

Small molecular inhibitors of Amyloid β
and α Synuclein amyloidogenic
aggregation, toxicity and *in silico* design of
amyloid-binding ligands

Sukanya Das, M.Sc.

Discipline of Pharmacology

Adelaide Medical School, Faculty of Health and
Medical Sciences, The University of Adelaide

May 2018

A thesis submitted for the degree of Doctor of Philosophy

Table of Contents

Abstract.....	i
Declaration.....	iii
Acknowledgements	iv
Statements of Authorship.....	vi
List of Abbreviations	xi
Chapter 1 : Introduction	1
1.1 Dementia and neurodegenerative diseases	1
1.1.1 Overview.....	1
1.1.2 Dementia and Alzheimer’s disease (AD) prevalence	2
1.1.3 Prevalence of Parkinson’s disease (PD)	3
1.1.4 Neuropathology of Alzheimer’s disease.....	4
1.1.5 Neuropathology of Parkinson’s disease.....	5
1.2 Current treatments for AD and PD	6
1.3 The amyloidogenic proteins Aβ and αS	7
1.3.1 Amyloidogenesis.....	7
1.3.2 The amyloid hypothesis	8
1.3.3 Structures of A β and α S.....	10
1.3.4 Amyloidogenic protein aggregation	12
1.4 Mechanisms of toxicity by Aβ and αS amyloidogenic proteins	13
1.4.1 Toxicity related to A β and α S aggregation	13
1.4.2 Oxidative stress and lipid peroxidation from A β and α S aggregation.....	14
1.4.3 Inflammatory responses associated with A β and α S aggregation	14
1.4.4 Other mechanisms of toxicity by A β and α S aggregates	15

1.4.5	Synaptic dysfunction by α S amyloidogenic aggregation.....	16
1.5	Different approaches to reduce Aβ and αS accumulation.....	18
1.5.1	Reducing A β and α S production.....	18
1.5.2	Inhibiting A β and α S aggregation.....	19
1.5.3	Clearance of A β and α S aggregates	20
1.6	Natural products as inhibitors of amyloidogenic protein aggregation	20
1.6.1	Advantages of natural products in drug discovery	20
1.6.2	Health benefits of natural polyphenols	21
1.6.3	Polyphenols that inhibit amyloidogenic protein aggregation and toxicity	22
1.6.4	Publication 1: Book Chapter.....	25
1.6.5	Clinical application of natural products as amyloidogenic protein aggregation inhibitors	29
1.7	Search for new inhibitors of Aβ amyloidogenic aggregation from synthetic origin	29
1.8	Biochemical and cell-based assays coupled with molecular modelling for identifying new amyloid inhibitors.....	30
1.8.1	Monitoring amyloidogenic protein aggregation by Thioflavin T assay	30
1.8.2	Visualisation of amyloidogenic aggregation by Electron Microscopy.....	31
1.8.3	Probing the structural conversion of α SA53T protein by ion mobility-mass spectrometry.....	31
1.8.4	Study of neuronal cell viability using the MTT assay for neuroprotection	32
1.8.5	Studying the interaction of molecules with A β and α SA53T by molecular docking.....	33
1.9	Research Aims.....	34

Chapter 2	<i>Bioactive polyphenol interactions with β amyloid: a comparison of binding modelling, effects on fibril and aggregates formation and neuroprotective capacity.....</i>	39
------------------	--	-----------

2.1	Publication 2	41
<i>Chapter 3 : Identification of dibenzyl imidazolidine and triazole acetamide derivatives through virtual screening targeting amyloid beta aggregation and neurotoxicity in PC12 cells.....</i>		
3.1	Publication 3 : Appendix A. Supplementary Material	53
<i>Chapter 4 : Exploring the structural diversity in inhibitors of α synuclein amyloidogenic folding, aggregation and neurotoxicity</i>		
4.1	Publication 4 : Appendix A. Supplementary Material	67
<i>Chapter 5 : Inhibition of α synuclein and amyloid β aggregation by diverse bioactives reveal a common antiaggregative role of magnolol</i>		
5.1	Introduction.....	83
5.2	Materials and methods	85
5.2.1	Reagents and Chemicals	85
5.2.2	α SA53T Protein expression and purification.....	86
5.2.3	Thioflavin T kinetic assay of α SA53T and A β ₁₋₄₂ fibrillisation	86
5.2.4	Transmission Electron Microscopy of A β fibrils and aggregates.....	87
5.2.5	Computational modelling of bioactive optimized conformation binding to A β ₁₋₄₂ and α SA53T	88
5.2.6	Statistical Analysis.....	89
5.3	Results	89
5.3.1	Effects of bioactives on α SA53T and A β ₁₋₄₂ fibrillisation.....	89
5.3.2	Transmission Electron Microscopy of α SA53T and A β ₁₋₄₂ fibrils and aggregates	92
5.3.3	Molecular modelling of bioactive interactions with α SA53T and A β ₁₇₋₄₂	94

5.4	Discussion.....	97
5.5	Conclusion	101

Chapter 6 : Molecular docking guided design of novel amyloid binding ligands using natural polyphenols and a synthetic heterocyclic ring system as templates 102

6.1	Introduction and background.....	102
6.1.1	Ligand-based drug design	102
6.1.2	Application of pharmacophore-based drug design for A β	103
6.1.3	Virtual screening	104
6.1.4	A combined approach: pharmacophore-based drug design with virtual screening	105
6.1.5	The neolignan biphenyl as template for anti-A β ligand design	106
6.2	Methodology	108
6.2.1	Design strategy for honokiol-derivatives using molecular docking	108
6.2.2	Computational methods	109
6.2.3	Design of Derivative 1, 2, 3 and 4	109
6.2.4	Design of Derivative 5,6 and 7: combining virtual screening hit with existing ligand.....	110
6.2.5	Other Derivatives	111
6.2.6	The core fragment of the derivatives	111
6.3	Results and Discussion.....	111
6.3.1	Honokiol and Derivative 1 molecular properties and interaction with A β	111
6.3.2	Derivative 2 molecular properties and interaction with A β	114
6.3.3	Derivative 3 interaction with A β	115
6.3.4	Derivative 4 interaction with A β	117
6.3.5	Derivative 5 interaction with A β	118
6.3.6	Derivative 6 interaction with A β	120

6.3.7	Derivative 7 interaction with A β	122
6.3.8	Docking of derivatives with α Synuclein A53T	125
6.3.9	Core fragment and scaffold hopping.....	127
6.3.10	General considerations.....	128
6.4	Conclusion and future direction.....	131
<i>Chapter 7 : Final Discussion and Conclusions</i>		132
7.1	Significance of the study.....	132
7.2	The neolignan biphenyl scaffold for developing disease modifying therapy in AD and PD.....	133
7.3	The novel dibenzyl imidazolidine scaffold and the ‘core’ fragment	136
7.4	The novel Derivative design as A β and α S ligand.....	137
7.5	Amyloid hypothesis as a target: still work to do.....	138
7.6	Limitations of this study and future directions	140
7.7	Conclusions.....	142
<i>Chapter 8 : Bibliography</i>		144

Abstract

Alzheimer's disease (AD) and Parkinson's disease (PD) are the most common forms of dementia and a leading cause of death amongst the older population worldwide. Pathologically, both AD and PD are characterized as progressive neurodegenerative disorders, in which there is a progressive loss of neuronal structure and function leading to loss of neurons in parts of the brain associated with cognition, memory and movement. Amyloidogenic protein misfolding and aggregation is at the centre of the neurodegenerative processes associated with AD and PD. In the case of AD, the amyloidogenic protein is amyloid β ($A\beta$) and in PD, it is the α Synuclein (αS) protein, or its mutant forms such as $\alpha SA53T$ found in familial PD which aggregates and exerts toxicity. In both AD and PD, we lack truly disease-modifying drug treatments, with current medications largely providing only modest and transient symptomatic improvement.

Therefore, the aim of this project was to identify a diverse set of new molecules from both natural and synthetic origin, that can alter $A\beta$ and $\alpha SA53T$ aggregation and fibril formation. Mostly small molecule binding has been studied by molecular docking and effects on $A\beta$ and $\alpha SA53T$ aggregation investigated using a ligand-binding fluorescence kinetic assay (Thioflavin T) and transmission electron microscopy (TEM). For neuroprotection studies, a mitochondrial viability (MTT) assay of neuronal cells (PC-12) was used. Finally, using molecular docking and density functional theory (DFT) approaches, a set of novel amyloid-binding ligands was designed *in silico* through ligand-based drug design. In the first study, four polyphenolic bioactives including a neolignan, ellagitannin and two flavonoid class of compounds have been comparatively studied for their binding interactions with $A\beta$, effects on fibril and aggregate formation and neuroprotection. In the second study, a structure-based

virtual screening method based on molecular docking has been implemented to identify new small molecule inhibitors of A β aggregation and neurotoxicity. Five heterocyclic compounds were selected and tested using the anti-aggregation and neuroprotection methods. Of these, the two best ‘hits’ bearing a novel molecular scaffold have been used in further studies. In the third study, the two virtual screening hits, polyphenolic bioactives from first study and two structurally related flavonoids were tested for inhibition of amyloidogenic aggregation and neuroprotection of the pathological α S mutant, α SA53T. Seven molecules have been compared as per the first and second study. Additionally, the impact on native α SA53T protein conformation was investigated by ion mobility mass spectrometry (IM-MS). In the fourth study, a diverse set of natural bioactives including a neolignan, flavonoid, chalcone, diterpene and alkaloid class of compound were tested for antiaggregative effects on both α SA53T and A β proteins. Additionally, their direct interactions with these amyloidogenic protein targets were studied by molecular docking.

The final study employed molecular docking and small molecular structure optimization using DFT method for rational design of a set of novel amyloid ligands. The favourable molecular attributes gleaned from both the bioactive neolignan in the first study and a favourable molecular scaffold in the second study were used to optimise binding for potential anti-aggregation. These ligands were predicted to have improved binding to A β and α SA53T *in silico*. Since there is an urgent need of disease-modifying therapies in both AD and PD, identification of anti-amyloidogenic and neuroprotective molecules would facilitate future drug discovery efforts. Design of a novel amyloid binder would be valuable for research and development of a therapeutic candidate or may assist in further design of an amyloid tracer molecule for diagnostic imaging.

Declaration

I certify that this work contains no material which has been accepted for the award of any other degree or diploma in my name, in any university or other tertiary institution and, to the best of my knowledge and belief, contains no material previously published or written by another person, except where due reference has been made in the text. In addition, I certify that no part of this work will, in the future, be used in a submission in my name, for any other degree or diploma in any university or other tertiary institution without the prior approval of the University of Adelaide and where applicable, any partner institution responsible for the joint-award of this degree.

I acknowledge that copyright of published works contained within this thesis resides with the copyright holder(s) of those works.

I also give permission for the digital version of my thesis to be made available on the web, via the University's digital research repository, the Library Search and through web search engines, unless permission has been granted by the University to restrict access for a period of time.

I acknowledge the support I have received for my research through the provision of an Australian Government Research Training Program Scholarship.

.....

Sukanya Das

22/5/18
.....

Date

Acknowledgements

I would like to thank my supervisor, Dr Scott Smid for his support, advice and encouragement throughout my candidature. His encouragement and support have motivated me to successfully complete the project. I would also like to thank my co-supervisor, Dr. Tara Pukala for her support and insights on my project. In addition, I would like to thank my other co-supervisor, Dr. Ian Musgrave for his advice and encouragement during my project.

Without financial support, this project would not have been possible. I would like to thank the Australian Research Training program as well as the Faculty of Health Sciences Divisional Scholarship for my scholarship. Travel to Australasian Society for Clinical and Experimental Pharmacologists and Toxicologists (ASCEPT) annual meeting, 2017 was supported by Dr. Scott Smid, Discipline of Pharmacology, Faculty of Health and Medical Sciences. Other travel support was provided by ASCEPT for presentation at the ASCEPT Drug Discovery special interest group symposium, 2016.

I would also like to acknowledge Lisa O'Donovan and Lynette Waterhouse from Adelaide Microscopy for training me on the Transmission Electron Microscope operation.

In addition, I would like to thank all my colleagues and the visiting students in The Neuroprotection lab in The Discipline of Pharmacology, who made the work environment more enjoyable and lively. Thanks to Rong, Dylan, Stefan and all the members of Dr. Tara Pukala's lab for all their support, friendship and fun filled conversations over lunches.

I would also like to extend my thanks to all the staff of Adelaide Campus Child Care Centre for looking after my child during my candidature. Without them I would not be able to balance my PhD and sole parenting role.

Last but not least, I would like to thank my family and friends for helping and encouraging me in the PhD journey. I am thankful to my little daughter Ruchira for making me more resilient.

Abbreviations

¹ H NMR	hydrogen nuclear magnetic resonance spectroscopy
3D	three dimensional
AA	arachidonic acid
AD	Alzheimer's disease
ANOVA	analysis of variance
APC	amyloid plaque core
APP	amyloid precursor protein
ASK1	apoptosis signal-regulating kinase1
AU	arbitrary unit
AUC	area under the curve
A β	amyloid β
A β ₁₋₄₀	amyloid β , sequence 1-40
A β ₁₋₄₂	amyloid β , 1-42 sequence
B3LYP	Becke's three-parameter hybrid functional
BACE1	beta site amyloid cleaving enzyme 1
BSA	bovine serum albumin
Ca ²⁺	calcium ion
CCS	collision cross section
CHC	central hydrophobic core
CNS	central nervous system
CNS	central nervous system
COMFA	comparative molecular field analysis
CoMSIA	comparative molecular similarity index analysis
COMT	catechol- <i>O</i> -methyltransferase
COX	cyclooxygenase
DA	dopamine

DDW	drug discovery workbench
DFT	density functional theory
DJ1	commonly used name for Parkinson protein 7
DLB	dementia with Lewy bodies
DMEM	Dulbecco's Modified Eagles Medium
DMSO	dimethyl sulfoxide
DNA	deoxy ribonucleic acid
EDTA	ethylenediaminetetraacetic acid
EGCG	(-) epigallocatechin-3-gallate
FAD	familial Alzheimer's disease
FBDD	fragment-based drug discovery
FCS	foetal calf serum
FDA	Food and Drug Administration
FMH	five-membered heterocycle
GAIM	general amyloid interaction motif
GBA1	glucosylceramidase beta
GCase	β -glucocerebrosidase
GTP	guanosine triphosphate
H-bonding	hydrogen bonding
HMDB	Human Metabolome Database
HNE	hydroxyl-2-nonenal
HSP	heat-shock protein
HTS	high throughput screening
IAPP	islet amyloid polypeptide
IDP	intrinsically disordered protein
IDP	intrinsically disordered protein
IL	interleukin
IM-MS	ion mobility-mass spectrometry

LB	Lewy body
LogP	logarithm of the octanol-water partition coefficient (P)
LOX	lipoxygenase
LP	Lewy pathology
LRRK2	leucine-rich repeat kinase 2
LTs	leukotrienes
<i>m/z</i>	mass to charge ratio
MAO-B	monoamine oxidase B
MAPK/JNK	mitogen activated protein kinase/c-Jun N-terminal kinase
MD	molecular dynamics
MM-PBSA	molecular mechanics Poisson-Boltzman surface area
MS	mass spectrometry
MSA	multiple system atrophy
mTOR	mammalian target of rapamycin
MTT	thiazolyl blue tetrazolium bromide salt
NAC	non-amyloid β component
NADH	nicotinamide adenine dinucleotide
NEAA	non-essential amino acids
NFT	neurofibrillary tangles
NLR	NOD-like receptors
NLRP3	NOD-like receptors pyrin domain containing 3
nm	nano meter
NMDA	<i>N</i> -methyl-D-aspartic acid
NMEs	new molecular entities
NMR	nuclear magnetic resonance spectroscopy
NOD	nucleotide-binding oligomerization domain
PBS	phosphate buffered saline
PC-12	phaeochromocytoma-12

PD	Parkinson's disease
PDB	protein data bank
PET	positron emission tomography
PINK1	PTEN (phosphatase and tensin homolog on chromosome 10) induced
PLANTS _{PLP}	protein-ligand ANT system (ant colony optimization) with pairwise linear potential
PrP	prion protein
PRR	pattern recognition receptors
	putative kinase 1
QSAR	quantitative structure activity relationship
RAGE	receptor for advanced glycation endproducts
REMD	replica exchange molecular dynamics
RFU	relative fluorescence unit
RMSD	root mean square deviation
RNA	riboxy nucleic acid
RNAi	riboxy nucleic acid interference
ROS	reactive oxygen species
RPMI	Roswell Park Memorial Institute
S	sulphur
SEVI	semen-derived enhancer of virus infection
sh	short hairpin
siRNA	small interfering RNA
SIRT1	silent mating type information regulation-2 homolog
SN	substantia nigra
SNARE	soluble N-ethylmaleimide-sensitive factor attachment protein receptor
SNCA	substantia nigra parc compacta
TEM	transmission electron microscopy
ThT	thioflavin T

TLR2	toll-like receptor 2
TNF α	tumour necrosis factor α
VAMP-2	vesicle associated membrane protein 2
VPS35	vacuolar protein sorting 35
VS	virtual screening
α S	α Synuclein
α SA53T	α Synuclein mutant for alanine 53 threonine
μ M	micro molar

Chapter 1: Introduction

1.1 Dementia and neurodegenerative diseases

1.1.1 Overview

Dementia commonly refers to the state of significant cognitive decline that interferes with the normal social functioning of older individuals as a result of neurodegeneration. Neurodegeneration or neurodegenerative disorder is a term collectively used for a variety of ailments that primarily affect the structure and function of neurons in the brain in a progressive manner. As the term ‘degeneration’ implies, in a neurodegenerative disorder there is progressive damage and eventual loss of neurons in specific regions of the brain. This pathology is exemplified by some of the most common forms of neurodegenerative diseases, such as Alzheimer’s disease (AD) and Parkinson’s disease (PD). Primarily, these diseases are associated with protein misfolding that leads to protein aggregation (Bucciantini, Giannoni et al. 2002). Since the majority of cases (50% – 70%) of dementia are AD, it can be divided into two broad classes: Alzheimer-type dementia and non-Alzheimer type dementia. Alzheimer-type dementia is predominantly characterised by memory loss along with other cognitive impairments in skilled motor function (apraxia), language (aphasia) or perception and visual or other (agnosias). The non-Alzheimer type dementia can be divided into three categories: Lewy body dementia, frontotemporal dementia and vascular dementia. PD is common form of Lewy body dementia, where cognitive decline is accompanied by movement disorders.

1.1.2 Dementia and AD prevalence

AD is one of the leading causes of death among older individuals aged over 65 years, globally (Figure 1) (Alzheimer's Association 2015). Figure 1 provides the global distribution of dementia and estimation for future with a higher total number of dementia patients in low- and middle-income countries. This is due to the greater overall population in those countries. According to the crude estimated prevalence in the World Alzheimer's report 2015, 4.7% and 4.6% of the total population of Asia and Africa have been suffering with dementia, respectively. Whereas, 6.4% and 5.9% of the total population of North America and Europe have been suffering from dementia, respectively. According to the World Alzheimer Report 2016, it is estimated that there were 46.8 million people suffering from AD in 2015 worldwide. This number is estimated to rise to 131.5 million by 2050 and 68% of this total number of dementia patients would be in the low- and middle-income countries (Ferri, Prince et al. 2006, Prince, Bryce et al. 2013).

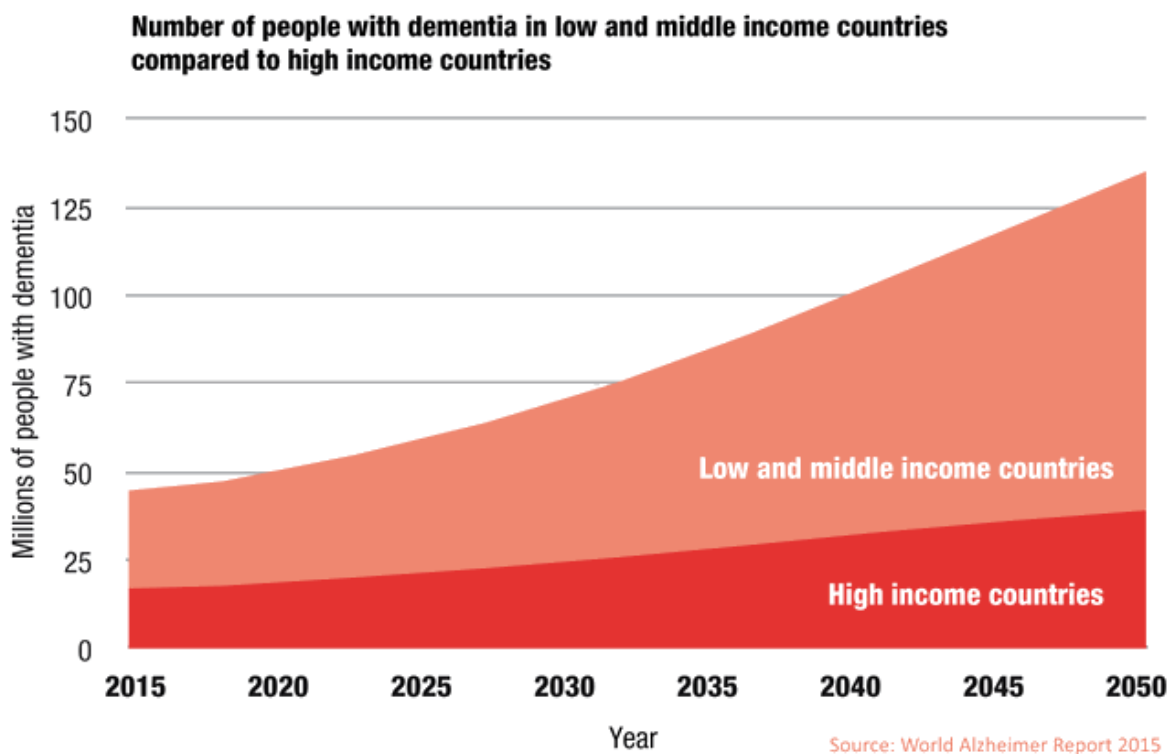


Figure 1. Global distribution of dementia and estimation for future, in both developing and developed world. *Source: World Alzheimer Report, 2015.*

The 2015 worldwide consensus study on the prevalence of dementia estimated that a new case of dementia is reported every 7 seconds (Ferri, Prince et al. 2006). Even though dementia is prevalent among older individuals, a 2017 report based on the American population estimated about 700,000 Americans (aged below 65 years) will have AD when they die and many of them will die because of the complications of AD (Alzheimer's Association 2017). In Australia, recent dementia statistics have reported that dementia is the second leading cause of death contributing to 5.4% of all deaths in males and 10.6% in all deaths in females each year (Australian Bureau of Statistics, 2017). In 2018, there is an estimated 425,416 patients are living with dementia which is estimated to increase to 1,100,890 by 2056 (Economic Cost of Dementia in Australia 2016-2056).

1.1.3 Prevalence of PD

PD is another complex neurodegenerative disease that affects 1 - 3% of the population aged over 60 years (Poewe, Seppi et al. 2017, Tysnes and Storstein 2017). In addition to cognitive decline, PD is also regarded as a movement disorder due to motor neuron degeneration with three cardinal signs; tremor, rigidity and bradykinesia (Tysnes and Storstein 2017). Recent studies have highlighted the non-motor symptoms of PD as an early indication (Schrag, Horsfall et al. 2015). Epidemiological studies have found a higher prevalence of PD in developed countries such as the US, Europe and Australia than in Asia among people aged over 70 years (Pringsheim, Jette et al. 2014). Out of the total PD cases, single gene mutations related to PD account for 5–10% (Lill 2016). Predominantly, autosomal dominant mutations in the *SNCA*, *LRRK2* and *VPS35* genes and autosomal recessive mutations in *PINK1*, *DJI* and

Parkin genes are linked to PD with high penetrance (Lill 2016). Consequently, the socio-economic burden of dementia is also on the rise. The World Alzheimer Report 2016 mentioned the total estimated worldwide cost of dementia is US\$818 billion. By 2018, this cost will increase to a trillion \$USD. Given the scenario where majority of dementia patients live in developing countries, disease management will become challenging due to both complex socio-economic factors and health costs associated with disease management globally.

1.1.4 Neuropathology of AD

The defining neuropathology of AD involves two primary lesions in the hippocampal region of the brain; development of senile or neuritic plaques and neurofibrillary tangles (NFT) (Perl 2010). Studies of senile plaques, a hallmark of AD, consistently revealed the presence of a central core of amyloid β ($A\beta$) protein, termed as amyloid plaque core (APC) (Figure 2a). $A\beta$ is a 4 kD protein arranged in a radial fashion within the plaques and is surrounded by a corona of abnormally configured neuronal processes or neurites (Figure 2a). The aggregation of $A\beta$ displays a beta-pleated sheet conformation. In addition to $A\beta$, microglial cells and reactive astrocytes are found at the periphery (Perl 2010) (Figure 2a). Another form of $A\beta$ aggregates are the diffuse plaques, where focal diffuse deposits of $A\beta$ protein may occur in the cerebral cortex in the absence of accompanying dystrophic neurites (Yamaguchi, Hirai et al. 1989) (Figure 2b). The other lesion, NFTs consist of hyperphosphorylated tau protein, a microtubule associated protein (Figure 2b). Abnormal accumulation of tau in the perikaryal cytoplasm of diseased neurons creates NFTs inside the neuron (Figure 2b).

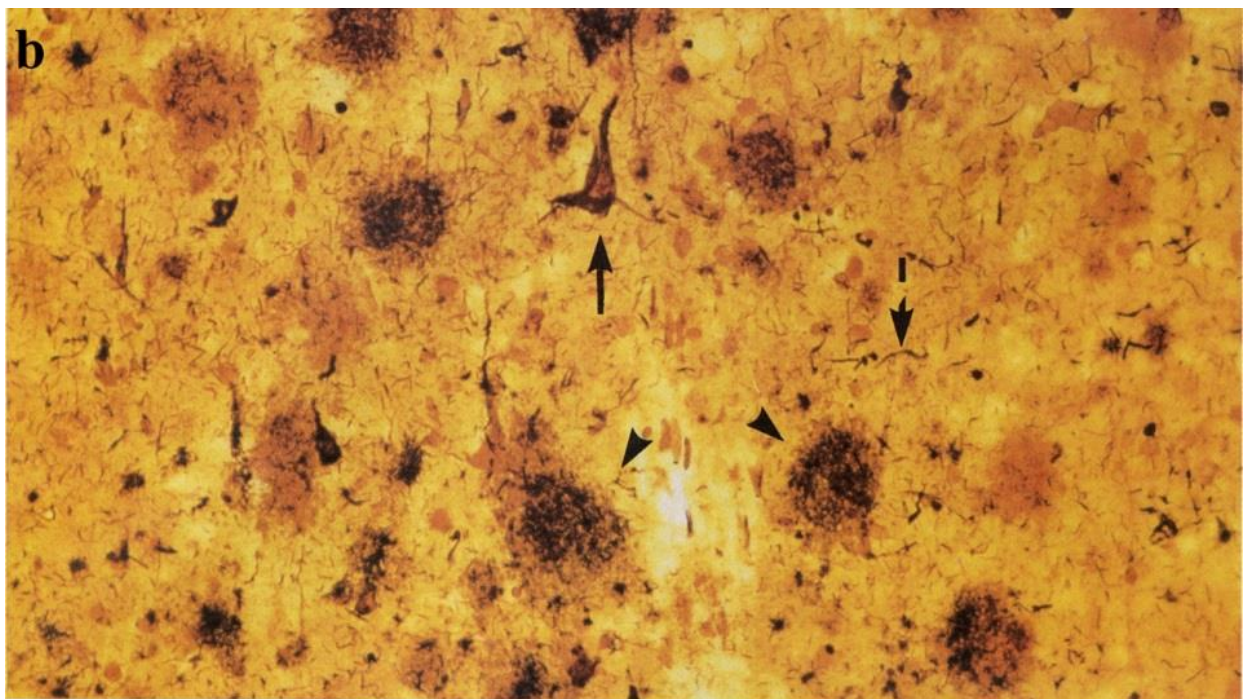
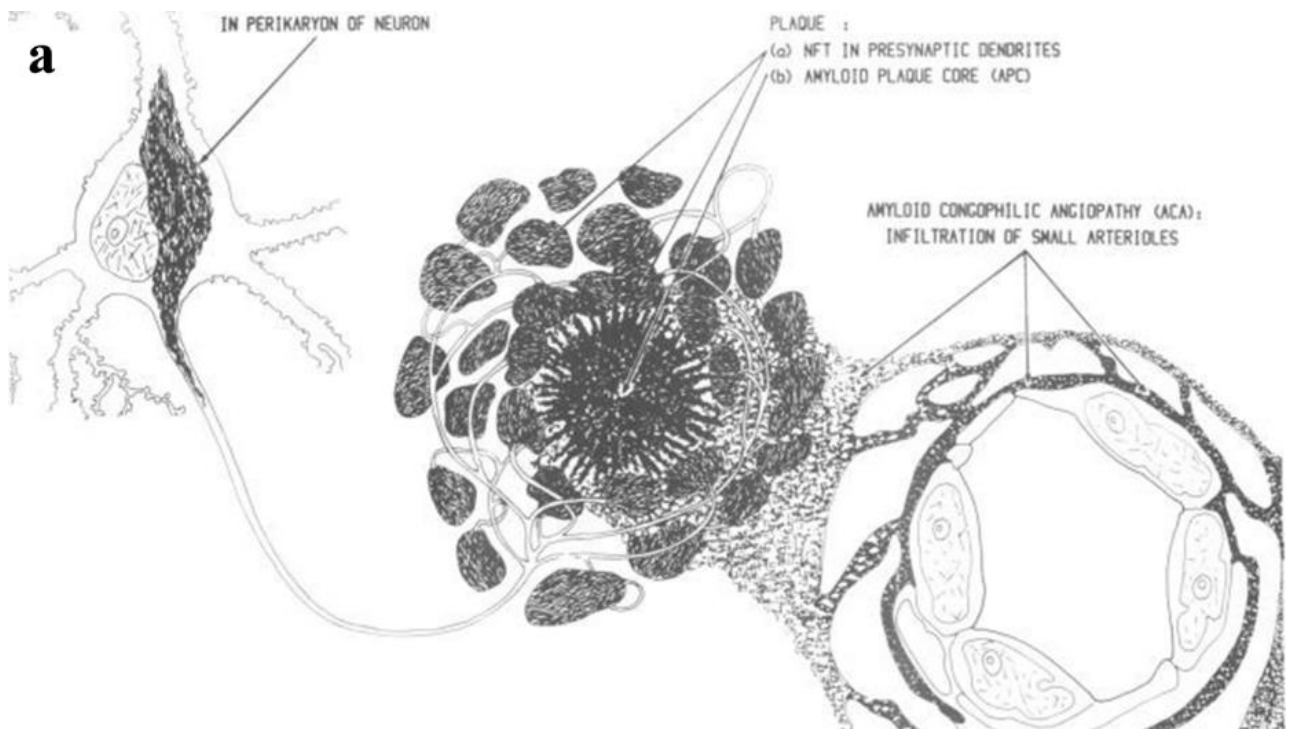


Figure 2. (a) Schematic diagram of the A β plaque and neurofibrillary tangles. These deposited proteins form the amyloid fibrils which may crystallize within the center of a plaque to form an A β plaque core (APC). Adapted from Masters et. al. (Masters, Multhaup et al. 1985). (b) A section of the cerebral cortex from an AD patient showing A β plaques (arrowheads), NFT

(arrow) and neutrophil threads (broken arrow) by Bielschowsky's stain. Adapted from Yanker et. al. (Yankner and Mesulam 1991).

1.1.5 Neuropathology of PD

In PD there is a loss of dopaminergic neurons in the substantia nigra pars compacta (SNCA) (Baba, Nakajo et al. 1998). Autopsy evidence of PD patient's brains show accumulation of Lewy bodies (LB) or Lewy pathology (LP) in both degenerating neurons as well as in extracellular spaces of the SNCA region. The aggregation of cytosolic protein α Synuclein (α S) is found to be associated with LB formation, as α S aggregates are the primary component of LB found in PD and dementia with Lewy bodies (DLB) (Baba, Nakajo et al. 1998) (Figure 3a and b). Moreover, pathological α S can transmit from cell to cell contributing towards progressive neurodegeneration in PD (Luk, Kehm et al. 2012). Although α S performs normal physiological and cellular functions such as vesicle trafficking, maintenance of the synaptic SNARE complex and vesicle pools and regulation of dopamine (DA) metabolism, under pathological conditions it becomes susceptible to amyloidogenic aggregation. Apart from the wild type α S, missense point mutations in the SNCA gene can lead to more aggregation-prone α SA1a53Thr (α S53T) protein (Li, Uversky et al. 2001). This α SA53T mutation not only causes familial PD, but these mutant protein carriers have also been shown to be associated with frontotemporal dementia in some patients (Bougea, Koros et al. 2017). Interestingly, LB-containing α S was found in the majority of sporadic AD patient's brains in the amygdala region (Lippa, Fujiwara et al. 1998, Hamilton 2000). This highlights the common overlap of amyloidogenic protein aggregation between AD and PD (Bucciantini, Giannoni et al. 2002).

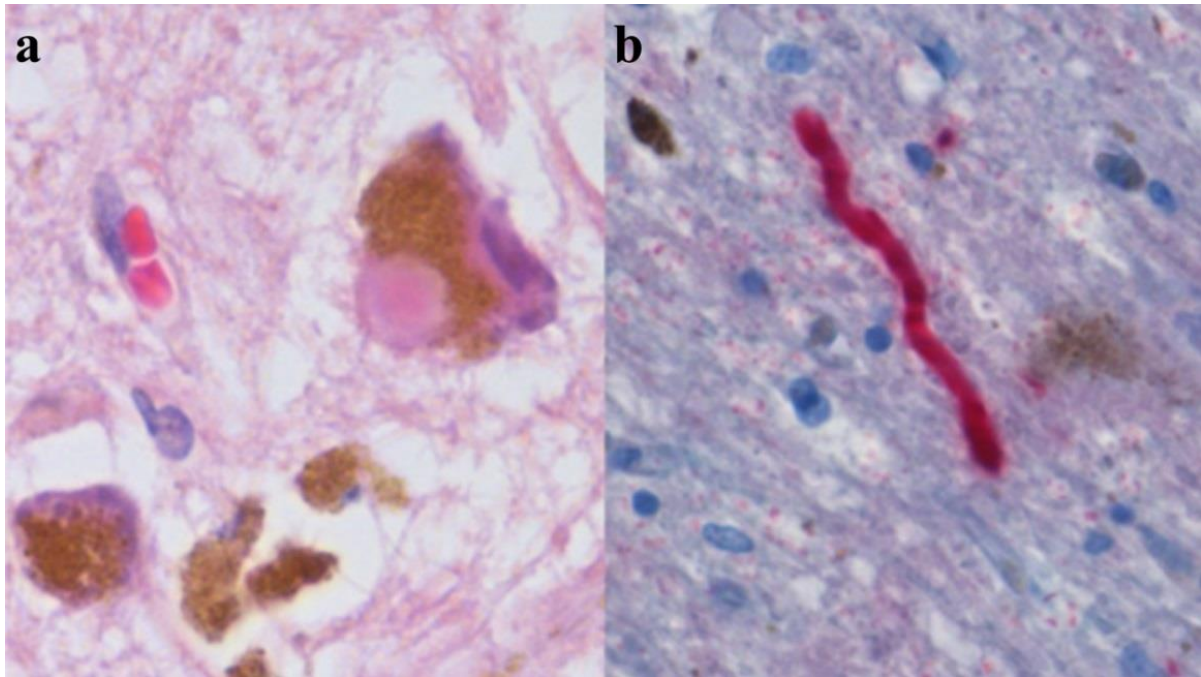


Figure 3: Sections of Substantia nigra in Parkinson's disease. **(a)** Substantia nigra pars compacta neuron with a Lewy body, extracellular neuromelanin and pigment-laden macrophages by haematoxylin/eosin stain, 500x. **(b)** α Synuclein positive Lewy neurite, 400x. Adapted from Werner et. al. (Werner, Heyny-von Haussen et al. 2008).

1.2 Current treatments for AD and PD

Despite the huge disease burden of both AD and PD, there is no cure for these diseases. Present medications are symptomatic and provide transient relief; however, they do not alter the course of disease progression. For AD, most of the approved drugs are classified as cholinesterase inhibitors that are used in various stages of AD. Since neurodegeneration of cholinergic neurons is profound, inhibition of cholinesterase has been shown to temporarily maintain acetylcholine levels for memory functioning (Nordberg and Svensson 1998, Trinh, Hoblyn et al. 2003). Another drug, memantine, works as a NMDA receptor antagonist and protects neuronal loss from excess glutamate toxicity (Tariot, Farlow et al. 2004). However, memantine does not protect neurons from the progression of the disease. Since 2003, no new drug has been approved for the treatment of AD.

The treatment of PD includes medications and surgical therapy. The medications are primarily dopamine replacement therapy in the form of levodopa, which has adverse side effects (DeMaagd and Philip 2015, Ferrazzoli, Carter et al. 2016). Dopamine receptor agonists have also been used (DeMaagd and Philip 2015). The efficacy of dopamine replacement therapy or levodopa depends on its enzymatic degradation by catechol-o-methyltransferase (COMT) and monoamine oxidase B (MAO-B) in the brain. In order to have a prolonged efficacy of levodopa treatment, a combination of levodopa and COMT inhibitor treatment is used (Ruottinen, H. and Rinne, U. K., 1998). Similarly, MAO-B is a major metabolising enzyme of dopamine. Therefore, COMT and MAO-B enzymes are attractive drug target for PD treatment to slow down dopamine degradation in the brain (Riederer, P. and Laux, G., 2011, Rabey, Sagi et al. 2000, Gonçalves, Alves et al. 2017). A cholinesterase inhibitor like donepezil, which is a prescribed drug for AD, has also been used in PD to manage dementia (Aarsland, Laake et al. 2002). Like AD, these medications are used for managing symptoms and do not address the underlying neurodegenerative pathology.

1.3 The amyloidogenic proteins A β and α S

1.3.1 Amyloidogenesis

Both A β and α S belong to the class of amyloidogenic proteins due to their high propensity for aggregation and transition to potentially cytotoxic β -sheet rich conformations. A β is generated due to the abnormal proteolysis of the large membrane protein, amyloid precursor protein (APP). APP is a complex protein and normally plays an important role in neural growth and repair in its full length configuration (Turner, O'Connor et al. 2003). Its fragmentation by

dedicated proteases such as beta-secretase (beta-site amyloid precursor protein cleaving enzyme 1, or BACE 1) followed by γ -secretase leads to the generation of neurotoxic 39-43 residue A β proteins (Mori, Takio et al. 1992, Iwatsubo, Saido et al. 1996). Out of these variable sequences, A β ₁₋₄₀ and A β ₁₋₄₂ are more predominant and frequently connected to AD pathology (Lemere, Lopera et al. 1996). Elevated plasma concentrations of A β ₁₋₄₂ were observed in familial AD related mutations (Scheuner, Eckman et al. 1996) and also in AD affected brain tissue (Kuo, Emmerling et al. 1996). A β ₁₋₄₂ is considered the most toxic species (Lambert, Barlow et al. 1998) related to neuronal cell death due to its high propensity for self-assembly (Chromy, Nowak et al. 2003).

α S, on the other hand, is a widely expressed cytosolic protein that is involved with important biological functions as mentioned earlier. Despite being primarily associated with PD, it is also known for multipathogenicity in other synucleinopathy diseases like DLB and multiple system atrophy (MSA), amongst others (Gai, Power et al. , Spillantini and Goedert 2000). It is a 140 amino-acid sequence protein belonging to the class of intrinsically disordered proteins (IDP), as it lacks a defined three-dimensional structure but comprises an ensemble of various conformations (Uversky 2011).

1.3.2 The amyloid hypothesis

The amyloid hypothesis or the amyloid cascade hypothesis dates back to 1906, when Alois Alzheimer first described the plaques and tangles in the brain as the pathognomonic signs of AD (Alzheimer 1911). Subsequent studies have characterised these plaques as made up of mostly A β protein aggregates. Further discovery of the autosomal dominant mutations for

familial AD (FAD) has been a cornerstone of the understanding of AD pathobiology and led to the development of the amyloid hypothesis (Goate, Chartier-Harlin et al. 1991, Hardy and Higgins 1992). It proposes that AD is essentially a disease of imbalance between the production and clearance of various pathogenic species of A β , occurring very early and often as an initiating factor of the disease (Hardy and Selkoe 2002) (Figure 4). According to the amyloid hypothesis, other neuropathologic lesions such as tau accumulation or NFT formation are subsequent events to A β aggregation (Hardy and Selkoe 2002) (Figure 4).

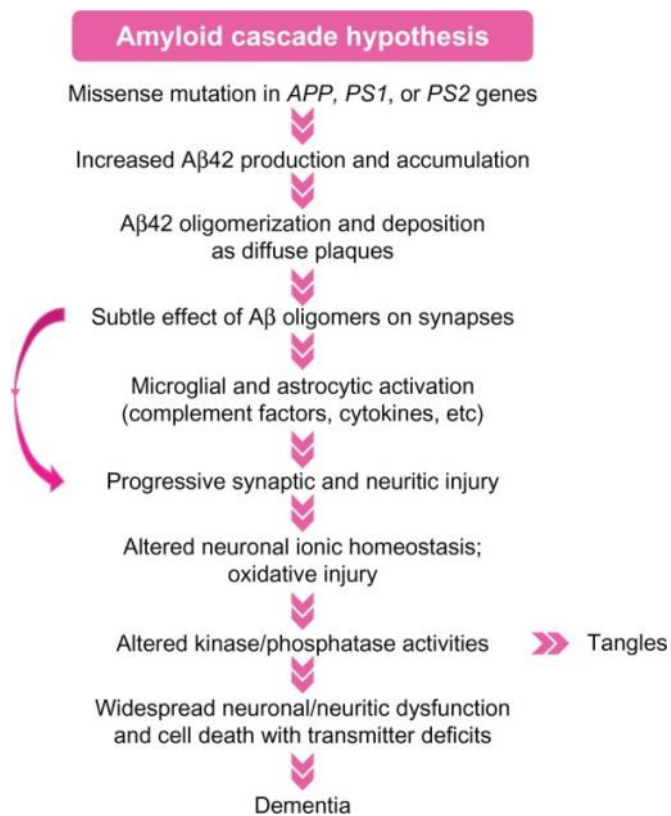


Figure 4. The amyloid hypothesis describing the sequential pathogenic events that occur in the development of AD. Adapted from Hardy. J and Selkoe. D. (Hardy and Selkoe 2002).

Since A β plaque formation often occurs decades earlier than the clinical diagnosis of the disease, the amyloid hypothesis is believed to be a route for disease-modifying therapeutics.

Autopsy samples from AD patient's brains showed formation of A β plaques and purification of amyloid plaque core protein revealed the presence of A β fibrillar structures (Masters, Simms et al. 1985, Lu, Qiang et al. 2013). Therefore, neurotoxicity of A β fibrils was previously believed to be the basis for the amyloid cascade hypothesis in AD (Hardy and Higgins 1992). Subsequent research demonstrated that small oligomeric, soluble A β aggregates were more related to neurotoxicity and neurodegeneration rather than the fibrils (Lambert, Barlow et al. 1998, Hartley, Walsh et al. 1999, Walsh, Hartley et al. 1999).

1.3.3. Structures of A β and α S

At the molecular level, most amyloidogenic proteins including A β and α S display structural polymorphisms. This implies that these proteins are capable of misfolding into different structural conformations that are associated with toxicity (Tycko 2015). For A β , a number of structural conformations ranging from monomers, oligomers and polymers have been reported to be associated with its toxicity (Luhers, Ritter et al. 2005, Xiao, Ma et al. 2015, Gremer, Scholzel et al. 2017). NMR and cryo-EM analysis suggest the presence of parallel- β -sheet segments in these A β conformations have been associated with aggregation and fibril growth. The oligomeric conformation (PDB ID: 2BEG) and the monomeric conformation (PDB ID: 1IYT) available from the Protein Data Bank have been used in this study for understanding ligand binding to A β (Figure 5a and b). The α -helical conformation of A β monomer in solution has a similarity with a viral protein that has also been implicated with toxicity (Crescenzi, Tomaselli et al. 2002) (Figure 5a). Additionally, the structure of the A β monomer comes from a ¹H NMR study undertaken in a mixture of trifluoroethanol (TFE) and water. TFE is an apolar solvent that encourages intramolecular hydrogen bonds, in contrast to water which readily hydrogen bonds with peptides and surface-exposed amino acids in proteins. As a result, since

A β is a relatively short peptide (40-42 amino acids in length), it adopts an unstructured conformation in water (Figure 5a). The mostly α -helical A β structure of Crescenzi et al. (Figure 5a) is most likely the conformation that the peptide adopts in a hydrophobic environment, for example when it binds to a membrane (Figure 5a). The structures of A β oligomer and A53T α -synuclein in Figures 5b, c are for the protein when incorporated into the amyloid fibrillar form, as determined by solid state NMR studies.

α S is a 140-residue protein whose structure is divided into three distinct regions; the N-terminal lipid binding region from residue 1-60, the non-amyloid β component or NAC region from residue 60-90 and the acidic C-terminal region from residue 90–140 (Culvenor, McLean et al. 1999). The various structural conformations of α S covering the complete sequence of the protein is not very well understood, due to its intrinsically disordered nature. Nevertheless, a recent NMR study revealed the full sequence structure of a pathologic α S conformation (Tuttle, Comellas et al. 2016). This structure presents characteristic amyloid features such as β -sheet segments and hydrophobic-core residues. Since there is not a complete sequence structure of the α SA53T mutant available in the Protein Data Bank (PDB), the above-mentioned structure has been mutated and used in this study (Figure 5c).

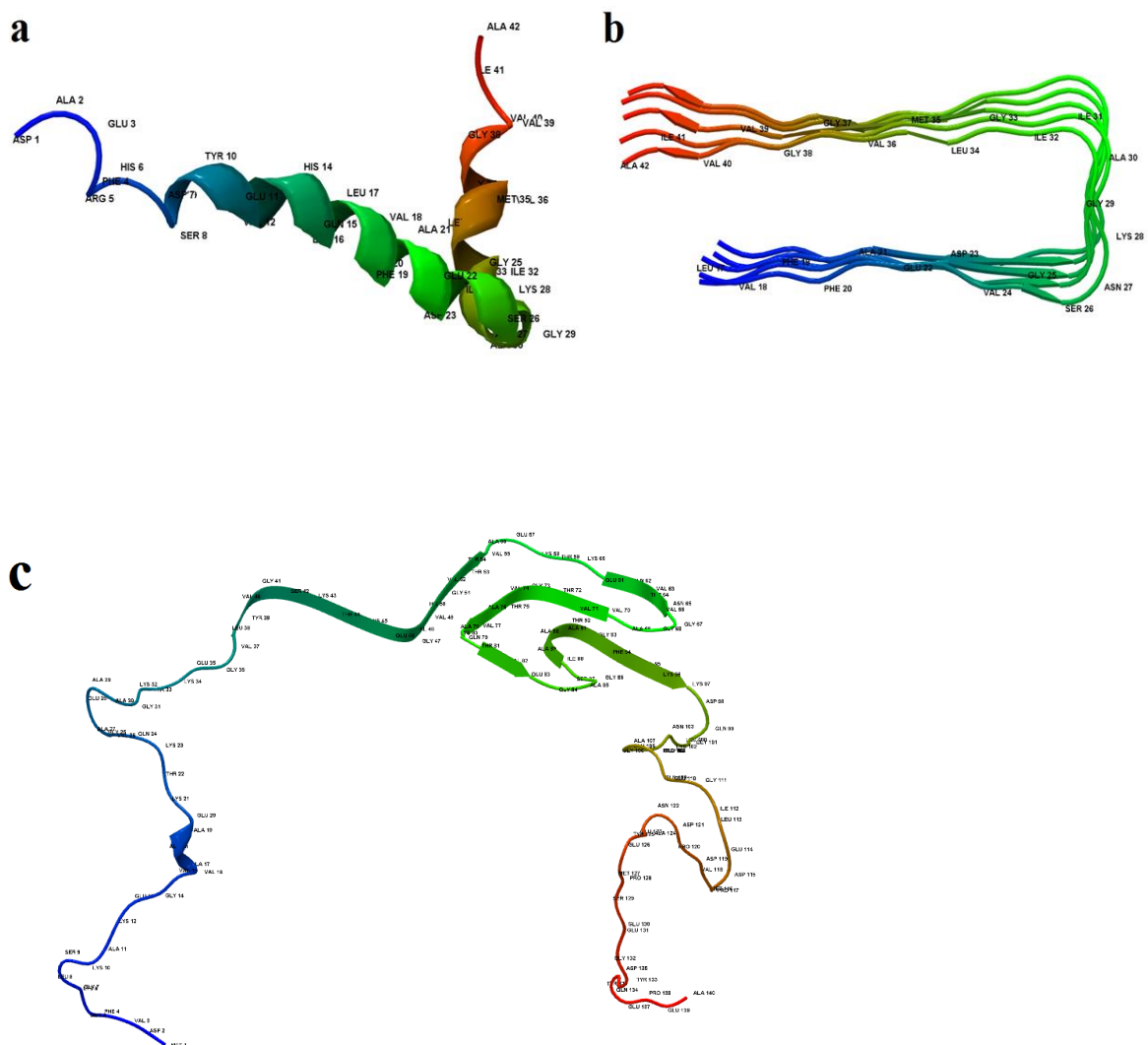


Figure 5. NMR structures of amyloidogenic proteins that are used in this study in the molecular modelling (a) A β monomer (PDB ID: 1IYT), (b) A β oligomer (PDB ID: 2BEG) and (c) α SA53T monomer (PDB ID: 2N0A).

1.3.4 Amyloidogenic protein aggregation

Various mechanisms have been proposed in the literature regarding the conversion of A β monomers to oligomers of different size and shape. Since A β ₁₋₄₀ and A β ₁₋₄₂ are primarily associated with neurotoxicity, they have been studied extensively for their structural/conformational changes that lead to further A β fibril development. Overall, there are

four suggested stages of amyloid fibril assembly from the native monomeric structure (Harper, Wong et al. 1999). Firstly, the monomer misfolds and aggregates into small oligomeric species that leads to protofibril initiation, which is a nucleation-dependent event. This may require fewer than 20 A β molecules (Walsh, Lomakin et al. 1997). The initiation process is followed by protofibril elongation, where coalescence of smaller protofibrils occur. This process has been explained experimentally and computationally (Kowalewski and Holtzman 1999, Cheon, Chang et al. 2007). The protofibril association stage includes winding and a conformational change into a β -sheet rich segment, as elucidated computationally (Cheon, Chang et al. 2007). The final step is the fibril elongation that can be initiated by the addition of preformed fibrillar seeds to A β protofibrils for growth of fibrils *in vitro* (Harper, Lieber et al. 1997).

1. 4 Mechanisms of toxicity by A β and α S amyloidogenic proteins

1.4.1 Toxicity related to A β and α S aggregation

The aggregation of amyloidogenic proteins into small soluble oligomers and mature fibrils leads to toxic actions toward neuronal cells (Harte, Klyubin et al. 2015). A β displays structural polymorphisms during its aggregation and forms a heterogeneous population of small oligomers and protofibrils in addition to fibrillar conformations. Recent studies on amyloid toxicity revealed that the small oligomeric conformations are more toxic than the mature fibrils, as they can form annular protofibrils or ‘amyloid pores’ that may interrupt membrane permeabilization (Lashuel, Hartley et al. 2002, Bieschke, Herbst et al. 2011). A β oligomers trigger toxicity by enhancing oxidative stress, disrupting membranes and initiating cellular organelle dysfunction. Consistent with the toxicity of amyloidogenic proteins such as A β , conformational changes and folding of α S into oligomers and prefibrillar species are the most toxic and pathogenic forms (Ingelsson 2016). The mutant forms of α S such as A53T form a

different conformational ensemble than the wild type α S during self-assembly (Tosatto, Horrocks et al. 2015). Release of α S by unconventional exocytosis into extracellular space elicits neurodegeneration, progressive spreading of α S pathology and neuroinflammation (Lee, Bae et al. 2014).

1.4.2 Oxidative stress and lipid peroxidation from A β and α S aggregation

One of the mechanisms of A β -induced neurotoxicity is where A β produces reactive oxygen species (ROS) which then activates apoptosis signal-regulating kinase 1 (ASK1) (Kadowaki, Nishitoh et al. 2004). The other mechanism involves generation of hydroxyl-2-nonenal (HNE) as a result of oxidative lipid damage as found in both AD and PD (Lovell, Ehmann et al. 1997, Castellani, Perry et al. 2002). Misfolded A β produces oxidative damage to lipid membranes by acting as a prooxidant. This oxidative lipid damage produces HNE, which in turn promotes more A β misfolding (Murray, Liu et al. 2007). A β promotes copper-mediated HNE generation that covalently modifies the histidine residue of A β , rendering it more aggregation-prone (Murray, Liu et al. 2007). Another study also reported that a pathologically thin lipid bilayer occurs as a result of oxidative damage in AD pathology, which in turn promotes A β toxic aggregation (Korshavn, Satriano et al. 2017). Likewise, HNE generation due to oxidative damage of lipids is also implicated in protein misfolding and neurotoxicity to nigral neurons in PD (Yoritaka, Hattori et al. 1996). Additionally, protein carbonyl generation due to free radical attack on amino acids has been observed in the substantia nigra (SN) of PD patients (Floor and Wetzel 1998).

1.4.3 Inflammatory responses associated with A β and α S aggregation

In addition to oxidative stress, aggregation of A β can activate inflammatory responses via pattern recognition receptors (PRR) such as Toll-like, NOD-like (nucleotide-binding oligomerization domain) receptors or NLR, formyl peptide, receptor for advanced glycation end product (RAGE) and scavenger receptors on glial cells and neurons that contribute to AD pathology (Salminen, Ojala et al. 2009). Not surprisingly, amyloidogenic folding of α S also triggers inflammatory responses by activating similar types of receptors such as Toll like receptor 2 (TLR2) and NOD-like receptors pyrin domain containing 3 (NLRP3) inflammasome (Gustot, Gallea et al. 2015).

In PD, the activation of microglial and astroglial cells brings about major inflammatory responses. Based on the staining for microglial activation and post-mortem analysis of PD affected brains, it is postulated that the dopaminergic neurodegeneration occurring early in the disease process is accompanied by the widespread activation of microglial cells (McGeer, Itagaki et al. 1988, Gerhard, Pavese et al. 2006). Alvarez-Erviti et. al. have also reported that release of α S or its pathological mutant A53T by neuronal cells activates proinflammatory cytokines from glial cells *in vitro* (Alvarez-Erviti, Couch et al. 2011). The α S aggregates released from the neuronal cells are taken up by astrocytes resulting in induction of proinflammatory cytokines and chemokines. This inflammatory response is due to the transmission of α S aggregates from neurons to glial cells, correlated with the extent of glial accumulation of α S aggregates and changes in glial gene expression profiles to an inflammatory response (Lee, Suk et al. 2010).

1.4.4 Other mechanisms of toxicity by A β and α S aggregates

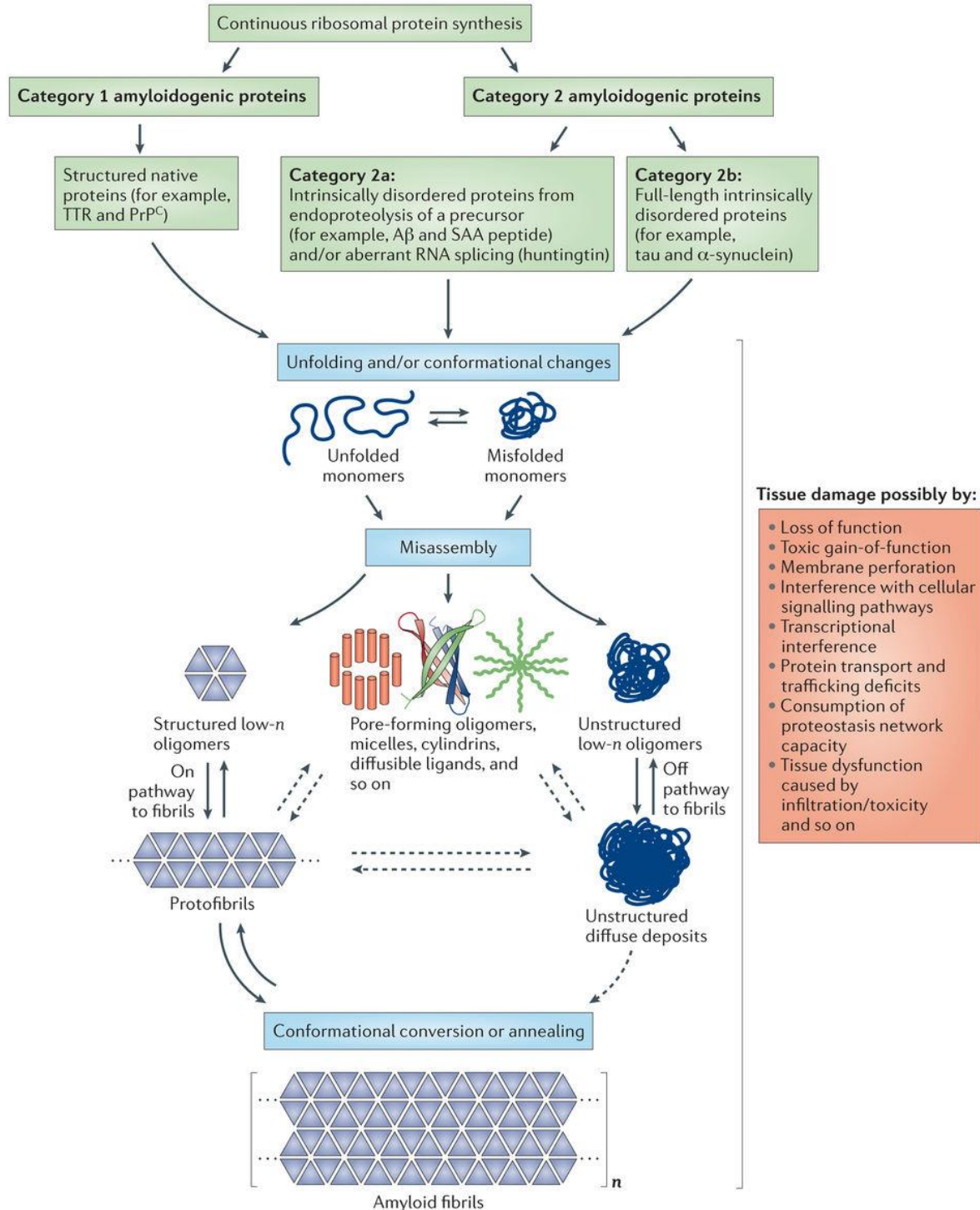
It is worth mentioning that the impaired mitochondrial electron transport chain is a primary source of oxidative stress. In PD, a defect in the mitochondrial NADH-ubiquinone reductase (complex 1) in the substantia nigra (SN) region has been observed (Mizuno, Ohta et al. 1989, Schapira, Cooper et al. 1990). Similarly, a significant decrease in cytochrome oxidase (complex IV) activity has been reported in AD (Parker, Filley et al. 1990, Mutisya, Bowling et al. 1994). Furthermore, A β interaction with the cell membrane leads to increased intraneuronal Ca²⁺ ions and disrupted calcium homeostasis (Hardy and Higgins 1992). Studies connecting oxidative stress with inflammatory responses from A β aggregation have demonstrated that in AD, A β deposition increases ROS production resulting in lipid and protein peroxidation. This occurs through an extracellular signal-regulated phospholipase A2 cascade for formation of arachidonic acid (AA) from membrane phospholipids (Adibhatla and Hatcher 2008, Hsieh and Yang 2013), which triggers COX-mediated inflammatory responses such as release of IL-1 (Mrak and Griffin 2005, Adibhatla and Hatcher 2008).

1.4.5 Synaptic dysfunction by α S amyloidogenic aggregation

Deposition of α S oligomers and aggregates in the presynaptic region can interact with the N-terminal domain of VAMP-2 and block presynaptic SNARE-mediated vesicle docking, which leads to inhibition of dopamine release (Choi, Choi et al. 2013). Abnormal interaction of α S with the Rab GTPase family like Rab3A and rabphilin is implicated with exocytosis of neurotransmitters associated with Lewy body diseases (Dalfo, Barrachina et al. 2004). The misfolded oligomeric and other amyloid forms of α S trigger misregulation of synaptic proteins leading to functional impairment of the presynaptic terminal (Volpicelli-Daley, Luk et al. 2011). This impairment is shown to be progressive and selective to dopaminergic neurons (Janezic, Threlfell et al. 2013). Since degeneration of dopaminergic neurons is a primary

phenotype of PD, synaptic dysfunction by α S oligomers and aggregates implies that inhibition of α S aggregation is a potential disease modifying strategy.

Dynamic process of protein aggregation leads to the dysfunction and loss of postmitotic tissue



Nature Reviews | Drug Discovery

Figure 6. Amyloidogenic protein, A β and α S aggregation process that leads to neurotoxicity in AD and PD. The self-assembly of native unfolded monomer or misfolded monomer of A β and α S can drive the formation of toxic oligomeric conformations that trigger a chain of toxic injuries to neuronal cells and eventual neurodegeneration. Adapted from the review study of Eisele et. al. (Eisele, Monteiro et al. 2015).

1. 5. Different approaches to reduce A β and α S accumulation

1.5.1 Reducing A β and α S production

Studies aiming at a reduction of A β have largely been focused on β -site amyloid-precursor-protein-cleaving enzyme 1 (BACE 1); that is, the aspartic protease that cleaves APP at the β -secretase site and generates A β . Earlier studies have identified many naturally occurring compounds such as green tea catechins, punicalagin and ellagic acid as non-competitive BACE1 inhibitors (Jeon, Bae et al. 2003, Kwak, Jeon et al. 2005). Small molecule drug discovery endeavours in AD have been intensely focused towards BACE1 inhibitor design as seen by a plethora of clinical candidates from major pharmaceutical companies (Yan and Vassar 2014). Despite the challenges, BACE 1 inhibitors are the first class of disease-modifying small molecule drugs for A β that have entered into clinical trials (Kennedy, Stamford et al. 2016, Ufer, Rouzade-Dominguez et al. 2016, Yan 2016). However, the results from the small molecule inhibitor of BACE1 (verubecestat 1) have not been promising and others are still at a trial stage (Mullard 2017).

Unlike A β , which has been generated by sequential cleavage of proteolytic enzymes, α S is a cytosolic protein and therefore its reduction might require intervention at the RNA translation level. RNA interference (RNAi) approaches including short hairpin (sh) α S RNA delivery via a lentiviral vector and small interfering (siRNA) directed against α S, have been reported to reduce brain α S level in rats (Zharikov, Cannon et al. 2015). In respect of the important

physiological functions performed by α S in the CNS however, reductions in α S level might be approached with caution. The other approach has been to modify the transcription of the α S gene, where a recent study has identified beta-2-adrenoreceptor agonism as a mechanism to reduce α S gene expression (Mittal, Bjørnevik et al. 2017).

1.5.2 Inhibiting A β and α S aggregation

Studies on inhibition of A β aggregation are mostly in preclinical development and have employed either small molecular inhibitors or peptidic anti-aggregators (Nakagami, Nishimura et al. 2002, Lecanu, Yao et al. 2004, Jillian, Xiaoyan et al. 2009, Doig and Derreumaux 2015). There have been various natural small molecule inhibitors of A β and α S investigated. Out of the various natural products, EGCG, curcumin and resveratrol have been studied extensively for inhibition of different amyloidogenic protein aggregates (Marambaud, Zhao et al. 2005, Yang, Lim et al. 2005, Ehrnhoefer, Bieschke et al. 2008, Ahmad and Lapidus 2012). Other natural products such as baicalein have demonstrated inhibition of α S aggregation by stabilizing its toxic oligomers and inhibiting oligomer formation in living cells (Hong, Fink et al. 2008, Lu, Ardah et al. 2011). In addition, baicalein inhibited A β oligomerization, disaggregated preformed A β aggregates and prevented A β fibril-induced toxicity in PC-12 cells (Lu, Ardah et al. 2011). A detailed introduction about the antiaggregative and anti-amyloid properties of natural small molecules, has been provided in Publication 1: Book Chapter (section 1.6.4).

Among other inhibitors, small heat shock proteins (HSP) have been documented to act as molecular chaperones that prevent amyloidogenic aggregation (Hatters et al. 2001, Rekas et al. 2004, Gorenberg and Chandra 2017). Another protein therapeutic is a combination of human immunoglobulin and a general amyloid interaction motif (GAIM), which binds to α S as a

generic amyloid inhibitor and is in a clinical trial (Krishnan, Tsubery et al. 2014). Another recent approach features the use of small antibody fragments called intrabodies to inhibit α S aggregation (Bhatt, Messer et al. 2013). Intrabodies are typically composed of 140–250 amino acids and target antigens intracellularly with high specificity and affinity for target epitopes.

1.5.3 Clearance of A β and α S aggregates

Antibody-based immunotherapy has predominantly accounted for clearance of A β aggregates and plaques from AD-affected patient's brains. Monoclonal antibodies have recently gained attention, with the promising results of aducanumab in clinical trials (Sevigny, Chiao et al. 2016). Strategies for clearance of α S employ an enhancement of the autophagic process. Rapamycin and its analogues, acting through the mammalian target of rapamycin (mTOR) to increase macroautophagic functions, have been shown to reduce α S aggregation (Moors, Hoozemans et al. 2017). Another autophagy-enhancing approach involves the lysosomal enzyme β -glucocerebrosidase (GCase), as mutations in the GCase encoding gene *GBA1* have been reported as a common risk factor for α S aggregation-related disorders, primarily due to reduced GCase activity (Sardi, Cheng et al. 2015). For degrading and clearing extracellular α S aggregation, active and passive immunotherapies in the form of monoclonal antibodies have been trialled recently (Schenk, Koller et al. 2017, Brys, Ellenbogen et al. 2018).

In view of the recent multimodal approach to overcome the amyloidogenic proteinopathy caused by A β and α S, it is essential to identify new molecular inhibitors that can generically target amyloidogenic aggregation.

1. 6 Natural products as inhibitors of amyloidogenic protein aggregation

1.6.1 Advantages of natural products in drug discovery

Presently there is neither any disease-modifying approach in both AD and PD nor any therapeutic agent that targets amyloidogenic protein aggregation. Provided the multifarious health benefits and a rich diversity of molecular structures, natural products offer an attractive collection to search for amyloid inhibitors that can be further developed as therapeutics (Ganesan 2008). Historically, small molecules found in natural products or inspired by a natural product have served as the key active ingredient in many drugs and candidates in clinical trials (Chin, Balunas et al. 2006, Newman and Cragg 2007, Harvey 2008). Recent drug discovery efforts extensively relied on natural product structures for design of new molecular entities (NMEs) (Patridge, Gareiss et al. 2016, Rodrigues, Reker et al. 2016). In addition, target oriented synthetic tractability and structural flexibility of small molecules help building focused libraries for classical drug discovery (Schreiber 2000).

1.6.2 Health benefits of natural polyphenols

Polyphenols are by definition organic molecules with multiple phenol rings that are widely distributed in various dietary sources as micronutrients and in other plant sources as a stress protective mechanism (Manach, Scalbert et al. 2004). Polyphenols cover an extensive group of compounds such as flavonoids, curcuminoids, stilbenes, lignans, tannins, phenolic acids, anthocyanidins, chalcones and other compounds. The anti-oxidant properties of various polyphenols are often highlighted in their health benefits against several diseases associated with oxidative stress (Manach, Scalbert et al. 2004). Based on the present understanding, polyphenols exert their powerful antioxidant effects by three mechanisms; H atom transfer, single electron transfer and metal chelation (Leopoldini, Russo et al. 2011). A comprehensive study of polyphenol metal chelation activity demonstrated that ‘gallol’ or ‘catechol’ group in

polyphenols, mostly found in flavonoids, exhibited higher antioxidant property due to chelation of iron and copper ions (Perron and Brumaghim 2009). Additionally, flavonoids can scavenge reactive oxygen molecules by suppressing xanthine oxidase activity (Hanasaki, Ogawa et al. 1994). The powerful antioxidant property and reduction of reactive oxygen species (ROS) of polyphenols contribute toward protection from cardio-vascular disease, various cancers, diabetes and age related disorders including neurodegenerative disease (Pandey and Rizvi 2009).

In addition to antioxidant effects, polyphenols also possess anti-inflammatory properties. Flavonoids and their glycoside derivatives reduce inflammation by various pathways such as inhibiting cyclooxygenase (COX) and lipoxygenase (LOX) responsible for generating leukotrienes (LTs) (Moroney, Alcaraz et al. 1988). Also, some flavonoids such as quercetin inhibit the phospholipase A2 enzyme as part of their anti-inflammatory response (Lee, Matteliano et al. 1982). Since oxidative stress and inflammatory responses are some of the primary mechanisms of amyloidogenic protein toxicity, antioxidant and anti-inflammatory compounds might provide benefit towards protecting neurons from these toxic injuries.

1.6.3 Polyphenols that inhibit amyloidogenic protein aggregation and toxicity

Various polyphenol bioactive compounds have demonstrated interactions with amyloidogenic proteins which inhibit their aggregation. Among these, flavonoids are the most effective group of compounds in altering amyloidogenic protein aggregation (Shimmyo, Kihara et al. 2008, Bieschke, Russ et al. 2010, Meng, Munishkina et al. 2010, Lu, Ardah et al. 2011). Flavonoids collectively represent molecules with a benzopyran ring connected with a phenyl ring, termed

a B-ring. They are further subdivided into flavone, flavanol, flavanone, flavanonol, flavan, flavan-3-ol, isoflavone and anthocyanidin classes. The flavan-3-ol, epigallocatechin-3-gallate (commonly known as EGCG) and flavone myricetin have been demonstrated to cause inhibition of amyloidogenic protein aggregation including A β and α S (Shimmyo, Kihara et al. 2008, Bieschke, Russ et al. 2010). Moreover, EGCG remodelled amyloidogenic fibrils into off-target non-toxic pathways and disrupted preformed amyloid aggregates (Ehrnhoefer, Bieschke et al. 2008). Other catechol-type (two or more adjacent hydroxyl groups) flavonoids such as taxifolin, epicatechin, quercetin and fisetin have also elicited significant inhibition of amyloid aggregation (Bastianetto, Yao et al. 2006, Porat, Abramowitz et al. 2006, Ansari, Abdul et al. 2009, Sato, Murakami et al. 2013, Ahmad, Ali et al. 2017). The non-catechol type flavonoids such as morin, datiscetin, kaempferol have also shown antiaggregative activities towards A β (Hanaki, Murakami et al. 2016). Baicalein, another catechol-type flavonoid caused extensive inhibition of α S aggregation by stabilizing its oligomeric conformations into an off-target pathway (Hong, Fink et al. 2008). In addition to inhibiting protein aggregation, flavonoids also protected neuronal cells *in vitro* and *in vivo* from amyloid pathology (Hong, Fink et al. 2008, Rezai-Zadeh, Arendash et al. 2008, Bieschke, Russ et al. 2010, Lu, Ardah et al. 2011, Lorenzen, Nielsen et al. 2014).

Aside from flavonoids, curcumin is the most widely researched bioactive polyphenol for inhibition of amyloidogenic aggregation and toxicity. Curcumin reduces A β levels by several mechanisms, of which binding to A β deposits and inhibiting oligomer and fibril formation *in vivo* is noteworthy (Yang, Lim et al. 2005). Moreover, curcumin decreased A β levels by attenuating the maturation of its precursor protein, APP (Zhang, Browne et al. 2010). Curcumin also reduced α S aggregation by binding to monomers, increasing its reconfiguration rate which makes the protein more diffusive (Ahmad and Lapidus 2012). The stilbene resveratrol has also

been studied extensively for its potential to mitigate amyloid toxicity through degradation of A β by a proteasome-dependent mechanism (Marambaud, Zhao et al. 2005). The antioxidant property of resveratrol can activate the neuroprotective sirtuin protein, SIRT1 (silent mating type information regulation-2 homolog) to protect neuroblastoma cells from oxidative stress caused by α S aggregation (Albani, Polito et al. 2009). Figure 7 shows the chemical structures of EGCG, curcumin and resveratrol, three commonly known natural product amyloidogenic aggregation inhibitors as discussed above.

The search for natural products to develop therapeutics for neurodegeneration has identified other classes of bioactive compounds such as terpenoids, alkaloids and carotenoids as effective agents against dementia (Papandreou, Kanakis et al. 2006, Yoo and Park 2012). Terpenoid-rich Ginkgo biloba extracts and ginkgolides have been studied thoroughly for protection against A β and α S-induced toxicity (Wu, Wu et al. 2006, Shi, Zhao et al. 2009, Yu, Chen et al. 2017).

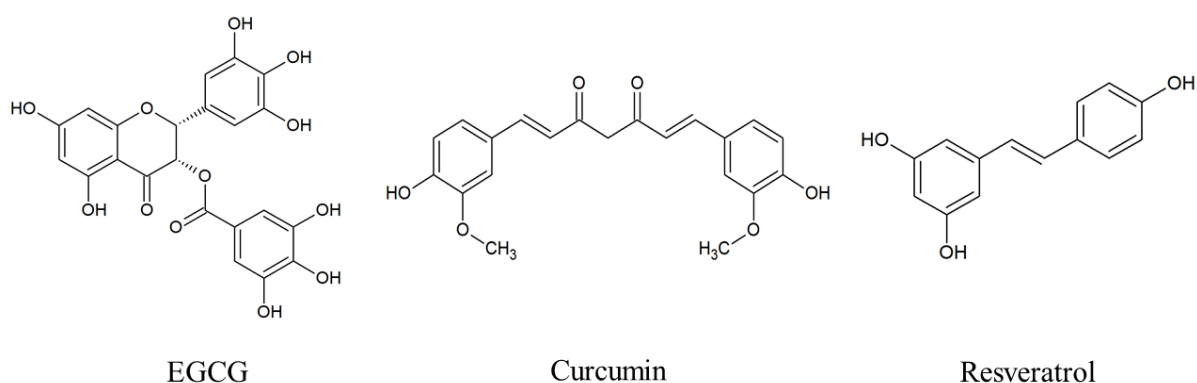


Figure 7: Chemical structures of the commonly known polyphenols as inhibitors of amyloidogenic protein aggregation.

1.6.4 Publication 1.

The Antiaggregative, Antiamyloid Properties of Bioactive Polyphenols in the Treatment of Alzheimer's Disease

Das, S., Smid SD.

Book: *Bioactive Nutraceuticals and Dietary Supplements*, Chapter 8, 73-76, (ISBN: 9780124114623)

Statement of Authorship

Title of book chapter	The Antiaggregative, Anti-amyloid Properties of Bioactive Polyphenols in the Treatment of Alzheimer's Disease
Publication Status	<input checked="" type="checkbox"/> Published <input type="checkbox"/> Accepted for Publication <input type="checkbox"/> Submitted for Publication <input type="checkbox"/> Unpublished and Unsubmitted work written in manuscript style
Publication Details	Book 'Bioactive Nutraceuticals and Dietary Supplements in Neurological and Brain Disease', 2015, chapter 8, page 73-76.

Principal Author

Name of Principal Author (Candidate)	Sukanya Das			
Contribution to the book chapter	I performed the literature search and wrote the manuscript.			
Overall percentage (%)	90%			
Certification:	This paper reports on original research I conducted during the period of my Higher Degree by Research candidature and is not subject to any obligations or contractual agreements with a third party that would constrain its inclusion in this thesis. I am the primary author of this paper.			
Signature	<table border="1" style="width: 100%;"> <tr> <td style="width: 60%;"></td> <td style="width: 20%;">Date</td> <td style="width: 20%;">17/5/18</td> </tr> </table>		Date	17/5/18
	Date	17/5/18		

Co-Author Contributions

By signing the Statement of Authorship, each author certifies that:

- i. the candidate's stated contribution to the publication is accurate (as detailed above);
- ii. permission is granted for the candidate to include the publication in the thesis; and
- iii. the sum of all co-author contributions is equal to 100% less the candidate's stated contribution.

Name of Co-Author	Scott Smid			
Contribution to the Paper	Provided intellectual engagement and reviewed manuscript.			
Signature	<table border="1" style="width: 100%;"> <tr> <td style="width: 60%;"></td> <td style="width: 20%;">Date</td> <td style="width: 20%;">17/5/2018</td> </tr> </table>		Date	17/5/2018
	Date	17/5/2018		

The Antiaggregative, Antiamyloid Properties of Bioactive Polyphenols in the Treatment of Alzheimer's Disease

Sukanya Das, Scott D. Smid

Discipline of Pharmacology, School of Medical Sciences, Faculty of Health Sciences,
University of Adelaide, Adelaide, Australia

OUTLINE

Introduction	73	Resveratrol	75
(-) Epigallocatechin-3-gallate	74	Conclusion	75
Curcumin	74	References	75

INTRODUCTION

Alzheimer's disease (AD) is a progressive neurodegenerative disorder for which current drug treatments are not considered disease modifying. Therefore, new therapeutic approaches targeting the cause of the disease are desirable. Aggregation of β -amyloid ($A\beta$), the hallmark protein associated with brain plaques in AD, involves a process of oligomerization of $A\beta$ protein monomers (typically 1–40 and 1–42 fragments) to form fibrils and/or protofibrils (Ferreira and Klein, 2011; Newman et al., 2007). $A\beta$ aggregates through intermolecular β sheet formation and elicits neurotoxicity via multiple mechanisms in the brain.

$A\beta$ is produced by unconventional proteolysis of membrane-bound amyloid precursor protein (APP) by β and γ secretase via a process termed the amyloidogenic pathway. Misfolded $A\beta$ monomers have the propensity to self-aggregate and form neurotoxic oligomers and fibrils that are associated with neuronal inflammation, excitotoxicity, and oxidative stress (Canevari et al., 2004). Inflammatory responses can be evoked in

astrocyte and microglial cell populations in the brain (Fioravanzo et al., 2010; Jana et al., 2008), resulting in the generation of inflammatory mediators such as cytokines and reactive oxygen species (ROS; Behl et al., 1994), and oxidative stress is believed to be one of the major contributing factors to neurodegenerative disease progression (Milton et al., 2008).

Understanding the primary neurotoxic mechanisms of $A\beta$ has fuelled research interest towards an array of naturally occurring polyphenolic compounds able to elicit neuroprotection via multiple mechanisms (Smid et al., 2012). Among such compounds, flavonoids are the largest group of polyphenolics that have gained recognition for various health benefits, including neuroprotection (Ramassamy, 2006). Flavonoids have demonstrated activity in reducing oxidative stress and inflammatory responses to $A\beta$. In our discussion, we focus on selected flavonoids with a widely recognized potential as antiamyloid treatments (Rossi et al., 2008), and further focus on the direct interaction of such compounds with the formation or stability of aggregated, toxic $A\beta$ species.

(-) EPIGALLOCATECHIN-3-GALLATE

The green tea polyphenol (-) epigallocatechin-3-gallate (EGCG) has a demonstrable capacity to protect neuronal cells from A β -mediated toxicity *in vitro*. Its direct anti-amyloid interaction occurs via inhibition of the formation of β -amyloid fibrils and disruption of mature fibrils (Ehrnhoefer et al., 2008; Harvey et al., 2011). It can remodel and inactivate preformed fibrils to nontoxic, unstructured, or 'off-target' forms (Bieschke et al., 2010). The remarkable β sheet disruptive capacity of EGCG extends not only to actions at A β but also includes α -synuclein and other amyloidogenic proteins such as plasmodium merozoite surface protein (Chandrashekar et al., 2010, 2011), prion scrapie protein (Rambold et al., 2008), semen-derived enhancer of virus infection (SEVI) amyloid (Hauber et al., 2009), and transthyretin (Miyata et al., 2010).

Experimentally, EGCG has been found to protect neuronal cells against A β and pro-oxidant evoked neurotoxicity. In neuronal cells, EGCG pretreatment significantly reduced A β mediated neurotoxicity *in vitro* (Harvey et al., 2011). Hippocampal neurons pretreated with EGCG when exposed to A β for 48 hours had elevated cell survival and decreased caspase activity (Choi et al., 2001). EGCG also has a protective effect against A β -induced neuronal apoptosis through scavenging ROS (Jung et al., 2007).

Importantly, EGCG promotes remodeling of preformed oligomers of A β that may allow elimination of accumulated toxic A β species during amyloidogenesis. Blocking seeded polymerization is of importance from a therapeutic standpoint, because patients diagnosed with AD are already likely to have accumulated preformed A β fibrils and aggregates. The remodeling of mature fibrils or misfolded proteins such as A β_{1-40} *in vitro* is also dependent on the auto-oxidation of EGCG, and binding with hydrophobic regions of A β plays an important role in EGCG-mediated remodeling. Oxidized EGCG molecules may react with free amines within the amyloid fibril through formation of Schiff base, cross-linking the fibrils that may prevent dissociation and toxicity (Palhano et al., 2013).

In terms of direct anti-amyloid interactions, EGCG can halt fibrillogenesis by hydrogen-bonding with A β , modifying its pathway to allow formation of nontoxic oligomers (Ehrnhoefer et al., 2008). EGCG traps A β and α -synuclein in monomeric and oligomeric forms with a diminished ability to participate in amyloidogenesis. This probably prevents the conformational rearrangements within oligomers required to nucleate aggregation. The unstructured oligomers induced by EGCG are unable to seed further aggregation; instead they are believed to follow an alternative, nontoxic pathway

(Kayed et al., 2003). These oligomers are more susceptible to disaggregate by molecular chaperones or protein-remodeling factors than toxic oligomers.

Studies using molecular dynamics (MD) and molecular mechanics Poisson-Boltzman surface area (MM-PBSA) free energy calculations have shown that nonpolar interactions, mainly van der Waals forces, contributed the major interactions in EGCG/A β_{1-42} binding, whereas polar interactions such as hydrogen bonding were secondary (Liu et al., 2011). NMR investigation of EGCG-induced, nontoxic A β oligomer formation corroborated that EGCG interferes with the aromatic hydrophobic core of A β (Lopez del Amo et al., 2012). Twelve important residues of A β_{1-42} strongly interact with EGCG; all contribute significantly to the EGCG and A β_{1-42} interaction (Liu et al., 2011). Direct binding of EGCG to A β_{1-42} expels water from its surface as a process to elicit conformational changes to A β , and inhibition of the A β_{1-42} conformational transition by EGCG is dose dependent. Similarly, EGCG has a site-specific interaction with SEVI amyloid precursor peptide PAP₂₄₈₋₂₈₆ monomers. It interacts with two side chain regions of primarily charged residues, particularly lysine, by the pH-dependent Schiff-base, allowing formation of a tightly bound complex (Popovych et al., 2012).

An atomistic replica exchange molecular dynamics (REMD) study of A β_{1-42} secondary structure and its conformational changes due to EGCG found that binding with small molecule EGCG causes remarkable changes in the A β_{1-42} dimer in an aqueous solution (Zhang et al., 2013). In the presence of EGCG, A β secondary structures demonstrated a reduction in β sheet content, increased coil and α -helix content, and reduced interchain and intrachain content. Thermodynamic analysis of the molecular interactions between A β and EGCG revealed that hydrogen bonding occurred mainly in regions 1–16 and hydrophobic bonding in regions 17–42 of A β (Shi-Hui Wang, 2010, 2012).

However, EGCG binds to unfolded proteins in a non-selective fashion as well, which may have unanticipated consequences in therapeutic settings. For example, EGCG interfered with proteins involved in mitigating cell damage, such as the normal cellular prion protein PrP(C), rendering cells susceptible to oxidative stress (Rambold et al., 2008).

CURCUMIN

The natural polyphenol curcumin, (bis-4-hydroxy-3-methoxyphenyl)-1,6-diene-3,5-dione, is present in the yellow curry spice turmeric derived from *Curcuma longa*. Over the last decade, several studies have demonstrated that it possesses anti-amyloid and anti-aggregative

properties relevant to AD pathogenesis and progression. Clinical trials with curcumin are ongoing, but so far they have demonstrated limitations in curcumin bioavailability and efficacy in regards to improvements in cognitive function (Ringman et al., 2012). Nonetheless, animal studies have shown that both curcumin and turmeric extract are effective at lowering A β burden in AD transgenic mice models. Curcumin is able to label plaques, block toxicity of oligomers, and significantly reduce amyloid levels following oral dosing (Begum et al., 2008; Shytle et al., 2012). High level *ab initio* molecular modeling of curcumin reveals that the molecule possesses unique charge and bonding characteristics to enable penetration through the blood–brain barrier and binding to A β protein (Balasubramanian, 2006).

Overall, curcumin's direct antiaggregative capacity can be attributed to both inhibition of A β aggregation and disaggregation of preformed amyloid fibrils. Curcumin can bind and inhibit fibril formation, including full-length A β sequence and A β ₁₋₂₈, A β ₁₂₋₂₈, and A β ₂₅₋₃₅ fragments. However, curcumin's effects did not depend on A β sequence but were instead dependent on fibril-related conformation. Despite the common overlapping sequence of these fibrillogenic peptides, amino acids 25–28, curcumin cannot bind nonaggregating peptides that span this A β ₁₇₋₂₈ region (Yang et al., 2005). Multi-scale computational methods have demonstrated that, when compared, both EGCG and curcumin preferentially interact with the central hydrophobic core (CHC) region of the A β ₁₇₋₄₂ trimer (Chebaro et al., 2012).

RESVERATROL

The phytoalexin stilbenoid resveratrol (3,5,4'-trihydroxy-*trans*-stilbene) is commonly found in grapes and red wines and has neuroprotective properties against A β -evoked toxicity (Richard et al., 2011). Resveratrol dose-dependently inhibits A β ₁₋₄₂ fibril formation and neurotoxicity, with part of its activity attributed to directly interfering with A β aggregation and oligomer conformation (Feng et al., 2009), including remodeling to off-target conformations (Ladiwala et al., 2010). Structural analogues of resveratrol can more potently inhibit A β accumulation in cells compared to resveratrol (Vingtdeux et al., 2011). Modelling of resveratrol binding to the A β ₁₇₋₄₂ model trimer revealed varying binding sites compared to EGCG and curcumin; however, a similar affinity for the CHC region was evidenced (Chebaro et al., 2012). Extensive replica exchange molecular dynamics simulations also revealed that resveratrol blocks the lateral growth of single-layered β sheet oligomer in human IAPP segments 22–27, which contributes to a reduction in aggregation levels (Jiang et al., 2011).

CONCLUSION

Among the numerous primary antioxidants studied for their potential neuroprotective abilities, EGCG, curcumin, and resveratrol have been among the most widely studied natural product compounds for further consideration as nutraceutical-based therapeutic treatments for AD or other amyloidoses. Among these three examples of dietary polyphenols, EGCG has demonstrated diverse properties in relation to binding with A β oligomers, disrupting mature A β fibril formation, or otherwise modulating the amyloidogenic processing pathway from APP. Of the three, EGCG possesses significant development potential for consideration as a neuroprotective therapeutic option in clinical trials in AD. Notwithstanding the core clinical challenges of AD-modifying therapies generally, EGCG still has significant limitations to overcome (e.g., bioavailability) before it can be considered a viable therapeutic option (Mereles and Hunstein, 2011).

References

- Balasubramanian, K., 2006. Molecular orbital basis for yellow curry spice curcumin's prevention of Alzheimer's disease. *J. Agric. Food Chem.* 54, 3512–3520.
- Begum, A.N., Jones, M.R., Lim, G.P., Morihara, T., Kim, P., Heath, D.D., Rock, C.L., Pruitt, M.A., Yang, F., Hudspeth, B., Hu, S., Faull, K.F., Teter, B., Cole, G.M., Frautschy, S.A., 2008. Curcumin structure-function, bioavailability, and efficacy in models of neuroinflammation and Alzheimer's disease. *J. Pharmacol. Exp. Ther.* 326, 196–208.
- Behl, C., Davis, J.B., Lesley, R., Schuber, T.D., 1994. Hydrogen peroxide mediates amyloid β protein toxicity. *Cell* 77, 817–827.
- Bieschke, J., Russ, J., Friedrich, R.P., Ehrnhoefer, D.E., Wobst, H., Neugebauer, K., Wanker, E.E., 2010. EGCG remodels mature alpha-synuclein and amyloid-beta fibrils and reduces cellular toxicity. *Proc. Natl. Acad. Sci. U S A* 107, 7710–7715.
- Canevari, L., Abramov, A.Y., DuChen, M.R., 2004. Toxicity of amyloid β peptide: tales of calcium, mitochondria, and oxidative stress. *Neurochem. Res.* 29, 637–650.
- Chandrashekar, I.R., Adda, C.G., Macrauld, C.A., Anders, R.F., Norton, R.S., 2010. Inhibition by flavonoids of amyloid-like fibril formation by plasmodium falciparum merozoite surface protein 2. *Biochemistry* 49, 5899–5908.
- Chandrashekar, I.R., Adda, C.G., Macrauld, C.A., Anders, R.F., Norton, R.S., 2011. EGCG disaggregates amyloid-like fibrils formed by plasmodium falciparum merozoite surface protein 2. *Arch. Biochem. Biophys.* 513, 153–157.
- Chebaro, Y., Jiang, P., Zang, T., Mu, Y., Nguyen, P.H., Mousseau, N., Derreumaux, P., 2012. Structures of abeta 17-42 trimers in isolation and with five small-molecule drugs using a hierarchical computational procedure. *J. Phys. Chem. B.* 116, 8412–8422.
- Choi, Y.T., Jung, C.H., Lee, S.R., Bae, J.H., Baek, W.K., Suh, M.H., Park, J., Park, C.W., Suh, S.I., 2001. The green tea polyphenol (-)-epigallocatechin gallate attenuates beta-amyloid-induced neurotoxicity in cultured hippocampal neurons. *Life Sci.* 70, 603–614.
- Ehrnhoefer, D.E., Bieschke, J., Boeddrich, A., Herbst, M., Masino, L., Lurz, R., Engemann, S., Pastore, A., Wanker, E.E., 2008. EGCG redirects amyloidogenic polypeptides into unstructured, off-pathway oligomers. *Nat. Struct. Mol. Biol.* 15, 558–566.

- Feng, Y., Wang, X.P., Yang, S.G., Wang, Y.J., Zhang, X., Du, X.T., Sun, X.X., Zhao, M., Huang, L., Liu, R.T., 2009. Resveratrol inhibits beta-amyloid oligomeric cytotoxicity but does not prevent oligomer formation. *Neurotoxicology* 30, 986–995.
- Ferreira, S.T., Klein, W.L., 2011. The abeta oligomer hypothesis for synapse failure and memory loss in Alzheimer's disease. *Neurobiol. Learn. Mem.* 96, 529–543.
- Fioravanzo, L., Venturini, M., Di Liddo, R., Marchi, F., Grandi, C., Parnigotto, P.P., Folin, M., 2010. Involvement of rat hippocampal astrocytes in beta-amyloid-induced angiogenesis and neuroinflammation. *Curr. Alzheimer. Res.* 7, 591–601.
- Harvey, B.S., Musgrave, I.F., Ohlsson, K.S., Fransson, Å., Smid, S.D., 2011. The green tea polyphenol (–)-epigallocatechin-3-gallate inhibits amyloid- β evoked fibril formation and neuronal cell death in vitro. *Food Chemistry* 129, 1729–1736.
- Hauber, I., Hohenberg, H., Holstermann, B., Hunstein, W., Hauber, J., 2009. The main green tea polyphenol epigallocatechin-3-gallate counteracts semen-mediated enhancement of HIV infection. *Proc. Natl. Acad. Sci. U S A* 106, 9033–9038.
- Jana, M., Palencia, C.A., Pahan, K., 2008. Fibrillar amyloid-beta peptides activate microglia via TLR2: implications for Alzheimer's disease. *J. Immunol.* 181, 7254–7262.
- Jiang, P., Li, W., Shea, J.E., Mu, Y., 2011. Resveratrol inhibits the formation of multiple-layered beta-sheet oligomers of the human islet amyloid polypeptide segment 22–27. *Biophys. J.* 100, 1550–1558.
- Jung, J.-Y., Mo, H.-C., Yang, K.-H., Jeong, Y.-J., Yoo, H.-G., Choi, N.-K., Oh, W.-M., Oh, H.-K., Kim, S.-H., Lee, J.-H., Kim, H.-J., Kim, W.-J., 2007. Inhibition by epigallocatechin gallate of CoCl_2 -induced apoptosis in rat PC12 cells. *Life Sci.* 80, 1355–1363.
- Kayed, R., Head, E., Thompson, J.L., McIntire, T.M., Milton, S.C., Cotman, C.W., Glabe, C.G., 2003. Common structure of soluble amyloid oligomers implies common mechanism of pathogenesis. *Science* 300, 486–489.
- Ladiwala, A.R., Lin, J.C., Bale, S.S., Marcelino-Cruz, A.M., Bhattacharya, M., Dordick, J.S., Tessier, P.M., 2010. Resveratrol selectively remodels soluble oligomers and fibrils of amyloid A β into off-pathway conformers. *J. Biol. Chem.* 285, 24228–24237.
- Liu, F.F., Dong, X.Y., He, L., Middelberg, A.P., Sun, Y., 2011. Molecular insight into conformational transition of amyloid beta-peptide 42 inhibited by (–)-epigallocatechin-3-gallate probed by molecular simulations. *J. Phys. Chem. B.* 115, 11879–11887.
- Lopez Del Amo, J.M., Fink, U., Dasari, M., Grelle, G., Wanker, E.E., Bieschke, J., Reif, B., 2012. Structural properties of EGCG-induced, nontoxic Alzheimer's disease abeta oligomers. *J. Mol. Biol.* 421, 517–524.
- Mereles, D., Hunstein, W., 2011. Epigallocatechin-3-gallate (EGCG) for clinical trials: more pitfalls than promises? *Int. J. Mol. Sci.* 12, 5592–5603.
- Milton, R.H., Abeti, R., Averaimo, S., Debiasi, S., Vitellaro, L., Jiang, L., Curmi, P.M., Breit, S.N., Duchon, M.R., Mazzanti, M., 2008. CLIC1 function is required for beta-amyloid-induced generation of reactive oxygen species by microglia. *J. Neurosci.* 28, 11488–11499.
- Miyata, M., Sato, T., Kugimiya, M., Sho, M., Nakamura, T., Ikemizu, S., Chirifu, M., Mizuguchi, M., Nabeshima, Y., Suwa, Y., Morioka, H., Arimori, T., Suico, M.A., Shuto, T., Sako, Y., Momohara, M., Koga, T., Morino-Koga, S., Yamagata, Y., Kai, H., 2010. The crystal structure of the green tea polyphenol (–)-epigallocatechin gallate-transferrin complex reveals a novel binding site distinct from the thyroxine binding site. *Biochemistry* 49, 6104–6114.
- Newman, M., Musgrave, I.F., Lardelli, M., 2007. Alzheimer disease: amyloidogenesis, the presenilins and animal models. *Biochimica. et Biophysica. Acta.* 1772, 285–297.
- Palhano, F.L., Lee, J., Grimster, N.P., Kelly, J.W., 2013. Toward the molecular mechanism(s) by which EGCG treatment remodels mature amyloid fibrils. *J. Am. Chem. Soc.* 135, 7503–7510.
- Popovych, N., Brender, J.R., Soong, R., Vivekanandan, S., Hartman, K., Basrur, V., MacDonald, P.M., Ramamoorthy, A., 2012. Site specific interaction of the polyphenol EGCG with the SEVI amyloid precursor peptide PAP(248–286). *J. Phys. Chem. B.* 116, 3650–3658.
- Ramassamy, C., 2006. Emerging role of polyphenolic compounds in the treatment of neurodegenerative diseases: a review of their intracellular targets. *Eur. J. Pharmacol.* 545, 51–64.
- Rambold, A.S., Miesbauer, M., Olschewski, D., Seidel, R., Riemer, C., Smale, L., Brumm, L., Levy, M., Gazit, E., Oesterheld, D., Baier, M., Becker, C.F., Engelhard, M., Winklhofer, K.F., Tatzelt, J., 2008. Green tea extracts interfere with the stress-protective activity of PrP and the formation of PrP. *J. Neurochem.* 107, 218–229.
- Richard, T., Pawlus, A.D., Iglesias, M.L., Pedrot, E., Waffo-Teguo, P., Merillon, J.M., Monti, J.P., 2011. Neuroprotective properties of resveratrol and derivatives. *Ann. N. Y. Acad. Sci.* 1215, 103–108.
- Ringman, J.M., Frautschy, S.A., Teng, E., Begum, A.N., Bardens, J., Beigi, M., Gyls, K.H., Badmaev, V., Heath, D.D., Apostolova, L.G., Porter, V., Vanek, Z., Marshall, G.A., Hellemann, G., Sugar, C., Masterman, D.L., Montine, T.J., Cummings, J.L., Cole, G.M., 2012. Oral curcumin for Alzheimer's disease: tolerability and efficacy in a 24-week randomized, double blind, placebo-controlled study. *Alzheimers Res. Ther.* 4, 43.
- Rossi, L., Mazzitelli, S., Arciello, M., Capo, C.R., Rotilio, G., 2008. Benefits from dietary polyphenols for brain aging and Alzheimer's disease. *Neurochem. Res.* 33, 2390–2400.
- Shi-Hui Wang, F.-F.L., Dong, Xiao-Yan, Sun, Yan, 2010. Thermodynamic analysis of the molecular interactions between amyloid β -peptide 42 and (–)-epigallocatechin-3-gallate. *J. Phys. Chem.* 114, 11576–11583.
- Shi-Hui Wang, X.-Y.D., Sun, Yan, 2012. Thermodynamic analysis of the molecular interactions between amyloid β -protein fragments and (–)-epigallocatechin-3-gallate. *J. Phys. Chem. B.* 116, 5803–5809.
- Shytle, R.D., Tan, J., Bickford, P.C., Rezai-Zadeh, K., Hou, L., Zeng, J., Sanberg, P.R., Sanberg, C.D., Alberte, R.S., Fink, R.C., Roschek Jr, B., 2012. Optimized turmeric extract reduces beta-amyloid and phosphorylated tau protein burden in Alzheimer's transgenic mice. *Curr. Alzheimer. Res.* 9, 500–506.
- Smid, S.D., Maag, J.L., Musgrave, I.F., 2012. Dietary polyphenol-derived protection against neurotoxic beta-amyloid protein: from molecular to clinical. *Food Funct.* 3, 1242–1250.
- Vingtdeux, V., Chandakkar, P., Zhao, H., D'Abramo, C., Davies, P., Marambaud, P., 2011. Novel synthetic small-molecule activators of AMPK as enhancers of autophagy and amyloid-beta peptide degradation. *FASEB. J.* 25, 219–231.
- Yang, F., Lim, G.P., Begum, A.N., Ubada, O.J., Simmons, M.R., Ambegaokar, S.S., Chen, P.P., Kaye, R., Glabe, C.G., Frautschy, S.A., Cole, G.M., 2005. Curcumin inhibits formation of amyloid beta oligomers and fibrils, binds plaques, and reduces amyloid in vivo. *J. Biol. Chem.* 280, 5892–5901.
- Zhang, T., Zhang, J., Derreumaux, P., Mu, Y., 2013. Molecular mechanism of the inhibition of EGCG on the Alzheimer Abeta (1–42) dimer. *J. Phys. Chem. B.* 117, 3993–4002.

1.6.5 Clinical application of natural products as amyloidogenic protein aggregation inhibitors

The demonstrated preclinical efficacy of the noted amyloidogenic aggregation inhibitor natural molecules such as EGCG has not translated into efficacy in clinical studies due to poor bioavailability (Cascella, Bimonte et al. 2017). Other polyphenols such as curcumin and resveratrol, have been used in AD clinical trials where they too have lacked efficacy (Mecocci and Polidori 2012). Additionally, AD clinical trials investigating the effect of standardised Ginkgo biloba extract known as EGb761 have not been promising (Sandrine, Pierre-Jean et al. 2008). EGCG has also been studied for inhibition of α S aggregation that may result in delayed progression of disability in patients with multiple system atrophy (MSA), another α S aggregation-related disease (ClinicalTrials.gov Identifier: NCT02008721 (Levin, Maaß et al. 2016). Clinical trials involving amyloidogenic protein aggregation inhibitors have consistently fallen short of benchmarks for efficacy. Rational design of new small molecules inspired from natural products and their further design for desirable drug-like properties may improve clinical translation of small molecular amyloidogenic aggregation inhibitors.

1.7 Search for new inhibitors of amyloidogenic aggregation from synthetic origin

The search for amyloidogenic protein aggregation inhibitors outside natural origin involves identification of novel synthetic compounds based on standard drug discovery methods. Fragment-based drug discovery (FBDD) is an established and alternative approach to traditional high throughput screening (HTS) for identifying novel small molecular structures for a drug target (Shuker, Hajduk et al. 1996, Erlanson 2012, Murray, Verdonk et al. 2012). This structure-based method has made a significant contribution in successful development of anti-A β drug classes such as BACE1 inhibitors (Stamford and Strickland 2013). This method

requires a fragment library and employs screening methods to detect binders for further development. Computer-aided screening methods such as ‘virtual screening’ is also widely used for screening a compound library. Nonetheless, screening studies for compounds bearing a fragment of interest, such as heterocyclic rings targeted to A β are limited. In this thesis (Chapter 3), a virtual screening study has been employed to identify compounds bearing fragments of interest that can directly interact with A β .

1.8 Biochemical and cell-based assays coupled with molecular modelling for identifying new amyloid binders

1.8.1 Monitoring amyloidogenic protein aggregation by thioflavin T assay

Thioflavin T (ThT) is a dye that specifically binds to amyloid structures of protein and gives fluorescence output at an approximate wavelength of 482 nm when excited at 450 nm (Naiki, Higuchi et al. 1989). Chemically, it is a benzothiazole salt where the benzothiazole group is connected to a dimethylammonobenzene group by a non-planar conformation at ground state. Upon excitation, ThT undergoes twisted internal charge transfer as a molecular rotor that accounts for its fluorescence output (Stsiapura, Maskevich et al. 2007). When ThT binds to the amyloid structures of a protein, this intramolecular rotation cannot take place due to steric hinderance and produces high fluorescence output which is proportional to the amount of amyloid protein present in solution (Ban, Hamada et al. 2003, Stsiapura, Maskevich et al. 2007). The ThT assay has been considered a standard method for determining amyloid aggregation and fibrillisation kinetics *in vitro*. Furthermore, the ThT assay can also shed light on how the presence of a compound impacts the aggregation of an amyloid protein, whereby decreased fluorescence may be indicative of inhibition of amyloid aggregation. The result of this assay is analysed by ‘Area under the curve’ (AUC) analysis. Following analysis, the AUC

graph is expressed as X-axis (time) value multiplied by Y-axis (relative fluorescence unit or RFU in arbitrary unit or AU) value. This statistical analysis provides information about the significance of an aggregation inhibitor. Hence, the ThT assay can be useful in comparing the anti-aggregatory effects of various compounds towards A β and α S. In the present study, a kinetic ThT assay for both A β and α SA53T aggregation and the effect of a diverse group of molecules have been performed to understand their potential anti-aggregative effects.

1.8.2 Visualisation of amyloidogenic aggregation by electron microscopy

Despite the advantage of monitoring amyloidogenic aggregation by the ThT assay, there are some inherent limitations of this method. The assay can be susceptible to fluorescence quenching by the presence of some flavonoids owing to the reactivity of the oxidised-flavonoid quinone formed (Coelho-Cerqueira, Pinheiro et al. 2014). This quenching can present false positive results for inhibition. Additionally, some compounds can interact with ThT or compete with the binding site on the amyloid protein which can lead to erroneous results (Hudson, Ecroyd et al. 2009). Therefore, visualisation of amyloid aggregates and fibrils by electron microscopy, along with the ThT assay, is advantageous for a more rigorous determination of an anti-aggregative effect of a compound. In this regard, transmission electron microscopy (TEM) can uncover valuable information about the actual effect of each compound on amyloid aggregation, fibril formation and morphology (Petkova, Leapman et al. 2005). In the present study, visualisation of A β and α SA53T aggregates and fibrils has been carried out by TEM in addition to the ThT assay.

1.8.3 Probing the structural conversion of α SA53T protein by Ion mobility-mass spectrometry

Ion mobility-mass spectrometry (IM-MS) is a powerful tool to investigate the early structural conversion of amyloidogenic proteins. Since amyloidogenic proteins such as α S exhibit structural polymorphism during the early aggregation process and form a heterogeneous population, sensitive biochemical techniques capable of monitoring all the transient species would be beneficial. IM-MS methods combining ion mobility with mass spectrometry are particularly informative, as it can study the conformation of each charge state of a protein and measure their cross sections (Jurneczko and Barran 2011). Additionally, it can retain the weak non-covalent interactions in gas phase between a protein and its ligand, which makes it suitable for studying the effect of various compounds on α SA53T (Sarni-Manchado and Cheynier 2002).

It is well known that α S belongs to the class of intrinsically disordered proteins (IDP) that lack a detectable secondary structure (Eliezer, Kutluay et al. 2001). Given the advantages of mass spectrometry and IMMS in particular in being able to study the structural changes of IDP, it would be suitable to study the change of the structural conformation of α S from interaction with a ligand that might inhibit amyloidogenic aggregation, and is employed in Chapter 4 of this thesis (Leavell, Gaucher et al. 2002, Touboul, Maillard et al. 2009, Frimpong, Abzalimov et al. 2010, Jurneczko, Cruickshank et al. 2012).

1.8.4 Study of neuronal cell viability using the MTT assay for neuroprotection

As mentioned earlier, both A β and α S or its pathological mutant α SA53T can evoke damage to neuronal cells by oxidative stress, inflammatory responses and other perturbations. Mitochondrial dysfunction is a major driver of the neurodegeneration observed in the

neurotoxicity of A β and α S aggregates. As a result, measuring mitochondrial activity as an indicator of viable cells is an established method to study amyloid toxicity *in vitro*. Living cells with active mitochondrial function can reduce the MTT dye, which is a yellow tetrazole salt reduced by cellular oxidoreductase enzymes to give a purple colour. The intensity of the produced purple colour is correlated with the number of viable cells under experimental conditions. The MTT assay is thus a standard colorimetric assay that is used to study the neurotoxicity exerted by A β and α S towards cultured neuronal cells and the subsequent neuroprotection by a compound. In this study, rat phaeochromocytoma (PC-12) cells have been used to study the neuroprotective effect of various compounds as well as to study the oxidative stress and lipid peroxidation arising from prooxidant *tert*-butyl hydrogen peroxide (*t*-bhp) exposure.

1.8.5 Studying the interaction of molecules with A β and α SA53T by molecular docking

Computational simulation methods such as molecular docking provide valuable information regarding small molecule or ligand prospective interactions with a target macromolecule or protein. It is a key tool that enables the interaction study and comparison of a large number of ligands towards a target in a very short time and relatively inexpensively. The goal of docking is to predict the optimal binding solutions of a protein-ligand complex in a three-dimensional representation that can be comparable to other structural biological findings such as X-ray crystallography. All docking methods employ a scoring function in order to rank its predicted binding solutions. The scoring function considers the available knowledge about the ligand and the target. In this study, molecular docking methods have been used extensively to study the interaction of each compound with different A β and α SA53T structures. Moreover, docking has been used here for a ligand-based drug design approach for designing novel amyloid

binding ligands. The scoring function used in the docking mode presented in this study is termed as piecewise linear potential or PLANTS_{PLP} scoring function (Korb, Stützle et al. 2009).

Due to its efficiency, molecular docking approaches have been employed for virtual screening databases to find novel fragments or ligands (Meng, Zhang et al. 2011, Grinter and Zou 2014). Nevertheless, the predictability of the scoring function and benchmarking in docking methodology play an important role in the success of docking, as well as in virtual screening. Hence, combining docking with an experimental ligand binding assay allows a platform of testable predictions. In this present study, a structure-based virtual screening study using both molecular docking and experimental testing has been undertaken to validate the docking predictions. Subsequently, the docking insights have been used to design novel ligands following ligand-based drug design methods.

1.9 Research hypothesis:

The main hypothesis of this thesis is to test whether the *in silico* molecular modelling predictions about favourable binding profile of a small molecule would lead to inhibition or alteration of aggregation *in vitro*. The molecular docking performed here in this thesis provide an inexpensive, fast and computationally guided ligand selection or screening tool as opposed to experimental throughput screening. Therefore, it is of great value to validate the reliability of molecular docking simulations for identifying new small molecular binder of amyloidogenic proteins. Chapter 3 in particular, has tested this hypothesis where the small molecules for *in vitro* experiments have been selected based on their docking profiles. Chapter 2, 4 and 5 have

partially tested the hypothesis as the molecular docking prediction has been in agreement with the *in vitro* results.

1.10 Research Aims: Identification, characterization and design of molecules for dual inhibition of A β and α S aggregation and toxicity

Studies investigating inhibition of amyloidogenic protein aggregation such as A β and α S by various molecules provide insight into the chemical structures that might be useful in drug design targeting amyloid proteins. However, compounds that are well-known for inhibition of A β and α S aggregation *in vitro* have generally not been effective in clinical trials (Mereles and Hunstein 2011). Despite serious research endeavours, there seems to be inherent limitations in using some previously identified natural molecules for rational drug-design (Baell 2016, Nelson, Dahlin et al. 2017). Therefore, identification of new natural molecules that are structurally distinct from EGCG or curcumin and can suppress pathogenic amyloid aggregation would be important for designing therapeutics targeting both AD and PD. Additionally, identification of new synthetic molecules that can work as effectively as the natural molecules towards mitigating A β and α S aggregation and toxicity would be valuable for drug-discovery, since synthetic molecules possess certain advantages in the early drug candidate selection. Finally, the design of novel ligands predicted to have superior binding towards amyloidogenic proteins would be valuable for both novel therapeutics or diagnostic imaging after further structure optimization for selective binding to an amyloid target.

Research aims addressed in Publication 2 (Chapter 2)

1. To identify new bioactive polyphenols outside the flavonoid group that can be a potent inhibitor of A β ₁₋₄₂ aggregation, alter fibril morphology and protect neuronal cells from A β ₁₋₄₂ mediated neurotoxicity.
2. To investigate the effect of the neolignan honokiol on A β ₁₋₄₂ aggregation and fibril morphology in comparison with the characterised flavonoids myricetin and luteolin.
3. To determine whether punicalagin, the antioxidant ellagitannin in pomegranate, can potently inhibit A β ₁₋₄₂ aggregation and alter fibril morphology in comparison with myricetin, luteolin and honokiol.
4. To investigate if the anti-aggregative action of honokiol and punicalagin is correlated with neuroprotection from A β ₁₋₄₂ toxicity in neuronal (PC-12) cells in comparison with the neuroprotection conferred by myricetin and luteolin.
5. To study the binding interaction of honokiol and punicalagin to different A β ₁₋₄₂ conformations in comparison with select flavonoids.

Research aims addressed in Publication 3 (Chapter 3)

1. To identify new binders of A β ₁₋₄₂ through virtual screening of an open source chemical database, filtered for a five-membered heterocycle (FMH) ring with only nitrogen or nitrogen and oxygen as the heteroatom and with no exocyclic C=O/S/N group.
2. Test *in vitro* virtual screening ‘hit’ compounds for translating whether their low docking score with A β ₁₋₄₂ correlates to inhibition of A β ₁₋₄₂ aggregation and alteration of fibril morphology.

3. To study the concentration-dependent toxicity profile of each selected 'hit' compound in cultured PC-12 cells.
4. Based on the toxicity profile, to further test the non-toxic compounds for neuroprotection of PC-12 cells from A β ₁₋₄₂ mediated toxicity.
5. To undertake a comparative analysis of the proposed binding interactions according to docking of selected 'hit' compounds to identify a novel molecular scaffold that can bind to A β ₁₋₄₂ to inhibit toxic amyloidogenic aggregation.

Research aims addressed in Publication 4 (Chapter 4)

1. To explore the effects of various molecular structures identified previously on α SA53T early conformational change leading to amyloidogenic aggregation, aggregate or fibril morphology and exogenous toxicity to PC-12 cells.
2. To examine the effect of different structures for inhibition of α SA53T amyloidogenic aggregation:
 - a. Whether only B-ring trihydroxylation as occurs in the semi-synthetic flavone 2-D08 can inhibit α SA53T toxic amyloidogenic aggregation in comparison to myricetin.
 - b. Comparison of effectiveness of dihydroxylation in both the A and B-ring with myricetin or 2-D08
3. To investigate whether the small neolignan honokiol can inhibit α SA53T amyloidogenic aggregation and neurotoxicity in comparison with flavones.

4. To examine the effect of the bulky and extensively hydroxylated ellagitannin molecule punicalagin on α SA53T amyloidogenic aggregation and neurotoxicity in comparison with select flavones and honokiol.
5. Exploring the effect of two synthetic compounds bearing a novel molecular scaffold on α SA53T amyloidogenic aggregation and neurotoxicity in comparison with natural flavones, neolignan and ellagitannin.

Research aims addressed in Chapter 5

1. To test the effect of magnolol, another neolignan that is structurally similar to honokiol, on both A β and α SA53T amyloidogenic protein aggregation, fibril morphology and neuroprotection.
2. To characterize the anti-aggregative properties of a structurally diverse set of bioactives including two diterpenes, cryptotanshinone and tanshinone I, the alkaloid neferine, chalcone phloretin and flavone galangin on A β and α SA53T.

Research aims addressed in Chapter 6

1. To utilise the neolignan pharmacophore for an *in-silico* ligand-based drug design approach to design improved novel amyloid binders, specifically for A β and α S.
2. To incorporate the novel molecular scaffold identified from virtual screening into the novel ligand design.

a. To design a novel 'core' molecular structure/fragment and study how other commonly used five membered heterocycle (FMH) rings affect the binding to A β and α SA53T.

Chapter 2: Bioactive polyphenol interactions with β amyloid: a comparison of binding modelling, effects on fibril and aggregate formation and neuroprotective capacity

Sukanya Das, Lina Stark, Ian F. Musgrave, Tara Pukala and Scott D. Smid (2016), 'Bioactive polyphenol interactions with β amyloid: a comparison of binding modelling, effects on fibril and aggregate formation and neuroprotective capacity', *Food & Function*, 7, 1138 – 1146.

Reprinted as per Royal Society of Chemistry authors deposition and sharing rights as per the licence to publish, 2018.

This study was focused on identifying new naturally occurring bioactive polyphenols that can potently inhibit $A\beta_{1-42}$ amyloidogenic aggregation and alter $A\beta_{1-42}$ fibril or aggregate morphology. The other aim of this study was to determine whether the inhibition of $A\beta_{1-42}$ aggregation results in neuroprotection from $A\beta_{1-42}$ mediated toxicity *in vitro*. Additionally, this study was focused on comparing the effects of different structural features present in natural polyphenolic compounds on $A\beta_{1-42}$ amyloidogenic aggregation and neurotoxicity. A neolignan polyphenol, honokiol and a bulky ellagitannin polyphenol, punicalagin were studied and compared with the flavones myricetin and luteolin. Both flavones contain the catechol (vicinal hydroxyl) group in their B-ring that is considered as a favourable structural feature in flavonoids for binding $A\beta$ to mitigate toxicity (Sato, Murakami et al. 2013). Myricetin contains a trihydroxyl and luteolin contains a dihydroxyl group in their flavone B-ring. Myricetin was previously shown to alter the $A\beta$ conformation that reduces toxicity (Shimmyo, Kihara et al.

2008), while luteolin was known to inhibit A β aggregation and act as a neuroprotectant against A β toxicity (Cheng, Hsieh et al. 2010, Churches, Caine et al. 2014). The comparative analysis of honokiol and punicalagin with these two flavones addressed the similarity or differences in the effect of neolignan biphenyl and ellagitannin structures on A β_{1-42} aggregation, as compared to catechol-type flavones.

In addition, the other aim addressed in this study was the comparison of these four polyphenols and their proposed binding interaction with model A β_{1-42} monomeric and oligomeric structures. As discussed earlier, the A β monomeric structures shown in this figure are very unlikely to be the conformation of the peptide in water (which is unstructured) but rather what it adopts in a membrane-like environment. A β interacts readily with cell membranes and it may elicit its toxic effects by forming pores in the membrane leading to cell death, so the structures of the α -helical peptide with the bioactives bound has relevance. This direct binding comparison facilitated our understanding of different structural features participating in proposed binding interactions according to docking models. The results indicated that honokiol has a higher probability of sterically interacting with the model A β_{1-42} targets and therefore was used in subsequent studies (Chapter 6) as a template for the design of an effective amyloid binding small molecule.

Overall, this study identified the potent antiaggregatory property of honokiol along with its ability to mitigate A β_{1-42} -induced toxicity in neuronal PC-12 cells. Additionally, this study identified punicalagin as a potent inhibitor of A β_{1-42} aggregation that can also protect PC-12 cells from A β_{1-42} toxicity. The anti-amyloid activity of honokiol and punicalagin is comparable to the noted flavone anti-amyloid bioactives, myricetin and luteolin.

Statement of Authorship

Title of Paper	Bioactive polyphenol interactions with β amyloid: a comparison of binding modelling, effects on fibril and aggregate formation and neuroprotective capacity.
Publication Status	<input checked="" type="checkbox"/> Published <input type="checkbox"/> Accepted for Publication <input type="checkbox"/> Submitted for Publication <input type="checkbox"/> Unpublished and Unsubmitted work written in manuscript style
Publication Details	Journal 'Food & Function', 2016, vol. 7, page 1138-1146.

Principal Author

Name of Principal Author (Candidate)	Sukanya Das		
Contribution to the Paper	I performed all the modelling works and the antiaggregative assays. I also performed the electron microscopic studies of three bioactives and cell viability assays of two bioactives. The manuscript was jointly written by me and my primary supervisor Dr. Scott Smid.		
Overall percentage (%)	80%		
Certification:	This paper reports on original research I conducted during the period of my Higher Degree by Research candidature and is not subject to any obligations or contractual agreements with a third party that would constrain its inclusion in this thesis. I am the primary author of this paper.		
Signature		Date	17/5/18

Co-Author Contributions

By signing the Statement of Authorship, each author certifies that:

- i. the candidate's stated contribution to the publication is accurate (as detailed above);
- ii. permission is granted for the candidate to include the publication in the thesis; and
- iii. the sum of all co-author contributions is equal to 100% less the candidate's stated contribution.

Name of Co-Author	Scott Smid		
Contribution to the Paper	I jointly compiled this manuscript together with the primary author, and provided intellectual engagement in the conceptual and experimental design of studies and interpretation. I assisted Sukanya with manuscript preparation.		
Signature		Date	17/05/2018

Name of Co-Author	Lina Stark		
Contribution to the Paper	Lina conducted a portion of the cell viability studies (2 compounds) while here on exchange studies over a semester equivalent.		
Signature		Date	18/05/2018

Name of Co-Author	Ian Musgrave		
Contribution to the Paper	Intellectual input in study design		
Signature		Date	17/5/18

Name of Co-Author	Tara Pukala		
Contribution to the Paper	Reviewed manuscript in preparation		
Signature		Date	21/5/2018



Cite this: *Food Funct.*, 2016, 7, 1138

Bioactive polyphenol interactions with β amyloid: a comparison of binding modelling, effects on fibril and aggregate formation and neuroprotective capacity

Sukanya Das,^a Lina Stark,^b Ian F. Musgrave,^a Tara Pukala^c and Scott D. Smid^{*a}

In this study we compared the effects of a diverse set of natural polyphenolics ligands on *in silico* interactive modelling, *in vitro* anti-aggregative properties and neuronal toxicity of β amyloid. The β amyloid-binding characteristics of optimised structural conformations of polyphenols with ascribed neuroprotective actions including punicalagin, myricetin, luteolin and honokiol were determined *in silico*. Thioflavin T and transmission electron microscopy were used to assess *in vitro* inhibitory effects of these polyphenols on $A\beta_{1-42}$ fibril and aggregation formation. Phaeochromocytoma (PC12) cells were exposed to $A\beta_{1-42}$, alone and in combination with test concentrations of each polyphenol (100 μ M) and viability measured using MTT assay. $A\beta_{1-42}$ evoked a concentration-dependent loss of cell viability in PC12 cells, in which all four polyphenols demonstrated significant inhibition of neurotoxicity. While all compounds variably altered the morphology of $A\beta$ aggregation, the flavonoids luteolin and myricetin and the lignan honokiol all bound in a similar hydrophobic region of the amyloid pentamer and exerted the most pronounced inhibition of $A\beta_{1-42}$ aggregation. Each of the polyphenols demonstrated neuroprotective effects in PC12 cells exposed to $A\beta_{1-42}$, including punicalagin. These findings highlight some structure–activity insights that can be gleaned into the anti-aggregatory properties of bioactive polyphenols based on modelling of their binding to β -amyloid, but also serve to highlight the more general cellular neuroprotective nature of such compounds.

Received 23rd October 2015,

Accepted 19th January 2016

DOI: 10.1039/c5fo01281c

www.rsc.org/foodfunction

Introduction

A diverse array of natural polyphenols have been ascribed neuroprotective properties in a number of models of neuronal damage and neurodegeneration, and are considered potential avenues for the development of neuroprotective drug therapies.^{1,2} Bioactive polyphenols such as flavonoids been shown to mediate neuroprotection against exposure to the toxic brain protein β -amyloid found in Alzheimer's disease *via* multiple actions.^{3,4}

Many naturally occurring compounds have demonstrated interactions with amyloid proteins resulting in inhibition of fibril or oligomer formation. Polyphenolic compounds,

individually or within extracts of their natural product sources, have been shown to directly disrupt and remodel amyloid fibrils into non-toxic conformations as part of their with neuroprotective action, exemplified by the green tea component epigallocatechin gallate (EGCG).^{5,6} Pomegranate juice or extract has been shown to reduce amyloid burden and microglial activation in transgenic mouse AD models,^{7,8} but the contribution from a constituent complex polyphenolic component ellagitannin, punicalagin, has not been ascertained. Additionally, the Magnolia-derived lignan honokiol has also demonstrated neuroprotective and anti-amyloid properties *in vitro*,^{9,10} yet an interaction directly affecting β -amyloid conformational states is unknown. As examples, these compounds all have a markedly divergent structure to other plant-derived flavonoids such as luteolin and myricetin, which have been identified as potent inhibitors of β amyloid induced memory impairment and β amyloid aggregation.^{11–14} It is not known if such structurally varying polyphenolics such as punicalagin and honokiol can interact directly in a common motif within β -amyloid to explain potential neuroprotective actions.

^aDiscipline of Pharmacology, School of Medical Sciences, Faculty of Health Sciences, The University of Adelaide, South Australia. E-mail: scott.smid@adelaide.edu.au; Fax: +61 8 82240685; Tel: +61 8 83135287

^bInstitute of Neuroscience and Physiology, The Sahlgrenska Academy, Göteborg University, Sweden

^cSchool of Chemistry and Physics, Faculty of Sciences, The University of Adelaide, South Australia

In this study we determined the capacity for such a set of structurally diverse and naturally occurring polyphenols to directly alter β -amyloid fibril formation and compared this with their neuroprotective effects *in vitro*. Additionally, we investigated the predictive capacity of selected polyphenolic binding to β amyloid through *in silico* approaches and compared this with their fibrillar inhibitory and neuroprotective capacity. In this way we aimed to better understand the structural basis of β amyloid interactions with naturally occurring polyphenols as a potential indicator of their neuroprotective ability.

Materials and methods

Reagents and chemicals

Human amyloid- β 1–42 protein ($A\beta_{1-42}$) was obtained from Abcam (Cambridge, MA, USA). Select polyphenols used in this study were the flavonoids luteolin and myricetin, the lignan honokiol and the ellagitannin punicalagin, the latter a component of pomegranate.¹⁵ All were sourced from Sigma-Aldrich (St Louis, MO, USA). Thiazolyl blue tetrazolium bromide (MTT), trypan blue, thioflavin T, DMSO, 10% neutral-buffered formalin, Roswell Park Memorial Institute 1640 (RPMI) medium, uranyl acetate, Dulbecco's Modified Eagles Medium (DMEM), poly-L-lysine solution, Triton \times 100 and foetal calf serum (FCS) were also obtained from Sigma-Aldrich. Non-essential amino acids (NEAA), penicillin/streptomycin, 10 \times trypsin EDTA and phosphate buffered saline (PBS) at pH 7.4 were obtained from Thermo Fisher Scientific (Scoresby, VIC, Australia). Bovine serum albumin (BSA) was obtained from Bovogen Biologicals (East Keilor, VIC, Australia).

PC12 cell culture

Rat pheochromocytoma cells (Ordway PC12) cells displaying a semi-differentiated phenotype with neuronal projections¹⁶ were kindly donated by Professor Jacqueline Phillips (Macquarie University, NSW, Australia) and maintained in RPMI-1640 media with 5% foetal calf serum (FCS), 1% L-glutamine, 1% non-essential amino acids and 1% penicillin/streptomycin. Cells were seeded at 2×10^4 cells per well in RPMI-1640 and 10% FCS. PC12 cells were equilibrated for 24 hours before treatment with bioactives and/or $A\beta_{1-42}$.

$A\beta$ preparation and treatment in PC12 cells

Native, non-fibrillar $A\beta_{1-42}$ was prepared by dissolving in 1% DMSO to yield a protein concentration of 3.8 mM. Sterile PBS was added to prepare a final concentration of 100 μ M. Amyloid was then dispensed into aliquots and immediately frozen at -70 °C until required.

Punicalagin, luteolin, honokiol and myricetin were diluted in PBS to their final stock concentrations prior to addition to cells. Undifferentiated PC12 cells were treated with each of these bioactives at 100 μ M, 15 minutes prior to incubation with $A\beta_{1-42}$ (0–2 μ M). Cells were then incubated for 48 hours at 37 °C, 5% CO₂ prior to measurement of cell viability.

Cell viability measurements

Viability was determined in PC12 cells using the thiazolyl blue tetrazolium bromide (MTT) assay. After incubation, 96-well plates had all media removed and replaced with serum-free media containing 0.25 mg ml⁻¹ of MTT. The plate was further incubated for 2 hours at 37 °C with 5% CO₂, then MTT solution removed and cells lysed with DMSO. Absorbance was measured at 570 nm using a PolarStar Galaxy microplate reader (BMG Labtech, Durham, NC, USA).

Thioflavin T assay and microscopy of $A\beta$ fibril and aggregate formation

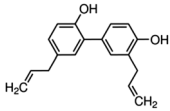
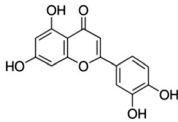
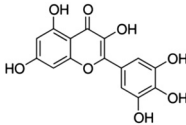
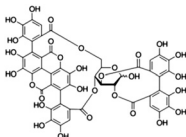
Thioflavin T (ThT) binds to β -amyloid fibrils with fluorescence increasing proportionally to the amount of fibrils present in solution. The ThT assay was used to confirm fibril formation over time with β -amyloid in cell-free solution, in addition to determining if fibril formation was directly affected by the polyphenolic compounds. ThT (10 μ M in PBS) was added to wells on a microplate together with non-fibrillar $A\beta_{1-42}$ (10 μ M) and the test polyphenol compound (each at 100 μ M). In addition, a range of concentration of each bioactive (0, 1, 10, 50 and 100 μ M) was tested against $A\beta_{1-42}$ (10 μ M) to determine the concentration–response relationship for inhibition of fibrillisation. Fluorescence was then measured at 37 °C every 20 minutes for 48 hours using a Synergy MX microplate reader (Bio-Tek, Bedfordshire, UK) with excitation and emission wavelengths at 446 nm and 490 nm respectively. ThT output from all treatment groups was normalised to blank values (ThT alone in PBS).

Transmission electron microscopy (TEM) was used to visualise $A\beta$ aggregates and fibrils and to investigate the effects of selected polyphenols on $A\beta$ morphology. Samples were prepared by incubating native $A\beta_{1-42}$ (10 μ M) in PBS, either alone or with flavonoids (100 μ M each) for 48 hours at 37 °C. A 5 μ l sample was then placed onto a 400 mesh formvar carbon-coated nickel electron microscopy grid (Proscitech, Kirwan, QLD, Australia). After 1 minute this sample was blotted off using filter paper and 10 μ l of contrast dye containing 2% uranyl acetate was then placed onto the grid, left for one minute and blotted off with filter paper. Grids were then loaded onto a specimen holder and then into a FEI Tecnai G2 Spirit Transmission Electron Microscope (FEI, Milton, QLD, Australia). Sample grids were then viewed using a magnification of 34 000–92 000 \times . Grids were extensively scanned manually in search of fibrils and representative images taken.

Computational modelling of polyphenol optimized conformation and binding to $A\beta_{1-42}$

For three polyphenols (luteolin, myricetin and honokiol), equilibrium geometries were optimized using density functional theory (DFT) approach¹⁷ that utilizes Becke's three-parameter hybrid functional known as B3LYP.¹⁸ A large basis set, aug-cc-pVDZ was used for approximation of molecular orbitals in optimized geometry for all three molecules. All the computations were carried out using Gaussian 09 package of codes

Table 1 Docking profile of bioactive polyphenols with A β_{1-42} monomer

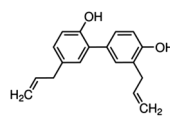
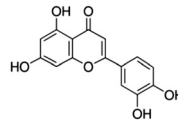
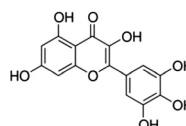
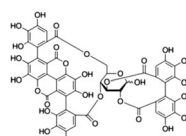
Bioactive	Molecular weight	Docking score	Steric interaction score	Hydrogen bonding score	RMSD (Å)	
Honokiol		266.33	-47.18	-47.54	-2.00	16.53
Luteolin		287.24	-41.36	-36.20	-5.75	9.07
Myricetin		319.24	-38.86	-36.06	-5.08	19.19
Punicalagin		1070.61	-47.14	-56.14	0.00	15.70

(<http://www.gaussian.com/>) at the Tizard supercomputer server of eResearch SA (<https://www.ersa.edu.au/tizard>). Calculations were carried out in no symmetry to facilitate full rearrangement and relaxation of the structures to their most stable form. For punicalagin, the optimized structure was extracted from Human Metabolome Database (HMDB ID: HMDB05795),

as geometry optimization through computation such as DFT-B3LYP or Hartree-Fock method was difficult to accomplish due to the large size and complexity of its molecular structure.

Fully optimized ligand structures were studied for their binding interactions with A β_{1-42} monomer (PDB ID: 1IYT) and

Table 2 Docking profile of bioactive polyphenols with A β_{1-42} oligomer (pentamer)

Bioactive	Molecular weight	Docking score	Steric interaction score	Hydrogen bonding score	RMSD (Å)	
Honokiol		266.33	-71.23	-71.93	-3.58	17.67
Luteolin		287.24	-65.07	-52.53	-12.67	21.06
Myricetin		319.24	-60.75	-46.74	-15.81	21.08
Punicalagin		1070.61	-52.40	-57.64	-4.00	16.43

oligomeric pre-fibrillar pentamer β -sheet structure (PDB ID: 2BEG) were modelled using the CLC Drug Discovery Workbench, version 1.5.1 (<http://www.clcbio.com/products/clc-drug-discovery-workbench>). This software uses a MolDock scoring function to identify the optimal solution from its docking algorithm based on a hybrid search algorithm denoted as guided differential evolution.¹⁹ The MolDock scoring function is based on a piecewise linear potential (PLP). Since $A\beta_{1-42}$ monomers and oligomers do not have any singular pharmacophore, a large search space was created covering the whole protein. All ligand structures were kept flexible to allow rotation of any bonds in order to bind $A\beta_{1-42}$. There were 100 iterations performed for each docking simulation for all four polyphenolic ligands. Results are summarized as a docking score in Tables 1 and 2.

Statistical analysis

Data obtained from the MTT assay was analysed *via* a two-way analysis of variance (ANOVA) to assess neuronal cell viability arising from incubation in $A\beta_{1-42}$, alone or in the presence of polyphenol ligands, with a Bonferroni's *post hoc* test used to determine the significance level for each polyphenol treatment interaction at each $A\beta_{1-42}$ concentration tested. Area under the curve analysis for Thioflavin T (ThT) fluorescence data was analysed using one way ANOVA with a Dunnett's multiple comparisons test used for determining the significance of bioactive effects *versus* $A\beta_{1-42}$. A significance value of $p < 0.05$ was used for all experiments. Data analysis and production of graphs was performed in GraphPad Prism 6 for Windows (GraphPad Software, San Diego, USA).

Results

Thioflavin T fluorescence of $A\beta_{1-42}$ fibrillisation kinetics

Thioflavin T (ThT)-based fibrillisation kinetics of $A\beta_{1-42}$ demonstrated a gradual increase in fluorescence output reaching a plateau by 900 min (15 h), indicative of maximum fibril and aggregate formation (Fig. 1a). Thereafter, ThT levels were stable over the duration of the assay up to 2880 min (48 h). All of the four polyphenols tested: myricetin, honokiol, luteolin and punicalagin (each at 100 μ M) markedly inhibited the development of ThT fluorescence, abolishing output both at the initial period of fibrillisation and continuing over the full 48 h time course of incubation. Area under the curve analysis showed extensive and significant overall inhibition of fibril formation in the presence of each of the bioactive polyphenols at 100 μ M over this time course (Fig. 1b). Inhibition of $A\beta_{1-42}$ fibrillisation was also demonstrated to be concentration-dependent for both luteolin and punicalagin within the range of 1–100 μ M as measured at the peak of the active fibril growth phase at 10 h (Fig. 2a and b). For myricetin, the lowest concentration tested (1 μ M) still demonstrated marked inhibition of ThT fluorescence (Fig. 2c), while honokiol also substantially attenuated ThT output at 1 μ M (Fig. 2d). The calculated relative inhibitory concentration (IC_{50}) of each polyphenol at 10 hours

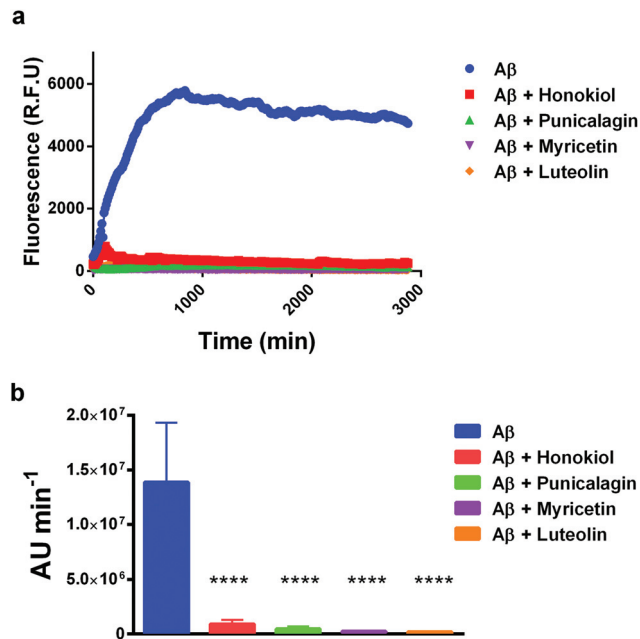


Fig. 1 (a) Thioflavin T (ThT) fluorescence indicative of amyloid $A\beta_{1-42}$ fibrillisation kinetics, alone and in the presence of each of four polyphenolic bioactives (100 μ M each) over 48 h in cell-free PBS solution. (b) Area under the curve analysis of ThT kinetics demonstrate significant overall inhibition of amyloid fibrillisation from incubation with polyphenolics (**** $P < 0.0001$; mean \pm SEM of $n = 4$ experiments).

was myricetin (0.25 μ M) > honokiol (0.55 μ M) = punicalagin (0.56 μ M) > luteolin (1.6 μ M). Inhibition at all polyphenol concentrations continued over 48 h of incubation (not shown).

Transmission electron microscopy of $A\beta_{1-42}$ fibrils and aggregates

On microscopic evidence, the morphology of the amyloid fibrils and aggregates was affected by incubation with each of the polyphenols, but to varying effect on both the extent and morphology of aggregation. For example, overall $A\beta_{1-42}$ aggregation was reduced and aggregates more amorphous in appearance in the presence of myricetin (Fig. 3b). Luteolin altered $A\beta_{1-42}$ aggregate morphology in a similar way to myricetin in appearance, although the extent of aggregation was more than that observed in myricetin-treated samples (Fig. 3e). Fibril and aggregate morphology in punicalagin (Fig. 3c) and honokiol-treated (Fig. 3d) $A\beta_{1-42}$ samples was similar, but in both cases overall fibril appearance was less dense than in control samples.

Effects of polyphenols on $A\beta_{1-42}$ mediated neuronal toxicity

MTT assay of cell viability demonstrated that $A\beta_{1-42}$ (0.1–2 μ M) evoked a concentration-dependent decrease in cell viability to a maximum of 60% over 48 h (Fig. 4). Notably, each of the polyphenols myricetin, honokiol, luteolin and punicalagin (each at 100 μ M) provided a significant degree of neuroprotection against β amyloid exposure over the full concentration range of $A\beta_{1-42}$.

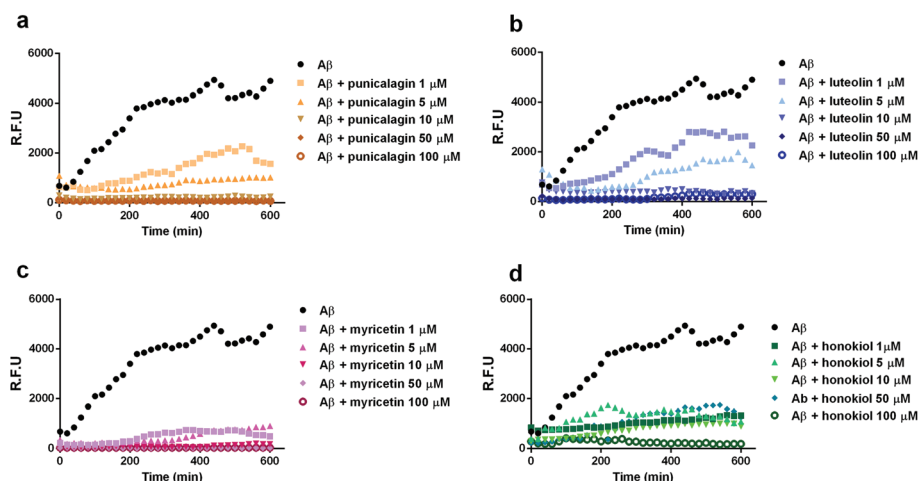


Fig. 2 Thioflavin T (ThT) fluorescence demonstrating amyloid Aβ₁₋₄₂ fibrillation kinetics over 10 h in cell-free PBS solution, alone and in the presence of increasing concentrations of polyphenolic bioactives (1–100 μM each): (a) punicalagin (b) luteolin (c) myricetin and (d) honokiol.

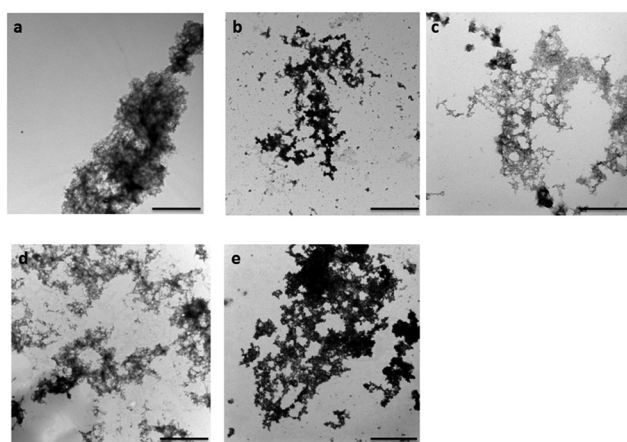


Fig. 3 Representative transmission electron micrographs of Aβ₁₋₄₂ fibril and aggregate formation, alone and following 48 h incubation with selected polyphenols (each at 100 μM): (a) Aβ₁₋₄₂ (b) Aβ₁₋₄₂ and myricetin (c) Aβ₁₋₄₂ and punicalagin (d) Aβ₁₋₄₂ and honokiol (e) Aβ₁₋₄₂ and luteolin. Scale bar: 1 μm.

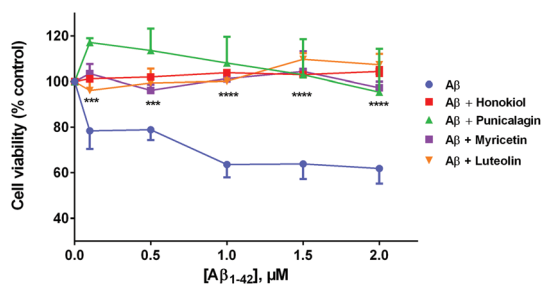


Fig. 4 MTT assay representing cell viability of PC12 cells following 48 h of Aβ₁₋₄₂ incubation, alone or with either punicalagin, luteolin, myricetin or honokiol (each at 100 μM). Each of the bioactive polyphenols exerted significant protection over the full concentration range of Aβ₁₋₄₂. *****p* < 0.0001 for each bioactive vs. Aβ₁₋₄₂ (1–2 μM); ****p* < 0.001 for each bioactive vs. Aβ₁₋₄₂ (0.1–0.5 μM); mean ± SEM of *n* = 4 experiments.

Molecular modelling of optimised polyphenol binding to Aβ monomer and pentamer

The optimised structures of each of the four polyphenols were docked to the model Aβ₁₋₄₂ monomer and pentamer. In the monomer, honokiol and myricetin bound to the same region (Fig. 5c and d) and interacted with key amino acid residues Glu3, His6, Asp7, Gly9 and Try10 (residues not shown). Luteolin bound to the rear side of the monomer (Fig. 5b) interacting with residues Gln15, Lys16 and Phe19, while punicalagin bound to the Aβ₁₋₄₂ monomer in the broader region of residue Leu17 to Val39 due to the larger size of the molecule (Fig. 5a). The Aβ₁₋₄₂ pentamer was made up of a chain of Aβ monomers (chain A, B, C, D, E) aligned side by side to form a β-sheet like structure (Fig. 6). Honokiol, luteolin and myricetin interacted with the hydrophobic binding pocket formed by Lys16, Leu17,

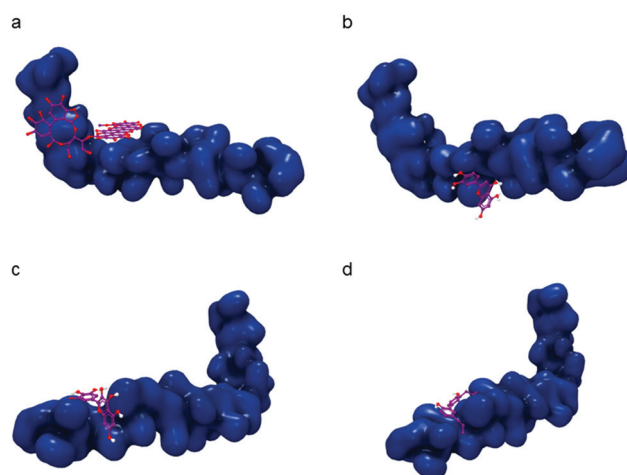


Fig. 5 Modelled bioactive ligand binding of each of the four optimised polyphenolic conformations to Aβ₁₋₄₂ monomer: (a) punicalagin, (b) luteolin, (c) myricetin and (d) honokiol. Binding properties of each polyphenol are provided in Table 1.

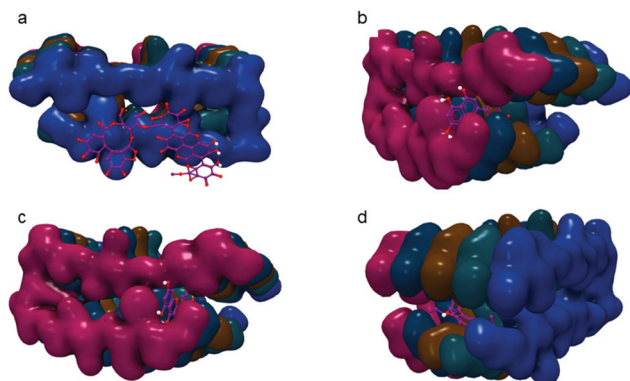


Fig. 6 Modelled bioactive ligand binding of each of the four optimised polyphenolic conformations to $A\beta_{1-42}$ pentamer: (a) punicalagin, (b) luteolin, (c) myricetin and (d) honokiol. Binding properties of each polyphenol are provided in Table 2.

Val18 and Phe19 residues of all chains of the $A\beta$ oligomer (amino acid residues not shown). Honokiol bound inside this binding pocket by forming hydrogen bonds with Leu17 and Gly38 of chains C and E. Myricetin and luteolin both formed hydrogen bonds with residue Leu17, Val18 and Phe19 of chain C, D and E. Punicalagin, unlike the other smaller ligands, bound to the exterior surface, possibly due to steric hindrance interacting with residue Leu17 to Ser26 and forming hydrogen bonding with residue Gly25.

Among the four bioactive molecules, punicalagin showed the lowest docking score of -52.40 and steric interaction score of -57.64 , hydrogen bonding score of -4.0 with the β -sheet conformation of $A\beta_{1-42}$ pentamer (Table 2). Honokiol, on the other hand, showed the highest docking score of -71.23 , steric interaction score of -71.93 and hydrogen bonding score of -3.58 . Luteolin and myricetin demonstrated similar docking scores of -65.07 and -60.75 respectively. Luteolin provided a higher steric interaction score than myricetin, whereas myricetin demonstrated the highest hydrogen bonding score overall. Optimal docking poses showed that the terminal hydroxyl groups of the flavonoids luteolin and myricetin were crucial for hydrogen bonding to $A\beta_{1-42}$ (Fig. 6).

Discussion

These studies have compared the neuroprotective properties of selected natural polyphenols with their capacity to structurally modify the aggregation of the major neurotoxic β amyloid fragment 1–42 *in vitro*. *In silico* modelling has also been used to compare the likely binding sites of such polyphenols to the β amyloid pentamer, as a further tool in which to investigate the most effective binding parameters that may predict the structural modification of β amyloid protein to potentially non-toxic conformations.

Of those polyphenols tested, there was a pattern related to the favourable molecular binding of the representative polyphenol to β amyloid protein and its effect on fibril and aggre-

gate morphology. This was inferred by both the extensive inhibition of ThT fluorescence and clear morphological evidence of fibril and aggregate modification *via* transmission electron microscopic imaging. The appearance of β amyloid in the presence of myricetin and luteolin resembled amorphous aggregates observed from the interaction of various other compounds with β amyloid, including the anti-fibrillar flavonoid epigallocatechin gallate.²⁰ Myricetin and luteolin have been previously documented to have an anti-aggregatory effect on β amyloid production^{21,22} and myricetin has also been shown to be effective against other ordered amyloid fibrils.²³ Such amorphous aggregates are likely to undergo loss of an extensive surface area present in the ‘meshwork’ of $A\beta$ fibrils in which ThT binds²⁴ to account for these marked reductions in output.

It was not possible to predict if such resultant forms of polyphenol-modified $A\beta$ were benign or toxic to neuronal cells solely from either inhibition of ThT fluorescence or from structural imaging alone. However, previous studies using various polyphenolic compounds, including flavonoids, have revealed not just inhibition of $A\beta$ fibril formation but also stabilisation of oligomers into off-target pathways that abrogate neurotoxicity,²⁵ so this is likely to have also occurred to mitigate $A\beta$ neurotoxicity in the present study. The most common disposition of $A\beta$ following incubation with flavonoids is as low molecular weight oligomers with some protofibrillar aggregates.²⁵ However, even within the large class of flavonoid compounds, small differences in chemical structure can result in marked differences in both the type of interaction with $A\beta$ and its resultant morphology.^{26–28} In addition, while we saw a varying composition of $A\beta$ species following incubation with all the polyphenols used in this study, the ability to modify β amyloid fibril formation is not a generalised property of all such naturally-occurring polyphenolics. A diverse range of phytochemicals that do not alter $A\beta_{1-42}$ fibril morphology include such compounds as cyanidin glucoside and gallic acid,²⁹ dihydrokaempferol, galangin and pinobanksin,²⁷ naringenin²⁵ and cannabidiol.²⁰

From the docking studies, it was found that all four polyphenolic molecules bind to $A\beta_{1-42}$ oligomer mainly through steric and hydrogen bonding interactions. Key amino acid residues involved in the interactions of honokiol, luteolin and myricetin are Lys16, Leu17, Val18 and Phe19 of chain C, D and E of the $A\beta_{1-42}$ oligomer. Interaction with Lys16 residue may be particularly relevant for these molecules to exert neuroprotection, as Lys16 residue appears to be an important factor in promoting $A\beta_{1-42}$ toxicity.³⁰ Interestingly, evidence suggests flavonoids may exert anti-aggregatory effects against $A\beta_{1-42}$ by the quinone-driven covalent modification of such a key lysine residue in $A\beta_{1-42}$, noting myricetin as one such example of a potent inhibitor.²⁷ Computational modelling of other small molecule inhibitors of $A\beta_{1-42}$, such as the flavonoid derivative 2-(4-benzyloxyphenyl)-3-hydroxy-chromen-4-one,³¹ demonstrated that it binds to the same hydrophobic groove of the $A\beta_{1-42}$ pentamer/oligomer (2BEG) interacting with similar amino acid residues as observed in our molecular docking studies.

Binding of both of these compounds to β amyloid was most favourable on the hydrophobic part of the pentamer surrounded by key residue Lys16, Leu17, Val18, Phe19, Gly38 and Val39. This occurs in a groove running parallel with the long axis of fibrils which is also associated with ThT binding.³² This may also explain why some polyphenolic compounds exert a strong degree of inhibition of ThT fluorescence without necessarily inhibiting fibril formation, *via* effective displacement of ThT from its binding site but lacking the structural interactions to alter fibrillisation itself.²⁰ This may also form one mechanism underlying the propensity for some polyphenolics to interfere with ThT fluorescence, leading to false positives for fibril inhibition and limiting the inferences that can be made from such experiments in isolation.³³

The amyloid anti-aggregatory and neuroprotective capacity of luteolin and myricetin are shared amongst other very similar flavonols and isoflavones, including such compounds as fisetin and transilutin.^{11,21} In such studies, modelling for flavonoid binding to β amyloid oligomers indicates extensive and stabilising hydrogen bonding between the flavonoid and amino acid side chains critical for β sheet formation and further fibrillisation.¹¹ Myricetin also destabilises the β -sheet conformation of A β _{25–35} peptide chains by forming hydrogen bonds with key residues responsible for β -sheet formation.³⁴ Coupled with the aforementioned potential of flavonoids for covalent modification of key A β amino acid side chains,²⁷ the findings of such exploratory studies generally reinforce the development potential of drugs derived from the core structure of selected flavonoids for further consideration as potential treatments for Alzheimer's disease.^{35,36} However, other naturally occurring non-flavonoid small molecules bind to a similar region in the exterior groove of β amyloid oligomers, eliciting remodelling *via* a combination of planar ring hydrophobic and hydrogen bonding interactions.³⁷

Punicalagin and honokiol both demonstrated a substantive and concentration-dependent degree of inhibition of fibril formation as judged by attenuation of ThT fluorescence. When viewed under the electron microscope, dense aggregates were absent, but some smaller and less developed fibrillar aggregates were still present and this may be sufficient to account for the residual ThT fluorescence following incubation with these compounds. In modelling the interaction of honokiol with the A β pentamer, it was seen to bind to the inner pore as distinct from the other flavonoids and punicalagin, and bound with the most favourable energy state of all the polyphenols tested. The molecular docking results indicate that steric interaction plays a major role for a bioactive molecule to bind A β _{1–42} along with hydrogen bonding. Honokiol, due to its small size and favourable intramolecular position of aliphatic/side chains is able to fit efficiently within the binding pocket resulting in a comparatively higher docking interaction score. Interestingly, honokiol was recently described to inhibit calcitonin aggregation,³⁸ suggestive of further potential as a small molecule template for anti-amyloid drug development.

In the aforementioned discussion of complexity of ligand binding and implications for fibril formation and morphology,

it may be a moot point how any polyphenol may bind or otherwise alter A β fibrillisation if the end result is cellular neuroprotection. Indeed, our observations of neuroprotection arising from incubation with each of the bioactives highlights the pleiotropic action of such polyphenols against β -amyloid evoked neurotoxicity. We have previously shown bioactive-evoked neuroprotection against β -amyloid toxicity to be concentration-dependent using EGCG.³⁹ This evidence, together with the concentration-dependent inhibition of ThT fluorescence by a number of compounds in the present study, is suggestive that the degree of neuroprotection is likely to be linked cumulatively to the extent of formation of ultimately benign forms of β -amyloid by such polyphenols.

Both luteolin and myricetin have been shown to provide neuroprotection against A β -mediated neurotoxicity through multiple actions.^{12,14,40–43} Punicalagin not only demonstrated significant neuroprotection against A β -mediated neurotoxicity, but also resulted in higher levels of cell viability than control; possibly indicative of a proliferative effect of the ellagitannin. As a major polyphenolic component of pomegranate extract, its presence may be responsible for the beneficial effects of pomegranate extract or juice in experimental animal AD models,⁷ which include attenuated amyloid burden, reduced microglial activation and lessened inflammation in a transgenic AD mouse model.⁸ Our results highlight for the first time an action on amyloid β aggregation as another potential neuroprotective mechanism of punicalagin. Additional amyloid-mitigating actions are implicated in the activities of this molecule, including BACE1 inhibition.¹⁵ Honokiol as a lignan is structurally dissimilar to the flavonoids luteolin and myricetin; however it also afforded neuroprotection to PC12 cells against β -amyloid exposure. This is supportive of a previous study that also demonstrated honokiol-mediated protection to PC12 cells following A β exposure.⁹ A degree of neuroprotection has been ascribed to honokiol *via* antioxidant, anti-inflammatory and neurotrophic actions,⁴⁴ and the closely related compound 4-*O*-methylhonokiol has also been demonstrated to have substantive neuroprotective and anti-inflammatory properties.^{45,46} Our results indicate an additional anti-aggregative action at β -amyloid to this molecule, the first reported to our knowledge.

Conclusions

In conclusion, diverse naturally occurring polyphenols show varying affinity and binding sites for β -amyloid and can differentially affect amyloid fibrillisation kinetics and morphology. Modelling of bioactive polyphenol binding to discrete sites in β -amyloid oligomers may be broadly predictive of altered fibril and aggregate morphology, but this alone is not predictive of neuroprotective effects of such compounds. In particular, diverse polyphenol structures such as punicalagin and honokiol are also able to disrupt the aggregative propensity of β amyloid and this may be implicated in their neuroprotective activity.

Acknowledgements

Thanks to Lyn Waterhouse for assistance with the transmission electron microscopy.

References

- J. Koppel and P. Davies, *J. Alzheimer's Dis.*, 2008, **15**, 495–504.
- J. Fernandez-Ruiz, C. Garcia, O. Sagredo, M. Gomez-Ruiz and E. de Lago, *Expert Opin. Ther. Targets*, 2010, **14**, 387–404.
- S. D. Smid, J. L. Maag and I. F. Musgrave, *Food Funct.*, 2012, **3**, 1242–1250.
- R. Campos-Esparza Mdel and M. A. Torres-Ramos, *Cent. Nerv. Syst. Agents Med. Chem.*, 2010, **10**, 269–277.
- J. Bieschke, J. Russ, R. P. Friedrich, D. E. Ehrnhoefer, H. Wobst, K. Neugebauer and E. E. Wanker, *Proc. Natl. Acad. Sci. U. S. A.*, 2010, **107**, 7710–7715.
- B. S. Harvey, I. F. Musgrave, K. S. Ohlsson, Å. Fransson and S. D. Smid, *Food Chem.*, 2011, **129**, 1729–1736.
- R. E. Hartman, A. Shah, A. M. Fagan, K. E. Schwetye, M. Parsadonian, R. N. Schulman, M. B. Finn and D. M. Holtzman, *Neurobiol. Dis.*, 2006, **24**, 506–515.
- L. Rojanathammanee, K. L. Puig and C. K. Combs, *J. Nutr.*, 2013, **143**, 597–605.
- C. P. Hoi, Y. P. Ho, L. Baum and A. H. Chow, *Phytother. Res.*, 2010, **24**, 1538–1542.
- B. Liu, N. Hattori, N. Y. Zhang, B. Wu, L. Yang, K. Kitagawa, Z. M. Xiong, T. Irie and C. Inagaki, *Neurosci. Lett.*, 2005, **384**, 44–47.
- Q. I. Churches, J. Caine, K. Cavanagh, V. C. Epa, L. Waddington, C. E. Tranberg, A. G. Meyer, J. N. Varghese, V. Streltsov and P. J. Duggan, *Bioorg. Med. Chem. Lett.*, 2014, **24**, 3108–3112.
- F. S. Tsai, H. Y. Cheng, M. T. Hsieh, C. R. Wu, Y. C. Lin and W. H. Peng, *Am. J. Chin. Med.*, 2010, **38**, 279–291.
- K. Ono, L. Li, Y. Takamura, Y. Yoshiike, L. Zhu, F. Han, X. Mao, T. Ikeda, J. Takasaki, H. Nishijo, A. Takashima, D. B. Teplow, M. G. Zagorski and M. Yamada, *J. Biol. Chem.*, 2012, **287**, 14631–14643.
- Y. Shimmyo, T. Kihara, A. Akaike, T. Niidome and H. Sugimoto, *J. Neurosci. Res.*, 2008, **86**, 368–377.
- H. M. Kwak, S. Y. Jeon, B. H. Sohng, J. G. Kim, J. M. Lee, K. B. Lee, H. H. Jeong, J. M. Hur, Y. H. Kang and K. S. Song, *Arch. Pharmacol. Res.*, 2005, **28**, 1328–1332.
- D. N. Dixon, R. A. Loxley, A. Barron, S. Cleary and J. K. Phillips, *In Vitro Cell. Dev. Biol.*, 2005, **41**, 197–206.
- W. Kohn, A. D. Becke and R. G. Parr, *J. Phys. Chem.*, 1996, **100**, 12974–12980.
- A. D. Becke, *J. Chem. Phys.*, 1993, **98**, 5648–5652.
- R. Thomsen and M. H. Christensen, *J. Med. Chem.*, 2006, **49**, 3315–3321.
- E. Janefjord, J. L. Maag, B. S. Harvey and S. D. Smid, *Cell. Mol. Neurobiol.*, 2014, **34**, 31–42.
- T. Akaishi, T. Morimoto, M. Shibao, S. Watanabe, K. Sakai-Kato, N. Utsunomiya-Tate and K. Abe, *Neurosci. Lett.*, 2008, **444**, 280–285.
- H. Ushikubo, S. Watanabe, Y. Tanimoto, K. Abe, A. Hiza, T. Ogawa, T. Asakawa, T. Kan and T. Akaishi, *Neurosci. Lett.*, 2012, **513**, 51–56.
- W. M. Berhanu and A. E. Masunov, *Biophys. Chem.*, 2010, **149**, 12–21.
- R. Khurana, C. Coleman, C. Ionescu-Zanetti, S. A. Carter, V. Krishna, R. K. Grover, R. Roy and S. Singh, *J. Struct. Biol.*, 2005, **151**, 229–238.
- Q. I. Churches, J. Caine, K. Cavanagh, V. C. Epa, L. Waddington, C. E. Tranberg, A. G. Meyer, J. N. Varghese, V. Streltsov and P. J. Duggan, *Bioorg. Med. Chem. Lett.*, 2014, **24**, 3108–3112.
- M. Hanaki, K. Murakami, K.-i. Akagi and K. Irie, *Bioorg. Med. Chem.*, 2016, **24**, 304–313.
- M. Sato, K. Murakami, M. Uno, Y. Nakagawa, S. Katayama, K.-i. Akagi, Y. Masuda, K. Takegoshi and K. Irie, *J. Biol. Chem.*, 2013, **288**, 23212–23224.
- M. Necula, R. Kayed, S. Milton and C. G. Glabe, *J. Biol. Chem.*, 2007, **282**, 10311–10324.
- D. Y. Wong, I. F. Musgrave, B. S. Harvey and S. D. Smid, *Neurosci. Lett.*, 2013, **556**, 221–226.
- S. Sinha, D. H. J. Lopes and G. Bitan, *ACS Chem. Neurosci.*, 2012, **3**, 473–481.
- S. Singh, R. Gaur, A. Kumar, R. Fatima, L. Mishra and S. Srikrishna, *Neurotoxic. Res.*, 2014, **26**, 331–350.
- M. R. H. Krebs, E. H. C. Bromley and A. M. Donald, *J. Struct. Biol.*, 2005, **149**, 30–37.
- S. A. Hudson, H. Ecroyd, T. W. Kee and J. A. Carver, *FEBS J.*, 2009, **276**, 5960–5972.
- M. Naldi, J. Fiori, M. Pistozzi, A. F. Drake, C. Bertucci, R. Wu, K. Mlynarczyk, S. Filipek, A. De Simone and V. Andrisano, *ACS Chem. Neurosci.*, 2012, **3**, 952–962.
- M. Prior, C. Chiruta, A. Currais, J. Goldberg, J. Ramsey, R. Dargusch, P. A. Maher and D. Schubert, *ACS Chem. Neurosci.*, 2014, **5**, 503–513.
- S. K. Singh, R. Gaur, A. Kumar, R. Fatima, L. Mishra and S. Srikrishna, *Neurotoxic. Res.*, 2014, **26**(4), 331–350.
- J. Bieschke, M. Herbst, T. Wiglenda, R. P. Friedrich, A. Boeddrich, F. Schiele, D. Kleckers, J. M. Lopez del Amo, B. A. Grüning, Q. Wang, M. R. Schmidt, R. Lurz, R. Anwyll, S. Schnoegl, M. Fändrich, R. F. Frank, B. Reif, S. Günther, D. M. Walsh and E. E. Wanker, *Nat. Chem. Biol.*, 2012, **8**, 93–101.
- C. Guo, L. Ma, Y. Zhao, A. Peng, B. Cheng, Q. Zhou, L. Zheng and K. Huang, *Sci. Rep.*, 2015, **5**, 13556.
- S. A. Hudson, H. Ecroyd, I. F. Musgrave, F. C. Dehle and J. A. Carver, *J. Mol. Biol.*, 2009, **392**, 689–700.
- N. Dragicevic, A. Smith, X. Lin, F. Yuan, N. Copes, V. Delic, J. Tan, C. Cao, R. D. Shytle and P. C. Bradshaw, *J. Alzheimer's Dis.*, 2011, **26**, 507–521.
- R. Liu, F. Meng, L. Zhang, A. Liu, H. Qin, X. Lan, L. Li and G. Du, *Molecules*, 2011, **16**, 2084–2096.

- 42 D. Sawmiller, S. Li, M. Shahaduzzaman, A. J. Smith, D. Obregon, B. Giunta, C. V. Borlongan, P. R. Sanberg and J. Tan, *Int. J. Mol. Sci.*, 2014, **15**, 895–904.
- 43 S. Bastianetto, S. Krantic, J. G. Chabot and R. Quirion, *Curr. Alzheimer Res.*, 2011, **8**, 445–451.
- 44 A. Woodbury, S. P. Yu, L. Wei and P. Garcia, *Front. Neurol.*, 2013, **4**, 130.
- 45 Y. J. Lee, D. Y. Choi, I. S. Choi, K. H. Kim, Y. H. Kim, H. M. Kim, K. Lee, W. G. Cho, J. K. Jung, S. B. Han, J. Y. Han, S. Y. Nam, Y. W. Yun, J. H. Jeong, K. W. Oh and J. T. Hong, *J. Neuroinflammation*, 2012, **9**, 35.
- 46 Y. J. Lee, D. Y. Choi, Y. K. Lee, Y. M. Lee, S. B. Han, Y. H. Kim, K. H. Kim, S. Y. Nam, B. J. Lee, J. K. Kang, Y. W. Yun, K. W. Oh and J. T. Hong, *J. Alzheimer's Dis.*, 2012, **29**, 677–690.

Chapter 3: Identification of dibenzyl imidazolidine and triazole acetamide derivatives through virtual screening targeting amyloid beta aggregation and neurotoxicity in PC12 cells

Sukanya Das, Scott D. Smid (2017) 'Identification of dibenzyl imidazolidine and triazole acetamide derivatives through virtual screening targeting amyloid beta aggregation and neurotoxicity in PC12 cells', *European Journal of Medicinal Chemistry*, 130: (354 - 364).

Reprinted with permission from Elsevier, Crown Copyright 2017.

This study was aimed at identifying new small molecule inhibitors of A β amyloidogenic aggregation and toxicity that contain a five membered heterocyclic (FMH) ring with nitrogen and/or oxygen as the heteroatom. Five membered heterocyclic (FMH) compounds are one of the key building blocks found in medicinal chemistry. Due to their high binding affinity with a variety of biological targets, some researchers classify FMH structures such as rhodanine and thiazolidine-2,4-dione as 'privileged scaffolds' in drug discovery (Tomasic and Masic 2009). However, debate exists for the suitability of the FMH ring with the exocyclic C=S group in early stage drug development, as the exocyclic C=S in rhodanine often offers a particularly high density of interaction sites which results in a promiscuous binding behaviour (Mendgen, Steuer et al. 2012). Despite this fact, FMH ring-bearing compounds remain a chemically attractive class of compounds that possess various intermolecular interaction points due to the presence of nitrogen and or sulphur in its ring (Mendgen, Steuer et al. 2012). Among this class of compounds, derivatives of thiohydantoin, rhodanine, hydantoin and thiazolidine are

commonly used in drug discovery (Meusel and Gütschow 2004, Jain, Vora et al. 2013). However, issues regarding the metabolic stability and toxicity of sulphur containing FMH ring-bearing compounds have been raised (Tang, Lee et al. 2015). Therefore, such compounds without any exocyclic C=S containing N-atom as the only heteroatom offer an alternative option for drug lead development.

Among the FMH ring-bearing compounds with only nitrogen as the heteroatom, imidazolidine or triazole compounds have shown bioactivity against various targets. For instance, imidazolidine-2,4-dione has been tested as a novel class of selective cannabinoid receptor agonists (van der Stelt, Cals et al. 2011), fatty acid amide hydrolase inhibitors (Muccioli, Fazio et al. 2006) and for antinociceptive effects in mice (de Queiroz, de Carvalho et al. 2015). A range of benzyl triazole derivatives act as γ -secretase modulators which lower A β levels *in vivo* (Fischer, Zultanski et al. 2011), while diphenyl triazole derivatives act as probe for detecting A β in human brain (Qu, Kung et al. 2007). However, the direct interaction of these FMH ring-bearing compounds, where nitrogen and/or oxygen are the heteroatom, with A β and its aggregation related toxicity is not well understood. An interaction of imidazolidine, triazole or benzoxazole derivatives against the pathologically relevant A β protein target would provide further insight towards suitability of these five membered heterocycle compounds without exocyclic C=O or C=S bonds as new aggregation inhibitors and neuroprotectants.

In view of this, the present study was aimed at identifying new FMH ring-bearing compounds with nitrogen and/or oxygen as the heteroatoms that can inhibit A β aggregation and toxicity. To address this, structure-based virtual screening by molecular docking was performed. ZINC is an open access database for commercially-available compounds, with a collection of many

millions of compounds. This database is designed to be suited for virtual screening, where the compounds have been divided into subsets based on their 'ring' structure. As a result, the ZINC database was well suited for the purpose of this study. Before conducting the structure-based virtual screening, the database was filtered for:

(a): FMH ring bearing compounds that have nitrogen and or oxygen as heteroatom and (b). No exocyclic C=O/S/N groups in the FMH ring.

This study has identified five new 'hit' compounds with predicted high binding scores to A β via molecular docking. Out of the five, four compounds inhibited A β aggregation in the thioflavin T assay of fibril kinetics. 100 μ M of each compound was tested against 10 μ M of A β in the anti-aggregation study. Finally, two compounds bearing a novel dibenzyl imidazolidine scaffold demonstrated inhibition of A β aggregation and neurotoxicity in neuronal (PC-12) cells.

Statement of Authorship

Title of Paper	Identification of dibenzyl imidazolidine and triazole acetamide derivatives through virtual screening targeting amyloid beta aggregation and neurotoxicity in PC12 cells
Publication Status	<input checked="" type="checkbox"/> Published <input type="checkbox"/> Accepted for Publication <input type="checkbox"/> Submitted for Publication <input type="checkbox"/> Unpublished and Unsubmitted work written in manuscript style
Publication Details	Journal 'European Journal of Medicinal Chemistry', 2017, vol.130, page 354-364.

Principal Author

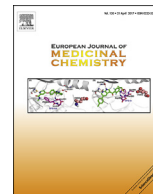
Name of Principal Author (Candidate)	Sukanya Das				
Contribution to the Paper	I have designed the virtual screening method and performed the database filtering and molecular modelling. I also, performed all the experiments and data analysis. I jointly worked with my primary supervisor Dr. Scott Smid for manuscript preparation.				
Overall percentage (%)	90%				
Certification:	This paper reports on original research I conducted during the period of my Higher Degree by Research candidature and is not subject to any obligations or contractual agreements with a third party that would constrain its inclusion in this thesis. I am the primary author of this paper.				
Signature	<table border="1" style="width: 100%;"> <tr> <td style="width: 80%;"></td> <td style="width: 20%;">Date</td> </tr> <tr> <td></td> <td>18/5/18</td> </tr> </table>		Date		18/5/18
	Date				
	18/5/18				

Co-Author Contributions

By signing the Statement of Authorship, each author certifies that:

- i. the candidate's stated contribution to the publication is accurate (as detailed above);
- ii. permission is granted for the candidate to include the publication in the thesis; and
- iii. the sum of all co-author contributions is equal to 100% less the candidate's stated contribution.

Name of Co-Author	Scott Smid				
Contribution to the Paper	Reviewed the final manuscript and input into the conceptual nature of studies.				
Signature	<table border="1" style="width: 100%;"> <tr> <td style="width: 80%;"></td> <td style="width: 20%;">Date</td> </tr> <tr> <td></td> <td>May 18, 2018</td> </tr> </table>		Date		May 18, 2018
	Date				
	May 18, 2018				



Research paper

Identification of dibenzyl imidazolidine and triazole acetamide derivatives through virtual screening targeting amyloid beta aggregation and neurotoxicity in PC12 cells



Sukanya Das, Scott D. Smid*

Discipline of Pharmacology, Adelaide Medical School, Faculty of Health Sciences, The University of Adelaide, South Australia, Australia

ARTICLE INFO

Article history:

Received 20 December 2016

Received in revised form

24 February 2017

Accepted 26 February 2017

Available online 28 February 2017

Keywords:

Alzheimer's disease

Amyloid β

Virtual screening

Imidazolidine

Triazole

Benzoxazole

ABSTRACT

Aggregation and neurotoxicity of amyloid β ($A\beta$) protein is a hallmark characteristic of Alzheimer's disease (AD). In this study we compared the anti-aggregatory and neuroprotective effects of five synthetic compounds against $A\beta$ protein; four of which possessed a five membered heterocycle ring scaffold (two dibenzyl phenyl imidazolidines and two triazole sulfanyl acetamides) and one with a fused five membered heterocycle (benzoxazole) ring, selected thorough virtual screening from ZINC database. Molecular docking of their optimized structures was used to study $A\beta$ binding characteristics. As predicted from molecular docking, strong steric binding of imidazolidines and H-bonding of both triazoles to $A\beta$ were translated into anti $A\beta$ aggregation properties. Subsequent transmission electron microscopy (TEM) was used to assess their effects on $A\beta_{1-42}$ fibril formation. Four compounds variably altered morphology of $A\beta$ fibrils from long, intertwined fibrils to short, loose structures. Thioflavin T assay of $A\beta$ fibrillisation kinetics demonstrated that one imidazolidine and both triazole compounds inhibited $A\beta$ aggregation. Rat pheochromocytoma (PC12) cells were exposed to $A\beta_{1-42}$, alone and in combination with the heterocyclic compounds to assess neuroprotective effects. $A\beta_{1-42}$ -evoked loss of neuronal cell viability was significantly attenuated in the presence of both imidazolidine compounds, while the triazole acetamides and benzoxazole compound were toxic to PC12 cells. These findings highlight the $A\beta$ anti-aggregative and neuroprotective propensity of a dibenzyl phenyl imidazolidine scaffold (Compound 1 and 2). While the triazole sulfanyl acetamide scaffold also possessed $A\beta$ anti-aggregation properties, they also demonstrated significant intrinsic neurotoxicity. Overall, the predictive efficacy of *in silico* methods enables the identification of novel imidazolidines that act both as inhibitors of $A\beta$ aggregation and neurotoxicity, and may provide a further platform for the development of novel Alzheimer's disease-modifying pharmacotherapies.

Crown Copyright © 2017 Published by Elsevier Masson SAS. All rights reserved.

1. Introduction

Deposition of amyloid beta ($A\beta$) protein is a pathological hallmark of Alzheimer's disease (AD), due to its high propensity for self-aggregation and conversion into toxic conformations. Under pathological conditions, the 42 residue amyloid beta ($A\beta_{1-42}$) protein rapidly converts into neurotoxic oligomers, protofibrils and fibrils that lead to the deposition of β amyloid plaques [1,2]. Soluble oligomers and protofibrillar forms of $A\beta_{1-42}$ are more toxic than mature fibrils and associated with neurodegeneration [3].

Consequently, disrupting the aggregative properties of $A\beta_{1-42}$ provides a potentially disease-modifying approach that merits the intensive search for small molecules that can impede self-aggregation and attenuate toxicity [4].

Various natural polyphenolic compounds such as EGCG, myricetin and curcumin suppress $A\beta_{1-42}$ aggregation and are also associated with a neuroprotective capacity [5–8]. However, there are limitations for using natural polyphenolic compounds as lead compound in structure-based drug discovery in this field. This is often related to poor bioavailability [9,10], with several novel small molecules, including natural compounds lacking conclusive outcomes in clinical trials [4,11]. Hence, identification and further development of new small molecules targeting $A\beta_{1-42}$ would be highly desirable for AD therapy.

* Corresponding author. Discipline of Pharmacology, Adelaide Medical School, Faculty of Health Sciences, The University of Adelaide, Adelaide, SA 5005, Australia.
E-mail address: scott.smid@adelaide.edu.au (S.D. Smid).

The increasing versatility of *in silico* approaches provides predictive information on small molecules that may favourably bind A β , and thus be used in the identification of compounds or molecular scaffolds for rational drug design targeting A β aggregation. Here we have studied the interaction of five such synthetic compounds, termed as Compound 1–5, selected from the ZINC chemical database through virtual screening methods. The database was filtered and screened for compounds in the single and double ring subsets; a five membered heterocycle ring (FMH) with nitrogen heteroatom (N) and a fused double ring with either a nitrogen or a nitrogen and an oxygen heteroatom in the FMH ring, but no heteroatom in its six membered ring and having no exocyclic C=O,S,N group. From the screening, four of the selected compounds contained either two or three N atoms in their FMH ring. They were an imidazolidine ring (Compound 1 and 2) or a triazole ring (Compound 3 and 4). Compound 5 containing a fused FMH; a benzoxazole ring was also selected (Fig. 1). We then investigated their A β _{1–42} docking interactions and subsequently assessed the effects of each of these compounds on A β _{1–42} aggregation kinetics, fibril morphology and neuroprotective capacity *in vitro*.

2. Materials and methods

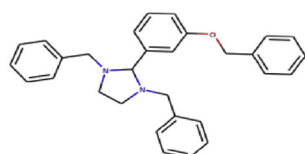
2.1. Reagents and chemicals

Human amyloid- β 1–42 protein (A β _{1–42}) was obtained from

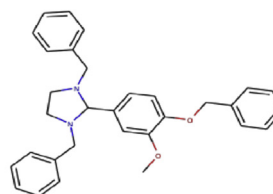
rPeptide (Bogart, GA, USA). Compound 1, 3 and 4 were sourced from Specs, a screening compound manufacturer (<https://www.specs.net>) while Compound 2 and 5 were sourced from ChemDiv (<http://www.chemdiv.com>). Compound 2 and 5 were assessed as >90% pure by manufacturer. For Compound 1 and 4, purity was assessed through ¹H NMR analysis (supplementary material, Figs. 1 and 2). For cell culture experiments, thiazolyl blue tetrazolium bromide (MTT), trypan blue, Thioflavin T, DMSO, Roswell Park Memorial Institute 1640 (RPMI) medium and fetal calf serum (FCS) were obtained from Sigma-Aldrich (St Louis, MO, USA). Non-essential amino acids (NEAA), penicillin/streptomycin, 10 × trypsin EDTA and phosphate buffered saline (PBS) at pH 7.4 were obtained from Thermo Fisher Scientific, (Scoresby, VIC, Australia). Bovine serum albumin (BSA) was obtained from Bovogen Biologicals (East Keilor, VIC, Australia).

2.2. Database selection, structure/ligand searching and selection process

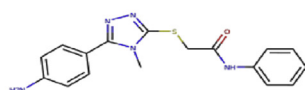
ZINC15 (<http://zinc15.docking.org/>) is a free database that contains over 120 million commercially available “drug-like” compounds from various suppliers in a ready-to-dock structural format [12]. We began our search from its single ring subset using i) in nature and ii) for-sale filters and subsequently consolidated into 11 different types of single ring five-membered heterocycles (FMH) with only nitrogen heteroatom. Similarly, in the double ring



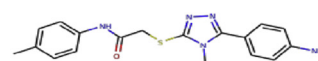
Compound 1 1,3-dibenzyl-2-[3-(benzyloxy)phenyl]imidazolidine
ZINC ID: 1932959533



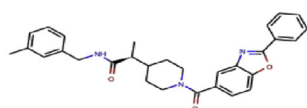
Compound 2 1,3-dibenzyl-2-[4-(benzyloxy)-3-methoxyphenyl]imidazolidine
ZINC ID: 19329512



Compound 3 2-{[5-(4-aminophenyl)-4-methyl-4H-1,2,4-triazol-3-yl]sulfanyl}-N-phenylacetamide
ZINC ID: 368131



Compound 4 2-{[5-(4-aminophenyl)-4-methyl-4H-1,2,4-triazol-3-yl]sulfanyl}-N-(4-methylphenyl)acetamide
ZINC ID: 694123



Compound 5 N-[(3-methylphenyl)methyl]-2-[1-(2-phenyl-1,3-benzoxazole-5-carbonyl)piperidin-4-yl]propanamide
ZINC ID: 65005672

Fig. 1. 2-D structure of five selected compounds with their chemical names and ZINC IDs.

compounds, we consolidated towards 5 types of FMH rings with either only one nitrogen or a nitrogen and an oxygen fused with a six membered ring. Each of these 16 types of ring-bearing compound subsets were further filtered for i) anodyne compounds with known non-reactivity and ii) bb, compounds commercially available in preparative quantity. Thereafter, each subset was screened through docking using PLANTS_{PLP} scoring function [13] in speed mode 4 that uses a 3s average ligand docking time with no iteration (Fig. 2).

All ligand screening simulations, further molecular docking and image collection were conducted in CLC Drug Discovery Workbench (CLC DDW), version 1.5.1 (http://resources.qiagenbioinformatics.com/manuals/clcdrugdiscoveryworkbench/current/index.php?manual=Introduction_CLC_Drug_Discovery_Workbench.html). The best 10 docking results from all subsets were visually inspected and ranked based on score, binding pose and region and molecular weight (300–500 g/mol). The number of compounds from the 16 types of ring subsets used in the virtual screening is also provided (Table 1, Supplementary Material).

2.3. Computational modelling of compound optimized conformations and binding to A β ₁₋₄₂

In order to gain further insights into the A β ₁₋₄₂ binding interactions for each selected compound from screening, all ligand

structures were first optimized and then individually re-docked to both A β ₁₋₄₂ monomer and oligomer with normal speed (docking time as required) with 300 iterations per docking. For all five compounds, equilibrium molecular geometries were optimized using density functional theory (DFT) method [14] that utilizes Becke-Lee-Yang-Parr three-parameter hybrid functional commonly known by the acronym B3LYP. A large basis set, aug-cc-pVDZ was used in approximation of optimized geometry for all five molecules. DFT-B3LYP level of calculations combining with a larger basis set is considered as standard and reliable method for estimating optimized molecular geometry [17]. Prior to docking, DFT calculations were used to ascertain the accurate bond distances, angles, dihedrals and optimized conformations in the lowest energy state of each of the selected compounds in this study. All the computations were carried out using Gaussian 09 package of codes (<http://www.gaussian.com/>) at the Tizard supercomputer server of eResearch SA (<https://www.ersa.edu.au/tizard>). Calculations were carried out in no symmetry to facilitate full rearrangement and relaxation of the structures to their most stable form.

Fully optimized ligand structures were then allowed to dock with the model A β ₁₋₄₂ monomer and oligomeric pre-fibrillar pentamer β -sheet structures. The docking software used a PLANTS_{PLP} empirical scoring function to identify the optimal solution from its docking based on a hybrid search algorithm, denoted as guided differential evolution [13,18]. A β ₁₋₄₂ monomer structure in solution

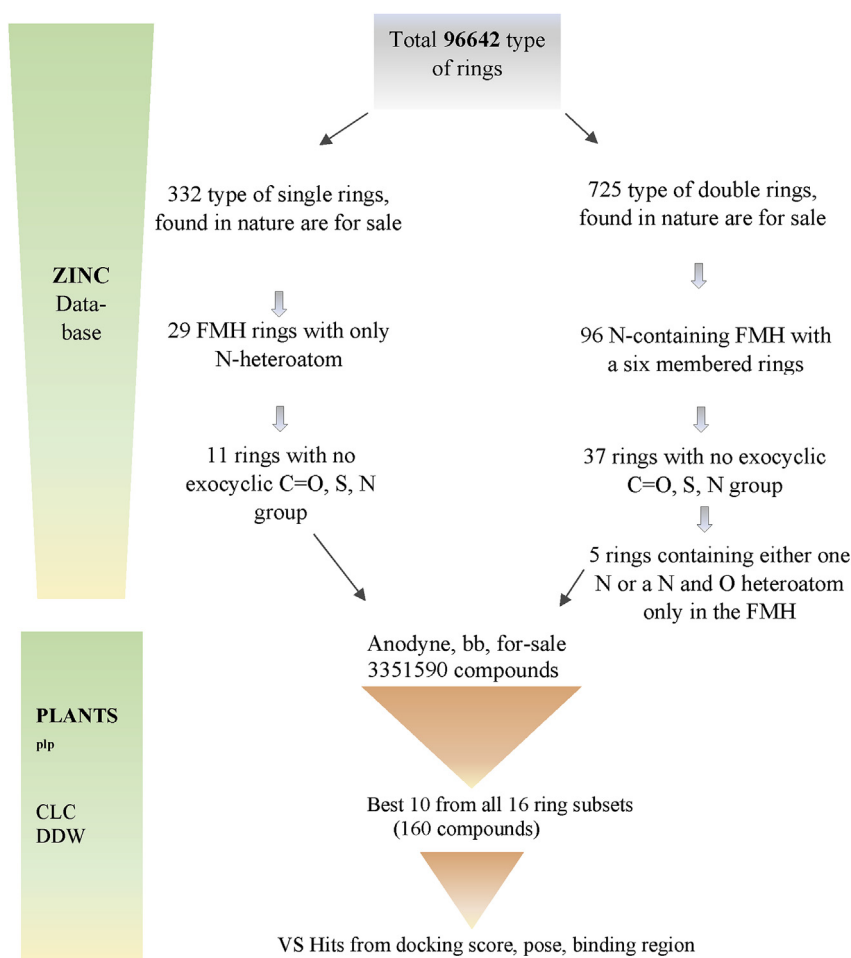


Fig. 2. Schematic of the VS protocol. The ring subsets of ZINC database was filtered for N-heteroatom FMH single and double rings, found in nature. Subsequently, 16 ring subsets were further filtered for anodyne, bb, and for-sale and then docked with PLANTS_{PLP} scoring function. Best 10 compounds from all subsets were visually inspected for their binding interaction. Finally five compounds were selected and redocked with their optimized structures.

as determined by NMR (PDB ID: 1IYT) and A β _{17–42} oligomer forming parallel, in register beta-sheet structures as determined by NMR (PDB ID: 2BEG) were used as model A β structures without any further modification. The A β _{1–42} monomer structure possessed an alpha helical conformation with a beta-turn in solution, which was suggested to be associated with membrane poration [19]. The oligomeric β -sheet structure showed a correlation with neurotoxicity and provided a structural basis for studies with fibrillation inhibitors [20]. A β _{1–42} does not have any known singular pharmacophore and no crystalized A β _{1–42} structure with small molecule, co-crystalized ligand was available. Therefore, a large search space was created covering the whole protein for binding sites. During docking, all ligand structures were kept flexible to allow rotation of any bonds in order to bind A β _{1–42}. Out of the top ten docking results, the best binding poses with a high score were analysed. The docking scores of the Thioflavin T molecule, a known binder of A β _{1–42}, was used as a standard value. Results were summarized as a docking score and interacting residues in Tables 1 and 2.

2.4. Thioflavin T assay and microscopy of A β fibril and aggregate formation

Thioflavin T (ThT) binds to β -amyloid fibrils, with fluorescence increasing proportionally to the amount of fibrils present in solution. The ThT assay was used to confirm fibril formation over time with β -amyloid in cell-free solution, in addition to determining if fibril formation was directly affected by the test compounds. In order to avoid any interference with the fluorescence output, all compounds were first dissolved in DMSO at 37 °C and vortexed repeatedly until it dissolved fully. They were then further diluted in

PBS to the desired working concentration. ThT (10 μ M in PBS) was added to wells on a microplate together with non-fibrillar A β _{1–42} (10 μ M) and the test compound (each at 100 μ M). Fluorescence was then measured at 37 °C every 10 min for 48 h using a Synergy MX microplate reader (Bio-Tek, Bedfordshire, UK) with excitation and emission wavelengths at 446 nm and 490 nm respectively. ThT output from all treatment groups was normalized to blank values (ThT alone in PBS).

Transmission electron microscopy (TEM) was used to visualize A β aggregates and fibrils and to investigate the effects of selected compounds on A β morphology. Samples were prepared by incubating native A β _{1–42} (10 μ M) in PBS, either alone or with test compounds (100 μ M each) for 48 h at 37 °C. A 400 mesh formvar carbon-coated nickel electron microscopy grid (Proscitech, Kirwan, QLD, Australia) was first treated in a plasma cleaning system (Solarus 950 Gatan Advanced Plasma System) to make it more hydrophilic. Then a 5 μ l sample was placed onto the grid and after 1 min this sample was blotted off using filter paper. 10 μ l of contrast dye containing 2% uranyl acetate was then placed onto the grid, left for 1 min and blotted off with filter paper. Grids were then loaded onto a specimen holder and then into a FEI Tecnai G2 Spirit Transmission Electron Microscope (FEI, Milton, QLD, Australia). Sample grids were then viewed using a magnification of 34000–92000 \times . Grids were extensively scanned manually in search of fibrils and representative images were taken.

2.5. Neuronal cell culture

Rat Phaeochromocytoma cells (Ordway PC12) displaying a semi-differentiated phenotype with neuronal projections were kindly

Table 1
Docking profile of test compounds with A β _{1–42} monomer (PDB ID: 1IYT).

Ligand	Interacting residues	H-bond forming residues	Docking score	Steric interaction score	H-bond score	RMSD (Å)
Compound 1	Lys 16, Leu 17, Val 18, Phe 20, Ala 21 Val 24, Gly 25, Ile 31, Leu 34, Met 35	–	–58.01	–61.29	0.00	8.46
Compound 2	His 14, Leu 17, Val 18, Phe 19, Ala 21 Glu 22, Val 24, Gly 25, Ser 26	Glu 22	–54.52	–54.03	–4.00	9.47
Compound 3	Gln 15, Lys 16, Val 18, Phe 19, Glu 22	Lys 16	–46.21	–46.79	–2.00	9.43
Compound 4	Asp 7, Ser 8, Gly 9, Glu 11, Val 12, Gln 15, Lys 16, Phe 19	Asp 7 Gln 15	–49.26	–51.28	0.00	10.42
Compound 5	His 6, Gly 9, Tyr 10, Val 12, His 13,14 Gln 15, Leu 17, Val 18, Ala 21	–	–50.84	–54.51	0.00	15.11
Thioflavin T	Val 12, His 13, Gln 15, Lys 16, Phe 19	–	–41.80	–43.32	0.00	8.48

Table 2
Docking profile of test compounds with A β _{17–42} oligomer (PDB ID: 2BEG).

Ligand	Interacting residues	H-bond forming residues	Docking Score	Steric interaction score	H-bonding score	RMSD (Å)
Compound 1	Leu 17 ^{A,B,C,D,E} , Val 18 ^{A,B,C,D,E} Phe 19 ^{A,B,C,D,E} , Gly 37 ^{C,D,E} , Gly 38 ^{C,D,E} Val 39 ^{B,C,D,E} , Val 40 ^{B,C,D,E} , Ala 42 ^{D,E}	–	–87.69	–90.24	0.00	19.07
Compound 2	Leu 17 ^{C,D,E} , Val 18 ^{B,C,D,E} , Phe 19 ^{B,C,D,E} Phe 20 ^E , Gly 37 ^{D,E} , Gly 38 ^{D,E} Val 39 ^{D,E} , Val 40 ^{C,D,E}	–	–77.71	–81.25	0.00	23.75
Compound 3	Leu 17 ^{A,B,C,D,E} , Val 18 ^{A,B,C,D,E} Phe 19 ^{A,B,C,D,E} , Gly 37 ^D , Gly 38 ^{D,E} Val 39 ^{B,C,D,E} , Val 40 ^{B,C,D,E}	Leu 17 ^C	–73.86	–73.08	–3.62	18.44
Compound 4	Leu 17 ^{A,B,C,D,E} , Val 18 ^{A,B,C,D,E} Phe 19 ^{A,B,C,D,E} , Gly 37 ^{D,E} Gly 38 ^{D,E} , Val 39 ^{B,D,E} , Val 40 ^{B,C,D,E}	Leu 17 ^C	–71.44	–71.91	–2.00	18.53
Compound 5	Leu 17 ^{A,B,C,D,E} , Val 18 ^{A,B,C,D,E} Phe 19 ^{A,B,C,D,E} , Gly 37 ^{D,E} , Gly 38 ^{D,E} Val 39 ^{B,D,E} , Val 40 ^{B,C,D,E}	Leu 17 ^C Val 39 ^E	–77.91	–80.62	–3.04	21.77
Thioflavin T	Leu 17 ^{C,D,E} , Val 18 ^{B,C,D,E} Phe 19 ^{B,C,D,E} , Gly 37 ^{C,D,E} , Gly 38 ^{C,D,E} Val 39 ^{C,D,E} , Val 40 ^{C,D,E}	–	–65.53	–69.45	0.00	21.00

donated by Professor Jacqueline Phillips (Macquarie University, NSW, Australia) [21]. Cells were maintained in RPMI-1640 media with 10% fetal calf serum (FCS), 1% L-glutamine, 1% non-essential amino acids and 1% penicillin/streptomycin. Cells were seeded at 2×10^4 cells per well in RPMI-1640 with 10% FCS. PC12 cells were equilibrated for 24 h before treatment with test compounds and/or A β_{1-42} .

2.6. A β and compound preparation

Native, non-fibrillar A β_{1-42} was prepared by dissolving in 1% DMSO to yield a protein concentration of 3.8 mM. Sterile PBS was added to prepare a final concentration of 100 μ M. Amyloid was then dispensed into aliquots and immediately frozen at -70 °C until required. All test compounds were initially diluted in DMSO and then in PBS to their final stock concentrations prior to addition to cells.

2.7. Neuronal cell treatment and viability measurements

Undifferentiated PC12 cells were treated with each of these compounds at 100 μ M, 15 min prior to incubation with A β_{1-42} (0–0.5 μ M). Cells were then incubated for 48 h at 37 °C, 5% CO $_2$ prior to measurement of cell viability. To assess each of the test compound's direct effects on cell viability, each compound was incubated with PC12 cells for 48 h at 37 °C, 5% CO $_2$ along with a vehicle over a concentration range 0–100 μ M. After 48 h, PC12 cell viability was determined using the thiazolyl blue tetrazolium bromide (MTT) assay. After incubation, 96-well plates had all media removed and replaced with serum-free media containing 0.25 mg/ml of MTT. The plate was further incubated for 2 h at 37 °C with 5% CO $_2$, then MTT solution was removed and cells were lysed with DMSO. Absorbance was measured at 570 nm using a Synergy MX microplate reader (Bio-Tek, Bedfordshire, UK).

2.8. Statistical analysis

Data obtained from the MTT assay was analysed via a two-way analysis of variance (ANOVA) to assess neuronal cell viability arising from incubation in A β_{1-42} , alone or in the presence of test compounds, with a Bonferroni's post-hoc test used to determine the significance level for each test compound treatment interaction at each A β_{1-42} concentration. Area under the curve analysis for Thioflavin T (ThT) fluorescence data was analysed using one way ANOVA with a Dunnett's multiple comparisons test used for determining the significance of these tested compounds effects versus A β_{1-42} . A significance value of $p < 0.05$ was used for all experiments. Data analysis and production of graphs was performed in GraphPad Prism 6 for Windows (GraphPad Software, San Diego, USA).

3. Results

3.1. Selection of compounds by virtual screening method

In this study we attempted to identify compounds which bear a N-heteroatom five membered heterocycle (FMH) ring without any exocyclic C=O, C=S or C=N group, as opposed to common five membered multi-heterocyclic (FMMH) lead-like molecules, which may bind and alter A β_{1-42} aggregation. The 16 type of rings filtered from ZINC contained FMH rings bearing between 1 and 4 nitrogen heteroatoms. Out of their best 10 screening results, the five highest scoring ligands from three subsets were selected. These subsets were imidazolidine (2 nitrogen FMH), triazole (3 nitrogen FMH) and benzoxazole (1 nitrogen, 1 oxygen fused FMH) groups.

Extensive molecular docking screening simulations demonstrated that the saturated 2-nitrogen rings such as imidazolidine, followed by pyrazolidine, exhibited higher docking scores than unsaturated ring types. Between the 2-nitrogen ring ligands, the dibenzyl phenyl imidazolidine structures with the FMH at the center and both N atoms bonded to dibenzyl side chains exhibited the highest binding scores. Both Compound 1 and 2 were selected in order to understand i) whether the dibenzyl phenyl imidazolidine scaffold, present in both compounds, would render anti-aggregation properties as predicted from docking, and ii) the impact of an extra O-methyl group in the phenyl group with respect to this scaffold's effects on A β_{1-42} aggregation and associated neurotoxicity. Since they both possessed a common scaffold, a positive *in vitro* result for both compounds would corroborate the anti A β_{1-42} potential of this scaffold. The triazole compounds (triazole sulfanyl acetamide scaffold of Compound 3 and 4) were the next subset that displayed high binding scores against both A β_{1-42} conformations (Table 1). They were selected to in order to gain an understanding of the 3-nitrogen FMH scaffold and any role of an extra terminal methyl group related to effects on A β_{1-42} aggregation. Thereafter, we were interested in selecting compounds with 1-nitrogen in the FMH. Of these, benzoxazole ligands showed favourable binding scores when compared to other 1-nitrogen FMH ligands. Compound 5, being a fused benzoxazole ring provided a docking score similar to Compound 2 and so provided insights into how such structural variations comparatively affected A β_{1-42} aggregation.

3.2. Molecular modelling of compounds optimized structures: effects on binding to A β monomer and oligomer

The optimized structure of Compound 1 and 2 revealed that Compound 2 had a different ground state conformation than Compound 1 (supplementary material, Fig. 3). Compound 1 was more planar than Compound 2, with the terminal benzene ring puckered and sitting out of plane in Compound 2. The optimized structures of each of the five compounds were allowed to dock to the model A β_{1-42} monomer and oligomer. In the monomer, Compound 1 bound near the hinge region of the protein (Fig. 3a, nearby residues were shown). Compound 2 bound to the front of the protein (Fig. 3b, nearby residues were shown). One functionality of the docking algorithm PLANTS is 'ligand torsional potential' as implemented in the Tripos force field that is calculated for all the rotatable bonds available in the ligand molecule, with the exception of terminal hydrogen bond-donating groups [22]. Since Compound 1 had 8 rotatable bonds and Compound 2 had 9 rotatable bonds, they were likely to undergo a higher torsional optimization of their molecular geometry as calculated by the DFT method after docking. As seen in Fig. 3a–b and Fig. 4a–b, the docked conformations of both Compound 1 and 2 were more twisted when compared to their optimized 3D conformation (Fig. 3, Supplementary Material).

Compound 3 and 4 bound to the same region underneath the protein surface (Fig. 3c and d, nearby residues were shown). Compound 3 was positioned in the binding pocket and formed H-bonding with Lys 16, whereas Compound 4 bound in the pocket by bending at the sulfanyl group (Fig. 3c and d, nearby residues are shown). Compound 5 docked in a binding pocket anterior to the protein (Fig. 3e, nearby residues are shown).

The oligomeric A β_{17-42} conformation was made up of five chains of A β (chain A,B,C,D,E), aligned side by side to form a β -sheet like structure. All the compounds bound with different docking poses to the hydrophobic pocket formed by chain B,C,D,E; residues Leu 17, Val 18, Phe 19 and Gly 37, Gly 38, Val 39, Val 40 (Fig. 4a–e). Compound 1 bound inside this pocket with a benzyl ring posing outward and parallel to the plane of the protein (Fig. 4a), therefore interacting with most of the residues in the pocket but without

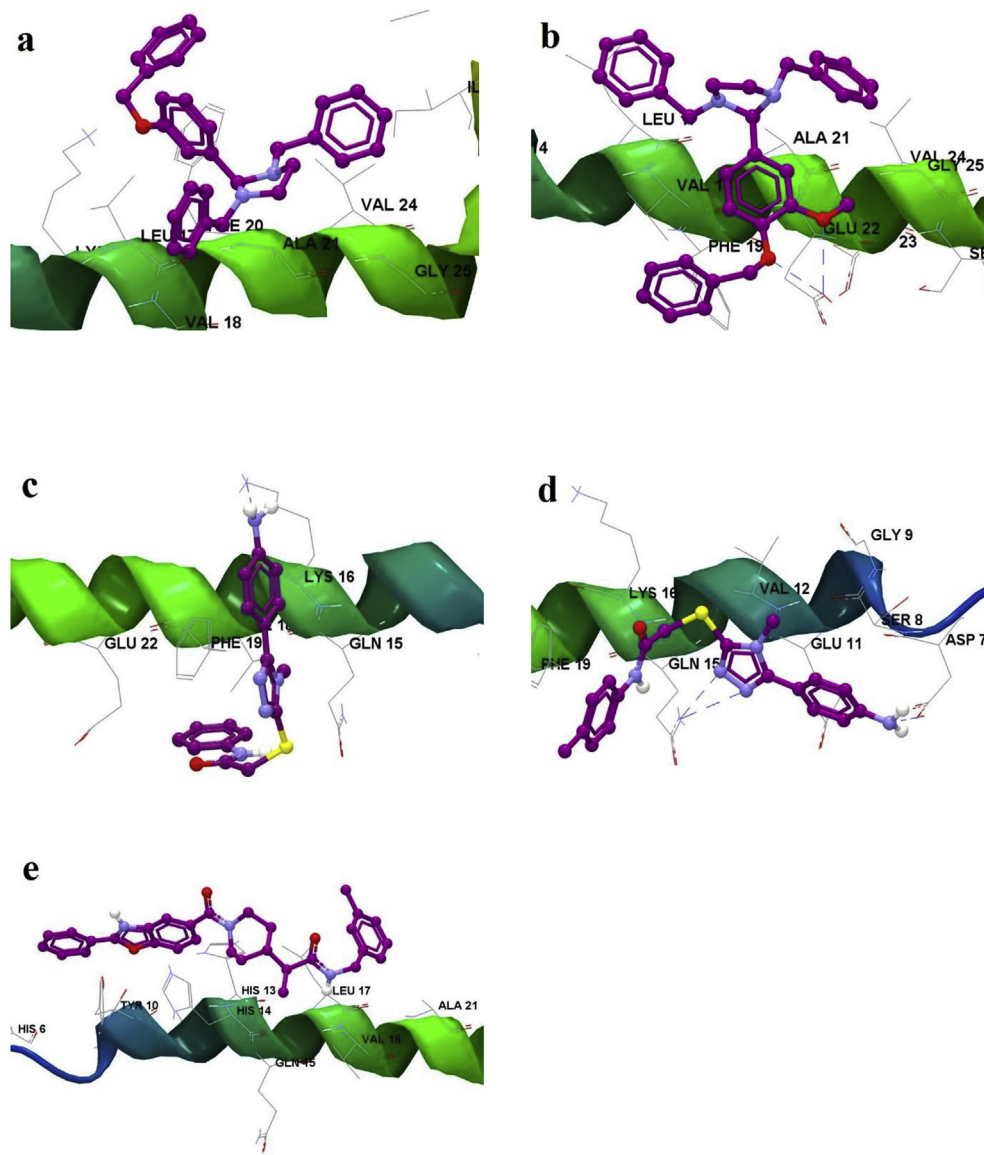


Fig. 3. Binding of each of the five optimized compound conformations to $A\beta_{1-42}$ monomer (PDB ID: 1IYT): (a) Compound 1, (b) Compound 2, (c) Compound 3, (d) Compound 4 and (e) Compound 5. Binding properties are provided in Table 1.

forming hydrogen bonding. Compound 2 bound to this pocket with its phenyl group, but its dibenzyl imidazolidine moiety was placed outside the protein structure (Fig. 4b). Like Compound 1, it did not form any hydrogen bonding. Compound 3 and 4 bound inside the pocket, forming hydrogen bonding (Fig. 4c, Table 2). Compound 5 bound across the pocket with its phenyl group connected to benzoxazole ring, positioned outside the oligomer (Fig. 4d). Among the five compounds, Compound 1 showed the highest docking score (Table 2). Compound 2 and 5 had similar scores, but with different poses. Compound 3 and 4 had similar scores, while Compound 3 showed higher H-bond score than Compound 4.

3.3. Thioflavin T fluorescence of $A\beta_{1-42}$ fibrillisation kinetics

Thioflavin T (ThT)-based fibrillisation kinetics of $A\beta_{1-42}$ demonstrated a gradual increase in fluorescence output until approximately 600 min (10 h), indicative of maximum fibril and aggregate formation (Fig. 5a). Thereafter, ThT fluorescence levels increased steadily up to 1560 min (26 h) and stabilized over the

duration of the assay, up to 2880 min (48 h). Among the five test compounds, Compound 2, 3 and 4 (imidazolidine and triazole acetamides respectively) notably inhibited the development of ThT fluorescence from the initial period of fibrillisation and continuing over the duration of assay. Area under the curve analysis showed extensive and significant overall inhibition of fibril formation in the presence of each of Compound 2, 3 and 4 (each at 100 μ M) over this time course (Fig. 5b). By contrast, Compound 1, another imidazolidine, did not affect the ThT fluorescence output over the duration of assay (Fig. 5c). Compound 1 itself did not generate auto fluorescence, either alone or with ThT (data not shown). Interestingly however, when Compound 5 was incubated with $A\beta_{1-42}$, it showed markedly higher fluorescence output than $A\beta_{1-42}$ alone (Fig. 5c). Further examination revealed that even in absence of $A\beta_{1-42}$, Compound 5 and ThT yielded higher fluorescence output than Compound 5, $A\beta_{1-42}$ and ThT combined (Fig. 5c). Whereas, Compound 5 alone, in the absence of ThT, produced very low fluorescence. This indicated a possible spectroscopic/fluoroscopic interaction between Compound 5 and Thioflavin T.

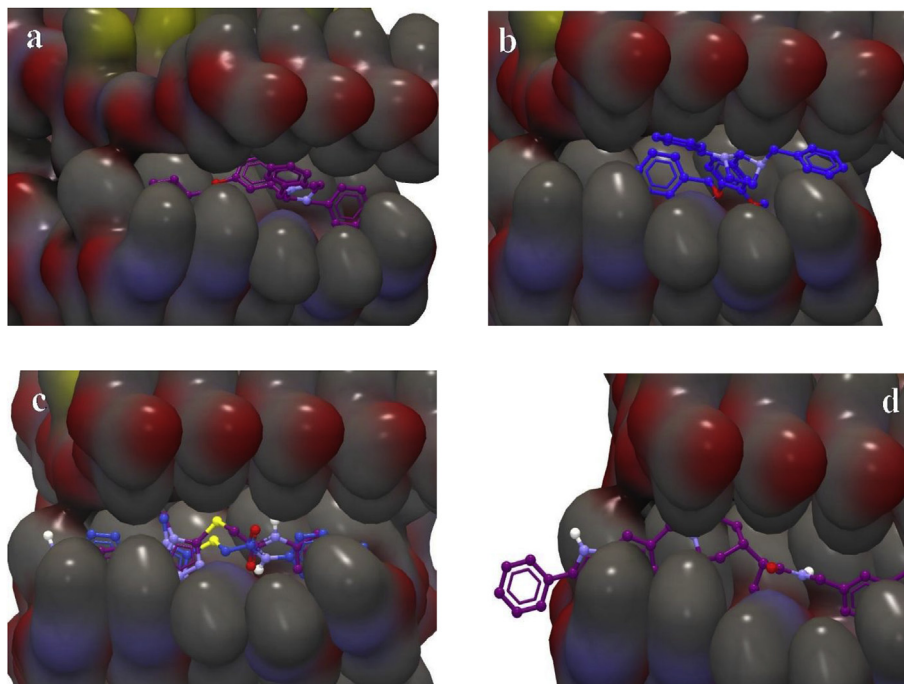


Fig. 4. Binding of each of the five compounds optimized conformations to A β_{17-42} oligomer (PDB ID: 2BEG): (a) Compound 1, (b) Compound 2, (c) Compound 3 and 4 together in the same binding region, (d) Compound 5. Binding properties are provided in Table 2.

3.4. Transmission electron microscopy of A β_{1-42} fibrils

On microscopic evidence, the morphology of β amyloid fibrils was affected by incubation with each of the compounds to varying degrees. For A β_{1-42} alone, the fibrils were relatively long, slightly rough edged and intertwined in a rope-like manner (Fig. 6a). In the presence of Compound 1, the fibrils appeared to be thinner, shorter in length and loosely attached to each other (Fig. 6b). Compound 2 also elicited thinner, loosely attached and relatively shorter fibrils (Fig. 6c). However, in Compound 1 treated samples, the fibrils appeared to be smoother, whereas in Compound 2 treated samples, the fibrils appeared to be relatively uneven. Fibrils in Compound 3 and 4 treated samples appeared to be thinner, uneven and with some mesh-like structures indicative of small and punctate aggregates (Fig. 6d–e). With the exception of Compound 5, overall fibril appearance was less dense when compared to A β_{1-42} control samples. In contrast, treatment with Compound 5 showed visibly more fibrils than A β_{1-42} control samples (Fig. 6f). These fibrils were more prevalent than control with an extended length and smoothed appearance.

3.5. Effects of compounds on neuronal cell viability

The MTT assay of cell viability demonstrated that Compounds 1 and 2 did not elicit significant toxicity to PC12 cells over the full concentration range of 1–100 μ M after 48 h (Fig. 7). By contrast, Compound 3 exhibited moderate (20%–25%) toxicity and Compound 4 caused comparatively higher toxicity (60%) than Compound 3 after 48 h at 100 μ M. Compound 5 demonstrated the highest toxicity among the five compounds, with 35% toxicity at 10 μ M increasing in a concentration-dependent manner to over 87% at 100 μ M.

3.6. Effects of test compounds on A β_{1-42} mediated neurotoxicity

Incubation with A β_{1-42} (0.1–0.5 μ M) over 48 h evoked a

significant decrease in cell toxicity by a maximum of 35% (Fig. 8). Notably, treatment with Compound 1 and 2 (100 μ M) provided a significant degree of neuroprotection against A β exposure over the full concentration range of A β_{1-42} . Treatment with Compound 3 (100 μ M) maintained 73%–78% cell viability over the full concentration range of A β_{1-42} , consistent with its intrinsic modest toxicity profile as demonstrated in Fig. 6. The effects of Compounds 4 and 5 against A β -mediated neuronal toxicity on PC12 cells could not be measured, due to their intrinsic toxicity to PC12 cells. However, the toxicity of Compound 3, 4 and 5 did not increase in combination with A β exposure (data only shown for Compound 3).

4. Discussion

These studies have successfully applied virtual screening methods and identified and compared the A β_{1-42} anti-aggregative properties of five synthetic heterocyclic compounds. Among them, two (Compound 1 and 2) were neuroprotective against A β induced toxicity *in vitro*. All of these compounds bear an N-containing five membered heterocycle ring, without exocyclic C=S/O/N groups. Both Compound 1 and 2 possessed a dibenzyl phenyl imidazolidine scaffold and Compound 3 and 4 possessed a triazole sulfanyl acetamide scaffold. Compound 5 possessed a benzoxazole piperidine propanamide scaffold. To the best of our knowledge, these five membered heterocyclic scaffolds, such as an imidazolidine linked with a di-benzyl group, or triazole linked with a sulfanyl acetamide group, have not been reported previously for their potential as A β_{1-42} aggregation inhibitors. *In silico* virtual screening simulations have been used to identify potential A β_{1-42} inhibitors from a chemical database containing desired functional groups previously [24]. In the present study, the *in silico* modelling was also used to compare the probable binding sites and affinity in the A β monomer and oligomer as a predictive tool for the interaction with A β_{1-42} protein that may mitigate aggregation and toxicity.

Compound 1 and 2 both exhibited higher binding scores with monomeric as well as oligomeric A β , blunted the elongated fibril

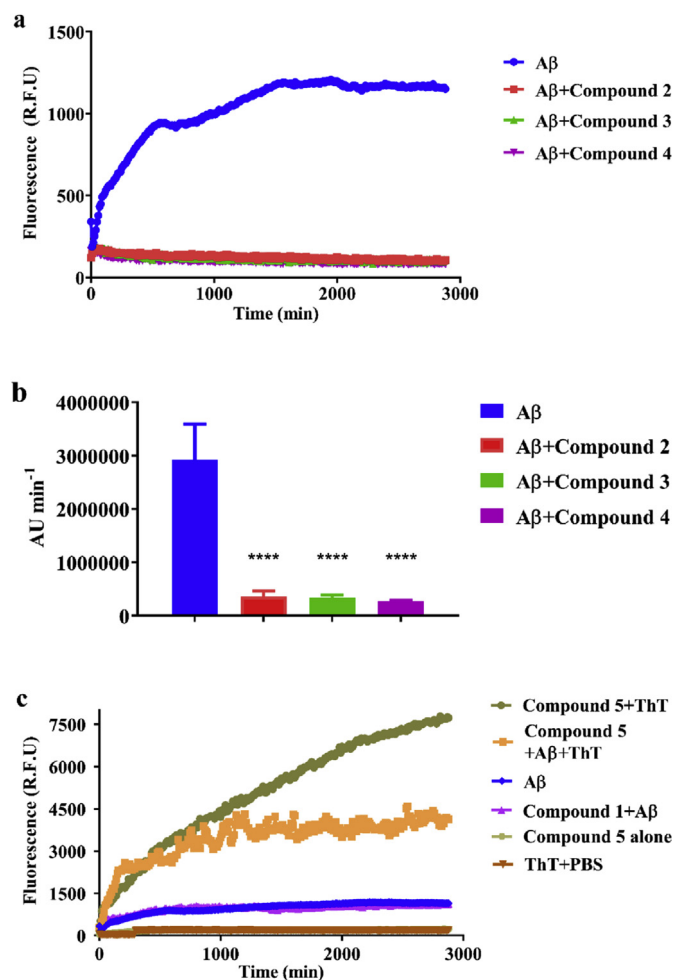


Fig. 5. (a) Thioflavin T (ThT) fluorescence indicative of amyloid A β_{1-42} fibrillation kinetics, alone and in the presence of each of the Compound 2, 3 and 4 (100 μ M each) over 48 h in cell-free PBS solution. Each of Compound 2, 3 and 4 significantly inhibited ThT fluorescence throughout 48 h. (b) Area under the curve analysis of ThT kinetics demonstrated significant overall inhibition of amyloid fibrillation from incubation with Compounds 2, 3 and 4. (c) ThT fluorescence indicative of amyloid A β_{1-42} fibrillation kinetics, alone and in the presence of each of the Compound 1 and 5 (100 μ M each) over 48 h in cell-free PBS solution. Additional curves in absence of A β_{1-42} , exhibited ThT fluorescence of Compound 5 with ThT, Compound 5 alone and ThT alone over 48 h in cell free PBS solution. Compound 1 did not inhibit ThT fluorescence. Compound 5 with A β_{1-42} increased ThT fluorescence and fluorescence was the highest with only ThT, excluding A β_{1-42} . (**** $P < 0.0001$; mean \pm SEM of $n = 4$ experiments).

morphology and demonstrated significant neuroprotection against A β_{1-42} mediated neurotoxicity in PC12 cells. Compound 2 significantly inhibited ThT fluorescence, however Compound 1 had no influence on ThT fluorescence. DFT-B3LYP level of calculation for structure optimization revealed that although Compound 1 and 2 are structurally similar in possessing a dibenzyl phenyl imidazolidine scaffold, the addition of one methoxy group and displacement of the benzyloxy group from C7 to C8 in the phenyl ring disrupted the planarity of Compound 2 (Fig. 3, supplementary material), possibly due to two vicinal oxygen atoms. Compound 1 was relatively more planar with regards to the phenyl extension from the imidazolidine ring than Compound 2. Co-planarity of aromatic moieties have been considered important for actions against amyloid fibril formation and attributed to favourable hydrophobic and π -stacking interactions in some natural compounds [23]. It was likely that the planarity of Compound 1 facilitated binding to A β in a way that altered toxic fibril formation, but did not impede Thioflavin T

integration into the developing fibrils. While Compound 1 bound to a similar pocket as Thioflavin T in the β -sheet oligomer, Compound 2 bound to a different pocket (Fig. 4a–b, supplementary material). Conversely, Compound 2 had multiple binding pockets in that hydrophobic region making it a more flexible binder. As discussed by Murugan et al. [24], having similar binding regions in the hydrophobic core of the A β oligomer increased the possibility of cross interaction between a highly specific binder and a tracer molecule. As a result, interpretation of A β binding from a tracer molecule like ThT should be carefully evaluated. It was possible that Compound 1 was unable to displace ThT within the competing binding pocket of A β , which resulted in no inhibition of ThT fluorescence. In contrast, Compound 2, as a flexible binder, was less prone to a competing cross interaction with ThT and therefore still able to bind in multiple sites of A β and inhibit fluorescence [25]. Compound 1 exhibited a high steric interaction score to the A β_{17-42} pentamer (Table 2), indicating the formation of a stable, bound complex with the oligomeric form of the protein. Avid binding to the A β pentamer is of particular importance in terms of reducing toxicity, as the oligomeric form has been suggested to be the most neurotoxic [26]. Other modes of neuroprotection against A β_{1-42} exposure are the stabilization of oligomers rather than complete ablation of aggregation, diverting alloforms into off-target pathways that abrogate neurotoxicity [27]. A similar phenomenon may have also occurred to mitigate A β neurotoxicity in the present study.

In the case of the other dibenzyl phenyl imidazolidine (Compound 2), a clear correlation was observed related to its favourable molecular binding to A β protein and its anti-fibrillar action. This was inferred by both the extensive inhibition of ThT fluorescence and morphological evidence of fibril modification via TEM imaging, with its A β anti-aggregatory activity also translating to a neuroprotective capacity. The non-planar conformation of Compound 2 might contribute to its ability to bind at multiple sites in the A β_{1-42} monomer and oligomer. Hydrogen bonding did not seem to play a major role for the A β interaction with each of these two imidazolidine compounds. From this study, we can infer that with respect to neuroprotection against A β , that i) non-planar conformation of dibenzyl phenyl imidazolidine scaffold might assist in attenuating ThT kinetics but are not important for neuroprotection, and ii) Compound 1 might have other modes of protection against A β_{1-42} -mediated neurotoxicity than solely via anti-aggregation. These findings, combined with a lack of intrinsic neurotoxicity, suggest that the dibenzyl phenyl-imidazolidine scaffold is a useful template for further development.

The other two structurally related triazole sulfanyl acetamides, Compound 3 and 4 also exhibited a correlation related to the favourable molecular binding to A β protein and its effect on fibril morphology and aggregate formation. This was ascertained by both the extensive inhibition of ThT fluorescence and evidence of fibril morphology modification via TEM imaging. The appearance of A β_{1-42} in the presence of Compound 3 resembled thin, unevenly textured fibrils. Additionally, in the presence of Compound 4, some small mesh-like structures were also observed. Such fibrillar structures were likely to undergo the loss of surface area present in the longer ‘rope-like’ A β fibrils in which ThT binds to account for these significant reduction in fluorescence output [28]. Appearance of these thin fibrillar structures after co-incubation with triazoles somewhat resembled that of another noted A β aggregation inhibitor, the N-containing heterocyclic aromatic (benzotrizinone) compound by Catto et al. [29]. Reviewing the docking study showed both Compound 3 and 4 demonstrated high binding scores, however, unlike the imidazolidines, H-bonding interactions played a key role in their binding. With the monomer, Compound 3 formed H-bond with residue Lys 16. A study on natural polyphenol binding to A β had shown that residue Lys 16 appears to be

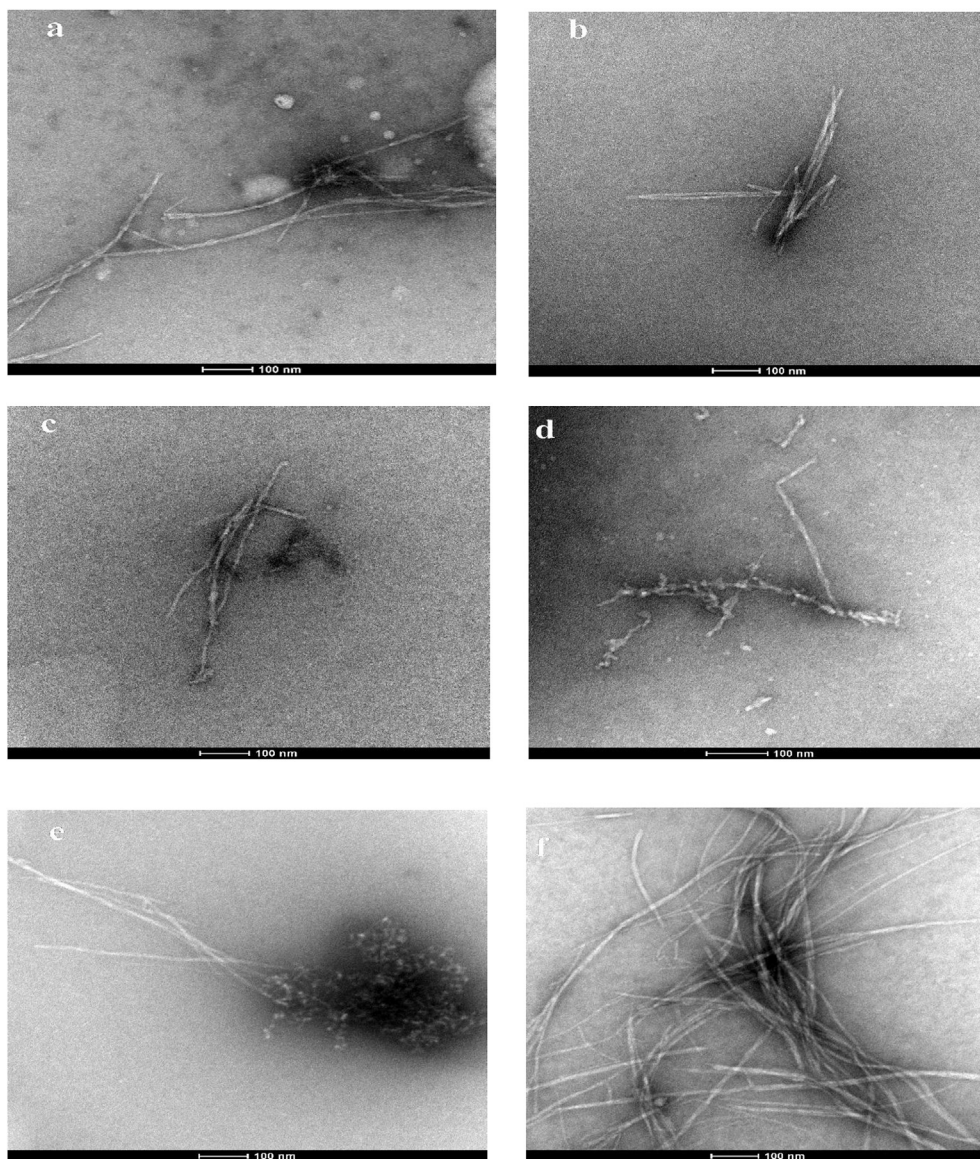


Fig. 6. Representative transmission electron micrographs of $A\beta_{1-42}$ fibrils, alone and following 48 h incubation with all five compounds (each at 100 μM): (a) $A\beta_{1-42}$, (b) $A\beta_{1-42}$ and compound 1, (c) $A\beta_{1-42}$ and compound 2, (d) $A\beta_{1-42}$ and compound 3, (e) $A\beta_{1-42}$ and compound 4 and (f) $A\beta_{1-42}$ and compound 5. Scale bar: 100 nm.

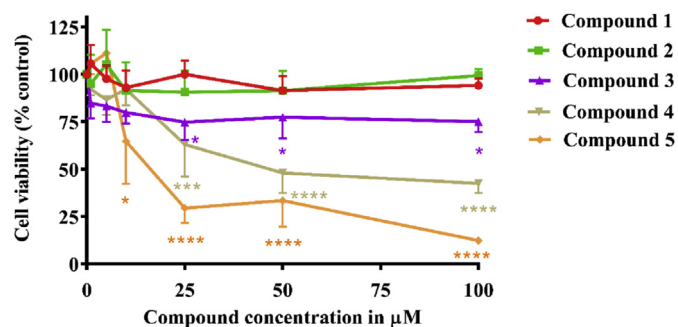


Fig. 7. MTT assay representing neuronal PC12 cell viability following 48 h incubation with Compounds 1–5 (1–100 μM). Compound 1 and 2 did not have any significant toxicity at any of the test concentrations. Compound 3 had moderate toxicity at 10 μM or higher concentration. Compound 4 showed significant toxicity from 25 μM . Compound 5 was the most toxic among these compounds. (**** $P < 0.0001$ for each compounds vs. control; mean \pm SEM of $n = 4$ experiments).

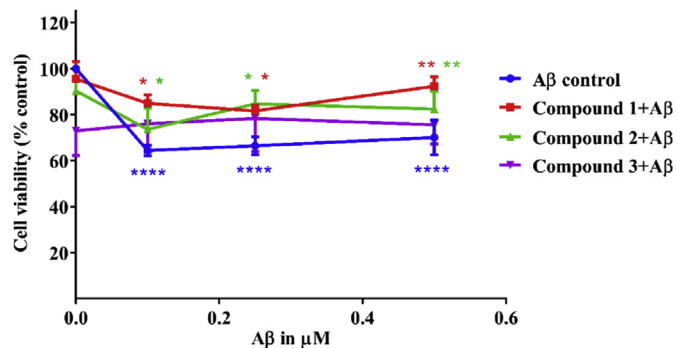


Fig. 8. MTT assay representing PC12 cell viability following 48 h of $A\beta_{1-42}$ incubation, alone or with each of Compounds 1–3 (100 μM). Compound 1 and 2 exerted significant neuroprotection over the full concentration range of $A\beta_{1-42}$. Increase in cell viability seen with Compound 3 was not significant. Compound 4 and 5 was not shown due to their significant toxicity to PC12 cells. (**** $P < 0.0001$ for each compounds vs $A\beta_{1-42}$ (0.1–0.5 μM); mean \pm SEM of $n = 4$ experiments).

an important factor in promoting A β ₁₋₄₂ toxicity [30]. Nevertheless, it was not possible to predict whether the resultant triazole sulfanyl acetamide-modified A β was benign or toxic to neuronal cells solely from the cell viability assay. Individually Compound 3 displayed moderate toxicity to PC12 cells at test concentration of 100 μ M. Compound 4, which shared the same structure with compound 3 except for an additional terminal methyl group, was found to be substantially more toxic to PC12 cells. This may be due to the sulfanyl 1,2,4 triazole group's anti-proliferative property, as seen with several other structurally related amino sulfanyl 1,2,4 triazole derivatives [31]. Thus, while the A β anti-aggregative property of this triazole sulfanyl acetamide scaffold was mechanistically insightful, further development may be hampered by its intrinsic toxicity.

Among the five selected compounds, Compound 5 was the most unique due to its size and presence of various functional groups, including the fused benzoxazole ring. It showed reasonably high binding scores to both forms of A β from the docking data. However, its unusually high background ThT fluorescence output (even in the absence of A β ₁₋₄₂) and its enhancement of A β ₁₋₄₂ fibrillisation, together with marked neurotoxicity, limited its further utility in this study. The direct fluoroscopic interaction with ThT might have been due to steric hindrance to the intramolecular rotation of ThT. Additionally, the benzoxazole group in Compound 5 might behave like the benzothiazole group in ThT, both by binding to A β ₁₋₄₂ and generating fluorescence [33]. TEM imaging in Compound 5 also revealed both a greater amount and extended length of fibrils compared to A β ₁₋₄₂ control. From docking of Compound 5 to A β oligomer, we hypothesized that the phenyl group placed outside the oligomer promoted further fibril elongation as seen in the TEM imaging, by attracting hydrophobic elements of the monomer which might in part contribute to higher ThT fluorescence than A β alone. Other compounds bearing a similar phenyl benzoxazole moiety as Compound 5 exhibited DNA intercalating and pro-apoptotic properties in a melanoma cell line [34]. This property of the phenyl benzoxazole moiety might in part contribute to its cell toxicity. So, while collectively the fibril-promoting and fluorophoric nature of Compound 5 was interesting, its marked neurotoxicity limited its further investigation.

5. Conclusions

In conclusion, imidazolidines and triazole acetamide scaffolds have demonstrated anti-aggregatory properties against A β ₁₋₄₂. Their varying affinity and binding sites differentially affected A β ₁₋₄₂ fibrillisation kinetics and morphology in addition to a spectrum of effects on cell viability. Nonetheless, we have identified a novel dibenzyl phenyl imidazolidine scaffold that was shown to be favourable for both A β ₁₋₄₂ anti-aggregatory and neuroprotective actions, and as such might be a promising pharmacotherapeutic lead for further development in Alzheimer's disease.

Acknowledgements

The authors would like to thank Dr. Tara Pukala, School of Chemistry and Physics, The University of Adelaide for access to Gaussian'09 software and assistance with purity assessment of compounds through NMR analysis and Lyn Waterhouse, Microscopist, Adelaide Microscopy for assistance with TEM.

Appendix A. Supplementary data

Supplementary data related to this article can be found at <http://dx.doi.org/10.1016/j.ejmech.2017.02.057>.

References

- [1] M. Ahmed, J. Davis, D. Aucoin, T. Sato, S. Ahuja, et al., Structural conversion of neurotoxic amyloid- β 1-42 oligomers to fibrils, *Nat. Struct. Mol. Biol.* 17 (2010) 561–567.
- [2] D.M. Walsh, I. Klyubin, J.V. Fadeeva, W.K. Cullen, R. Anwyl, M.S. Wolfe, M.J. Rowan, D.J. Selkoe, Naturally secreted oligomers of amyloid β protein potently inhibit hippocampal long-term potentiation in vivo, *Nature* 416 (2002) 535–539.
- [3] W.L. Klein, G.A. Krafft, C.E. Finch, Targeting small A β oligomers: the solution to an Alzheimer's disease conundrum? *Trends Neurosci.* 24 (2001) 219–224.
- [4] A.J. Doig, P. Derreumaux, Inhibition of protein aggregation and amyloid formation by small molecules, *Curr. Opin. Struct. Biol.* 30 (2015) 50–56.
- [5] B.S. Harvey, I.F. Musgrave, K.S. Ohlsson, A. Fransson, S.D. Smid, The green tea polyphenol (–)-epigallocatechin-3-gallate inhibits amyloid- β evoked fibril formation and neuronal cell death in vitro, *Food Chem.* 129 (2011) 1729–1736.
- [6] S. Das, L. Stark, I.F. Musgrave, T. Pukala, S.D. Smid, Bioactive polyphenol interactions with [small beta] amyloid: a comparison of binding modelling, effects on fibril and aggregate formation and neuroprotective capacity, *Food & Funct.* 7 (2016) 1138–1146.
- [7] D.E. Ehrnhoefer, J. Bieschke, A. Boeddrich, M. Herbst, L. Masino, R. Lurz, S. Engemann, A. Pastore, E.E. Wanker, EGCG redirects amyloidogenic polypeptides into unstructured, off-pathway oligomers, *Nat. Struct. Mol. Biol.* 15 (2008) 558–566.
- [8] K. Ono, K. Hasegawa, H. Naiki, M. Yamada, Curcumin has potent anti-amyloidogenic effects for Alzheimer's β -amyloid fibrils in vitro, *J. Neurosci. Res.* 75 (2004) 742–750.
- [9] C. Manach, A. Scalbert, C. Morand, C. Rémésy, L. Jiménez, Polyphenols: food sources and bioavailability, *Am. J. Clin. Nutr.* 79 (2004) 727–747.
- [10] D. Merelles, W. Hunstein, Epigallocatechin-3-gallate (EGCG) for clinical trials: more pitfalls than promises? *Int. J. Mol. Sci.* 12 (2011) 5592–5603.
- [11] S. Molino, M. Dossena, D. Buonocore, F. Ferrari, L. Venturini, G. Ricevuti, M. Verri, Polyphenols in dementia: from molecular basis to clinical trials, *Life Sci.* 161 (2016) 69–77.
- [12] T. Sterling, J.J. Irwin, ZINC 15—ligand discovery for everyone, *J. Chem. Inf. Model.* 55 (2015) 2324–2337.
- [13] O. Korb, T. Stützel, T.E. Exner, Empirical scoring functions for advanced Protein–Ligand docking with PLANTS, *J. Chem. Inf. Model.* 49 (2009) 84–96.
- [14] W. Kohn, A.D. Becke, R.G. Parr, Density functional theory of electronic structure, *J. Phys. Chem.* 100 (1996) 12974–12980.
- [15] A.A. El-Azhary, H.U. Suter, Comparison between optimized geometries and vibrational frequencies calculated by the DFT methods, *J. Phys. Chem.* 100 (1996) 15056–15063.
- [16] R. Thomsen, M.H. Christensen, MolDock: a new technique for high-accuracy molecular docking, *J. Med. Chem.* 49 (2006) 3315–3321.
- [17] O. Crescenzi, S. Tomaselli, R. Guerrini, S. Salvadori, A.M. D'Urso, P.A. Temussi, D. Picone, Solution structure of the Alzheimer amyloid beta-peptide (1–42) in an apolar microenvironment. Similarity with a virus fusion domain, *Eur. J. Biochem.* 269 (2002) 5642–5648.
- [18] T. Luhrs, C. Ritter, M. Adrian, D. Riek-Loher, B. Bohrmann, H. Dobeli, D. Schubert, R. Riek, 3D structure of Alzheimer's amyloid- β (1–42) fibrils, *Proc. Natl. Acad. Sci. U. S. A.* 102 (2005) 17342–17347.
- [19] D.N. Dixon, R.A. Loxley, A. Barron, S. Cleary, J.K. Phillips, Comparative studies of PC12 and mouse pheochromocytoma-derived rodent cell lines as models for the study of neuroendocrine systems, *In Vitro Cell. Dev. Biol. - Animal* 41 (2005) 197–206.
- [20] M. Clark, R.D. Cramer, N. Van Opdenbosch, Validation of the general purpose tripos 5.2 force field, *J. Comput. Chem.* 10 (1989) 982–1012.
- [21] J.A. Carver, P.J. Duggan, H. Ecroyd, Y. Liu, A.G. Meyer, C.E. Tranberg, Carboxymethylated- κ -casein: a convenient tool for the identification of polyphenolic inhibitors of amyloid fibril formation, *Bioorg. Med. Chem.* 18 (2010) 222–228.
- [22] N.A. Murugan, C. Halldin, A. Nordberg, B. Långström, H. Ågren, The culprit is in the cave: the core sites explain the binding profiles of amyloid-specific tracers, *J. Phys. Chem. Lett.* 7 (2016) 3313–3321.
- [23] I.I.H. Levine, Multiple ligand binding sites on A β (1–40) fibrils, *Amyloid* 12 (2005) 5–14.
- [24] M. Ahmed, J. Davis, D. Aucoin, T. Sato, S. Ahuja, S. Aimoto, J.I. Elliott, W.E. Van Nostrand, S.O. Smith, Structural conversion of neurotoxic amyloid- β 1-42 oligomers to fibrils, *Nat. Struct. Mol. Biol.* 17 (2010) 561–567.
- [25] Q.I. Churches, J. Caine, K. Cavanagh, V.C. Epa, L. Waddington, C.E. Tranberg, A.G. Meyer, J.N. Varghese, V. Streltsov, P.J. Duggan, Naturally occurring polyphenolic inhibitors of amyloid beta aggregation, *Bioorg. Med. Chem. Lett.* 24 (2014) 3108–3112.
- [26] R. Khurana, C. Coleman, C. Ionescu-Zanetti, S.A. Carter, V. Krishna, R.K. Grover, R. Roy, S. Singh, Mechanism of thioflavin T binding to amyloid fibrils, *J. Struct. Biol.* 151 (2005) 229–238.
- [27] M. Catto, A.A. Berezin, D. Lo Re, G. Loizou, M. Demetriades, A. De Stradis, F. Campagna, P.A. Koutentis, A. Carotti, Design, synthesis and biological evaluation of benzo[e][1,2,4]triazin-7(1H)-one and [1,2,4]-triazino[5,6,1-jk]carbazol-6-one derivatives as dual inhibitors of beta-amyloid aggregation and acetylcholinesterase, *Eur. J. Med. Chem.* 58 (2012) 84–97.
- [28] M. Sato, K. Murakami, M. Uno, Y. Nakagawa, S. Katayama, K.-i. Akagi, Y. Masuda, K. Takegoshi, K. Irie, Site-specific inhibitory mechanism for

- amyloid β 42 aggregation by catechol-type flavonoids targeting the Lys residues, *J. Biol. Chem.* 288 (2013) 23212–23224.
- [31] Y.J. Shi, X.J. Song, X. Li, T.H. Ye, Y. Xiong, L.T. Yu, Synthesis and biological evaluation of 1,2,4-triazole and 1,3,4-thiadiazole derivatives as potential cytotoxic agents, *Chem. Pharm. Bull. (Tokyo)* 61 (2013) 1099–1104.
- [33] S. Stefansson, D.L. Adams, C.M. Tang, Common benzothiazole and benzoxazole fluorescent DNA intercalators for studying Alzheimer Abeta1-42 and prion amyloid peptides, *Biotechniques* 52 (2012).
- [34] A. Kamal, K.S. Reddy, M.N.A. Khan, R.V.C.R.N.C. Shetti, M.J. Ramaiah, S.N.C.V.L. Pushpavalli, C. Srinivas, M. Pal-Bhadra, M. Chourasia, G.N. Sastry, A. Juvekar, S. Zingde, M. Barkume, Synthesis, DNA-binding ability and anti-cancer activity of benzothiazole/benzoxazole–pyrrolo[2,1-c][1,4]benzodiazepine conjugates, *Bioorg. Med. Chem.* 18 (2010) 4747–4761.

Appendix A: Supplementary material

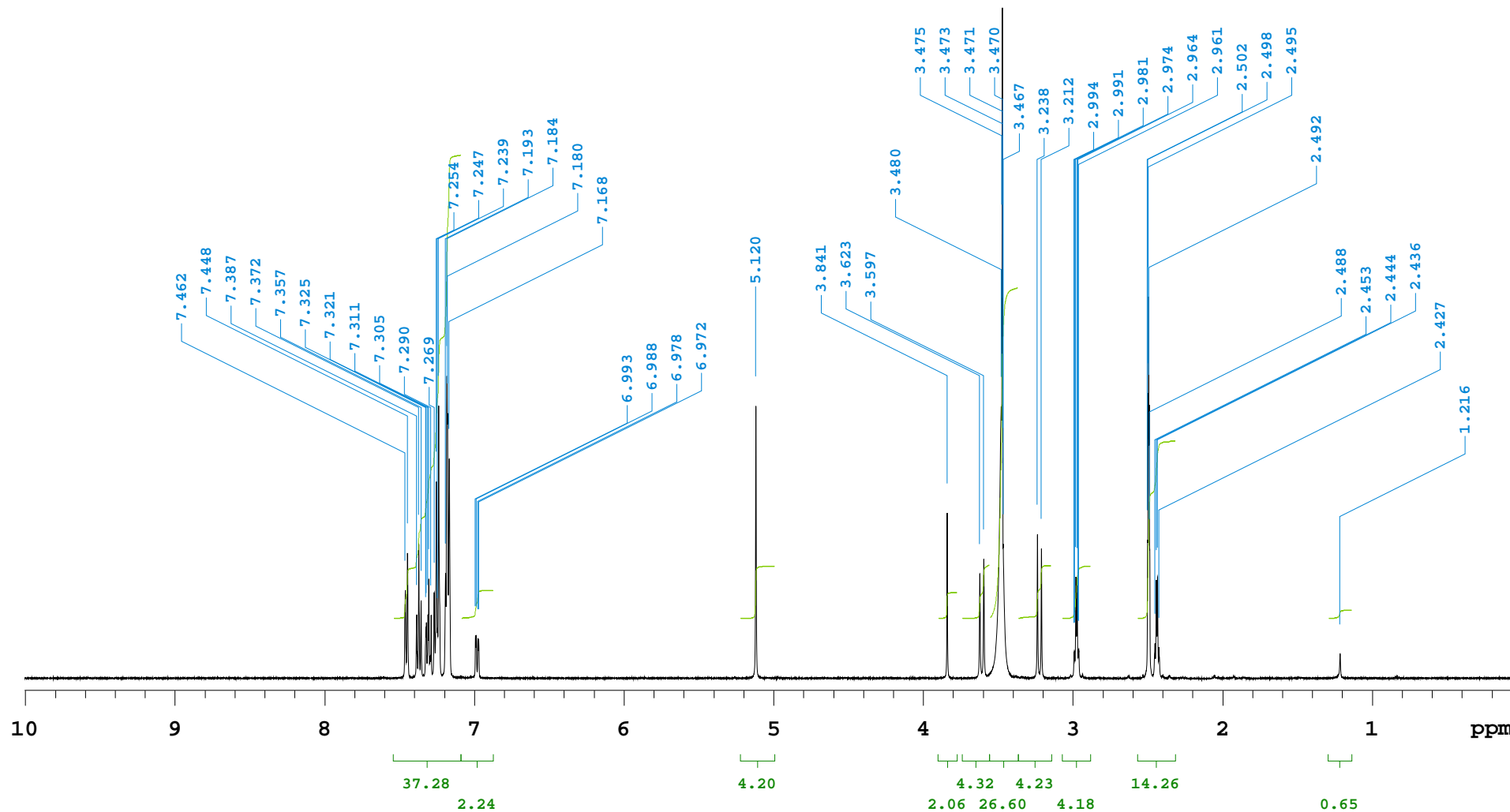


Sample Name Compound 1
Date collected 2015-05-25

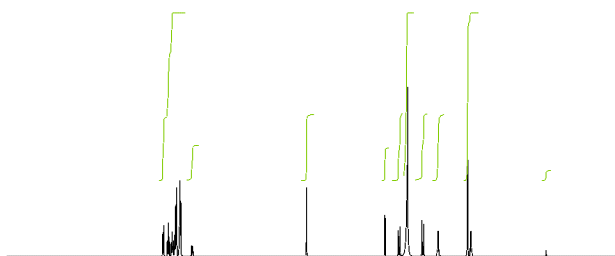
Pulse sequence PRESAT
Solvent dms

Temperature 26
Spectrometer nmr500.chemistry.adelaide.edu.au-vnmrs500

Study owner walkup



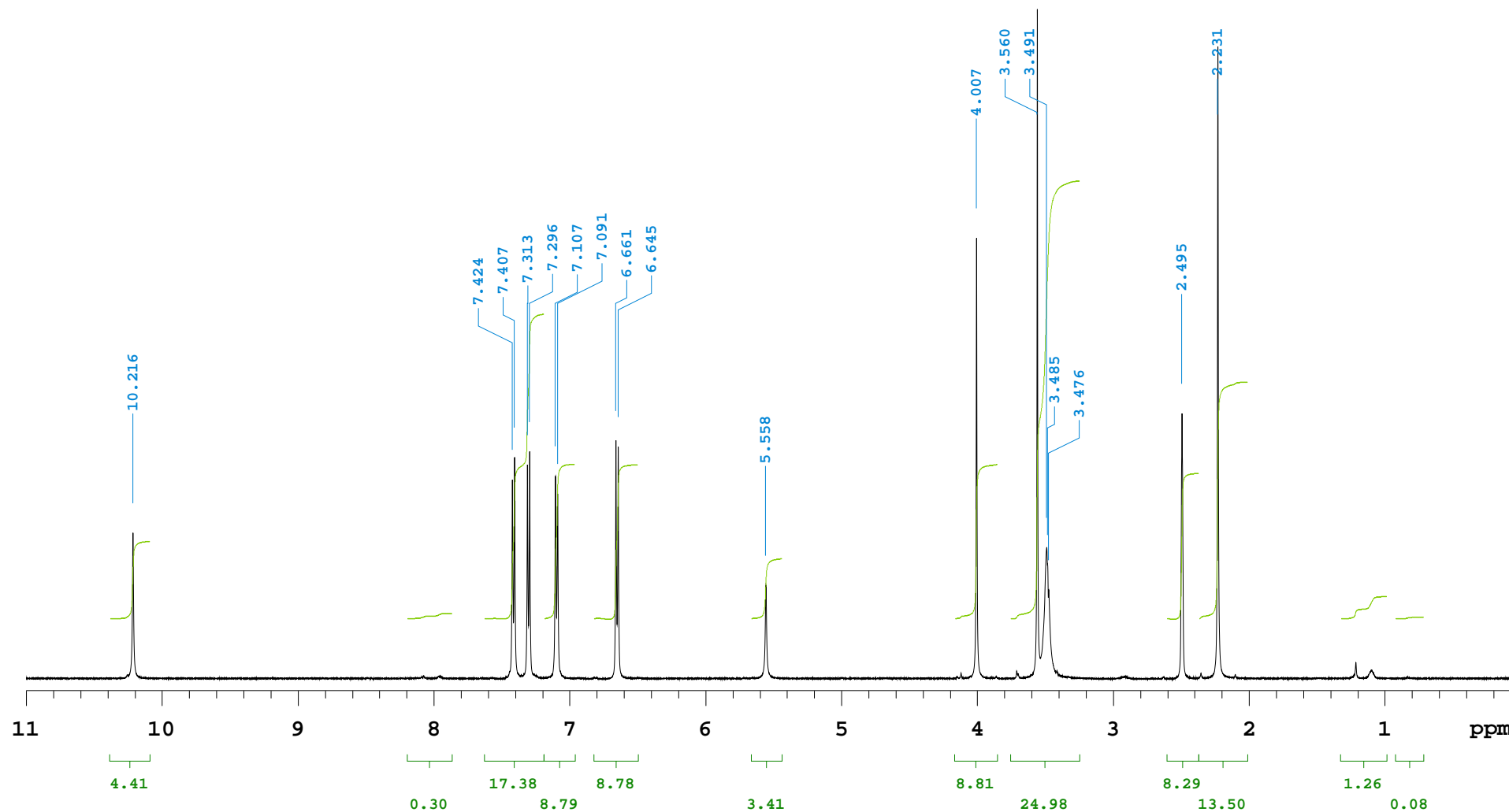
Supplementary Figure 1. ¹H-NMR of Compound 1 (1,3-dibenzyl-2-[3-(benzyloxy)phenyl]imidazolidine) in DMSO.



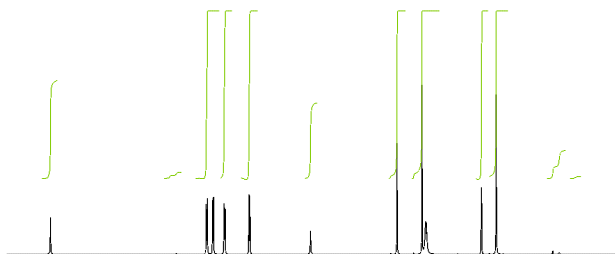
ai cdc ph

imidazolin in DMSO

SAMPLE		PRESATURATION	
date	May 25 2015	satmode	y
solvent	dms0	wet	n
file	/home/walkup/vnmrsys /data/walkup/TPimidazolin/ PRESAT_TPimidazolin_dms0_2 0150525_500_01	SPECIAL	
ACQUISITION		temp	26.0
sw	8012.8	gain	42
at	4.089	spin	0
np	65536	hst	0.008
fb	4000	pw90	7.200
bs	4	alfa	10.000
ss	1	FLAGS	
d1	2.000	il	n
nt	8	in	n
ct	8	dp	y
TRANSMITTER		hs	nn
tn	H1	PROCESSING	
sfrq	499.813	fn	not used
tof	499.8	DISPLAY	
tpwr	61	sp	1.4
pw	7.200	wp	4999.0
DECOUPLER		rfl	1007.6
dn	C13	rfp	0
dof	0	rp	-105.0
dm	nnn	lp	0
decwave	W40_onenmr_MR1203 W035	PLOT	
dpwr	39	wc	252
dmf	32258	sc	8
Plotname: PRESAT_TPimidazolin_dms0_20150525_500_01_plot01			
		vs	81
		th	4



Supplementary Figure 2. ¹H-NMR of Compound 4 (2-{{[5-(4-aminophenyl)-4-methyl-4H-1, 2, 4-triazol-3-yl] sulfanyl}-N-(4-methylphenyl) acetamide) in DMSO.



ai cdc ph

INTEGRAL VALUES

Integral	start(ppm)	end	value
1	10.3872	10.0893	4.412
2	8.1964	7.86339	0.301
3	7.62679	7.18863	17.376
4	7.18863	6.96078	8.793
5	6.82057	6.49633	8.784
6	5.66382	5.43598	3.415
7	4.16531	3.84984	8.814
8	3.75344	3.24517	24.976
9	2.60546	2.36885	8.294
10	2.36885	2.00956	13.499
11	1.32603	0.984259	1.261
12	0.922917	0.712599	0.075

Acetomide in DMSO

SAMPLE

date **May 25 2015**
 solvent **dms0**
 file **/home/walkup/vnmrsys**
/data/walkup/TPacetomide/P
RESAT_TPacetomide_dms0_201
50525_500_01

PRESATURATION

satmode **y**
 wet **n**

SPECIAL

temp **26.0**
 gain **38**
 spin **0**
 hst **0.008**
 pw90 **7.200**
 alfa **10.000**

ACQUISITION

sw **8012.8**
 at **4.089**
 np **65536**
 fb **4000**
 bs **4**
 ss **1**
 d1 **2.000**
 nt **8**
 ct **8**

FLAGS

il **n**
 in **n**
 dp **y**
 hs **nn**

TRANSMITTER

tn **H1**
 sfrq **499.813**
 tof **499.8**
 tpwr **61**
 pw **7.200**

PROCESSING

fn **not used**

DISPLAY

sp **1.4**
 wp **5496.8**
 rfl **1007.6**
 rfp **0**
 rp **-107.3**
 lp **0**

DECOUPLER

dn **C13**
 dof **0**
 dm **nnn**
 decwave **W40_onenmr_MR1203**
W035

PLOT

wc **252**
 sc **8**
 vs **99**
 th **7**

 Plotname: **PRESAT_TPacetomide_dms0_20150525_500_01_plot01**

Supplementary material

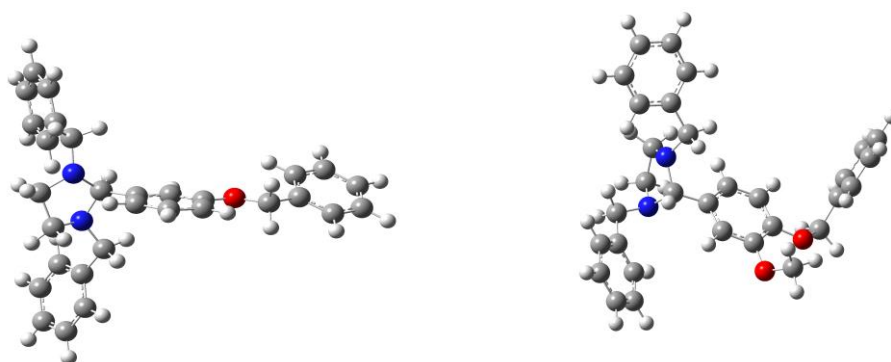


Figure. 3: Optimised structures (following DFT-B3LYP calculation) of Compounds 1 and 2. 3-D interactive structure files in .pdb format.

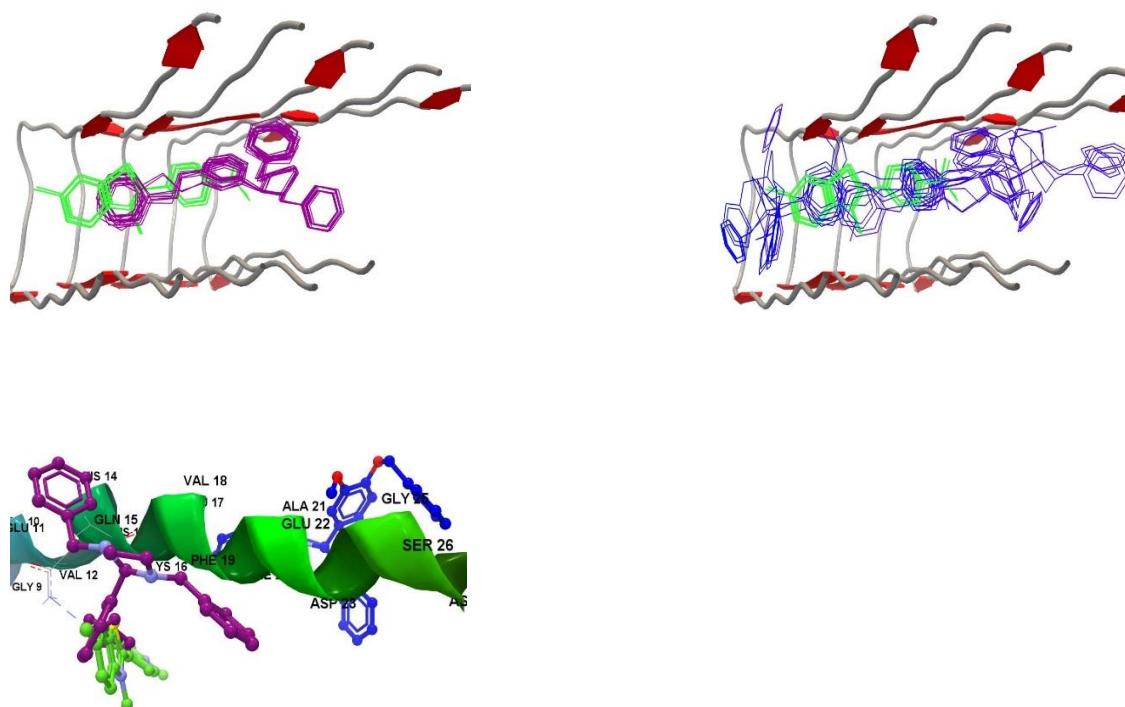


Figure 4: Binding of three ligands: optimised conformations of Compound 1, 2 and ThT to the Aβ₁₇₋₄₂ oligomer and Aβ₁₇₋₄₂ monomer. (a) Binding sites of Compound 1 and ThT in oligomer (b) Binding sites of Compound 2 and ThT in oligomer (c) Compound 1, 2 and ThT bound to Aβ₁₇₋₄₂ monomer. Compound 1=purple, Compound 2=blue and ThT=green.

Single ring type	Total purchasable compounds	Anodyne, bb, ready for sale
Tetrazole	2180726	86430
1H, 1_2_4 triazole	10193186	293256
2H triazole	3350821	163705
Imidazole	7445052	423322
Other imidazoles	54661	19605
1H Pyrazole	28150875	970728
3H Pyrazole	4631	114
Imidazolidine	30802	876
Pyrazolidine	8521	1048576
Pyrrole	3985252	166055
Pyrrolidine	36456053	1048576
Double ring type	Total purchasable compounds	Anodyne, bb, ready for sale
Indole	4160299	79320
Isoindole	487759	6376
1H indole	414276	16508
Indoline	1912779	40285
Benzoxazole	1136373	34754

Table 1: Type of rings after filtering the ZINC database, ring subsets. 11 single FMH rings with only N-heteroatom and 5 double rings, having single N-heteroatom FMH fused with a six membered ring. Total number of purchasable compounds from each ring is further filtered for anodyne, bb and compounds ready for sale. These filtered list of compounds from each ring was used in virtual screening.

Chapter 4: Exploring the structural diversity in inhibitors of α -synuclein amyloidogenic folding, aggregation and neurotoxicity

Das, S., Pukala, TL. and Smid, SD. (2018) 'Exploring the structural diversity in inhibitors of α -synuclein amyloidogenic folding, aggregation and neurotoxicity' *Frontiers in Chemistry – Medicinal and Pharmaceutical Chemistry*, 6: (181- 192) doi: 10.3389/fchem.2018.00181

Author's proof reprinted following Frontiers Copyright Statement, 2018.

The main purpose of this study is to investigate the effect of various structural features within a diverse set of molecules on α S (α SA53T) amyloidogenic folding, aggregation and exogenous toxicity to PC-12 cells. This study compared the effect of a flavone bearing B-ring trihydroxylation and a flavone with both A and B-ring dihydroxylation on α SA53T amyloidogenic folding, aggregation and toxicity. This was compared with the flavone myricetin, which has hydroxylation in all A, C and B-rings and is a known inhibitor of α SA53T aggregation (Liu, Graetz et al. 2015). The other aim of this study is to investigate the effect of the biphenyl neolignan, honokiol on α SA53T amyloidogenic folding, aggregation and neurotoxicity. The effect of large and extensively hydroxylated polyphenol such as ellagitannin is also addressed in this study, by characterising the punicalagin molecule's interaction with α SA53T and its effects on aggregation and toxicity. These molecules are comparatively studied to identify new flavone structures as well as non-flavone bioactive polyphenolic inhibitor of α SA53T toxic amyloidogenic aggregation. Additionally, this study has been aimed at

characterizing the effects of synthetic dibenzyl imidazolidine compounds, identified from virtual screening as ‘hits’ from our previous study (Chapter 3) on α SA53T amyloidogenic folding, aggregation and toxicity. An understanding of the impact of these inhibitors on the various conformations of α SA53T would be insightful to probe the early structural polymorphism observed during amyloidogenic aggregation. Thus, the IM-MS analysis presented in this study is aimed at improving our understanding of each molecule’s effect on α SA53T conformational ensembles. In addition, their proposed direct binding interactions are studied by molecular docking with model α SA53T to understand their binding affinity.

This study demonstrated the inhibitory effect of B-ring trihydroxylation in flavone (exemplified by the semi-synthetic flavone 2-D08) on α SA53T amyloidogenic folding, aggregation and toxicity. The comparative analysis of three flavones here, showed that only B-ring trihydroxylation has a distinct effect on α SA53T amyloidogenic aggregation and toxicity. Furthermore, this study identified that honokiol impacted α SA53T amyloidogenic aggregation in a comparable manner to the studied flavones. This study also highlighted the importance of the dibenzyl imidazolidine scaffold against α SA53T amyloidogenic aggregation. Additionally, punicalagin has also been identified for the first time as inhibitor of α SA53T amyloidogenic aggregation and toxicity. Overall, this study has demonstrated important structural elements, including the neolignan biphenyl structure, of flavone B-ring trihydroxylation, the dibenzyl imidazolidine scaffold and the bulky ellagitannin structure are all capable of inhibiting α SA53T amyloidogenic aggregation by preserving its native conformation, hence reducing its amyloidogenic aggregation and exogenous toxicity *in vitro*.

Statement of Authorship

Title of Paper	Exploring structural diversity in Inhibitors of α -Synuclein Amyloidogenic Folding, Aggregation and Neurotoxicity
Publication Status	<input type="checkbox"/> Published <input checked="" type="checkbox"/> Accepted for Publication <input type="checkbox"/> Submitted for Publication <input type="checkbox"/> Unpublished and Unsubmitted work written in manuscript style
Publication Details	Journal 'Frontiers in Chemistry; Medicinal and Pharmaceutical Chemistry', 2018, doi: 10.3389/fchem.2018.00181

Principal Author

Name of Principal Author (Candidate)	Sukanya Das
Contribution to the Paper	I, along with the co-authors conceived this study. I performed the experiments and molecular modelling. I performed the data analysis and interpretation with support from Dr. Tara Pukala and project supervision from Dr. Scott Smid. I wrote the manuscript and both co-authors helped in the manuscript preparation.
Overall percentage (%)	85%
Certification:	This paper reports on original research I conducted during the period of my Higher Degree by Research candidature and is not subject to any obligations or contractual agreements with a third party that would constrain its inclusion in this thesis. I am the primary author of this paper.
Signature	
	Date

Co-Author Contributions

By signing the Statement of Authorship, each author certifies that:

- the candidate's stated contribution to the publication is accurate (as detailed above);
- permission is granted for the candidate to include the publication in the thesis; and
- the sum of all co-author contributions is equal to 100% less the candidate's stated contribution.

Name of Co-Author	Tara Pukala
Contribution to the Paper	<i>Input to study design, data collection/analysis and manuscript preparation.</i>
Signature	
	Date
	<i>21/5/2018.</i>

Name of Co-Author	Scott Smid
Contribution to the Paper	Input into study design and reviewed final manuscript
Signature	
	Date
	May 18, 2018



Exploring the Structural Diversity in Inhibitors of α -Synuclein Amyloidogenic Folding, Aggregation, and Neurotoxicity

Sukanya Das¹, Tara L. Pukala^{2*} and Scott D. Smid¹

¹ Discipline of Pharmacology, Adelaide Medical School, Faculty of Health Sciences and Medicine, University of Adelaide, Adelaide, SA, Australia, ² Discipline of Chemistry, School of Physical Sciences, Faculty of Sciences, University of Adelaide, Adelaide, SA, Australia

OPEN ACCESS

Edited by:

Simona Rapposelli,
Università degli Studi di Pisa, Italy

Reviewed by:

Daniela Rodrigues de Oliveira,
Universidade Federal de Sao Paulo,
Brazil

Jyotirmayee Mohanty,
Bhabha Atomic Research Centre,
India

*Correspondence:

Tara L. Pukala
tara.pukala@adelaide.edu.au

Specialty section:

This article was submitted to
Medicinal and Pharmaceutical
Chemistry,
a section of the journal
Frontiers in Chemistry

Received: 01 March 2018

Accepted: 07 May 2018

Published: 25 May 2018

Citation:

Das S, Pukala TL and Smid SD (2018)
Exploring the Structural Diversity in
Inhibitors of α -Synuclein
Amyloidogenic Folding, Aggregation,
and Neurotoxicity.
Front. Chem. 6:181.
doi: 10.3389/fchem.2018.00181

Aggregation of α -Synuclein (α S) protein to amyloid fibrils is a neuropathological hallmark of Parkinson's disease (PD). Growing evidence suggests that extracellular α S aggregation plays a pivotal role in neurodegeneration found in PD in addition to the intracellular α S aggregates in Lewy bodies (LB). Here, we identified and compared a diverse set of molecules capable of mitigating protein aggregation and exogenous toxicity of α SA53T, a more aggregation-prone α S mutant found in familial PD. For the first time, we investigated the α S anti-amyloid activity of semi-synthetic flavonoid 2', 3', 4' trihydroxyflavone or 2-D08, which was compared with natural flavones myricetin and transilutin, as well as such structurally diverse polyphenols as honokiol and punicalagin. Additionally, two novel synthetic compounds with a dibenzyl imidazolidine scaffold, Compound 1 and Compound 2, were also investigated as they exhibited favorable binding with α SA53T. All seven compounds inhibited α SA53T aggregation as demonstrated by Thioflavin T fluorescence assays, with modified fibril morphology observed by transmission electron microscopy. Ion mobility-mass spectrometry (IM-MS) was used to monitor the structural conversion of native α SA53T into amyloidogenic conformations and all seven compounds preserved the native unfolded conformations of α SA53T following 48 h incubation. The presence of each test compound in a 1:2 molar ratio was also shown to inhibit the neurotoxicity of preincubated α SA53T using phaeochromocytoma (PC12) cell viability assays. Among the seven tested compounds 2-D08, honokiol, and the synthetic Compound 2 demonstrated the highest inhibition of aggregation, coupled with neuroprotection from preincubated α SA53T *in vitro*. Molecular docking predicted that all compounds bound near the lysine-rich region of the N-terminus of α SA53T, where the flavonoids and honokiol predominantly interacted with Lys 23. Overall, these findings highlight that (i) restricted vicinal trihydroxylation in the flavone B-ring is more effective in stabilizing the native α S conformations, thus blocking amyloidogenic aggregation, than dihydroxylation aggregation in both A and B-ring, and (ii) honokiol, punicalagin, and the synthetic imidazolidine Compound 2 also inhibit α S amyloidogenic aggregation by stabilizing its native conformations. This diverse set of molecules acting on a singular pathological target with predicted binding to α SA53T in the folding-prone N-terminal region may contribute toward novel drug-design for PD.

Keywords: α -synuclein, amyloid inhibition, 2-D08, transilutin, honokiol, punicalagin, dibenzyl imidazolidine

INTRODUCTION

Parkinson's disease (PD) neuropathology is characterized by loss of dopaminergic neurons, and in most cases, deposition of Lewy bodies in the brain (Hughes et al., 1992). Aggregation and amyloid formation of the cytosolic protein α -Synuclein (α S), in both intracellular and extracellular areas, have been implicated in the formation of Lewy pathology (LP) and degeneration of dopaminergic neurons in the substantia nigra pars compacta region of the brain (Baba et al., 1998; Volpicelli-Daley et al., 2011; Luk et al., 2012; Iyer et al., 2014). Human α S is a 140-amino acid residue polymorphic protein consisting of a membrane binding N-terminal region, a non-amyloid β component (NAC) region and an acidic C-terminal tail. This protein is associated with key biological activities such as vesicle trafficking, maintenance of the synaptic SNARE complex and vesicle pools, and regulation of dopamine (DA) metabolism (Cabin et al., 2002; Sidhu et al., 2004; Chandra et al., 2005; Cooper et al., 2006). Along with the sporadic form of PD caused by wild type α S, a missense point mutation in the *snca* gene results in the more aggregation prone mutant α SA1a53Thr (α SA53T), which has been found to be associated with a familial form of PD (Polymeropoulos et al., 1997; Narhi et al., 1999; Li et al., 2001; Papadimitriou et al., 2016). Since current treatments for PD aim only at replacing DA loss, and provide only transient symptomatic relief, there is an urgent need for treatments that can directly modify disease progression. Therefore, inhibition of α S aggregation, or its pathological mutant α SA53T, provides a disease-modifying therapeutic approach for PD, inclusive of its familial form.

The amyloidogenic aggregation of an intrinsically disordered protein (IDP) such as α S involves formation of heterogeneous and transient assemblies early in its aggregation pathway, that act as a precursor for fibrillization (Bousset et al., 2013). Considering the difficulty in gaining structural information on these conformational assemblies, ion mobility-mass spectrometry (IM-MS) is employed to monitor soluble α S conformations during the early aggregation process. IM-MS is a sensitive tool for structural study of conformational folding and other characterization (Lanucara et al., 2014), and has been used for high-throughput screening of amyloid inhibitors (Young et al., 2014). It allows measurement of both the mass and collision cross section (CCS) of an ion, and thereby can provide information on the structural changes of amyloidogenic proteins such as α S during aggregation and binding of small molecules (Bernstein et al., 2004; Vlad et al., 2011; Liu et al., 2015). Combined with kinetic analysis of fibrillization (such as from thioflavin T fluorescence assays) and visualization of the fibrils using transmission electron microscopy (TEM), IM-MS provides insights on the effect of exogenous compounds on native α SA53T conformations *in vitro*. This can inform on how such compounds interact during the early stage of toxic amyloidogenic aggregation. Evaluation of α SA53T neurotoxicity also provides valuable information on the toxic nature of the observed aggregation products, and possible neuroprotective effects of small molecule aggregation inhibitors.

Various natural compounds have been shown to inhibit α S aggregation or participate in remodeling of its fibrillization

pathway (Zhu et al., 2004; Masuda et al., 2006; Bieschke et al., 2010; Morshedi et al., 2015). The polyphenolic flavonoids baicalein and epigallo-catechin-3-gallate (EGCG) are amongst these (Hong et al., 2008; Bieschke et al., 2010). Structurally, baicalein possesses vicinal trihydroxyl groups only in the flavone A-ring, whereas EGCG possesses vicinal trihydroxylation in the B-ring and in the gallic acid moiety. Gallic acid, by itself, also demonstrated inhibition of α SA53T aggregation (Liu et al., 2014). A comprehensive study on flavonoid-induced inhibition of α S aggregation has shown that vicinal dihydroxylation or trihydroxylation improves inhibition irrespective of ring position (Meng et al., 2009). However, except for baicalin, other reported flavonoid inhibitors lack the localized single ring vicinal di or tri hydroxyl groups. Thus, the importance of position and extent of hydroxylation of flavonoids involved in inhibiting α S aggregation and neurotoxicity is unclear. In this study, we have investigated the anti-amyloid effect of semi-synthetic, 2', 3', 4' trihydroxy flavone (2-D08) that has only vicinal trihydroxylation in the B-ring. This flavone has shown improved inhibition of amyloid β ($A\beta$) aggregation and toxicity through its localized B-ring trihydroxylation (Marsh et al., 2017). We compared it with myricetin, a known inhibitor of α S aggregation (Meng et al., 2010; Liu et al., 2015) which also has vicinal trihydroxylation in the B-ring along with -OH groups at flavone 3, 5, and 7 positions. Transilitin was also investigated here to compare the effect of dihydroxylation in both A and B rings. Our study provides information on the role of select B-ring trihydroxylation for modulation of α S aggregation and toxicity.

Other bioactive polyphenols investigated here for the first time are the natural lignan compound honokiol and ellagitannin punicalagin. Honokiol has demonstrated anti-amyloid effects against amyloid beta ($A\beta$) (Hoi et al., 2010; Das et al., 2016). Punicalagin, found in pomegranate, is also a known inhibitor of $A\beta$ protein aggregation and has antioxidant and anti-inflammatory properties (Yaidikar et al., 2014; Yaidikar and Thakur, 2015; Das et al., 2016). Extending the structural diversity of molecules that can act on a common target of pathological α S aggregation, we also included two synthetic imidazolidine compounds, termed Compound 1 (1,3-dibenzyl-2-[3-(benzyloxy) phenyl] imidazolidine) and Compound 2 (1,3-dibenzyl-2-[4-(benzyloxy)-3-methoxyphenyl] imidazolidine), both bearing a five-membered heterocyclic (FMH) imidazolidine ring scaffold. We previously identified these compounds through virtual screening of the ZINC chemical database and highlighted the importance of this molecular scaffold with regards to preventing amyloid β aggregation (Das and Smid, 2017). A summary of the compounds investigated here is provided in **Figure 1**.

MATERIALS AND METHODS

Reagents and Chemicals

Myricetin, 2-D08, honokiol, and punicalagin were obtained from Sigma-Aldrich (Castle Hill, VIC, Australia). Transilitin was kindly provided by Dr. Peter Duggan at CSIRO Materials Division (Clayton South, VIC, Australia). Synthetic

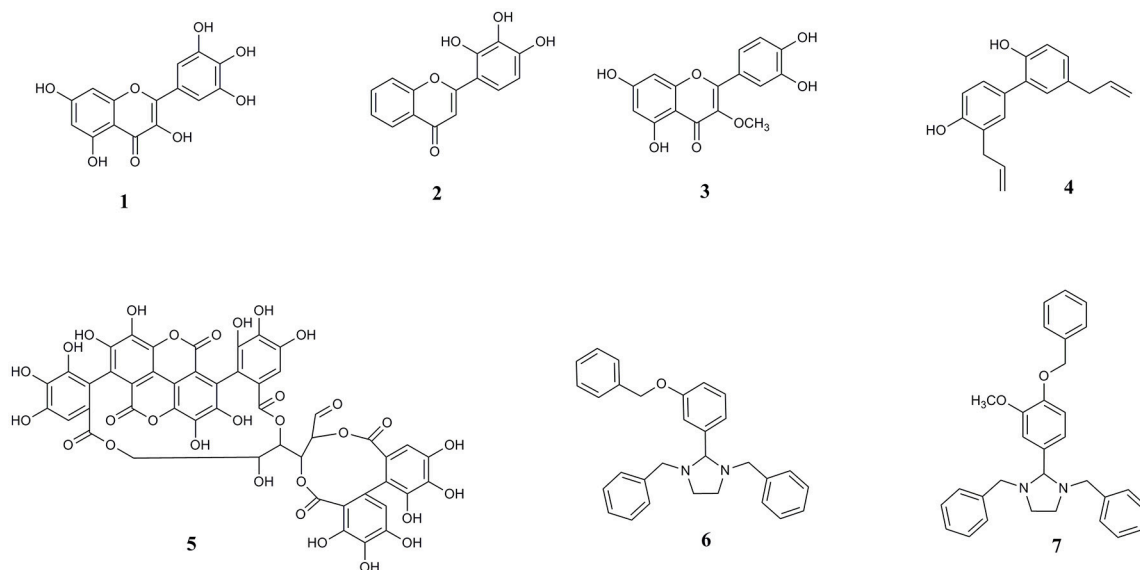


FIGURE 1 | Chemical structures of **(1)** myricetin, **(2)** 2', 3', 4' trihydroxy flavone or 2-D08, **(3)** transilutin, **(4)** honokiol, **(5)** punicalagin, **(6)** 1,3-dibenzyl-2-[3-(benzyloxy)phenyl]imidazolidine or Compound 1, and **(7)** 1,3-dibenzyl-2-[4-(benzyloxy)-3-methoxyphenyl]imidazolidine or Compound 2.

imidazolidine Compound 1 and Compound 2 were sourced from Specs (The Netherlands) and ChemDiv (U.S.A.) respectively, both screening compound manufacturers. Purity of Compound 1 was assessed to be >97% through ^1H NMR analysis (Supplementary Figure 1), Compound 2 was certified with a purity of >97%.

Thioflavin T, thiazolyl blue tetrazolium bromide (MTT), trypan blue, DMSO, Roswell Park Memorial Institute 1640 (RPMI) medium and fetal calf serum (FCS) were obtained from Sigma-Aldrich (St Louis, MO, USA). Non-essential amino acids (NEAA), penicillin/streptomycin, $1\times$ trypsin EDTA, and phosphate buffered saline (PBS) at pH 7.4 were obtained from Thermo Fisher Scientific, (Scoresby, VIC, Australia). Bovine serum albumin (BSA) was obtained from Bovogen Biologicals (East Keilor, VIC, Australia). Ammonium acetate was obtained from Sigma-Aldrich (Castle Hill, VIC Australia).

Protein Expression and Purification

αSA53T was expressed and purified as previously described (Volles and Lansbury, 2007). Cells were grown in normal lennox broth (LB) medium. Protein was purified by size exclusion chromatography using a Superdex 200 SEC column (Bio Rad), with a flow rate of 0.5 ml/min, in 20 mM ammonium acetate buffer. The purity of αSA53T was confirmed by mass spectrometry and samples were lyophilized and stored at -80°C until required.

Preincubation of αSA53T and Compound Preparation

αSA53T was dissolved in 50 mM ammonium acetate buffer (pH not adjusted) to make 1 mM stock solution, dispensed into aliquots and immediately frozen at -80°C until required. All test compounds were initially diluted in DMSO and then in 50 mM

ammonium acetate to their final stock concentrations prior to incubation with αSA53T . The final concentration of DMSO in each experiment was <1%. For the cell viability assay, $50\ \mu\text{M}$ αSA53T alone or in the presence of each compound ($100\ \mu\text{M}$) in 50 mM ammonium acetate buffer was shaken at 300 rpm for 72 h at 37°C .

Thioflavin T Fluorescence Assay

Thioflavin T (ThT) binds to β sheet rich structures present in amyloid fibrils, with fluorescence increasing proportionally to the quantity of fibrils present in solution. ThT (final concentration $100\ \mu\text{M}$) was added to wells in a Greiner 96-well plate together with αSA53T ($100\ \mu\text{M}$), in the absence or presence of each test compound (either at 200 or $100\ \mu\text{M}$) in 50 mM ammonium acetate buffer to a total volume of $100\ \mu\text{l}$ in each well. Fluorescence was measured at 37°C every 30 min for 100 h using a Fluostar Optima plate reader (BMG Lab technologies, Australia) with a 440/490 nm excitation/emission filter. The ThT assay was performed in duplicate and repeated three times. Results were normalized to blank values (ThT alone in 50 mM ammonium acetate buffer).

Transmission Electron Microscopy (TEM) Imaging

TEM was used to visualize αSA53T aggregates and fibrils and investigate the effects of selected compounds on fibril morphology. Samples were prepared by adding 5–10 μl of protein solution taken directly from the ThT assay after 100 h to a 400 mesh formvar carbon-coated nickel electron microscopy grid (Proscitech, Kirwan, QLD, Australia). After 1 min, this sample was blotted using filter paper. Ten microliters of contrast dye containing 2% uranyl acetate was then placed on the grid, left for 1 min and blotted with filter paper. Grids were then loaded

onto a specimen holder for analysis using a FEI Tecnai G2 Spirit Transmission Electron Microscope (FEI, Milton, QLD, Australia). Sample grids were viewed using a magnification of 34,000–92,000X. Grids were extensively scanned manually in search of fibrils and representative images were taken.

Ion Mobility-Mass Spectrometry (IM-MS)

Fifty micromolar α SA53T was prepared for IM-MS experiments in 50 mM ammonium acetate buffer in the absence and presence of each compound at a molar ratio of 1:2 (protein: compound). Samples were allowed to fibrillize by incubation at 37°C with constant shaking at 300 rpm. IM-MS analysis was performed on an Agilent 6560 Ion Mobility Q-ToF spectrometer with samples introduced by nano-electrospray ionization through platinum-coated capillaries (made in-house). Ions were analyzed in the positive mode, with parameters systematically selected to achieve optimal signal while avoiding any analysis induced structural transitions (full details of optimization will be reported in a manuscript currently in preparation). Typical instrument parameters included; capillary voltage 1,700 V, fragmentor voltage 400 V, gas temperature 0°C, gas flow 2 l/min, trap fill time 20000.0 μ s, trap release time 4000.0 μ s and CCS measurement was made using a multifold approach varying the IM drift tube voltage between 1,200 and 1,700 V. The acquired spectra were processed using Qualitative Analysis B.07.00 and IM-MS browser B.07.01 (both Agilent, Santa Clara, USA).

Neuronal Cell Culture, Treatment, and Viability Measurements

Rat pheochromocytoma cells (Ordway PC12) displaying a semi-differentiated phenotype with neuronal projections were kindly donated by Professor Jacqueline Phillips (Macquarie University, NSW, Australia) [21]. Cells were maintained in Roswell Park Memorial Institute 1640 (RPMI) media with 10% fetal calf serum (FCS), 1% L-glutamine, 1% non-essential amino acids, and 1% penicillin/streptomycin. Cells were seeded at 2×10^4 cells per well in RPMI with 10% FCS. PC12 cells were equilibrated for 24 h before treatment with preincubated α SA53T or preincubated α SA53T in presence of each test compound. Cells were then incubated for 48 h at 37°C, 5% CO₂ prior to measurement of cell viability. After 48 h, PC12 cell viability was determined using the thiazolyl blue tetrazolium bromide (MTT) assay. After incubation, 96-well plates had all media removed and replaced with serum-free media containing 0.25 mg/ml of MTT. The plate was further incubated for 2 h at 37°C with 5% CO₂, then the MTT solution was removed and cells were lysed with DMSO. Absorbance was measured at 570 nm using a Synergy MX microplate reader (Bio-Tek, Bedfordshire, UK).

Statistical Analysis

Area under the curve analysis for Thioflavin T (ThT) fluorescence data was interrogated using a one-way analysis of variance (ANOVA) with a Dunnett's multiple comparisons test to determine the significance of each tested compound's effect vs. α SA53T alone. Data obtained from the MTT assay was analyzed via a one-way ANOVA to assess neuronal cell viability with a Holm–Sidak's multiple comparison test used to determine

the significance level for each test compound interacting with α SA53T. A significance value of $p < 0.05$ was used for all experiments. Data analysis and production of graphs was performed in GraphPad Prism 6 for Windows (GraphPad Software, San Diego, USA).

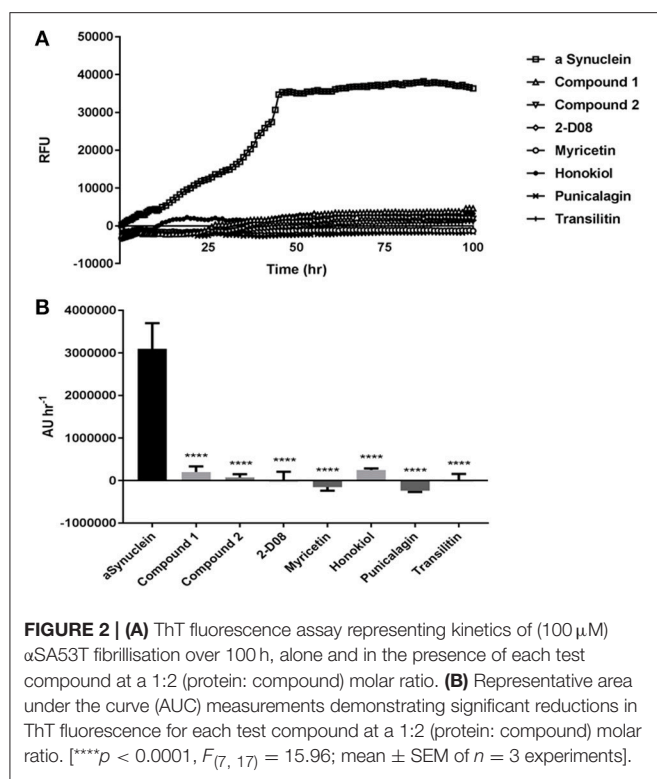
Molecular Docking of Compound Optimized Structure Binding to α Synuclein

To gain insight into the binding interactions of each selected compound (ligand) with α SA53T, all ligand structures were first optimized and then individually docked to α SA53T with 300 iterations per docking. Previous experimental evidence suggested that the flavonoid binding site in α synuclein is near the lysine-rich region of the N-terminus, with Lys21 or Tyr39 playing a pivotal role (Meng et al., 2009). Therefore, the docking search space was created centering this binding site with a radius of 25 Å covering these N-terminus residues. Ligand equilibrium molecular geometries were optimized using a density functional theory (DFT) method that utilizes the Becke–Lee–Yang–Parr three-parameter hybrid functional (B3LYP) to ascertain accurate bond distances, angles, dihedrals and optimized conformations in the lowest energy state, using the Gaussian09 package of codes (Frisch et al., 2016). A large basis set, aug-cc-pVDZ, was used in approximation of optimized geometry for each ligand. DFT-B3LYP level of calculations combined with a larger basis set is considered as a standard and reliable method for estimating optimized molecular geometry (El-Azhary and Suter, 1996). Fully optimized ligand structures were then allowed to dock with the model α SA53T. Since the full sequence α SA53T structure was not available, the solid-state NMR of pathogenic α synuclein fibril (PDB ID: 2N0A) was obtained from protein data bank and residue 53 mutated from alanine to threonine to generate the model protein monomer of α SA53T (Tuttle et al., 2016). The resultant α SA53T protein conformation, without any further adjustment, was used for docking, which employed CLC drug discovery workbench, version 2.4.1 using a PLANTSplp empirical scoring function (Korb et al., 2009).

RESULTS

Significant Inhibition of α SA53T Amyloid Fibril Formation by All Test Compounds

The amyloid fibrillization of α SA53T was measured by a ThT-based kinetic assay, which demonstrated a gradual increase in fluorescence (relative fluorescence unit or RFU) up to the first 50 h and then stabilized over the remainder of the assay, indicating α SA53T underwent a conformational transition to a cross- β -sheet rich structure characteristic of amyloid fibrils and aggregates (Figure 2A). All test compounds: 2-D08, myricetin, transilitin, honokiol, punicalagin, Compound 1 and Compound 2 inhibited the ThT fluorescence over the entire 100 h time course of the assay at a 1:2 (protein: compound) molar ratio. Area under the curve analysis showed extensive and significant overall inhibition of fibril formation in the presence of each of the test compounds at a 1:2 (protein: compound) molar ratio



(Figure 2B). Further ThT assays at a 1:1 (protein: compound) molar ratio also exhibited significant fibril inhibition, though Compound 1 was the least effective among all compounds tested (Supplementary Figures 2a,b). The mean RFU along with the respective standard error of mean (SEM) values for each compound are provided as Supplementary Table 1.

Transmission Electron Microscopy of α SA53T Fibrils and Aggregates

False positives for ThT inhibition can occur when some polyphenols undergo spontaneous oxidation in aqueous solution and strongly quench ThT fluorescence, and this also might have resulted in negative RFU for myricetin and punicalagin (Coelho-Cerqueira et al., 2014). Therefore, the inhibition of fibrillization observed in ThT assays was further confirmed by TEM, an essential qualitative technique to characterize the morphology of amyloid fibril and aggregate formation. The morphology of α SA53T fibrils and aggregates appeared to be affected by incubation with each of the test compounds at a 1:2 (protein: compound) molar ratio, after 100 h incubation (Figures 3a–h). TEM evidence demonstrated that α SA53T alone formed dense fibrillar aggregates where several fibrils were intertwined and arranged as rope-like mature amyloid fibrils, similar to those observed previously (Bharathi et al., 2007; Figure 3a). Incubation with Compound 2, myricetin and transilitin resulted in shorter, thinner, and loosely attached fibrils, but in low abundance (Figures 3c,e,h). Incubation with honokiol produced loosely attached, short and long fibrils while punicalagin incubation produces loosely attached, thin fibrils that were comparatively

longer (Figures 3f,g). Incubation with 2-D08 resulted in amorphous aggregates of very short fibrils (Figure 3d), while incubation with Compound 1 produce short fibrils and small dense aggregates (Figure 3b). In the presence of all test compounds, no rope-like aggregates were observed compared to α SA53T alone. Additional TEM images following 50 h incubation highlighted the formation of pre-fibrillar structures by α SA53T alone. In the presence of all compounds except punicalagin, small aggregate-like structures were observed. Punicalagin incubation resulted in a few protofibrillar α SA53T structures similar to those that were observed following 100 h incubation (Supplementary Figure 3).

Preservation of Early α SA53T Conformations by Test Compounds Monitored Using IM-MS

IM-MS was utilized to investigate the α SA53T conformational changes occurring early during aggregation in the presence and absence of each test compound. An effective amyloid inhibitor compound would not only prevent fibril formation, but also preserve the protein in its natively unfolded state. IM-MS has important application for investigating the early aggregation phenomena of amyloidogenic proteins, since the unfolded native proteins convert into a compact folded conformation that precedes fibrillization (Smith et al., 2010; Liu et al., 2014). The mass spectrum of α SA53T prior to incubation displayed a broad charge state distribution consistent with a natively unstructured protein (Konermann and Douglas, 1998; Figure 4A). The measured CCSs for monomeric α SA53T ions prior to incubation were plotted in Figure 4B, and are in agreement with previously reported IM-MS measurements of the α SA53T monomer (Liu et al., 2011). Lower charge states having a lower CCS represent the population of ions with more compact structure, while from charge states +8 to +9 the CCS measured increases significantly, indicative of a transition from compact to extended structures. A similar observation was reported previously for wild type α -synuclein (Bernstein et al., 2004).

Following 48 h incubation, IM-MS analysis showed that α SA53T ions of both lower and higher charge states from +7 to +12 underwent a structural collapse as indicated by a notable decrease in measured CCSs. Notably, when α SA53T was incubated in the presence of inhibitor compounds, the measured CCS values of the monomers revealed that the protein mostly remained in its native conformation after 48 h, with honokiol or 2-D08 shown to be most effective (Figure 4B). Among the flavones, CCSs of α SA53T in the presence of myricetin or 2-D08 or transilitin were comparable.

To simplify the analysis of α SA53T conformations in the presence of each test compound, we selected a single charge state, +11, for comparison of CCSs based on the data shown in Figure 4B. This charge state was selected as ion populations at higher charge states tend to display a single, narrow feature in the arrival time distribution and it showed remarkable collapse of unfolded conformations, from 2,937 to 2,520 \AA^2 following 48 h of incubation. Incubation of α SA53T in the presence of punicalagin, myricetin, transilitin, Compound 2

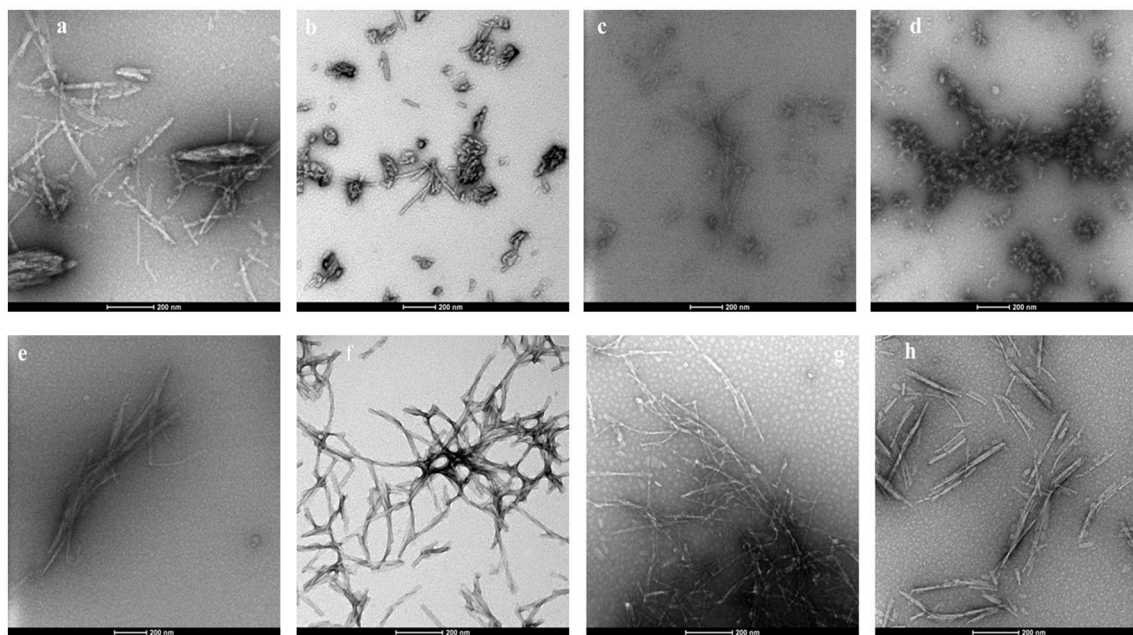


FIGURE 3 | Representative transmission electron micrographs of α SA53T fibril and aggregate formation, following 100 h incubation alone and with each test compound at a 1:2 (protein: compound) molar ratio; (a) α SA53T alone and in presence of (b) Compound 1, (c) Compound 2, (d) 2-D08, (e) myricetin, (f) honokiol, (g) punicalagin, and (h) transilitin. Scale bar: 200 nm.

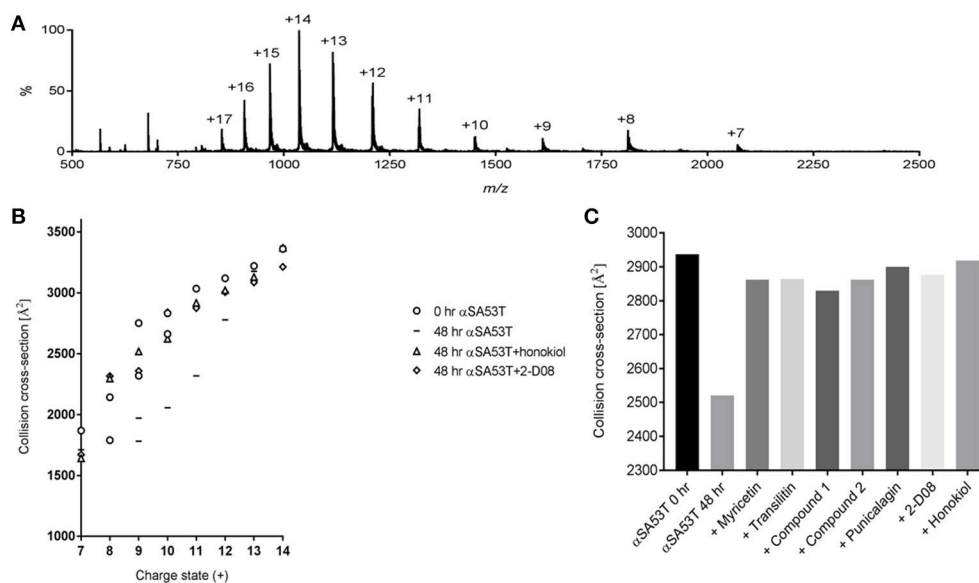
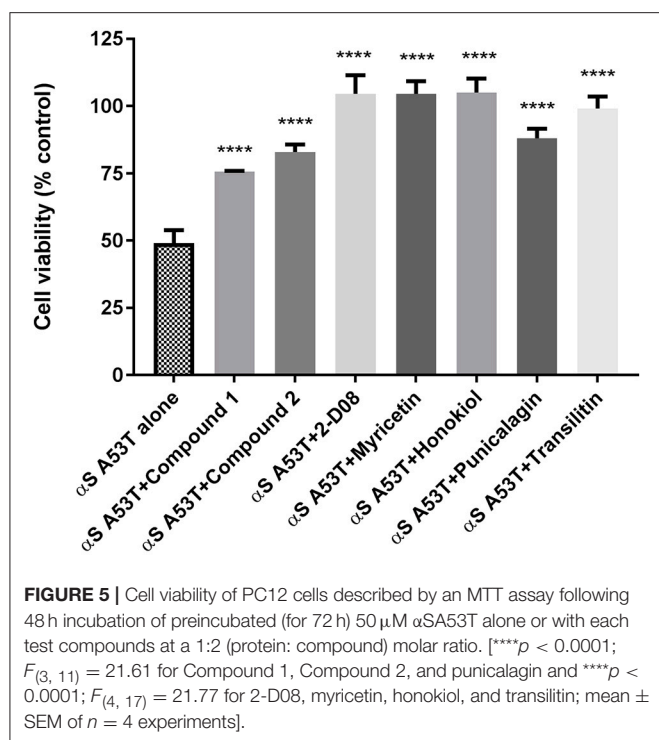


FIGURE 4 | (A) IM-MS spectrum of α SA53T (50 μ M) in 50 mM ammonium acetate. (B) Plot of CCS vs. charge state for the dominant peaks in the IM-MS spectrum measured for α SA53T at 0 h (circles) and following incubation in the absence (squares) and presence of 1:2 (protein: compound) honokiol (triangles) or 2-D08 (diamonds). Where multiple features were observed in the ATD, CCS is plotted for each feature. (C) Experimentally derived CCSs for the +11-charge state (m/z 1,317) of α SA53T following 48 h incubation at 37°C with shaking at 300 rpm.

and Compound 1 preserved the CCS of the 11+ ions close to the preincubation measurement after 48 h (Figure 4C). Detailed CCSs measurements of all these compounds for each charge state is provided in Supplementary Figures 4a–e. Overall, all seven

test compounds demonstrated inhibition of the early structural collapse of α SA53T during aggregation, with honokiol and 2-D08 being the most effective as evidenced by preventing the decrease in CCSs.



Effects of Compounds on Fibrillar α SA53T Mediated Neuronal Toxicity

Analysis of cell viability as determined by the MTT assay demonstrated that preincubated α SA53T (50 μ M) alone evoked about 50% loss of cell viability over 48 h (Figure 5). In contrast, preincubated α SA53T in the presence of each test compound at a 1:2 (protein: compound) molar ratio prevented the loss of cell viability significantly (Figure 5). PC12 cells exposed to preincubated α SA53T in the presence of 2-D08, myricetin, or honokiol (100 μ M each) did not show any loss of cell viability. This finding implies that interaction of these compounds with α SA53T inhibited the neurotoxicity of the resultant fibrils toward PC12 cells *in vitro*. The two synthetic imidazolidines, Compound 1 and Compound 2 also significantly mitigated the loss of cell viability compared to α SA53T alone, however, the degree of neuroprotection was not as pronounced as the other natural test compounds (Figure 5). In a 1:1 (protein: compound) molar ratio, only Compound 2, 2-D08, myricetin, honokiol, and punicalagin-treated significantly reversed the loss of cell viability from α SA53T (Supplementary Figure 5). The mean percentage cell viability along with respective SEM values for each compound are provided as Supplementary Table 2.

Molecular Modeling of Optimized Conformations of Test Compounds to α S A53T

Results from docking studies indicated that all the test compounds bound near the lysine-rich hinge area ranging from residue Ala 17 to Gly 36 in the predefined docking search space (Figures 6A–D and Supplementary Figures 6a–c). Both synthetic imidazolidines Compound 1 and Compound 2 displayed higher

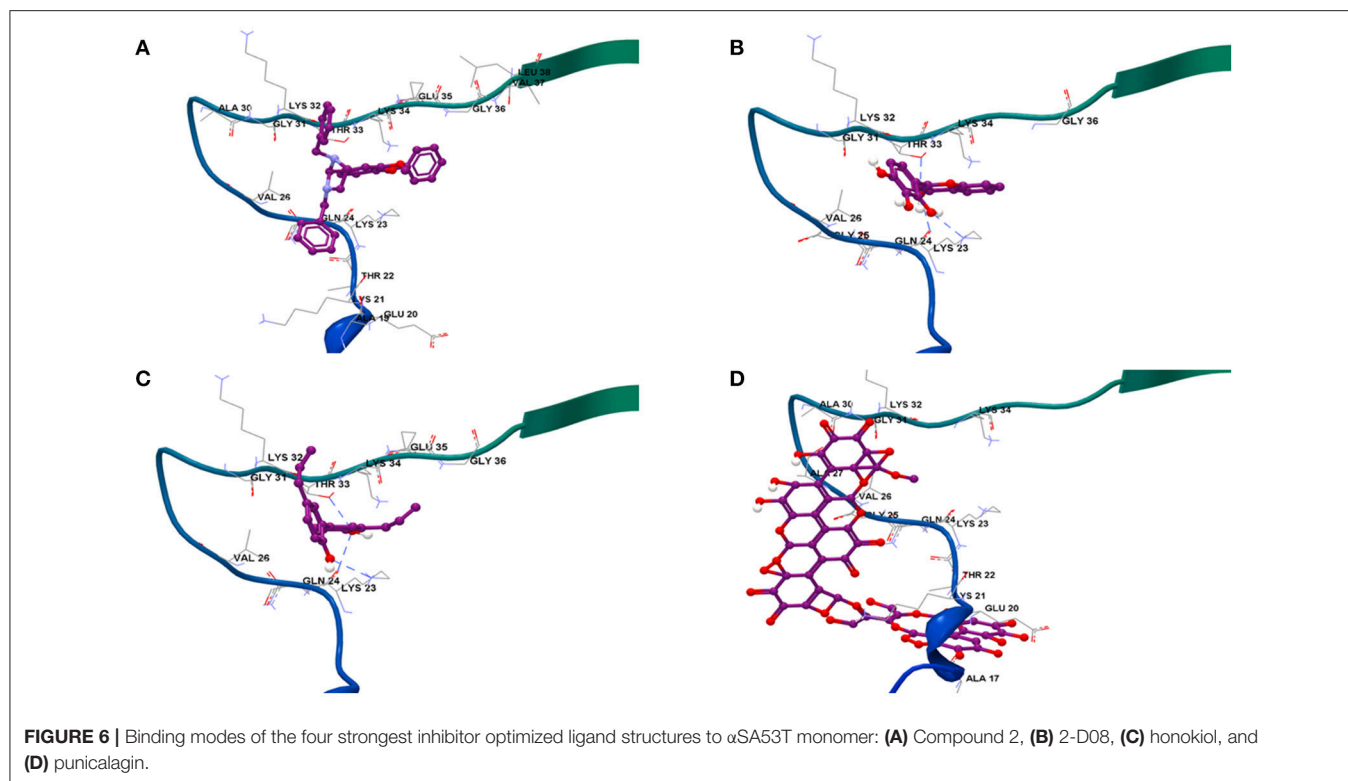
docking scores and steric interactions than the rest of the ligands; however, neither formed any H-bonding interactions (Table 1; Figures 6A,B). The two trihydroxy flavones, 2-D08 and myricetin, yielded similar scores, with myricetin forming more H-bonding interactions than 2-D08. Transilittin, a dihydroxy flavone, had similar docking and H-bonding scores as myricetin. The lignan honokiol had the highest score among the natural compounds, indicating strong interaction and H-bonding to Lys 23 and Thr 33 while the ellagitannin punicalagin had the lowest score, implying punicalagin might be a poor binder to α SA53T. H-bonding with key Lys residues, especially Lys 23 and Lys 21 was found in the case of all tested natural ligands.

DISCUSSION

A growing number of studies have emphasized that accumulation or aggregation of α -synuclein plays a key role in neurodegeneration via mitochondrial and lysosomal dysfunction (Hashimoto et al., 2003; Mazzulli et al., 2016). A search for α S aggregation inhibitors possessing different molecular scaffolds, other than the commonly used dopamine analogs would be insightful for rational drug design. This study has identified and compared the neuroprotective properties of common and novel flavones as well as other polyphenols, along with two synthetic imidazolidine compounds, which can attenuate the toxic aggregation of α SA53T *in vitro*. The seven compounds studied here can be broadly divided into four categories, based on their structures; (i) the flavones: myricetin, 2-D08 and transilittin, (ii) neolignan: honokiol, (iii) ellagitannin: punicalagin, and (iv) synthetic dibenzyl phenyl imidazolidines: Compound 1 and Compound 2. Molecular docking provided additional insight into their probable binding sites and the nature of interactions that might contribute to structural modification of α SA53T during fibrillization, to result in the formation of non-toxic aggregates.

Interaction of Flavones and Their Effect on α SA53T Conformation, Fibrillization, and Neurotoxicity

The three flavones studied here possessed a catechol-type vicinal tri-hydroxylation in the B-ring (myricetin and 2-D08) and dihydroxylation in both A and B-rings (transilittin). A major aim of this study was to investigate how restricted tri-hydroxylation in the flavone B-ring (2-D08) impacts α S amyloid aggregation. TEM imaging revealed that 2-D08 altered the fibril morphology more significantly than myricetin or transilittin, despite similar ThT fluorescence outputs, in particular, TEM images after 50 h incubation revealed that 2-D08 modified the α SA53T active fibrillisation phase differently than myricetin or transilittin. The amorphous α SA53T aggregates arising from incubation with 2-D08 are likely to possess a reduced hydrophobic surface that is critical for ThT micellar binding, thus lowering fluorescence (Khurana et al., 2005). These amorphous aggregates resemble α -Synuclein treated with baicalein as observed in a previous study (Hu et al., 2016). Notably, 2-D08 showed an exclusive interaction



with Lys 23, followed by Thr 33 and unlike transilitin and myricetin. Therefore, restriction of the *O*-quinone forming three -OH side groups in either the A or B-ring of the flavone might be favorable for binding to inhibit α S fibrillization as previously observed with baicalein (Hong et al., 2008). Nevertheless, the primary interaction of 2-D08 with α SA53T could be a low affinity, transient interaction between the protein and ligand rather than covalent modification of the Lys and Thr residues in the binding region, as we did not observe significant adduct formation in our IMMS study. Gallic acid had been shown to inhibit α SA53T structural collapse in a similar manner (Liu et al., 2014).

We previously reported that 2-D08 exerted a novel anti-aggregatory and neuroprotective effect against A β compared to transilitin and quercetin, which have A and C-ring hydroxylation (Marsh et al., 2017). In the present study, 2-D08 induced inhibition of α S aggregation and neuroprotection was as pronounced as myricetin, a generic amyloid aggregation inhibitor, and supports the idea that restricted B-ring trihydroxylation is adequate for targeting both α S and A β (Ono and Yamada, 2006; Hirohata et al., 2007; Zelus et al., 2012; Liu et al., 2015). From the TEM imaging, it appeared that transilitin modified the α SA53T fibrils in a similar way to myricetin, where only loose fibrils but no amorphous aggregates were seen. It is likely that these two flavones with A-ring hydroxylation share a common mechanism for inhibiting aggregation by reducing toxic amyloidogenic fibrils, whereas 2-D08 may inhibit amyloid fibrillization through formation of non-toxic amorphous aggregates. Consequently, within the

flavone molecular scaffold, both 2-D08 and transilitin appear to be generic inhibitors of α SA53T and A β aggregation, similar to myricetin. Comparing the strong inhibitory effect of transilitin with the flavonoid G-500 suggests that additional hydroxyl groups other than the two pairs in the A and C-rings might be redundant (Meng et al., 2010). Together, our findings emphasize the previously reported idea that vicinal trihydroxylation in the flavone is favorable for strong inhibition of α S aggregation, coupled with its precise position in the B-ring (Meng et al., 2010).

IM-MS is an emerging analytical method that retains weak non-covalent interactions in the gas-phase and maintains protein conformations from solution phase (Koneremann and Douglas, 1998; Sarni-Manchado and Cheyner, 2002; Wyttenbach and Bowers, 2011; Abzalimov et al., 2012). The IM-MS study presented here reinforces that soluble α SA53T undergoes a structural transition from natively unfolded to more compact amyloidogenic conformations at an early stage of aggregation, as measured by changes in CCSs. This is consistent with our ThT results, where the increasing fluorescence reaches its maximum by \sim 50 h, indicating the fibril plateau phase is reached in this time frame. Stabilization of unfolded α SA53T conformations to prevent amyloid formation was observed by IM-MS in the presence of all three flavones tested and was further supported by inhibition of ThT fluorescence during this early aggregation period.

No loss in PC12 cell viability was observed *in vitro* by preincubated α SA53T in the presence of 2-D08, even at an equimolar concentration, corroborating that the loose

TABLE 1 | Docking profiles of seven test compounds to α SA53T monomer.

Ligand	Docking score	H-bond forming residues	H-bond score	Steric interaction score	RMSD (Å)
Compound 1	-69.23	–	0.00	-73.48	133.13
Compound 2	-65.53	–	0.00	-68.25	136.99
2-D08	-44.89	Lys 23, Thr 33	-6.00	-40.88	137.15
Myricetin	-41.82	Ala 19, Lys 21, 23, Thr 22, Gln 24, Gly 25	-10.45	-32.68	129.40
Honokiol	-58.36	Lys 23, Thr 33	-6.00	-55.55	137.42
Punicalagin	-38.00	Lys 21, Lys 23	-5.83	-38.28	131.27
Transilitin	-50.09	Lys 23, Lys 32, Thr 33, Lys 34	-10.00	-44.82	136.70

amorphous aggregates formed under these conditions are not amyloidogenic or toxic. The prevention of structural collapse by 2-D08 effectively inhibited the toxic amyloid formation of α SA53T, providing a degree of neuroprotection as pronounced as myricetin. Transilitin, on the other hand, was less effective in halting α SA53T amyloidogenic aggregation and neurotoxicity at an equimolar concentration. Since there is some degree of α SA53T folding as measured by CCSs in the presence of transilitin, this might account for the reduced neuroprotection at a lower concentration. Combining the anti-aggregation and neuroprotection results, we can infer that flavone tri-hydroxylation is more effective against toxic α SA53T amyloidogenic aggregation than di-hydroxylation. An understanding of the precise flavone structural requirements for strong inhibition of α S toxic aggregation would facilitate improved drug design. As exemplified with quercetin, hydroxylation in the flavone 3 and 7 positions are susceptible to thiol formation with cellular proteins rather than being neutralized in the cellular antioxidant network (Jacobs et al., 2011). Therefore, not having any hydroxylation in these positions while retaining a strong inhibitory effect seems a valuable strategy for improved drug design. Consequently, 2-D08 would be more favorable than myricetin to serve as a template for flavone-based inhibitors of α S toxic aggregation.

Lignan Interaction With α SA53T During Fibrillization and Neurotoxicity

Outside the flavonoid class of compounds, other small molecule polyphenolics such as lignans have recently gained attention for amyloid inhibition. In the present study, honokiol showed a profound effect on α SA53T aggregation, as indicated by the TEM imaging and ThT assay. TEM images of honokiol-treated α SA53T fibrils to some extent resembled analogous samples with punicalagin when comparing the long fibrils, and transilitin when comparing the short fibrils. These modified fibrils might account for the residual ThT fluorescence. As a strong inhibitor, honokiol prevented the structural collapse of native monomeric α SA53T at a very early stage of aggregation, as observed for 2-D08, although treatment with honokiol did not produce any amorphous aggregates. TEM images following 50 h incubation suggested that honokiol effectively inhibited α SA53T fibrillization at an early stage, in agreement with the ThT and IM-MS results. The demonstrated neuroprotection by preincubated α SA53T fibrils in the presence of honokiol

highlights the non-toxic and non-amyloidogenic nature of the detached fibrils observed. Molecular docking results indicated that honokiol has the highest overall and steric binding scores among the natural compounds, while interacting strongly with key residues Lys 23 and Thr 33 through hydrogen-bonding, a similar interaction observed in the docking profile of 2-D08. This indicated a more sterically favorable interaction with this binding region to stabilize the unfolded α SA53T monomer. Nonetheless, honokiol lacks any *O*-quinone forming vicinal dihydroxyl structure like 2-D08 or other catechol-type flavones. Therefore, it might not covalently modify the target but interact through π - π stacking. Presumably, honokiol and tri-hydroxyflavones such as 2-D08 or myricetin might have different modes of interacting with α SA53T, nevertheless, they all result in similar degree of inhibition of amyloidogenic aggregation. Previously, honokiol was reported to be effective against toxicity related to A β and calcitonin aggregation (Guo et al., 2015; Das et al., 2016), and shown to be as effective as resveratrol and EGCG in an *in vivo* model of A β toxicity, inhibition of cholinesterase and metal chelation (Kantham et al., 2017). Together, honokiol has as pronounced an effect as the two tri-hydroxyflavones on inhibiting α SA53T aggregation and toxic amyloidogenic formation. Nonetheless, the molecular mechanism underlying this lignan based inhibition of α S aggregation is yet to be fully understood.

Effect of Ellagitannin on α SA53T Fibrillization and Neurotoxicity

Punicalagin, being the largest molecule tested, presents interesting information on the role of steric bulk. Like the flavones and honokiol, punicalagin also maintained the natively unfolded structure of α SA53T in its early stage of aggregation. Seemingly, the thin, long fibrils arising from punicalagin-treated α SA53T might not be toxic amyloid fibrils, as it exerted significant neuroprotection to α SA53T-exposed PC12 cells. These fibrils might have undergone a loss of hydrophobic surface area where ThT micelles could bind, thus diminishing fluorescence output (Khurana et al., 2005). Not surprisingly, molecular docking predicted that punicalagin was a poor binder to α SA53T, possibly due to steric hindrance as a result of its bulky size, however, it was predicted to form H-bonding interactions with key Lys 21 and 23 like other natural polyphenols tested here. Having multiple vicinal hydroxylation sites across the molecule, it is highly probable that punicalagin has several interaction

modes with polar residues in an unfolded protein. Therefore, it is possible that punicalagin interacted with these predicted residues to preserve an unfolded conformation that resulted in non-amyloidogenic fibril formation. This was further supported by the TEM study following 50 h incubation. Due to the bulky size, punicalagin might have weak, non-specific interactions, not binding to a particular pocket unlike other small molecule polyphenolics. There is a correlation between the antioxidant activity of flavonoids and their *in vitro* inhibitory effect on α S fibrillization (Meng et al., 2009). We previously showed that punicalagin was capable of inhibiting amyloid β aggregation and neurotoxicity (Das et al., 2016). Given punicalagin has some similarities in terms of being an extensively hydroxylated polyphenol, its high antioxidant activity might also contribute toward its inhibitory effect.

Novel Dibenzyl Imidazolidine Scaffold Effect on α SA53T Fibrillization and Neurotoxicity

Our previous study employing structure-based virtual screening for $A\beta_{1-42}$ inhibitors identified two compounds with anti-aggregatory and neuroprotective roles *in vitro* (Das and Smid, 2017). These two synthetic compounds bearing a novel dibenzyl imidazolidine scaffold could provide insight on the effect of this scaffold on α SA53T aggregation in comparison with natural polyphenolics. TEM imaging suggests that the α SA53T fibril morphology, modified by both compounds, is different than that induced by the polyphenolics. Nonetheless, the TEM study after 50 h incubation showed that α SA53T modified by Compound 2 resembled the morphology of myricetin-incubated samples. Furthermore, there is variable effect on fibril morphology between these two compounds. In the presence of Compound 1, the small dense aggregates look different than the amorphous aggregates produced by 2-D08. The presence of both aggregates and short fibrils indicate that Compound 1 might have more than one mechanism of interaction with α SA53T during aggregation. The docking study predicted no polar interactions between Compound 1 and α SA53T and showed higher docking scores, suggesting a non-stable protein-ligand interaction. The reduction of CCSs for some α SA53T charge states in the presence of Compound 1 indicates it is less effective in stabilizing the native α SA53T unfolded state. Therefore, interaction of Compound 1 with α SA53T might not completely prevent its amyloidogenic aggregation, especially at lower concentration, unlike the natural polyphenolics and Compound 2. This was further supported by the comparative neurotoxicity observed in PC12 cells, and a higher ThT fluorescence at equimolar concentrations of protein: compound.

In the case of Compound 2, the appearance of thin, long fibrils but no dense aggregates points toward a different mechanism of interaction with α SA53T than Compound 1. There is some degree of similarity between α SA53T fibrils formed by Compound 2 and myricetin. However, Compound 2 had a mostly sterically favorable binding to α SA53T, while myricetin has both steric and polar interactions observable from the docking study.

Compound 2 demonstrated significant neuroprotection and low ThT fluorescence at an equimolar concentration of protein: compound. Improved inhibition of α SA53T toxic amyloid aggregation by Compound 2 over Compound 1 is feasibly attributable to the additional -OCH₃ functional group adjacent to the phenyl group in the dibenzyl imidazolidine scaffold in Compound 2. This finding is consistent with our previous study on these compounds against $A\beta_{1-42}$, where we found that Compound 2 significantly inhibited $A\beta_{1-42}$ aggregation in both ThT and TEM analysis, whereas Compound 1 was not able to inhibit ThT fluorescence (Das and Smid, 2017). Considering the novel aspect and effectiveness of both compounds bearing this dibenzyl imidazolidine scaffold, our findings highlight the potential of this molecular scaffold when targeted against pathological amyloidogenic proteins.

CONCLUSION

Among the seven compounds tested and compared here, polyphenols such as 2-D08, honokiol, myricetin, punicalagin, and the synthetic imidazolidine, Compound 2 are the most effective inhibitors of α SA53T toxic amyloidogenic aggregation, while transilitin and other synthetic imidazolidines, such as Compound 1, were less effective. All of these compounds inhibited toxic amyloidogenic aggregation by stabilizing the native unfolded α SA53T conformations, which in turn altered α SA53T fibril morphology. This structurally diverse group of molecules could potentially facilitate improved drug design targeting the complexity of progressive neurodegenerative diseases associated with amyloidogenic protein aggregation.

AUTHOR CONTRIBUTIONS

SD, SS, and TP conceived the presented study. SD performed the experiments, computational modeling studies and data analysis with support from TP and project supervision from SS. The manuscript was written by SD with input from all authors.

ACKNOWLEDGMENTS

We thank Lisa Anne O'Donovan from Adelaide Microscopy for her assistance with setting up the TEM machine, and Julian Harrison and Celine Kelso from the University of Wollongong for contributions to optimization of the native IM-MS method. We also thank Agilent Technologies for support with ion mobility-mass spectrometry instrumentation. This research was supported partially by the Australian Government through the Australian Research Council's *Discovery Projects* funding scheme (project DP170102033).

SUPPLEMENTARY MATERIAL

The Supplementary Material for this article can be found online at: <https://www.frontiersin.org/articles/10.3389/fchem.2018.00181/full#supplementary-material>

REFERENCES

- Abzalimov, R. R., Frimpong, A. K., and Kaltashov, I. A. (2012). "Detection and characterization of large-scale protein conformational transitions in solution using charge-state distribution analysis in ESI-MS," in *Intrinsically Disordered Protein Analysis: Volume 2, Methods and Experimental Tools*, eds N. Vladimir Uversky and A. Keith Dunker (New York, NY: Springer New York), 365–373.
- Baba, M., Nakajo, S., Tu, P. H., Tomita, T., Nakaya, K., Lee, V. M., et al. (1998). Aggregation of alpha-synuclein in Lewy bodies of sporadic Parkinson's disease and dementia with Lewy bodies. *Am. J. Pathol.* 152, 879–884.
- Bernstein, S. L., Liu, D., Wyttenbach, T., Bowers, M. T., Lee, J. C., Gray, H. B., et al. (2004). α -Synuclein: stable compact and extended monomeric structures and pH dependence of dimer formation. *J. Am. Soc. Mass Spectrom.* 15, 1435–1443. doi: 10.1016/j.jasms.2004.08.003
- Bharathi, Indi, S. S., and Rao, K. S. J. (2007). Copper- and iron-induced differential fibril formation in α -synuclein: TEM study. *Neurosci. Lett.* 424, 78–82. doi: 10.1016/j.neulet.2007.06.052
- Bieschke, J., Russ, J., Friedrich, R. P., Ehrnhoefer, D. E., Wobst, H., Neugebauer, K., et al. (2010). EGCG remodels mature α -synuclein and amyloid- β fibrils and reduces cellular toxicity. *Proc. Natl. Acad. Sci. U.S.A.* 107, 7710–7715. doi: 10.1073/pnas.0910723107
- Bousset, L., Pieri, L., Ruiz-Arlandis, G., Gath, J., Jensen, P. H., Habenstein, B., et al. (2013). Structural and functional characterization of two alpha-synuclein strains. *Nat. Commun.* 4:2575. doi: 10.1038/ncomms3575
- Cabin, D. E., Shimazu, K., Murphy, D., Cole, N. B., Gottschalk, W., McIlwain, K. L., et al. (2002). Synaptic vesicle depletion correlates with attenuated synaptic responses to prolonged repetitive stimulation in mice lacking alpha-synuclein. *J. Neurosci.* 22, 8797–8807. doi: 10.1523/JNEUROSCI.22-20-08797.2002
- Coelho-Cerqueira, E., Pinheiro, A. S., and Follmer, C. (2014). Pitfalls associated with the use of Thioflavin-T to monitor anti-fibrillogenic activity. *Bioorg. Med. Chem. Lett.* 24, 3194–3198. doi: 10.1016/j.bmcl.2014.04.072
- Chandra, S., Gallardo, G., Fernandez-Chacon, R., Schluter, O. M., and Sudhof, T. C. (2005). Alpha-synuclein cooperates with CSPalpha in preventing neurodegeneration. *Cell* 123, 383–396. doi: 10.1016/j.cell.2005.09.028
- Cooper, A. A., Gitler, A. D., Cashikar, A., Haynes, C. M., Hill, K. J., Bhullar, B., et al. (2006). α -synuclein blocks ER-Golgi traffic and Rab1 rescues neuron loss in Parkinson's models. *Science* 313, 324–328. doi: 10.1126/science.1129462
- Das, S., and Smid, S. D. (2017). Identification of dibenzyl imidazolidine and triazole acetamide derivatives through virtual screening targeting amyloid beta aggregation and neurotoxicity in PC12 cells. *Eur. J. Med. Chem.* 130, 354–364. doi: 10.1016/j.ejmech.2017.02.057
- Das, S., Stark, L., Musgrave, I. F., Pukala, T., and Smid, S. D. (2016). Bioactive polyphenol interactions with [small beta] amyloid: a comparison of binding modelling, effects on fibril and aggregate formation and neuroprotective capacity. *Food Funct.* 7, 1138–1146. doi: 10.1039/C5FO01281C
- El-Azhary, A. A., and Suter, H. U. (1996). Comparison between optimized geometries and vibrational frequencies calculated by the DFT methods. *J. Phys. Chem.* 100, 15056–15063. doi: 10.1021/jp960618o
- Frisch, M. J., Trucks, G. W., Schlegel, H. B., Scuseria, G. E., Robb, M. A., Cheesema, J. R., et al. (2016). *Gaussian 09*. Wallingford, CT: Gaussian, Inc.
- Guo, C., Ma, L., Zhao, Y., Peng, A., Cheng, B., Zhou, Q., et al. (2015). Inhibitory effects of magnolol and honokiol on human calcitonin aggregation. *Sci. Rep.* 5:13556. doi: 10.1038/srep13556
- Hashimoto, M., Rockenstein, E., Crews, L., and Masliah, E. (2003). Role of protein aggregation in mitochondrial dysfunction and neurodegeneration in Alzheimer's and Parkinson's diseases. *Neuromol. Med.* 4, 21–35. doi: 10.1385/NMM:4:1-2:21
- Hirohata, M., Hasegawa, K., Tsutsumi-Yasuhara, S., Ohhashi, Y., Ookoshi, T., Ono, K., et al. (2007). The anti-amyloidogenic effect is exerted against Alzheimer's β -amyloid fibrils *in vitro* by preferential and reversible binding of flavonoids to the amyloid fibril structure. *Biochemistry* 46, 1888–1899. doi: 10.1021/bi061540x
- Hoi, C. P., Ho, Y. P., Baum, L., and Chow, A. H. (2010). Neuroprotective effect of honokiol and magnolol, compounds from *Magnolia officinalis*, on beta-amyloid-induced toxicity in PC12 cells. *Phytother. Res.* 24, 1538–1542. doi: 10.1002/ptr.3178
- Hong, D. P., Fink, A. L., and Uversky, V. N. (2008). Structural characteristics of α -synuclein oligomers stabilized by the flavonoid baicalein. *J. Mol. Biol.* 383, 214–223. doi: 10.1016/j.jmb.2008.08.039
- Hu, Q., Uversky, V. N., Huang, M., Kang, H., Xu, F., Liu, X., et al. (2016). Baicalein inhibits α -synuclein oligomer formation and prevents progression of α -synuclein accumulation in a rotenone mouse model of Parkinson's disease. *Biochim. Biophys. Acta* 1862, 1883–1890. doi: 10.1016/j.bbdis.2016.07.008
- Hughes, A. J., Daniel, S. E., Kilford, L., and Lees, A. J. (1992). Accuracy of clinical diagnosis of idiopathic Parkinson's disease: a clinico-pathological study of 100 cases. *J. Neurol. Neurosurg. Psychiatry* 55, 181–184. doi: 10.1136/jnnp.55.3.181
- Iyer, A., Petersen, N. O., Claessens, M. M. A. E., and Subramaniam, V. (2014). Amyloids of alpha-synuclein affect the structure and dynamics of supported lipid bilayers. *Biophys. J.* 106, 2585–2594. doi: 10.1016/j.bpj.2014.05.001
- Jacobs, H., Moalin, M., van Gisbergen, M. W., Bast, A., van der Vijgh, W. J., and Haenen, G. R. (2011). An essential difference in the reactivity of the glutathione adducts of the structurally closely related flavonoids monoHER and quercetin. *Free Radic. Biol. Med.* 51, 2118–2123. doi: 10.1016/j.freeradbiomed.2011.09.013
- Kantham, S., Chan, S., McColl, G., Miles, J. A., Veliyath, S. K., Deora, G. S., et al. (2017). Effect of the biphenyl neolignan honokiol on A β 42-induced toxicity in *Caenorhabditis elegans*, A β 42 fibrillation, cholinesterase activity, DPPH radicals, and iron(II) chelation. *ACS Chem. Neurosci.* 8, 1901–1912. doi: 10.1021/acschemneuro.7b00071
- Khurana, R., Coleman, C., Ionescu-Zanetti, C., Carter, S. A., Krishna, V., Grover, R. K., et al. (2005). Mechanism of thioflavin T binding to amyloid fibrils. *J. Struct. Biol.* 151, 229–238. doi: 10.1016/j.jsb.2005.06.006
- Konermann, L., and Douglas, D. J. (1998). Unfolding of proteins monitored by electrospray ionization mass spectrometry: a comparison of positive and negative ion modes. *J. Am. Soc. Mass Spectrom.* 9, 1248–1254. doi: 10.1016/S1044-0305(98)00103-2
- Korb, O., Stützel, T., and Exner, T. E. (2009). Empirical scoring functions for advanced protein–ligand docking with PLANTS. *J. Chem. Inf. Model.* 49, 84–96. doi: 10.1021/ci800298z
- Lanucara, F., Holman, S. W., Gray, C. J., and Evers, C. E. (2014). The power of ion mobility-mass spectrometry for structural characterization and the study of conformational dynamics. *Nat. Chem.* 6:281. doi: 10.1038/nchem.1889
- Li, J., Uversky, V. N., and Fink, A. L. (2001). Effect of familial Parkinson's disease point mutations A30P and A53T on the structural properties, aggregation, and fibrillation of human alpha-synuclein. *Biochemistry* 40, 11604–11613. doi: 10.1021/bi010616g
- Liu, Y., Carver, J. A., Calabrese, A. N., and Pukala, T. L. (2014). Gallic acid interacts with α -synuclein to prevent the structural collapse necessary for its aggregation. *Biochim. Biophys. Acta* 1844, 1481–1485. doi: 10.1016/j.bbapap.2014.04.013
- Liu, Y., Graetz, M., Ho, L., and Pukala, T. L. (2015). Ion mobility—mass spectrometry-based screening for inhibition of α -synuclein aggregation. *Eur. J. Mass Spectrom.* 21, 255–264. doi: 10.1255/ejms.1359
- Liu, Y., Ho, L. H., Carver, J. A., and Pukala, T. L. (2011). Ion mobility mass spectrometry studies of the inhibition of alpha synuclein amyloid fibril formation by (–)-epigallocatechin-3-gallate. *Aust. J. Chem.* 64, 36–40. doi: 10.1071/CH10334
- Luk, K. C., Kehm, V., Carroll, J., Zhang, B., O'Brien, P., Trojanowski, J. Q., et al. (2012). Pathological α -Synuclein transmission initiates Parkinson-like neurodegeneration in nontransgenic mice. *Science* 338, 949–953. doi: 10.1126/science.1227157
- Marsh, D. T., Das, S., Ridell, J., and Smid, S. D. (2017). Structure-activity relationships for flavone interactions with amyloid beta reveal a novel anti-aggregatory and neuroprotective effect of 2',3',4'-trihydroxyflavone (2-D08). *Bioorg. Med. Chem.* 25, 3827–3834. doi: 10.1016/j.bmc.2017.05.041
- Masuda, M., Suzuki, N., Taniguchi, S., Oikawa, T., Nonaka, T., Iwatsubo, T., et al. (2006). Small molecule inhibitors of α -synuclein filament assembly. *Biochemistry* 45, 6085–6094. doi: 10.1021/bi0600749
- Mazzulli, J. R., Zunke, F., Isacson, O., Studer, L., and Krainc, D. (2016). α -Synuclein-induced lysosomal dysfunction occurs through disruptions in protein trafficking in human midbrain synucleinopathy models. *Proc. Natl. Acad. Sci. U.S.A.* 113, 1931–1936. doi: 10.1073/pnas.1520335113
- Meng, X., Munishkina, L. A., Fink, A. L., and Uversky, V. N. (2009). Molecular mechanisms underlying the flavonoid-induced inhibition of α -synuclein fibrillation. *Biochemistry* 48, 8206–8224. doi: 10.1021/bi900506b

- Meng, X., Munishkina, L. A., Fink, A. L., and Uversky, V. N. (2010). Effects of various flavonoids on the α -synuclein fibrillation process. *Parkinson's Dis.* 2010:16. doi: 10.4061/2010/650794
- Morshedi, D., Aliakbari, F., Tayaranian-Marvian, A., Fassih, A., Pan-Montojo, F., and Perez-Sanchez, H. (2015). Cuminaldehyde as the major component of *Cuminum cyminum*, a natural aldehyde with inhibitory effect on alpha-synuclein fibrillation and cytotoxicity. *J. Food Sci.* 80, H2336–H2345. doi: 10.1111/1750-3841.13016
- Narhi, L., Wood, S. J., Steavenson, S., Jiang, Y., Wu, G. M., Anafi, D., et al. (1999). Both familial Parkinson's disease mutations accelerate alpha-synuclein aggregation. *J. Biol. Chem.* 274, 9843–9846. doi: 10.1074/jbc.274.14.9843
- Ono, K., and Yamada, M. (2006). Antioxidant compounds have potent anti-fibrillogenic and fibril-destabilizing effects for α -synuclein fibrils *in vitro*. *J. Neurochem.* 97, 105–115. doi: 10.1111/j.1471-4159.2006.03707.x
- Papadimitriou, D., Antonelou, R., Miligkos, M., Maniati, M., Papagiannakis, N., Bostantjopoulou, S., et al. (2016). Motor and nonmotor features of carriers of the p.A53T alpha-synuclein mutation: a longitudinal study. *Mov. Disord.* 31, 1226–1230. doi: 10.1002/mds.26615
- Polymeropoulos, M. H., Lavedan, C., Leroy, E., Ide, S. E., Dehejia, A., Dutra, A., et al. (1997). Mutation in the alpha-synuclein gene identified in families with Parkinson's disease. *Science* 276, 2045–2047. doi: 10.1126/science.276.5321.2045
- Sarni-Manchado, P., and Cheynier, V. (2002). Study of non-covalent complexation between catechin derivatives and peptides by electrospray ionization mass spectrometry. *J. Mass Spectrom.* 37, 609–616. doi: 10.1002/jms.321
- Sidhu, A., Wersinger, C., and Vernier, P. (2004). Does alpha-synuclein modulate dopaminergic synaptic content and tone at the synapse? *FASEB J.* 18, 637–647. doi: 10.1096/fj.03-1112rev
- Smith, D. P., Radford, S. E., and Ashcroft, A. E. (2010). Elongated oligomers in β 2-microglobulin amyloid assembly revealed by ion mobility spectrometry-mass spectrometry. *Proc. Natl. Acad. Sci. U.S.A.* 107, 6794–6798. doi: 10.1073/pnas.0913046107
- Tuttle, M. D., Comellas, G., Nieuwkoop, A. J., Covell, D. J., Berthold, D. A., Kloepper, K. D., et al. M. (2016). Solid-state NMR structure of a pathogenic fibril of full-length human alpha-synuclein. *Nat. Struct. Mol. Biol.* 23, 409–415. doi: 10.1038/nsmb.3194
- Vlad, C., Lindner, K., Karreman, C., Schildknecht, S., Leist, M., Tomczyk, N., et al. (2011). Autoproteolytic fragments are intermediates in the oligomerization- aggregation of Parkinson's disease protein alpha-synuclein as revealed by ion mobility mass spectrometry. *ChemBiochem* 12, 2740–2744. doi: 10.1002/cbic.201100569
- Volles, M. J., and Lansbury, P. T. Jr. (2007). Relationships between the sequence of α -synuclein and its membrane affinity, fibrillization propensity, and yeast toxicity. *J. Mol. Biol.* 366, 1510–1522. doi: 10.1016/j.jmb.2006.12.044
- Volpicelli-Daley, L. A., Luk, K. C., Patel, T. P., Tanik, S. A., Riddle, D. M., and Stieber, A. (2011). Exogenous α -synuclein fibrils induce lewy body pathology leading to synaptic dysfunction and neuron death. *Neuron* 72, 57–71. doi: 10.1016/j.neuron.2011.08.033
- Wytenbach, T., and Bowers, M. T. (2011). Structural stability from solution to the gas phase: native solution structure of ubiquitin survives analysis in a solvent-free ion mobility-mass spectrometry environment. *J. Phys. Chem. B* 115, 12266–12275. doi: 10.1021/jp206867a
- Yaidikar, L., Byna, B., and Thakur, S. R. (2014). Neuroprotective effect of punicalagin against cerebral ischemia reperfusion-induced oxidative brain injury in rats. *J. Stroke Cerebrovasc. Dis.* 23, 2869–2878. doi: 10.1016/j.jstrokecerebrovasdis.2014.07.020
- Yaidikar, L., and Thakur, S. (2015). Punicalagin attenuated cerebral ischemia-reperfusion insult via inhibition of proinflammatory cytokines, up-regulation of Bcl-2, down-regulation of Bax, and caspase-3. *Mol. Cell. Biochem.* 402, 141–148. doi: 10.1007/s11010-014-2321-y
- Young, L. M., Saunders, J. C., Mahood, R. A., Revill, C. H., Foster, R. J., Tu, L. H., et al. (2014). Screening and classifying small-molecule inhibitors of amyloid formation using ion mobility spectrometry-mass spectrometry. *Nat. Chem.* 7, 73–81. doi: 10.1038/nchem.2129
- Zelus, C., Fox, A., Calciano, A., Faridian, B. S., Nogaj, L. A., and Moffet, D. A. (2012). Myricetin Inhibits Islet Amyloid Polypeptide (IAPP) aggregation and rescues living mammalian cells from IAPP toxicity. *Open Biochem. J.* 6, 66–70. doi: 10.2174/1874091X01206010066
- Zhu, M., Rajamani, S., Kaylor, J., Han, S., Zhou, F., and Fink, A. L. (2004). The flavonoid baicalein inhibits fibrillation of alpha-synuclein and disaggregates existing fibrils. *J. Biol. Chem.* 279, 26846–26857. doi: 10.1074/jbc.M403129200

Conflict of Interest Statement: The authors declare that the research was conducted in the absence of any commercial or financial relationships that could be construed as a potential conflict of interest.

Copyright © 2018 Das, Pukala and Smid. This is an open-access article distributed under the terms of the Creative Commons Attribution License (CC BY). The use, distribution or reproduction in other forums is permitted, provided the original author(s) and the copyright owner are credited and that the original publication in this journal is cited, in accordance with accepted academic practice. No use, distribution or reproduction is permitted which does not comply with these terms.

Appendix A: Supplementary material

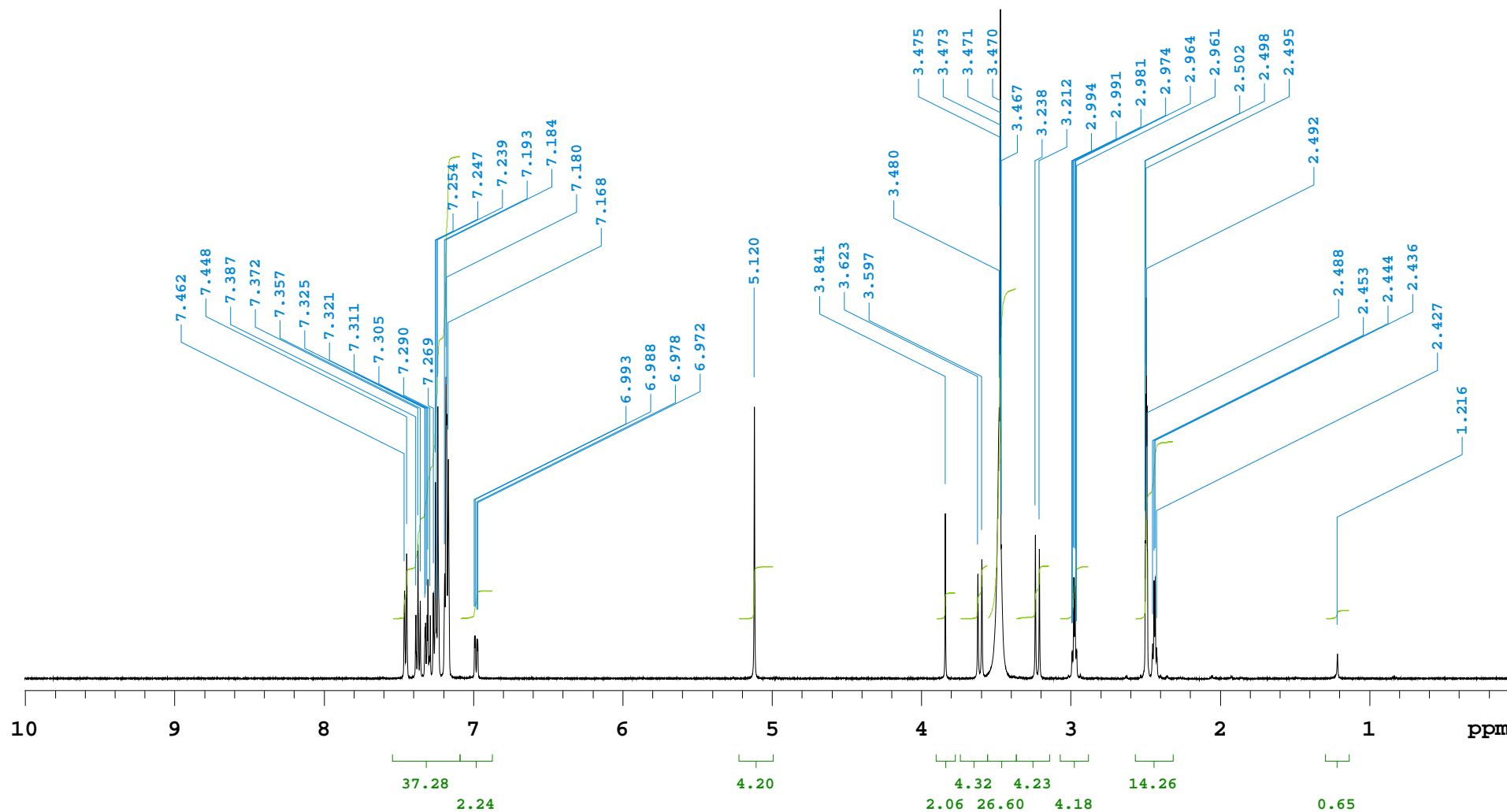


Sample Name Compound 1
Date collected 2015-05-25

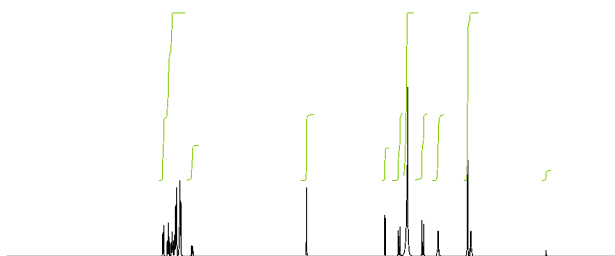
Pulse sequence PRESAT
Solvent dms

Temperature 26
Spectrometer nmr500.chemistry.adelaide.edu.au-vnmrs500

Study owner walkup



Supplementary Figure 1. ¹H-NMR of Compound 1 (1,3-dibenzyl-2-[3-(benzyloxy)phenyl]imidazolidine) in DMSO.



ai cdc ph

imidazolin in DMSO

SAMPLE		PRESATURATION	
date	May 25 2015	satmode	y
solvent	dms	wet	n
file	/home/walkup/vnmrsys /data/walkup/TPimidazolin/ PRESAT_TPimidazolin_dms_2 0150525_500_01	SPECIAL	
ACQUISITION		temp	26.0
sw	8012.8	gain	42
at	4.089	spin	0
np	65536	hst	0.008
fb	4000	pw90	7.200
bs	4	alfa	10.000
ss	1	FLAGS	
d1	2.000	il	n
nt	8	in	n
ct	8	dp	y
TRANSMITTER		hs	nn
tn	H1	PROCESSING	
sfrq	499.813	fn	not used
tof	499.8	DISPLAY	
tpwr	61	sp	1.4
pw	7.200	wp	4999.0
DECOUPLER		rfl	1007.6
dn	C13	rfp	0
dof	0	rp	-105.0
dm	nnn	lp	0
decwave	W40_onenmr_MR1203 W035	PLOT	
dpwr	39	wc	252
dmf	32258	sc	8
Plotname: PRESAT_TPimidazolin_dms_20150525_500_01_plot01			
		vs	81
		th	4

Supplementary material

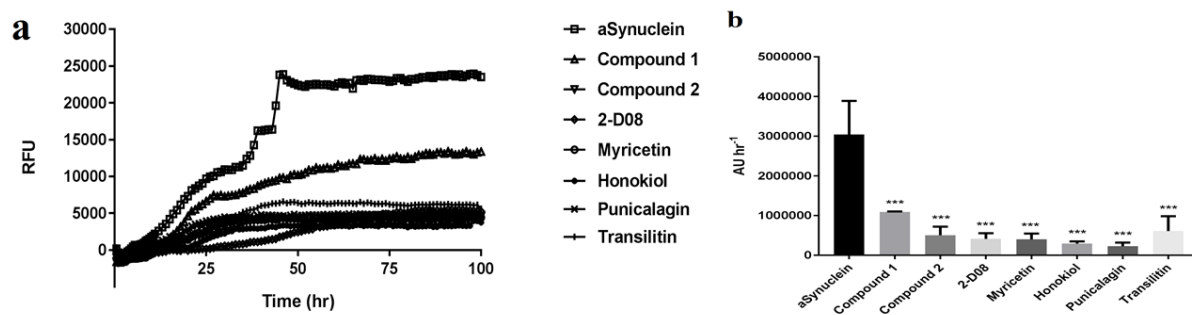


Figure 2: (a) ThT fluorescence assay representing kinetics of (100 μ M) α SA53T fibrillation over 100 hr, alone and in the presence of each test compound at a 1:1 (protein: compound) molar ratio. (b) Representative area under the curve (AUC) measurements demonstrating significant reductions in ThT fluorescence for each test compound at a 1:1 (protein: compound) molar ratio; (***) $p < 0.0001$, $F_{(7, 16)} = 7.294$, mean \pm SEM of $n = 3$ experiments).

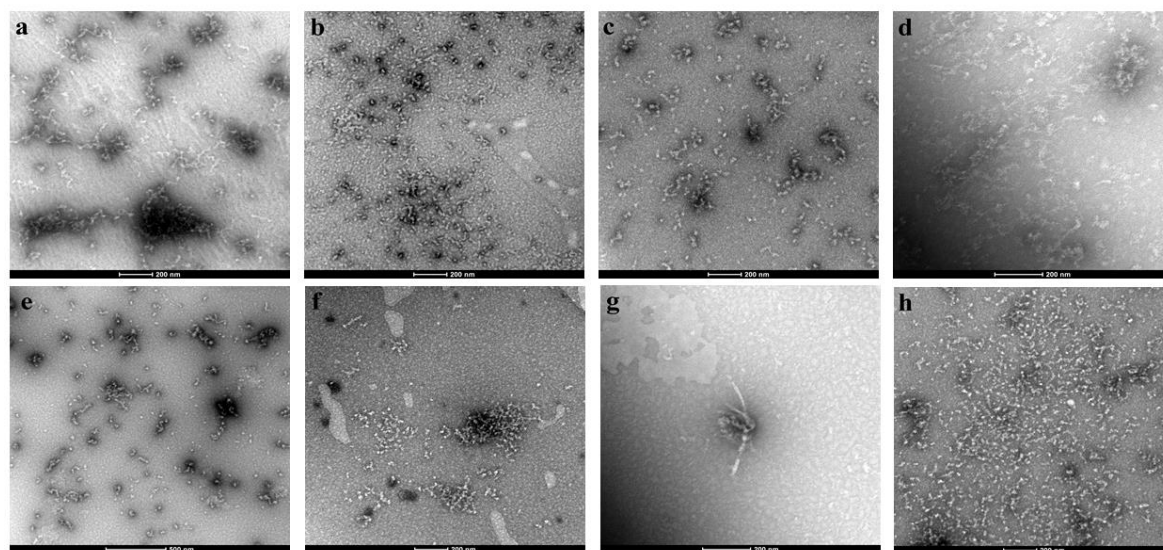


Figure 3: Representative transmission electron micrographs of α SA53T fibril and aggregate formation, after 50 hr incubation alone and with each test compound at a 1:2 (protein: compound) molar ratio; (a) A53T alone and in presence of (b) Compound 1, (c) Compound 2, (d) 2-D08, (e) myricetin, (f) honokiol, (g) punicalagin and (h) transilitin. Scale bar: 200 nm.

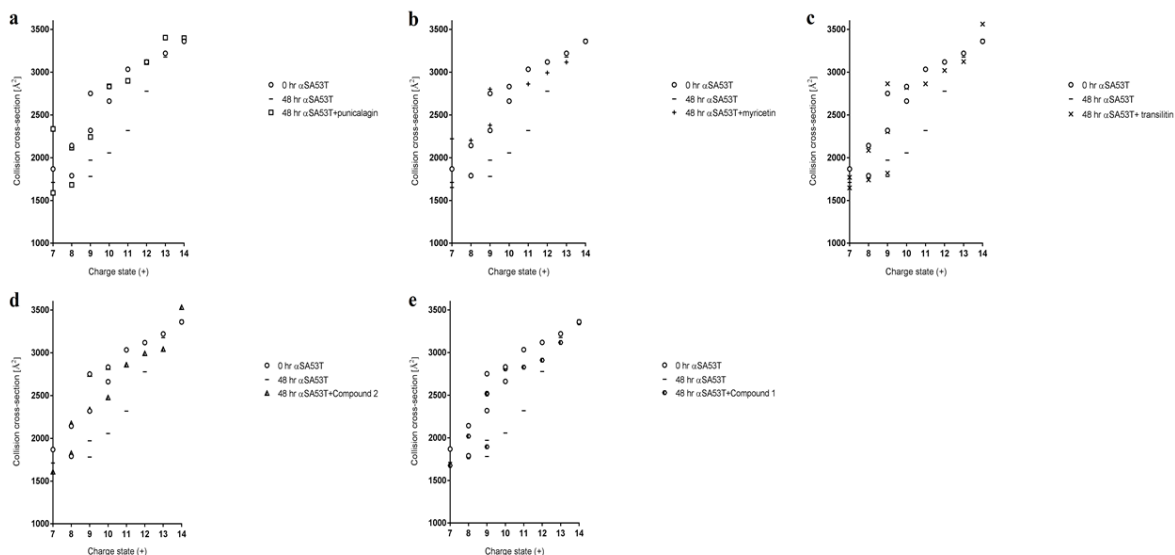


Figure 4: Plot of CCS versus charge state for the dominant peaks in the IM-MS spectrum measured for 50 μM αSA53T in 50 mM ammonium acetate at 0hr (circle) and following 48 hrs incubation at 37 $^{\circ}\text{C}$ with 300 rpm shaking, in absence (dash) and presence of (a) punicalagin (square), (b) myricetin (plus), (c) transilitin (cross), (d) Compound 2 (half-filled triangle) and (e) Compound 1 (half-filled hexagon) at a 1:2 (protein: compound) ratio.

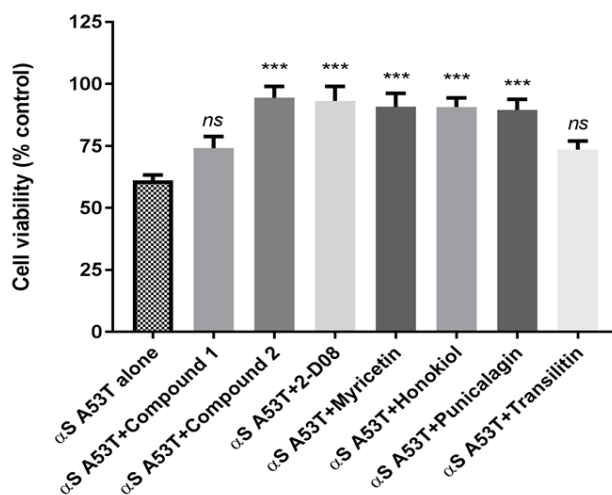


Figure 5: Cell viability of PC12 cells described by an MTT assay following 48hr incubation of preincubated (for 72 hr) 50 μM A53T αS alone or with each test compounds at a 1:1 (protein: compound) molar ratio. Compound 2, 2-D08, myricetin, honokiol and punicalagin showed significant protection. ($***p < 0.0005$, $F_{(5, 18)} = 7.736$ for Compound 2, 2-D08, myricetin, honokiol, punicalagin vs. A53T αS and $p > 0.05$, $F_{(2, 9)} = 4.057$ for Compound 1, transilitin vs. A53T αS ; mean \pm SEM of $n = 4$ experiments).

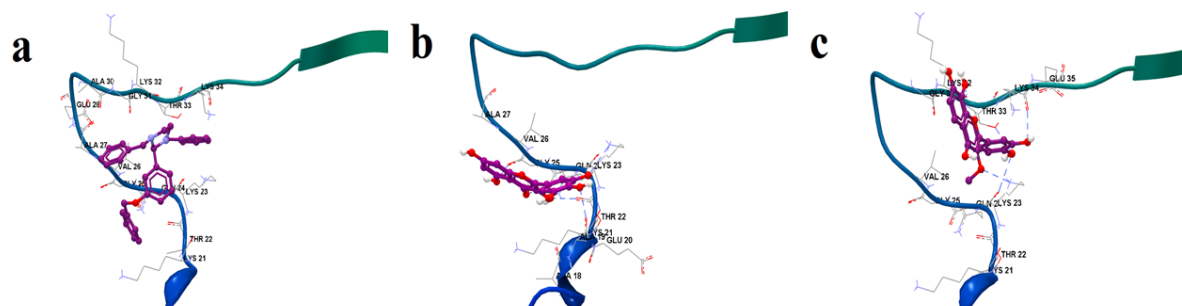


Figure 6: Binding modes of the other three inhibitor optimised ligand structures to α SA53T monomer: **(a)** Compound 1, **(b)** myricetin and **(c)** transilitin.

Chapter 5: Inhibition of α -synuclein and amyloid β aggregation by diverse bioactives reveals a common antiaggregative role of magnolol

5.1 Introduction

Protein aggregation in the form of amyloid fibrils is associated with the neuropathology of both PD and AD. In AD, the extracellular protein amyloid β ($A\beta$) misfolds into neurotoxic β -sheet rich fibrils, whereas in PD it is the cytosolic protein α synuclein (αS) that aggregates into neurotoxic amyloid fibrils eliciting cellular dysfunction. The $\alpha SA53T$ mutant form of αS is more aggregation-prone and associated with familial PD (Narhi, Wood et al. 1999). Consequently, studies have focused on identifying bioactive molecules capable of directly disrupting and remodelling amyloid fibrils of both $A\beta$ and αS into non-toxic conformations as part of their neuroprotective action, exemplified by the green tea flavonoid EGCG, flavone myricetin and saffron bioactive crocin (Papandreou, Kanakis et al. 2006, Bieschke, Russ et al. 2010, Inoue, Shimizu et al. 2017). A diverse array of natural polyphenols has been ascribed neuroprotective properties in a number of models of neuronal damage and neurodegeneration, with potential for the development of neuroprotective drugs (Koppel and Davies 2008, Fernandez-Ruiz, Garcia et al. 2010). Bioactive polyphenols such as flavonoids been shown to mediate neuroprotection against the neurotoxic $A\beta$ found in AD via anti-aggregation and other mechanisms (Smid, Maag et al. 2012).

Previous studies presented in this thesis have highlighted the inhibitory activity of the neolignan honokiol for both $\alpha SA53T$ and $A\beta$ amyloidogenic aggregation. Honokiol and magnolol have very similar chemical structures (found in the same plant genus *Magnolia*) and in the molecular docking studies showed a favourable binding profile comparable to honokiol.

Additionally, magnolol displayed neuroprotection against A β induced toxicity, in a previous study (Hoi, Ho et al. 2010). Other than A β , magnolol demonstrated neuroprotective and anti-aggregative properties against calcitonin, another amyloidogenic protein (Guo, Ma et al. 2015). Therefore, magnolol has been selected to study its direct effect on α SA53T and A β amyloidogenic aggregation and fibril morphology. Neferine, an alkaloid from lotus seed embryo, reduces amyloidogenic huntingtin protein levels and toxicity through inducing autophagy (Wong, Wu et al. 2015). It has been found to inhibit the BACE1 enzyme resulting in lower A β production (Jung, Jin et al. 2010). Neferine generated a lower docking score against both targets, hence this was selected for comparison. Tanshinone I, an abietane diterpene found in the medicinal herb Danshen, has been found to offer neuroprotection in PD pathology through antioxidant action and selectively suppressing pro-inflammatory gene expression associated with neurodegeneration (Wang, Jing et al. 2015, Jing, Wei et al. 2016). Similarly, cryptotanshinone, another abietane diterpenes, has been found to alleviate memory decline following A β injection in mice and reduce neuroinflammation (Maione, Piccolo et al. 2018). Both cryptotanshinone and tanshinone I have been shown to be neuroprotective against A β (Hanaki, Murakami et al. 2016). The chalcone structural scaffold has been used for developing imaging molecules for α S and A β aggregation (Kotzbauer, Tu et al. 2017, Chauhan, Tiwari et al. 2018). Phloretin, a dihydrochalcone found in apple leaves, has been associated with protecting cells from A β toxicity by blocking attachment to lipid bilayers (Hertel, Terzi et al. 1997). The flavone galangin, has reduced A β generation *in vitro* by inhibition of the BACE1 enzyme (Zeng, Huang et al. 2015). Our previous studies have shown that B-ring hydroxylation in the flavone is a favourable structural feature for inhibiting α SA53T and A β amyloidogenic aggregation and fibril morphology (Chapter 4 and (Marsh, Das et al. 2017). As galangin has no hydroxyl group in the B-ring, it enables us a useful comparator to further study

structure-activity relationships towards α SA53T and A β amyloidogenic aggregation and fibril morphology.

While previous studies highlight multiple sites of neuroprotection of naturally-occurring bioactives, a direct interaction of many of these bioactives with the common elements of toxic amyloidogenic proteins, such as A β and α SA53T has not been systematically documented. In this way, the study aims to better understand the structural features by which bioactive inhibitors may interact with the aggregation-prone and amyloidogenic proteins α SA53T and A β .

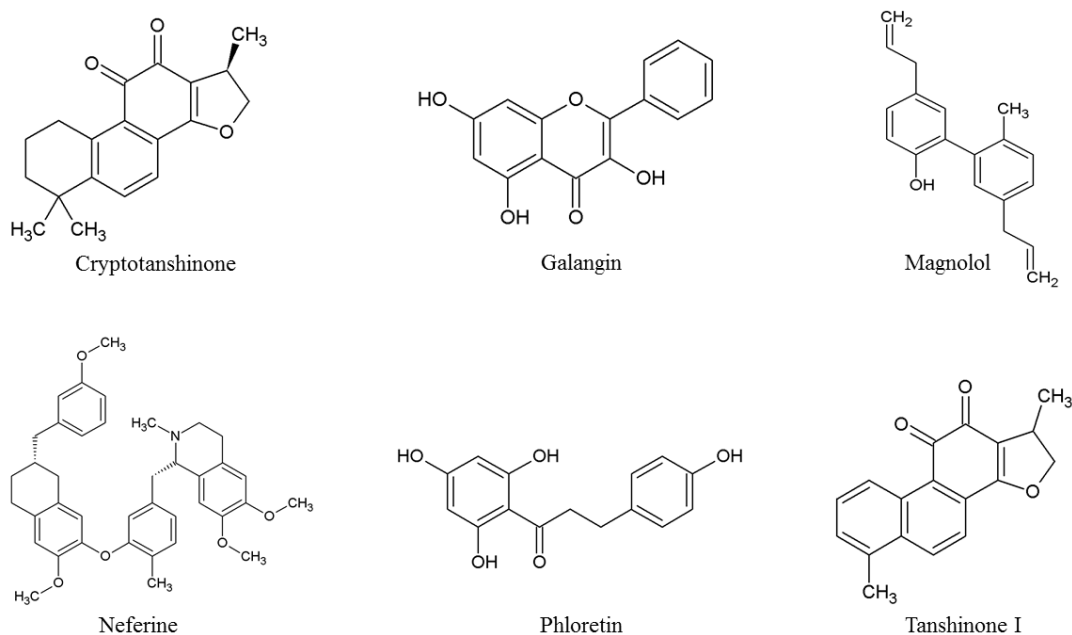


Figure 1. Chemical structures of the bioactive compounds used in this study.

5.2 Materials and Methods

5.2.1 Reagents and Chemicals

Human amyloid- β 1-42 protein ($A\beta_{1-42}$) was obtained from Abcam (Cambridge, MA, USA). Select bioactives used in this study were the flavonoid galangin, the lignin magnolol, the chalcone phloretin, alkaloid neferine and diterpenes tanshinone I and cryptotanshinone. All were sourced from Sigma-Aldrich (St Louis, MO, USA). thioflavin T, DMSO were also obtained from Sigma-Aldrich. Phosphate buffered saline (PBS) at pH 7.4 were obtained from Thermo Fisher Scientific, (Scoresby, VIC, Australia). Foetal calf serum (FCS) was obtained from Bovogen Biologicals (East Keilor, VIC, Australia).

5.2.2 α SA53T Protein expression and purification

α SA53T was expressed and purified as previously described (Volles and Lansbury Jr 2007). Cells were grown in normal Lennox broth (LB) medium. Protein was purified by size exclusion chromatography using a Superdex 200 SEC column (Bio Rad), with a flow rate of 0.5ml/min, in 20mM ammonium acetate buffer. The purity of α SA53T was confirmed by Q-ToF mass spectrometry on an Agilent 6560 Ion Mobility Q-ToF spectrometer with samples introduced by nanoelectrospray ionisation through platinum-coated capillaries (made in-house). Ions were analysed in the positive mode with typical instrument parameters included; capillary voltage 1700 V, fragmentor voltage 400 V, gas temperature 0°C, gas flow 2 l/min, trap fill time 20000.0 μ s, trap release time 4000.0 μ s. Protein was stored at -80°C until required.

5.2.3 Thioflavin T kinetic assay of α SA53T and $A\beta_{1-42}$ fibrillisation

The dye thioflavin T (ThT) binds to the β -sheet of amyloid fibrils, with fluorescence increasing proportionally to the amount of fibrils present in solution. The ThT assay was used to confirm fibril formation over time by α SA53T and $A\beta_{1-42}$ in cell-free solution, in addition to determining if the fibril formation was directly affected by the bioactive compounds. For α SA53T fibrillisation kinetics, ThT (100 μ M in PBS) was added to wells on a microplate together with non-fibrillar α SA53T (100 μ M) and test bioactive compounds at a 1:5 (protein: compound) molar ratio. Fluorescence was measured at 37°C every 30 minutes for 100 hours using a Fluostar Optima plate reader (BMG Lab technologies, Australia) with a 440/490 nm excitation/emission filter. For the $A\beta_{1-42}$ fibrillisation study, ThT (10 μ M in PBS) was added to wells on a microplate together with non-fibrillar $A\beta_{1-42}$ (10 μ M) and the test bioactive compounds (each at 100 μ M). Fluorescence was then measured at 37°C every 10 minutes for 48 hours using a Synergy MX microplate reader (Bio-Tek, Bedfordshire, UK) with excitation and emission wavelengths at 446nm and 490nm respectively. ThT output from all treatment groups were normalised to blank values (ThT alone in PBS).

5.2.4 Transmission Electron Microscopy of $A\beta$ fibrils and aggregates

Transmission electron microscopy (TEM) was used to visualise the effects of selected bioactives on α SA53T and $A\beta_{1-42}$ fibril and aggregate morphology. For α SA53T imaging, samples were directly taken from the ThT assay on completion (100 hrs). For $A\beta$ imaging, samples were prepared by incubating native $A\beta_{1-42}$ (10 μ M) in PBS, either alone or with each of the bioactive compounds (100 μ M) for 48 hours at 37°C. For both proteins, a 5 μ l sample was then placed onto a 400 mesh formvar carbon-coated nickel electron microscopy grid (Proscitech, Kirwan, QLD, Australia). After 1 minute this sample was blotted off using filter paper and 10 μ l of contrast dye containing 2% uranyl acetate was then placed onto the grid, left

for one minute and blotted off with filter paper. Grids were then loaded onto a specimen holder and then into a FEI Tecnai G2 Spirit Transmission Electron Microscope (FEI, Milton, QLD, Australia). Sample grids were extensively scanned manually in search of fibrils using a magnification of 34000-92000 \times and representative images taken.

5.2.5 Computational modelling of bioactive optimized conformation binding to A β ₁₋₄₂ and α SA53T

For the bioactive ligands, equilibrium geometries were optimized using density functional theory (DFT) approach that utilizes Becke's three-parameter hybrid functional known as B3LYP (Kohn, Becke et al. 1996). A large basis set, aug-cc-pVDZ was used for approximation of molecular orbitals in optimized geometry for all three molecules. All the computations were carried out using Gaussian 09 package of codes (M. J. Frisch 2016). Calculations were carried out in no symmetry to facilitate full rearrangement and relaxation of the structures to their most stable form.

Fully optimized ligand structures were studied for their prospective binding interactions according to docking model A β ₁₋₄₂ fibrillar β -sheet structure (PDB ID: 2BEG) using the CLC Drug Discovery Workbench, version 2.4.1, that uses a PLANTS_{plp} empirical scoring function (Thomsen and Christensen 2006). This NMR structure of A β oligomer has been shown to be toxic and serves as a good model for understanding the structural basis of fibrillisation inhibitors (Lührs, Ritter et al. 2005). As A β does not have any singular pharmacophore, a large search space was created covering the whole protein. For docking studies with α SA53T, the docking search space was created near the NAC (non-amyloid β component of AD amyloid) region of its lipid binding domain since this region is crucial for its aggregation (Rodriguez,

Ivanova et al. 2015). Since the full α SA53T structure was not available, the solid-state NMR of pathogenic α synuclein fibril (PDB ID: 2N0A) was obtained from the protein data bank and the residue 53 mutated from alanine to threonine to generate the model protein monomer of α SA53T (Tuttle, Comellas et al. 2016). The resultant α SA53T protein conformation was used for docking without any further adjustment. All ligand structures were kept flexible to allow rotation of any bonds to bind α SA53T or $A\beta_{1-42}$. There were 100 iterations performed for each docking simulation for each bioactive ligand. Results are summarized as a docking score in Table 1 and 2.

The compound structures were screened for PAINS (pan assay interference compound) moieties using the filter <http://zinc15.docking.org/patterns/home/>. No PAINS moiety was detected.

5.2.6 Statistical Analysis

Area under the curve analysis for thioflavin T (ThT) fluorescence data was analysed using one-way ANOVA with a Dunnett's multiple comparisons test used for determining the significance of bioactive effects versus α SA53T or $A\beta_{1-42}$. A significance value of $p < 0.05$ was used for all experiments. Data analysis and production of graphs was performed in GraphPad Prism 7 for Windows (GraphPad Software, San Diego, USA).

5.3 Results

5.3.1 Effects of bioactives on α SA53T and $A\beta_{1-42}$ fibrillisation

The mass spectrum of α SA53T confirmed the purity of the expressed protein (Fig. 2). Thioflavin T (ThT) fibrillation kinetics of α SA53T demonstrated a gradual increase in fluorescence from 24 hours (hrs) and reached at its highest at 70 hrs. This indicated that α SA53T underwent a conformational transition to a cross- β -sheet rich structure characteristic of amyloid fibrils and aggregates (Fig. 3a). Thereafter, the fluorescence stabilised over the remainder of the assay. Out of the six bioactive compounds tested at a 1:5 (protein: compound) molar ratio, only magnolol and cryptotanshinone significantly inhibited ThT fluorescence (Fig. 3a, b). Magnolol markedly suppressed fibril kinetics, while cryptotanshinone showed a small degree of residual fluorescence (Fig. 3a, b). Neferine showed a partial inhibition of ThT fluorescence, however, this was not statistically significant (Fig. 3a, b). Galangin, phloretin and tanshinone I had only a marginal and non-significant effect on the ThT fluorescence of α SA53T overall (Fig. 3a, c).

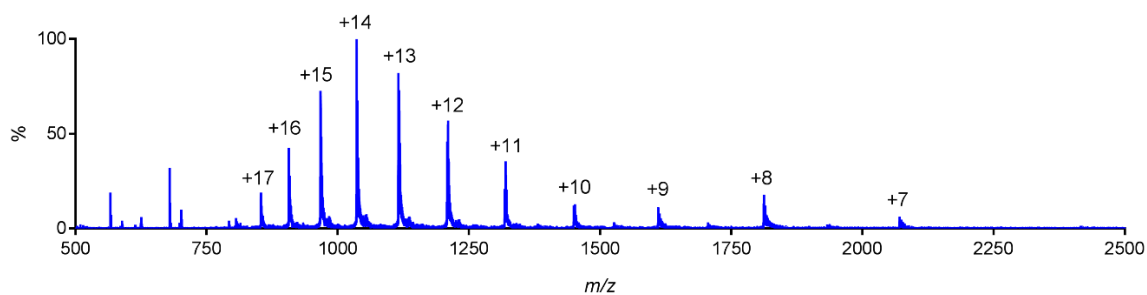


Figure 2. Mass spectrum of α SA53T (50 μ M) in 50mM ammonium acetate.

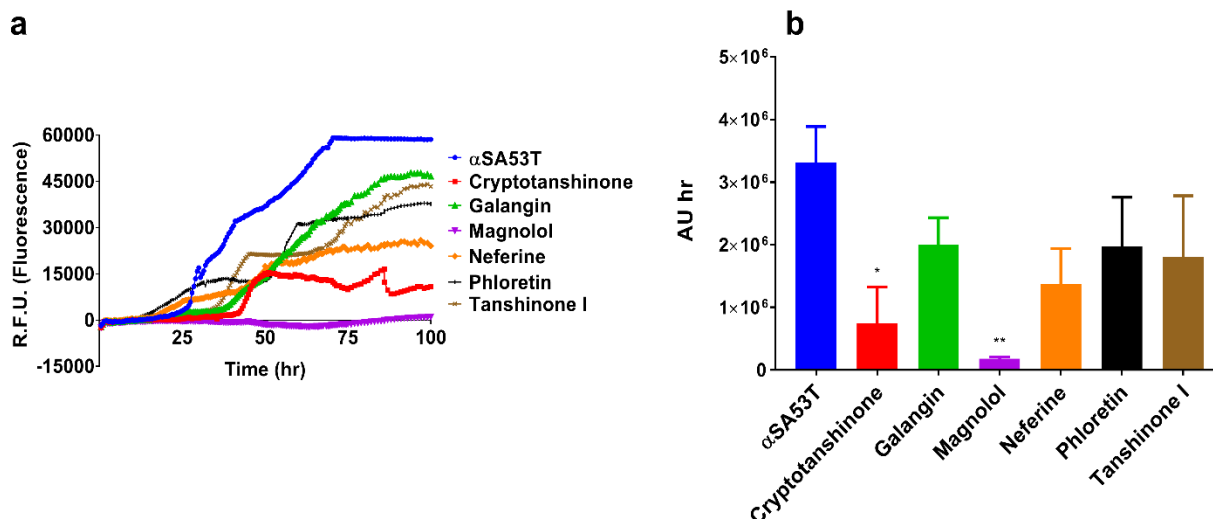


Figure 3: (a) ThT fluorescence assay representing kinetics of α SA53T (100 μ M) fibrillisation over 100 hrs, alone and in the presence of each test compound at a 1:5 (protein: compound) molar ratio. (b) Area under the curve (AUC) measurements demonstrating significant reductions in ThT fluorescence for each test compound at a 1:5 (protein: compound) molar ratio. ** $p < 0.01$ for magnolol and cryptotanshinone and $p > 0.05$ for galangin, phloretin, tanshinone I and neferine. Mean \pm SEM of $n = 3$ experiments.

The thioflavin T (ThT)-based fibrillisation kinetics of $A\beta_{1-42}$ demonstrated a gradual increase in fluorescence from 770 mins (~ 13 hrs) and reached a maximum at about 2250 minutes (mins) equivalent to 37 hrs, indicative of fibril and aggregate formation (Fig. 4a). Thereafter, ThT levels were mostly stable over the duration of the assay, up to 2880 mins (48 hrs). Initially, there was a minor increase in $A\beta_{1-42}$ fluorescence and a higher increase in fluorescence for all the test bioactives were observed. However, this increased fluorescence was diminished from around 800 mins (~ 13 hrs) when the $A\beta_{1-42}$ showed a persistent increase in fluorescence output (Fig. 4a). All the bioactives tested (each at 100 μ M) inhibited the development of ThT fluorescence significantly after around 13 hrs and continuing over the full 48 hr time course of incubation. Area under the curve analysis showed extensive and significant overall inhibition of fibril formation in the presence of each of the bioactive polyphenols (Fig. 4b). Galangin had

the most profound inhibition of A β ₁₋₄₂ fluorescence, followed by cryptotanshinone, magnolol, neferine, tanshinone I and phloretin.

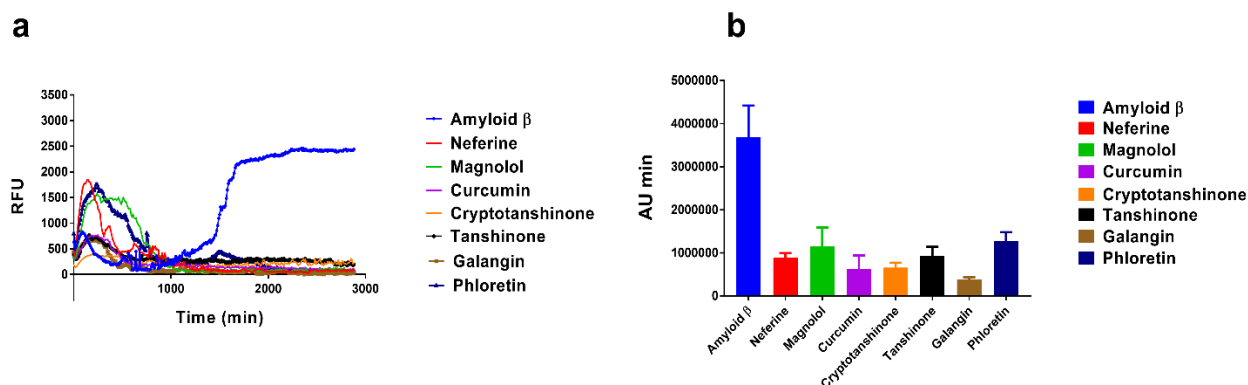


Figure 4: (a) Thioflavin T (ThT) fluorescence indicative of amyloid A β ₁₋₄₂ (10 μ M) fibrillation kinetics, alone and in the presence of each of the six bioactives (100 μ M each) over 48hrs in cell-free PBS solution. (b) Area under the curve analysis of ThT kinetics demonstrating significant overall inhibition of amyloid fibrillation from incubation with each of the bioactives ($^{****}P < 0.0001$; mean \pm SEM of n=3 experiments).

5.3.2 Transmission Electron Microscopy of α SA53T and A β ₁₋₄₂ fibrils and aggregates

The inhibition of α SA53T fibrillation observed in the ThT assay was further confirmed by transmission electron microscopy (TEM), an essential qualitative technique to directly visualise the morphology of amyloid fibril and aggregate formation. α SA53T alone formed dense fibrillar aggregates in high abundance following 100 hrs incubation (Fig. 5a), as observed previously (Liu, Carver et al. 2014). The morphology of α SA53T fibrils and aggregates was markedly altered after 100hrs incubation with magnolol, forming small amorphous aggregates at a 1:5 (protein: compound) molar ratio (Fig. 5d). Incubation with cryptotanshinone resulted in shorter, smoother and loosely attached fibrils in relatively low density and abundance (Fig. 5b). For the remainder of the bioactives, the density and abundance were only modestly reduced compared to control, with a meshwork of aggregates still present (Fig. 5c, e-g).

Overall, incubation with either galangin, neferine, phloretin or tanshinone I did not alter the overall morphology and abundance of dense fibrillar aggregates of α SA53T.

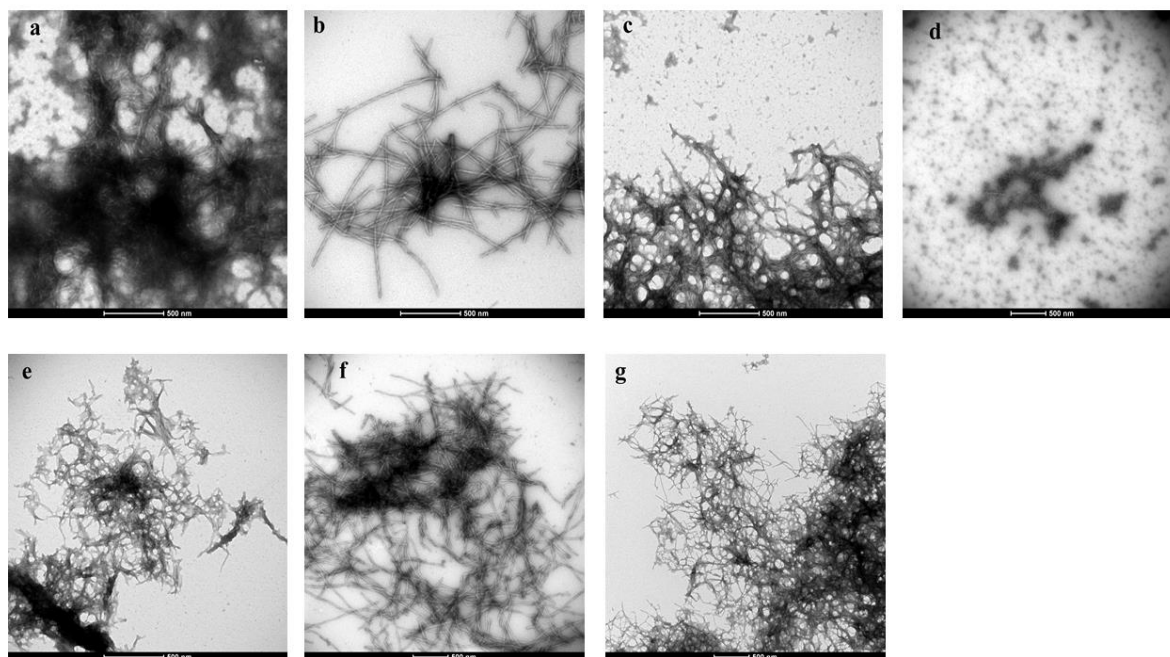


Figure 5: Representative transmission electron micrographs of α SA53T fibril and aggregate formation, following 100 hr incubation, alone and with each bioactive compound at a 1:5 (protein: compound) molar ratio; (a) A53T α S alone, and in presence of (b) cryptotanshinone, (c) galangin, (d) magnolol, (e) neferine, (f) phloretin and (g) tanshinone I (each at 100 μ M). Scale bar: 500 nm.

On microscopic evidence, the morphology of $A\beta_{1-42}$ fibrils and aggregates was affected by incubation with each of the bioactives, but to varying extents on both density and morphology. $A\beta_{1-42}$ alone formed dense aggregates, resembling a ‘meshwork’ after 48 hrs of incubation (Fig. 6a). Magnolol markedly reduced $A\beta_{1-42}$ aggregation, with the appearance of small and dense amorphous aggregates (Fig. 6d). Cryptotanshinone and tanshinone I altered $A\beta_{1-42}$ aggregate morphology into thin, long fibrils that were loosely attached and less dense than $A\beta_{1-42}$ alone (Fig. 6b, g). Incubation with neferine produced relatively thin and loosely attached fibrils, while no aggregates were observed (Fig. 6e), while phloretin did not visibly alter the morphology of

A β ₁₋₄₂ aggregates (Fig. 6f). In contrast to the other bioactives tested, incubation with galangin resulted in the presence of both dense aggregates and longer, interconnected fibrils in abundance (6c).

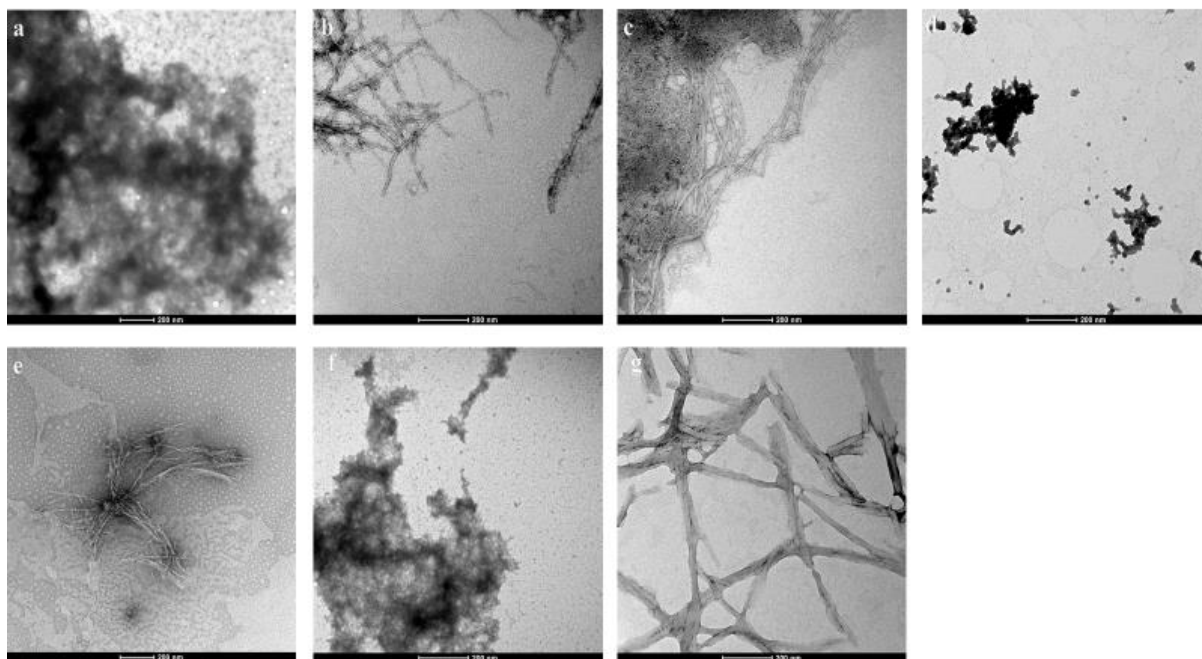


Figure 6: Representative transmission electron micrographs of A β ₁₋₄₂ fibril and aggregate formation, (a) alone and (b-g) following 48hrs incubation with each of the bioactives (each at 100 μ M): (a) A β ₁₋₄₂ (b) cryptotanshinone (c) galangin (d) magnolol (e) neferine (f) phloretin (g) tanshinone I. scale bar: 200nm.

5.3.3 Molecular modelling of bioactive prospective interactions with α SA53T and A β ₁₇₋₄₂

Results from docking studies indicated that all the test compounds bound near the hinge region of α SA53T, surrounded by residue Ala 85 to Ile 88 and Phe 94 to Glu 105 of the NAC (non-A β component) region, a critical part of the protein responsible for amyloidogenic aggregation, in the lipid binding domain (Fig. 7a-f) (Rodriguez, Ivanova et al. 2015). Due to the relatively larger size of the protein, only binding site with interacting residues are shown. Magnolol showed the lowest docking score, which was due to proposed shape complementarity within

this NAC region binding pocket, interacting with the Lys and Glu residues (Fig. 7c). Neferine had the second lowest docking score and interacted mostly with Gly residues (Fig 7d). Cryptotanshinone and Tanshinone I had similar docking scores and proposed hydrogen (H-bonding) interactions with similar binding poses (Fig. 7a, f). Galangin, having a high docking score, bound to a different pocket than rest of the bioactives and interacted with Ala 78 to Glu 83 residues (Fig. 7b). Phloretin had the highest docking score but a low H-bonding score and bound in a similar region to tanshinone I (Fig. 8e).

Table 1. Docking profile of bioactive polyphenols with α SA53T

Bioactive	Docking score	H-bonding score	H-bonding residue	Steric interaction score	RMSD (Å)
cryptotanshinone	-40.84	-6.01	Asn 103, Glu 104, 105	-34.83	171.99
galangin	-36.14	-6.0	Gln 79, Glu 83	-30.98	163.99
magnolol	-51.55	0.00	-	-54.41	170.61
neferine	-47.21	0.00	-	-56.02	185.45
phloretin	-35.04	-7.36	Gly 101, Asn 103, Glu 104,105	-34.59	172.75
Tanshinone I	-39.74	-6.0	Asn 103, Glu 104, 105	-33.74	170.84

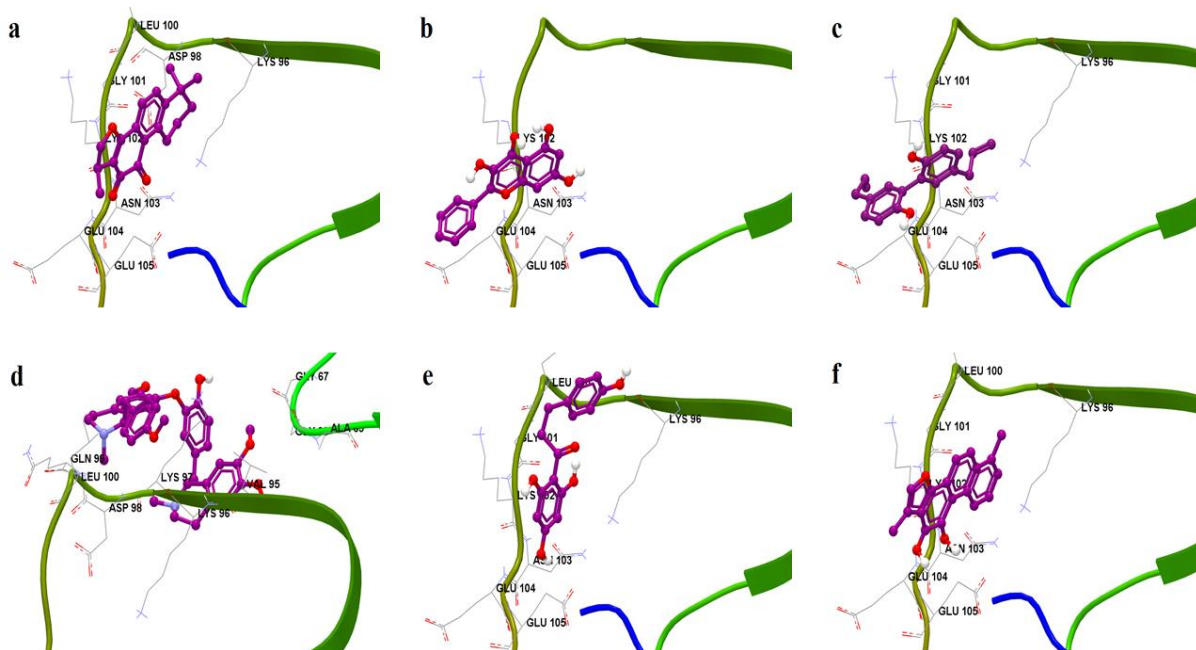


Figure 7: Modelled bioactive ligand binding of each of the optimised bioactives conformations to α SA53T (PDB ID: 2N0A) (a) cryptotanshinone, (b) galangin, (c) magnolol, (d) neferine (e) phloretin and (f) tanshinone I. Binding properties of each bioactives are provided in Table 1.

Molecular docking of each of the bioactives with the $A\beta_{17-42}$ oligomer suggested that all the test compounds bound in the hydrophobic binding pocket formed by Leu 17, Val 18, Phe 19 and Gly 38, Val 39, 40 of all chains (Fig. 8a-f). Due to the small size of $A\beta_{12-42}$ oligomer, the whole protein structure can be shown with interacting residues for all bioactives. Neferine had the lowest docking score which was primarily due to proposed shape complementarity, as it was able to interact with all the chains in the binding pocket according to docking model (Fig. 8d). Tanshinone I bound within this same pocket and had the second highest score with a high H-bond score (Fig. 8f). Despite having similar docking scores, magnolol binding was suggested to be through shape complementarity primarily, whereas galangin was suggested to have a higher probability of forming H-bond interactions in this pocket according to the docking model (Fig. 8b, c). Cryptotanshinone was predicted to have a different binding pose than Tanshinone I and displayed a weak binding score, with predicted less H-bond interactions

according to the docking model (Fig. 8a). Phloretin bound inside the pocket with a proposed high H-bond interaction; however, the overall docking score was high (Fig. 8e).

Table 2. Docking profile of bioactive polyphenols with A β ₁₇₋₄₂

Bioactive	Docking score	H-bonding score	H-bonding residue	Steric interaction score	RMSD (Å)
cryptotanshinone	-50.29	-1.57	Val 39 ^E	-48.72	21.42
galangin	-64.95	-14.08	Leu 17 ^{D, E} , Val 18 ^{C, D} , Phe 19 ^D	-51.73	20.34
magnolol	-65.24	-1.76	Leu 17 ^C	-67.86	17.66
neferine	-82.91	-3.53	Leu 17 ^C	-88.56	22.05
phloretin	-56.21	-10.78	Leu 17 ^{A, C, D} , Val 18 ^{A, C}	-53.33	17.01
Tanshinone I	-68.84	-10.8	Leu 17 ^{D, E} , Val 18 ^{C, D} , Phe 19 ^D	-58.04	21.10

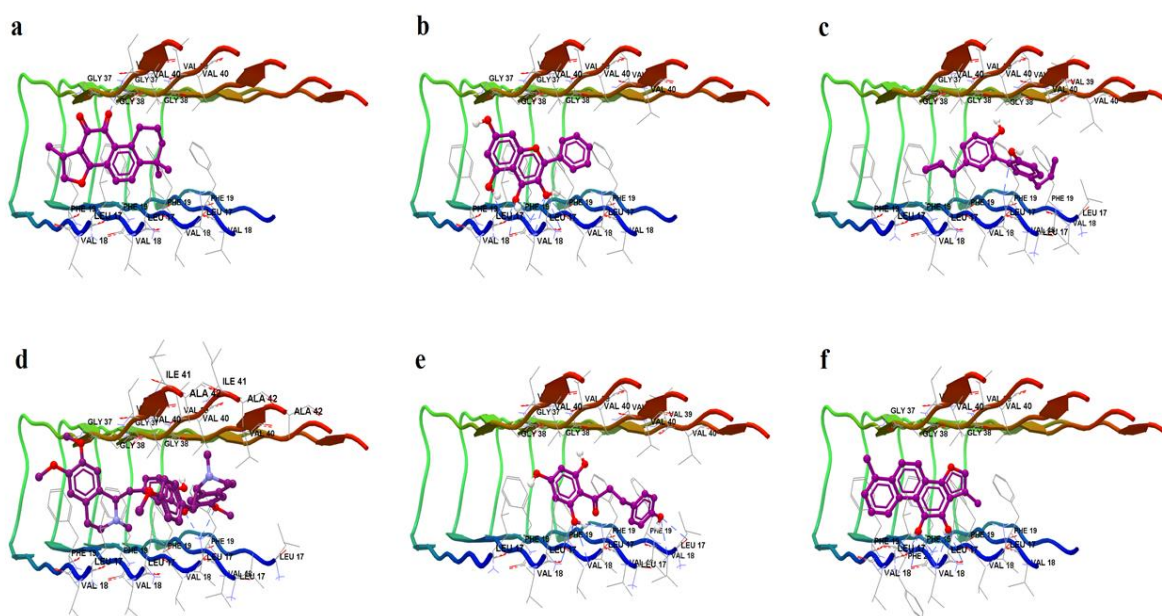


Figure 8: Modelled bioactive ligand binding of each of the optimised bioactives conformations to A β ₁₇₋₄₂ polymer (PDB ID: 2BEG) (a) cryptotanshinone, (b) galangin, (c) magnolol, (d) neferine (e) phloretin and (f) tanshinone I. Binding properties of each bioactives are provided in Table 2

5.4. Discussion

This study compared the capacity of selected natural bioactives to structurally modify the aggregation of the major neurotoxic α -synuclein (A53T) and β amyloid fragment 1-42 *in vitro*. *In silico* modelling was also used to compare the likely binding sites of such bioactives to the α -synuclein (A53T) and β amyloid oligomer, as a further tool in which to investigate the most effective binding parameters that may predict the structural modification of α -synuclein and β amyloid protein to potentially non-aggregative and non-neurotoxic conformations.

The ThT and TEM study of α SA53T aggregation suggests that magnolol is capable of significantly inhibiting α SA53T fibrillisation by forming small amorphous aggregates. These small amorphous aggregates are likely to undergo loss of an extensive surface area present in the ‘meshwork’ of A β fibrils in which ThT binds to account for these marked reductions in fluorescence output (Khurana, Coleman et al. 2005). In a previous study, Rekas et al. (2004) observed that α B-crystallin inhibited the aggregation of A53T α -synuclein by converting it into amorphous aggregates. The docking study of magnolol and α SA53T indicates strong steric interaction between magnolol and the binding site of α SA53T. This interaction might have resulted in formation of less abundant amorphous aggregates, rather than highly abundant long α SA53T fibrils present in control samples. The compounds inhibited α SA53T fibrillation at a relatively high compound concentration of 500 μ M. Therefore, it is possible that other mechanisms in addition to the reversible binding of an inhibitor molecule could contribute to inhibition of α SA53T aggregation.

Similar to α SA53T, magnolol inhibited $A\beta_{1-42}$ aggregation via ThT kinetics and resulted in the formation of small, amorphous aggregates as seen from TEM. The initial increase in ThT fluorescence for $A\beta_{1-42}$ in the first few hours of incubation with bioactives, including magnolol, may indicate that initial nucleation or elongation of amyloid oligomers can still occur, but that at a specific stage, $A\beta_{1-42}$ fibrils are exposed or vulnerable to small ligand interactions in which selected bioactive polyphenols seem particularly effective at inhibiting further progression. It is previously shown that ThT fluorescence can vary due to the addition of endogenous compounds such as polyphenols (Hudson et al. 2009). It should be noted that ThT fluorescence can over-represent fibril inhibition, as electron microscopy demonstrated that fibrils and aggregates can still be present even with markedly reduced ThT output. Magnolol, due to its small size and favourable intramolecular position of aliphatic/side chains, is able to fit efficiently within the binding pocket, resulting in a comparatively lower docking score. As observed in our docking simulations, the binding interaction of magnolol with both α SA53T and $A\beta$ oligomeric conformation is essentially one of shape complementarity. Therefore, it can be asserted that the biphenyl structure of the neolignan is favourable for sterically interacting with amyloidogenic proteins, leading to anti-aggregative activity. Our previous study with honokiol, a structurally similar neolignan, indicated that the neolignan biphenyl scaffold had a favourable shape for interacting with $A\beta$ and was a potent inhibitor of aggregation and may provide neuroprotection through multiple pathways (Das, Stark et al. 2016) (Kantham, Chan et al. 2017). Interestingly, magnolol was also demonstrated to inhibit calcitonin aggregation (Guo, Ma et al. 2015), suggestive of further potential as a small molecule template for anti-amyloid drug development.

The finding that galangin is ineffective in arresting α SA53T aggregation, as evidenced by both ThT and TEM, is probably due to the absence of vicinal di- or tri-hydroxylation in either of its

flavone A or B ring. Previous studies on α SA53T aggregation by various flavones have found that the presence of vicinal hydroxylation improves α synuclein aggregation inhibition (Meng, Munishkina et al. 2009, Meng, Munishkina et al. 2010). Our docking scores also indicate that galangin is a poor binder to α SA53T, which also might account for its ineffectiveness against α SA53T aggregation. In the docking study, the binding of galangin to A β was most favourable on the hydrophobic part of the pentamer, surrounded by key residues Leu17, Val18, Phe19, Gly38 and Val39. This occurs in a groove running parallel with the long axis of fibrils, which is also associated with ThT binding (Krebs, Bromley et al. 2005). While the ThT inhibition via galangin in presence of A β has been unexpected, other flavones without B ring hydroxylation have been shown previously to inhibit thioflavin T fluorescence, such as baicalein (Zhu, Choi et al. 2007, Espargaró, Ginex et al. 2017). However, as the TEM images still showed fibrils/aggregates, this is indicative that galangin may have quenched ThT fluorescence or otherwise displaced ThT from fibrils without impeding fibrillisation (Lee, Kerr et al. 2016). This may also explain why some polyphenolic compounds exert a strong degree of inhibition of ThT fluorescence without necessarily inhibiting fibril formation, via displacement of ThT from its amyloid binding site (Janefjord, Maag et al. 2014).

Cryptotanshinone, being anti-aggregative against α SA53T, modified fibrils in a similar manner to phloretin. However, these were relatively lower in abundance. Tanshinone I modified α SA53T fibril morphology to a minor extent, where the moderately abundant α SA53T fibrillar ‘meshwork’ was still evident from microscopic analysis. Although their docking profile to α SA53T was very similar, they may possess a different mode of interaction with α SA53T. Both tanshinones altered A β aggregation by producing loose fibrils, with no aggregates observed.

The alkaloid neferine demonstrated significant A β aggregation inhibition and visibly altered A β fibril morphology and reduced overall aggregation. This property, coupled with a favourable docking profile against A β oligomer, suggests that the size of the neferine molecule is amenable for interaction with a small amyloid protein such as the A β oligomer. Neferine, however, did not significantly inhibit α SA53T aggregation, albeit its docking profile pointed towards a weak interaction.

Phloretin had a modest effect on A β aggregation. Although, the TEM imaging implied no visible modification in appearance of aggregates in comparison to control, the overall abundance of aggregates was lower. A previous study demonstrated that phloretin prevented A β association to negatively charged lipid vesicles by means of electrostatic interactions, as a means of mitigating A β cytotoxicity (Hertel, Terzi et al. 1997). Our docking of phloretin with the A β oligomer also highlighted a high degree of electrostatic interaction between phloretin and the hydrophobic core of A β . In addition to electrostatic interaction, phloretin might also increase A β oligomerization as a result of direct interactions (Efimova, Zakharov et al. 2015). Phloretin modified α SA53T fibrils in a manner comparable to cryptotanshinone; however, the overall abundance of fibrils was much higher, suggesting that phloretin exerted a marginal effect on α SA53T aggregation and this was also reflected in the high docking scores.

5.5 Conclusion

Diverse naturally-occurring bioactives are variably able to disrupt the aggregative propensity of α SA53T and A β . Of all the bioactives tested, the neolignan magnolol and cryptotanshinone were the best in this regard, inhibiting both α Synuclein and β amyloid aggregation. In a preliminary cell viability study, both cryptotanshinone and tanshinone I displayed intrinsic neurotoxicity to PC-12 cells after 48 hour exposure at 50 μ M, but not magnolol (unpublished

data). Therefore, these findings suggest that magnolol may have the most potential among the six compounds tested and provide a favourable template for further drug development targeting amyloidogenic protein aggregation.

Chapter 6: Molecular docking guided design of novel amyloid binding ligands using natural polyphenols and a synthetic heterocyclic ring system as templates

6.1 Introduction and background

In silico drug design collectively represents various computational methods used at different stages of drug design and development in modern drug discovery. *In silico* approaches play an essential role in the ‘hit’ to ‘lead’ generation and ‘lead optimization’ process (Zoete, Grosdidier et al. 2009, Koutsoukas, Simms et al. 2011). Depending on the available knowledge of a drug target and molecules that bind to that target, different *in silico* methods can be applied in order to design a novel ligand. When the structure of the target binding site is well understood, *de novo* drug design and structure-guided methods can be employed for generating novel ligands (Honma, Hayashi et al. 2001, Honma 2003, Ji, Zhang et al. 2003). In the absence of adequate information of a drug target, other *in silico* methods such as ligand-based drug design and virtual screening have been shown to be able to successfully guide the drug discovery endeavour (Knehans, Schüller et al. 2011).

6.1.1 Ligand-based drug design

Ligand-based drug design is of great importance when there is a lack of information about the 3D structure of a target. It can provide valuable insight into the nature of interaction between a ligand and its target, which further reveal predictive optimization of the ligand structure is possible. For example, there is no clear understanding of the potential small molecule ligand binding sites in amyloid β or α synuclein proteins, or even if they have potential

pharmacophores. Therefore, ligand-based drug design would be an effective strategy in the case of these aggregation-prone amyloidogenic proteins, which can be additionally complex when considering their polymorphic propensity during aggregation (Kodali and Wetzel 2007).

Ligand-based drug design can be broadly divided into two approaches: a) pharmacophore-based design and b) 3D quantitative structure activity relationship (QSAR) computations (Table 1).

Table 1. Two major approaches for *in silico* ligand-based drug design.

Ligand-based drug design

<i>Pharmacophore-based design</i>	<i>3D-Quantitative Structure Activity Relationship (QSAR)</i>
<p><i>Ligands are designed based on pharmacophores: IUPAC defines a pharmacophore as ‘an ensemble of steric and electronic features that is necessary to ensure the optimal supramolecular interactions with a specific biological target and to trigger (or block) its biological response’. (Wermuth, Ganellin et al. 1998).</i></p>	<p><i>Comparative Molecular Field Analysis (COMFA)- This involves i) representing ligands by their steric and electrostatic fields in a three-dimensional lattice, ii) a new ‘field fit’ technique by statistical calculation, iii) analysis by partial least squares, PLS and iv) graphic representation of results (Cramer, Patterson et al. 1988).</i></p> <p><i>Comparative Molecular Similarity Indices Analysis (CoMSIA) – finds common features important in binding, by analysis of i) steric, ii) electrostatic features and hydrogen bond acceptor and donor properties using a Gaussian function in the similarity indices equation</i></p> $A^q_{F,K,(j)} = -\sum W_{probe,k} W_{ik} e^{-\alpha r^{2j}}$ <p><i>(Klebe, Abraham et al. 1994, Zheng, Kong et al. 2014)</i></p>

6.1.2 Application of pharmacophore-based drug design for Aβ

Aβ has several conformations that have been associated with its toxicity (Crescenzi, Tomaselli et al. 2002, Luhrs, Ritter et al. 2005). A diverse set of natural bioactives ranging from flavonoid, curcuminoid, lignan, chalcone, alkaloid and terpenoid structures have been characterized as

inhibitors of A β aggregation by directly interacting and modifying A β fibrils and aggregate morphology (Luo, Smith et al. 2002, Reinke and Gestwicki 2007, Bieschke, Russ et al. 2010, Kraziński, Radecki et al. 2011, Das, Stark et al. 2016, Fosso, McCarty et al. 2016). Among these natural bioactives, curcuminoid or curcumin structures have been extensively modified in order to design novel and improved A β binders (Yanagisawa, Shirai et al. 2010, Yanagisawa, Taguchi et al. 2015). Some studies have successfully developed flavonoid derivative compounds with improved A β binding, leading to anti-aggregation and neuroprotection (Li, Wang et al. 2013, Singh, Gaur et al. 2014), whereas chalcone derivatives have been designed as superior binders to A β for imaging and diagnostic purposes (Ono, Hori et al. 2007, Ono, Ikeoka et al. 2010, Fosso, McCarty et al. 2016). In contrast, the lignan structure has not been well investigated for use as an active scaffold or pharmacophore in ligand-based drug design targeting A β or other amyloidogenic proteins such as α SA53T, despite a recently identified anti-amyloidogenic action *in vitro* (Das, Stark et al. 2016, Kantham, Chan et al. 2017).

6.1.3 Virtual screening

As described in Chapter 1, virtual screening (VS) is an *in silico*, inexpensive and quicker alternative to traditional high throughput screening (HTS). It is applicable in the case of both known or unknown binding sites of a target. VS can further complement a *de novo* drug design approach by increasing chemical accessibility or the design of a compound library (Schneider, Clément-Chomienne et al. 2000, Katarkar, Haldar et al. 2015). For the ligand-based drug design method, structure-based VS can play an important role in pharmacophore-based drug design by generating hits bearing the desired pharmacophore(s) (Schneider, Neidhart et al. 1999, Knehans, Schüller et al. 2011).

6.1.4 A combined approach: pharmacophore-based drug design with virtual screening

In this Chapter, a combination of both drug design strategies has been employed in order to develop novel amyloid β_{1-42} ($A\beta_{1-42}$) binders. Modelling natural polyphenolic bioactives revealed that honokiol, a small molecule lignin, is structurally amenable for further development through molecular docking simulations. Additionally, the VS study of the ZINC chemical database identified a dibenzyl imidazolidine as a promising scaffold for structure-based drug design against $A\beta$ (Das and Smid 2017). Likewise, honokiol and the dibenzyl imidazolidine scaffold bearing compounds demonstrated direct interaction and inhibition of α Synuclein A53T ($\alpha SA53T$) aggregation, a more aggregation-prone mutant of α Synuclein (αS) associated with PD (Li, Uversky et al. 2001). A common ligand binding with higher affinity to $A\beta$ or $\alpha SA53T$ would be beneficial either from a drug discovery perspective or for amyloid imaging purposes with clinical applications. Therefore, in this work these molecular scaffolds or pharmacophores have been combined with the aim of designing novel and improved $A\beta$ binder(s), which were then docked against $\alpha SA53T$ for characterizing the generic amyloid binding affinity. A set of derivative molecules have been designed utilizing computational methods such as molecular docking and molecular geometry optimization, which consolidate the structural features of honokiol and the dibenzyl imidazolidine scaffold. Low docking score was used as a guide for *in silico* development. The steric interaction score as computed by the PLANTS_{PLP} docking algorithm provided information about the shape complementarity during docking interactions (Korb, Stütze et al. 2009). Lipinski's rule of five was also used as a guide for evaluating ligand structures, however, a marginal increase in *log P* value was considered to be advantageous where the ligand target would require access to the central nervous system (CNS).

6.1.5. The neolignan biphenyl pharmacophore as a template for anti-A β ligand design

Honokiol and magnolol are two structurally similar lignans, possessing the neolignan biphenyl or the biphenyl-hydroxy-propenyl molecular scaffold. Both of these molecules demonstrated direct interaction and inhibition of A β experimentally, with favourable docking profiles in molecular modelling (Chapter 5, (Das, Stark et al. 2016). Likewise, they both inhibited α SA53T aggregation, where honokiol inhibited the toxic conversion of unfolded α SA53T (Chapter 4). They have almost identical chemical structures except for one -OH group; however, their ground state conformations are slightly different (Fig. 1). Honokiol has both of its -OH groups on the same side of the biphenyl ring, while in magnolol, they are on the opposite sides. The docking studies presented in the earlier chapters of this thesis have shown that both honokiol and magnolol are strong binders to A β , while honokiol had a relatively higher score than magnolol (Chapter 2 and 4). This could be due to the conformation of honokiol. Additionally, honokiol obtained a lower docking score than other bioactive polyphenols such as myricetin, luteolin and punicalagin, particularly with oligomeric A β ₁₋₄₂ (Das, Stark et al. 2016). Since the oligomeric structure of A β ₁₋₄₂ was representative of an anti-parallel beta-sheet conformation that is associated with neurotoxicity, a lower docking score would be a desirable starting point for designing an improved A β ₁₋₄₂ binder (Lührens, Ritter et al. 2005).

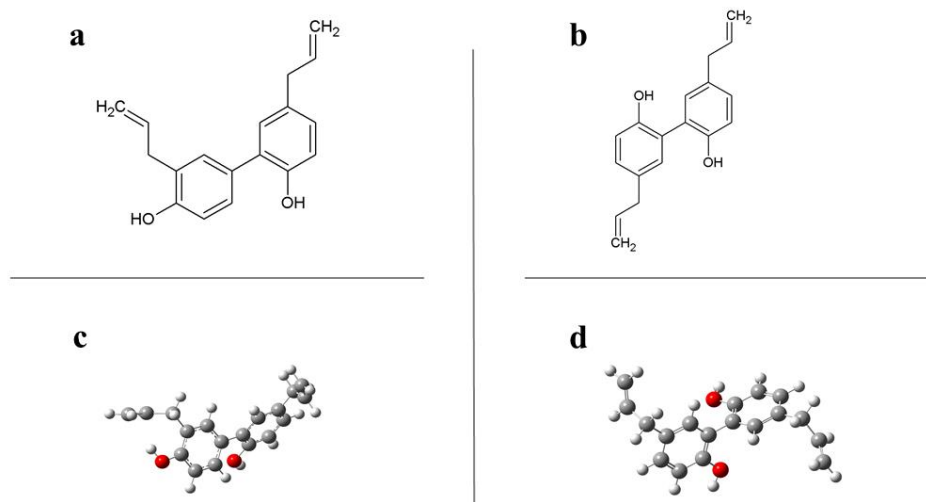


Figure 1. Chemical structures of (a) honokiol and (b) magnolol. Optimized conformations of (c) honokiol and (d) optimized conformation of magnolol.

Moreover, the structure of honokiol is more tractable for pharmacophore-based development than other A β inhibitors such as punicalagin, EGCG or other catechol-type flavones. Being a small molecule with a molecular weight of 266.33 g/mol, it resembles a fragment which could be developed further using *in silico* design. Therefore, the neolignan biphenyl molecular scaffold of honokiol (partially shared by magnolol too) was chosen as the initial pharmacophore for designing novel ligands that may be potentially superior binders to A β and other amyloidogenic proteins like α S.

Molecular stability of honokiol is higher than other noted amyloidogenic protein aggregation inhibitors such as EGCG and resveratrol (Kantham, Chan et al. 2017). Honokiol has been found to be stable over 48 hrs in phosphate buffered saline at 37 deg. C, whereas both EGCG and resveratrol showed degradation over this time period (Kantham, Chan et al. 2017). Aqueous

solubility is of high interest for enhancing bioavailability during the drug development process. Although honokiol is essentially a hydrophobic molecule with poor aqueous solubility, its nanoparticle formulation has been demonstrated to have dispersibility in water that may make it more amenable to an efficient drug-delivery system (Gou, Dai et al. 2008). Therefore, the biphenyl-hydroxy-propenyl fragment/scaffold of honokiol has been used as a pharmacophore for further development of novel derivatives targeting A β and α S amyloidogenic protein structures in this study.

6.2 Methodology

6.2.1 Design strategy for honokiol-derivatives using molecular docking

Molecular docking against A β monomer and oligomer structures were used as guide to design ligands with improved low docking scores and predicted H-bonding as part of their binding. The aim of this study was to enhance and improve the docking profile (low scores, electrostatic interaction and shape complementarity) as compared to honokiol. Using the biphenyl-hydroxy-propenyl pharmacophore, an iterative fragment growing strategy was employed to improve docking scores, which has been applied for other drug discovery strategies previously (Shang, Yuan et al. 2014). The oligomeric form of A β (PDB ID: 2BEG) is associated with toxicity and has been used in many *in silico* modelling studies to understand various small molecular suggested interactions with A β (Lührs, Ritter et al. 2005). Additionally, the monomeric form of A β serves as good model for docking, due to the full length (residues 1–42) and association with toxicity (Crescenzi, Tomaselli et al. 2002). In addition to A β , a high-resolution NMR structure of α S (PDB ID: 2N0A) was mutated from Ala to Thr at residue 53 to generate the structure of α SA53T (Tuttle, Comellas et al. 2016).

6.2.2 Computational methods

All the structural modifications and design of new ligand structures was performed in GaussView5.0 of the Gaussian'09 program (<http://gaussian.com/>) (Frisch, Trucks et al. 2016). For each of the new ligand, the structural geometry was optimized using a density functional theory (DFT) approach that utilizes Becke's three-parameter hybrid functional, commonly known by the acronym B3LYP (El-Azhary and Suter 1996). A large basis set, cc-pVDZ was used for optimized geometry of each designed ligand. All computations were carried out using Gaussian'09. Optimized ligands underwent molecular docking analyses in CLC Drug Discovery Workbench, version 1.5.1 using a PLANTS_{PLP} SCORING function (Korb, Stützle et al. 2009). The molecular properties related to their drug-likeness were calculated for each derivative, using the docking software. The first ligand structure, modified from the honokiol-based pharmacophore, was called Derivative 1. From Derivative 1, Derivative 2 was designed and this iterative fragment growing strategy continued until the design of Derivative 7. Scaffold hopping, another popular concept in drug design, was then used on Derivative 6 and 7 structures to develop other promising ligands (Böhm, Flohr et al. 2004). Each derivative ligand was docked to both the A β and α SA53T targets. This 'design – structure optimization – docking' loop was repeated for several rounds to ensure improved binding.

The whole design process was guided by rational intervention without any automated input from the docking software.

6.2.3 Design of Derivative 1, 2, 3 and 4

The main rationale behind modifying the structure of honokiol was to explore whether any derivative structure of this biphenyl neolignan scaffold can further improve binding probability

to amyloid targets. This, in turn, would inform a novel design of honokiol-derived amyloid binding ligands. Several strategies for modifying the honokiol structure were tried computationally which indicated that the structural modification followed in Derivative 1 would be favourable. In the first step, the A-ring of the neolignan biphenyl molecular scaffold of honokiol was modified. The -OH group at position 4 of the A-ring and the propenyl chain at position 3 were replaced by a conjugated alkene (buta-1,3-diene) chain at position 4 (Fig. 2a, b). This structure was called Derivative 1 (Fig 2). Next, a phenyl group was introduced to the conjugated buta-1,3-diene chain of Derivative 1 (Fig. 4). This resulted in the structure of Derivative 2. Derivative 3 was designed by introducing two -OH groups in the 1 and 3 positions of the buta-1,3-diene chain of Derivative 3 (Fig. 6). In the next step, an attempt was taken to investigate the effect of introducing a nucleophile such as O, N or S atom with the conjugated chain. Therefore, the two -OH groups of Derivative 3 were removed, and the phenyl group was converted into phenoxy group, which made the ligand structure of Derivative 4 (Fig. 8). This modification had the phenyl buta-1,3-diene-1,3-diol chain of Derivative 3 converted into a phenoxybuta-1,3-dien-1-yl chain of Derivative 4 (Fig. 8).

6.2.4 Design of Derivative 5,6 and 7: combining virtual screening hit with existing ligand

The structure-based virtual screening study using molecular docking used in Chapter 3 identified a novel dibenzyl imidazolidine scaffold with a phenyl group as an anti-aggregative and neuroprotective ligand against A β (Das and Smid 2017). This scaffold was additionally effective against α SA53T toxic aggregation (Chapter 4). For simplicity and to use less ring systems, only the ‘dibenzyl phenyl imidazolidine’ fragment was used from the ‘benzoxy phenyl imidazolidine scaffold’ of the virtual screening hits. Both of the ‘hit’ molecules possessed this fragment and showed low docking scores with a predicted favourable shape. Therefore, this

molecular scaffold was used in further design of derivative ligands to improve the docking scores. This combined approach of ligand-design by introducing fragments from screening ‘hits’ allowed us to search new chemical spaces and maintain a novel molecular design.

Since the structural modification from Derivative 3 to Derivative 4 did not yield any significant advantage in terms of the docking profile with A β , the structure of Derivative 3 was used for further modification. To design the next series of ligands, the dibenzyl (methoxy) phenyl imidazolidine fragment was introduced to the conjugated buta-1,3-diene chain, which was Derivative 5 (Fig. 10). Subsequently, the structure of Derivative 5 was further simplified in the design of Derivative 6, where the (methoxy)phenyl group from the imidazolidine ring was removed (Fig. 12). In the final stage of ligand optimization, the imidazolidine ring of Derivative 6 was replaced with an imidazole group, which resulted in the design of Derivative 7 (Fig. 14).

6.2.5 Other Derivatives

Several other derivatives were designed by changing the five-membered heterocyclic (FMH) imidazole ring into other FMH rings of the Derivative 7 structure (Table 4). These other FMH rings were selected from the top 100 most frequently occurring rings in small molecule traded drugs, as listed by the FDA (Taylor, MacCoss et al. 2014).

6.2.6 The core fragment of the derivatives

After docking all the derivative ligands, it was identified that the ‘core fragment’ of the high scoring derivative ligands shared the dibenzyl imidazole or other FMH ring scaffolds (Fig. 16). This ‘core’ fragment was also individually docked with A β .

6.3 Results and Discussion

6.3.1 Honokiol and Derivative 1 molecular properties and interaction with A β

The optimized ground state conformation of honokiol was non-planar. Introduction of a buta-1,3-diene chain at position 4 of the A-ring, by replacing the -OH and propenyl chain, made Derivative 1 more planar at the ground state optimized conformation, except for the other propenyl chain at position 5' of B-ring (Fig. 2c, d). The calculated molecular properties indicated that the structural modification from honokiol to Derivative 1 increased the LogP (Table 1). However, the hydrogen donor and hydrogen acceptor groups had been reduced to 1 from 2 in honokiol. The ability of honokiol to cross the blood brain barrier and act on various targets in the CNS, such as in gliosarcoma and neuroblastoma is attributed to essentially hydrophobic nature of honokiol (Wang, Duan et al. 2011, Lin, Chen et al. 2012).

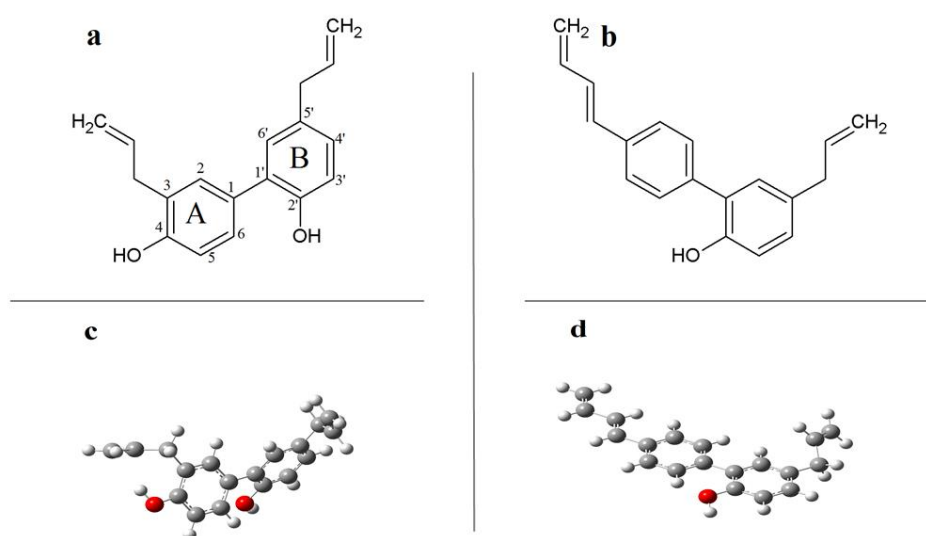


Figure 2. Development of Derivative 1 (**b, d**) ligand molecular structure from the neolignan biphenyl molecular scaffold of honokiol (**a, c**). The A-ring of honokiol (**a**) has been modified in Derivative 1 (**b**).

The docking study of Derivative 1 with the A β monomer did not show any significant difference from the docking profile of honokiol (Table 2), although the binding pose of Derivative 1 was slightly shifted from Asp 23 to Asn 27 (Fig 3a, b). In docking with the A β oligomer, the structural modification from honokiol to Derivative 1 did not change the overall docking score. Nonetheless, it is proposed to have increased interactions with the backbone amides group of key residues within this target as summarized by proposed H-bonding interactions (Table 3, Fig 3c, d). This predicted improvement in backbone amides interaction was possibly due to the conformational change, as planarity in some polycyclic compounds might appropriately orient the hydrogen donor or acceptor group of a ligand against A β (Churches, Caine et al. 2014). Backbone amides participate in stabilizing the overall protein conformation (Yang, Wang et al. 2004). A previous study on replacing the backbone amides with ester groups in islet amyloid polypeptide (IAPP) made the protein more stable in a

monomeric form (Cao and Raleigh 2010). However, the effect of this proposed increased interaction with backbone amides by a small molecular ligand is yet to be investigated for A β .

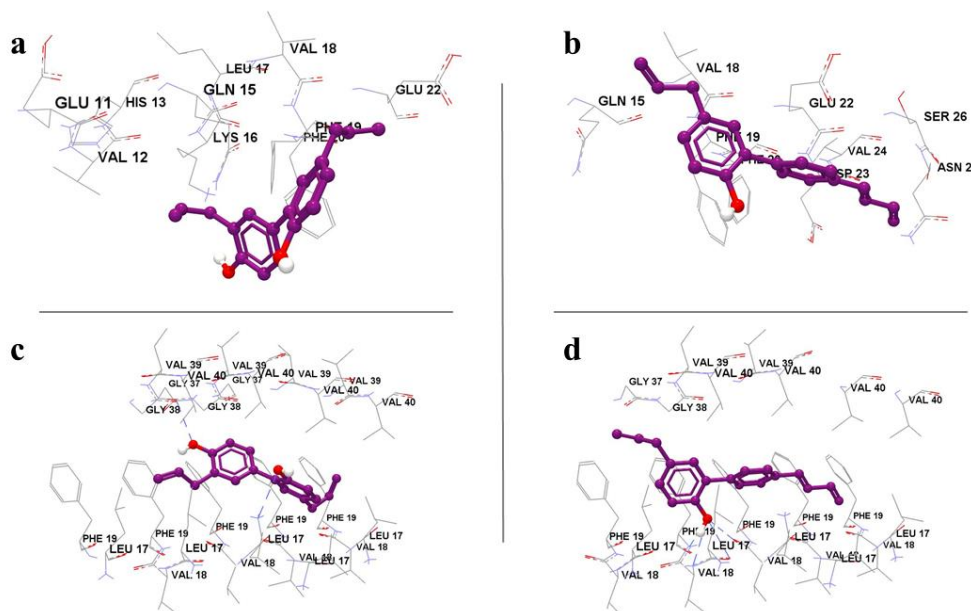


Figure 3. Comparison of docking binding poses between honokiol and Derivative 1 in A β (a) honokiol, (b) Derivative 1 bound to A β monomer, (c) honokiol and (d) Derivative 1 bound to A β oligomer. Only interacting residues are shown.

6.3.2 Derivative 2 molecular properties and interaction with A β

Derivative 2 had a mostly planar conformation, like Derivative 1 (Fig. 4). Not surprisingly, the introduction of an aromatic ring, a phenyl group to the buta-1,3-diene chain, markedly increased the LogP value (Table 1). The hydrophobic structure of Derivative 2 decreased the overall docking score against both A β monomer and oligomer, along with proposed increased H-bonding interactions to its binding pocket according to the docking model (Fig. 5a-d). In the case of the monomer, it is predicted to form H-bonding with Lys 16, a key residue responsible for A β toxicity (Table 2) (Sato, Murakami et al. 2013). The docking poses of Derivative 2 suggested that the terminal phenyl group improved the ligand orientation while

enabling the -OH group to interact with key residues (Fig. 5b, d). Therefore, in the subsequent steps, modifications were made either to this phenyl group or the linker buta-1,3-diene chain.

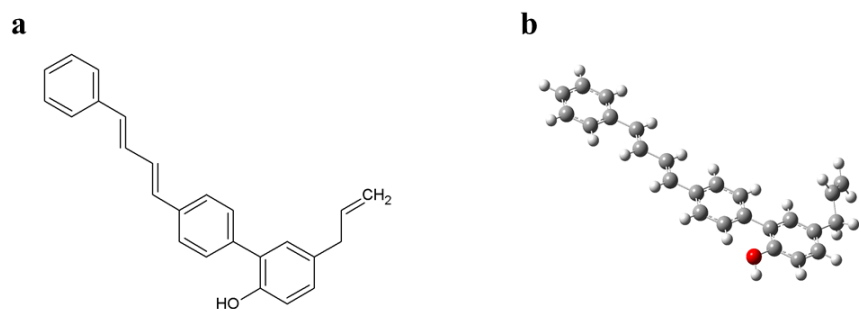


Figure 4. (a) Chemical structure and (b) ground state optimized structure of Derivative 2.

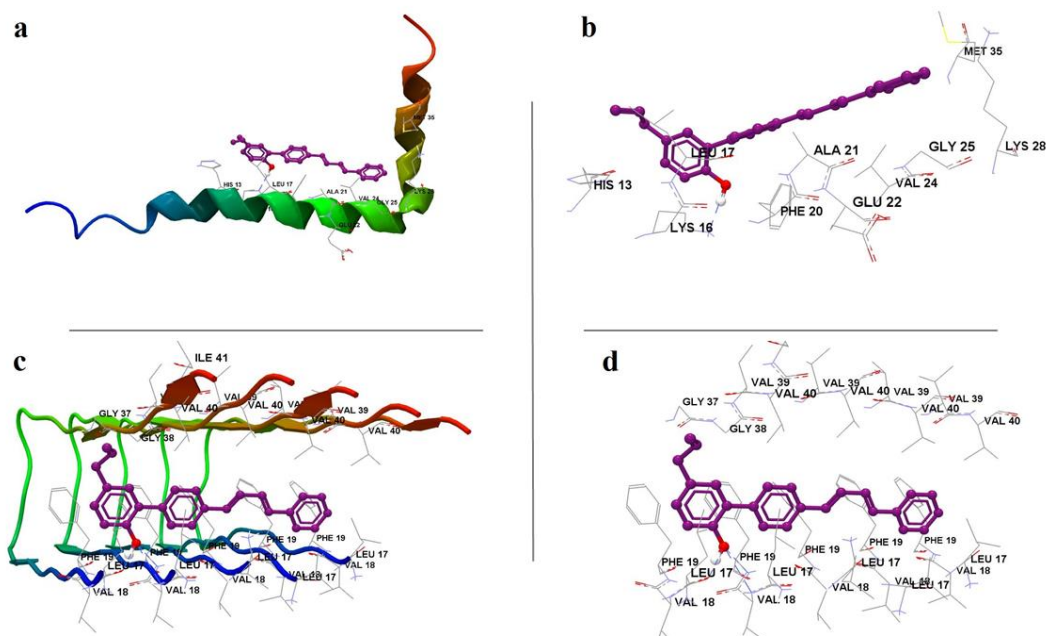


Figure 5. Docking poses of Derivative 2 with A β ; (a) monomer, (b) Derivative 2 showing proposed binding interaction residues of monomer, (c) oligomer and (d) Derivative 2 showing proposed binding interaction residues of oligomer.

6.3.3 Derivative 3 interaction with A β

In Derivative 3, the introduction of two -OH groups at position 1 and 3 of the buta-1,3-diene chain (Fig. 6) partially reduced the LogP; nevertheless, it increased H-bond donor and acceptor counts (Table 1). Interestingly, Derivative 3 had a higher docking score than Derivative 2 against both A β monomer and oligomer (Table 2, 3). Despite having more polar groups as H-bond donor/acceptors, it showed no H-bonding interaction while docked to the A β monomer (Fig. 7a, b). However, within the A β oligomer binding pocket it was predicted to have the highest H-bonding interactions with multiple residues from amongst all derivatives according to the docking result (Table 3). This suggested that the hydroxy buta-1,3-diene chain of Derivative 3 favours electrostatic interactions with many residues across the binding pocket of A β oligomer (Fig. 7c, d), whereas Derivative 2 interacted essentially through shape complementarity based on the docking model. A comparison of their binding poses also suggested that Derivative 2 fitted well within the binding pocket, a characteristic of favourable shape (Fig. 5c), while Derivative 3 spanned across the binding pocket in a different orientation (Fig. 7c).

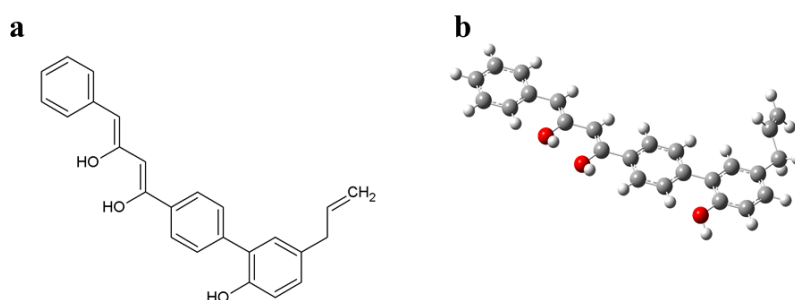


Figure 6. (a) Chemical structure and (b) ground state optimized structure of Derivative 3.

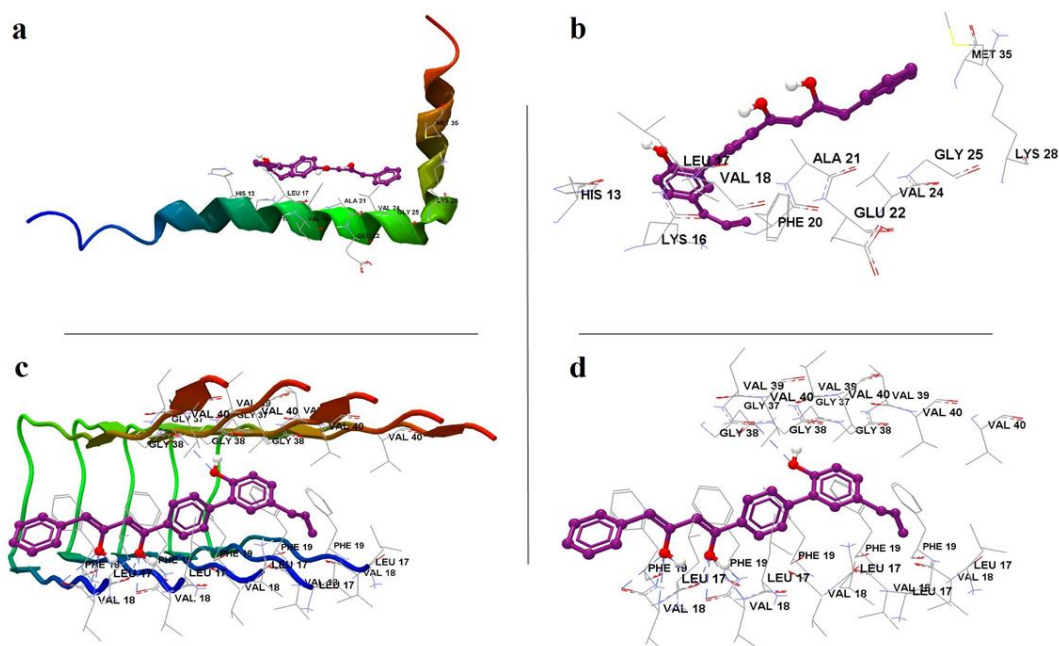


Figure 7. Docking poses of Derivative 3 with A β ; (a) monomer, (b) Derivative 3 showing proposed binding interaction residues of monomer, (c) oligomer and (d) Derivative 3 showing proposed binding interaction residues of oligomer.

6.3.4 Derivative 4 interaction with A β

The alternative approach taken in the design of Derivative 4 altered its geometry and disrupted the planarity of the molecular structure (Fig. 8a). However, there was a marginal increase in the LogP value and the ether group increased the number of H-bond acceptors (Table 1). Docking with the monomer suggested a marginal increase in score compared to Derivative 3, while the binding pocket and H-bond preference shifted to residue Glu 22 (Fig. 9a, b, Table 2). In regard to oligomer docking, no significant improvement was observed compared to either Derivative 2 or 3 (Fig. 9c, d, Table 3). Since the interaction with Lys residues would be a desirable property of an anti-A β ligand due to its impact on A β toxicity, the Derivative 4 structure was not considered suitable for further design (Sato, Murakami et al. 2013).

The merging of the Derivative 2 structure with the virtual screening ‘hit’ dibenzyl imidazolidine scaffold, as described previously, altered the molecular geometry from a mostly planar Derivative 2 to a non-planar Derivative 5 (Fig. 10). This marginally increased the LogP value as more hydrophobic groups were introduced (Table 1), but it also increased the H-bond acceptors in the ligand with more rotatable bonds. The lower docking score with A β monomer than previous Derivatives was probably due to more ring systems along with rotatable bonds in this ligand (Fig. 11, Table 2, 3). The virtual screening ‘hits’ Compound 1 and 2 bearing this scaffold demonstrated slightly lower docking scores compared to Derivative 5 (Das and Smid 2017). Docking of Derivative 5 to the A β oligomer resulted in a higher docking score than Compound 1. Nonetheless, it was predicted to have moderate interactions with the backbone amide groups of the key residues as summarized by proposed H-bonding interactions within the binding pocket of the A β oligomer according to the docking model (Fig. 11c, d, Table 3). This suggested that Derivative 5 was capable of both prospective H-bond and hydrophobic interactions, unlike Compound 1 and 2 according to docking model. Additionally, having a phenyl group such as the B-ring of honokiol connected to the dibenzyl group, seemed an effective design strategy for balancing polar and hydrophobic interactions with the A β monomer and oligomer.

Removal of the methoxyphenyl group from the dibenzyl imidazolidine fragment of Derivative 5 and addition of the -OH and -OCH₃ groups to the terminal phenyl group (as in Derivative 4) simplified the molecular geometry of Derivative 6 when compared to Derivative 5 (Fig. 12). Derivative 6 also possessed improved drug-likeness, as LogP was within the range of most approved drugs and it contained multiple H-bond acceptors, donors and flexible bonds (Table 1). Derivative 6 had the lowest docking score with the A β monomer, showing H-bonding to the key Lys 16 residue (Table 2). It was predicted to bind in a favourable region where it interacted with the majority of the hydrophobic residues along with Lys 28 and Met 35, responsible for A β toxicity (Fig. 13a, b) (Bitan, Tarus et al. 2003, Sato, Murakami et al. 2013). In the oligomer docking, Derivative 6 also displayed the highest score, yet not many prospective interactions with the key residues occurred, except for that with Gly 37 (Fig. 13c, d). This indicates towards a proposed non-polar interaction and a favourable shape of ligand according to docking model. Although Derivative 2 also displayed favourable shape for fitting within the A β oligomer binding pocket, the structure of Derivative 6 would be preferable in drug design, since more saturated carbons in a structure are associated with successful drug discovery (Lovering, Bikker et al. 2009).

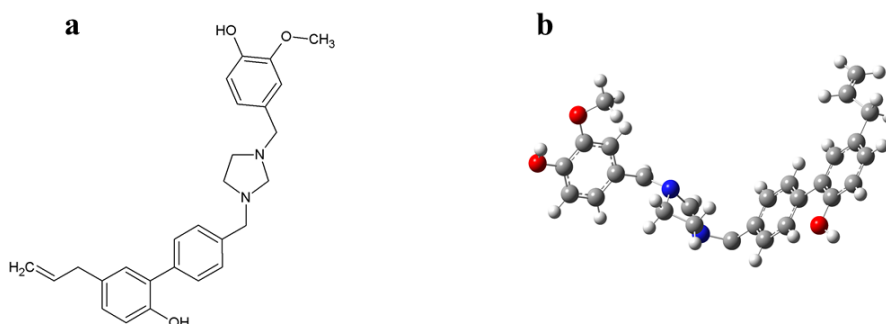


Figure 12. (a) Chemical structure and (b) ground state optimized structure of Derivative 6.

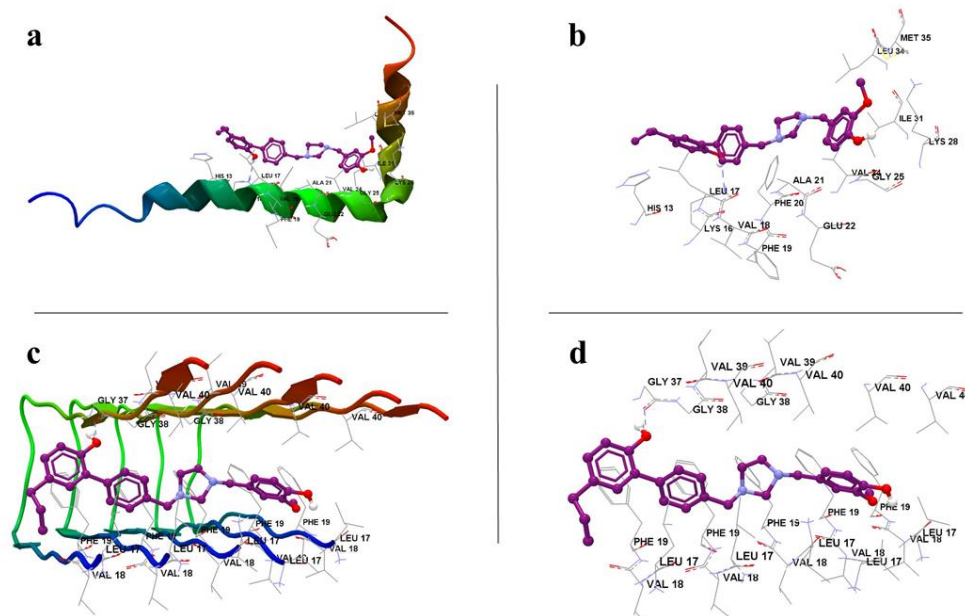


Figure 13. Docking poses of Derivative 6 with Aβ (a) monomer, (b) Derivative 6 showing proposed binding interaction residues of monomer, (c) oligomer and (d) Derivative 6 showing proposed binding interaction residues of oligomer.

6.3.7 Derivative 7 interaction with Aβ

Derivative 7 represented the final structural modification from the molecular docking guided and pharmacophore-based *in silico* design approach. Replacing the imidazolidine group of Derivative 6 with an imidazole group, as in Derivative 7, increased LogP > 6 (Table 1), while also increasing the H-bond donor count and marginally altering the molecular geometry (Fig. 14a). This modification improved the H-bond interaction while docked to Aβ monomer; however, the binding pocket was shifted and the interaction with the key Lys residues and overall score was decreased (Fig. 15a, b, Table 2). Therefore, Derivative 6 was considered as the optimized ligand from this *in silico* study against the Aβ monomer target.

Proposed interactions with the A β oligomer suggested that Derivative 7 engaged in prospective interactions with the backbone amide groups of the key residues as summarized by H-bonding interactions, as well as possessing a favourable shape for binding to the A β target, according to docking result (Table 3, Fig 15c, d). The minor change in molecular geometry from Derivative 6 to Derivative 7 probably positioned the lignan -OH groups well within the binding pocket (Fig. 15c). As a result, Derivative 7 seemed to be an optimized ligand for an improved docking profile showing both polar and hydrophobic interaction to the A β oligomer.

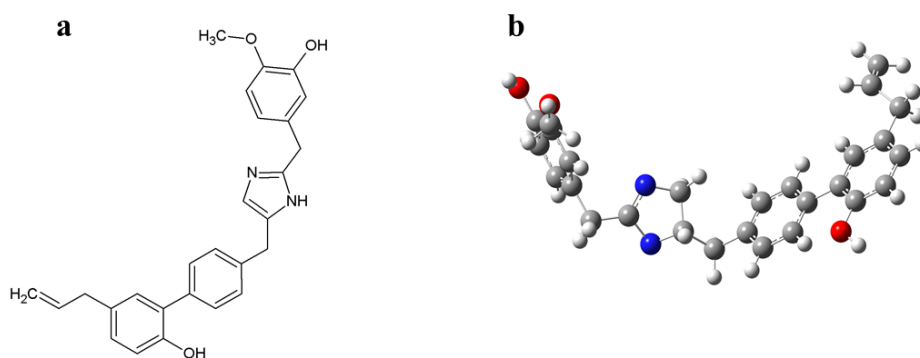


Figure 14. (a) Chemical structure and (b) ground state optimized conformation of Derivative 7.

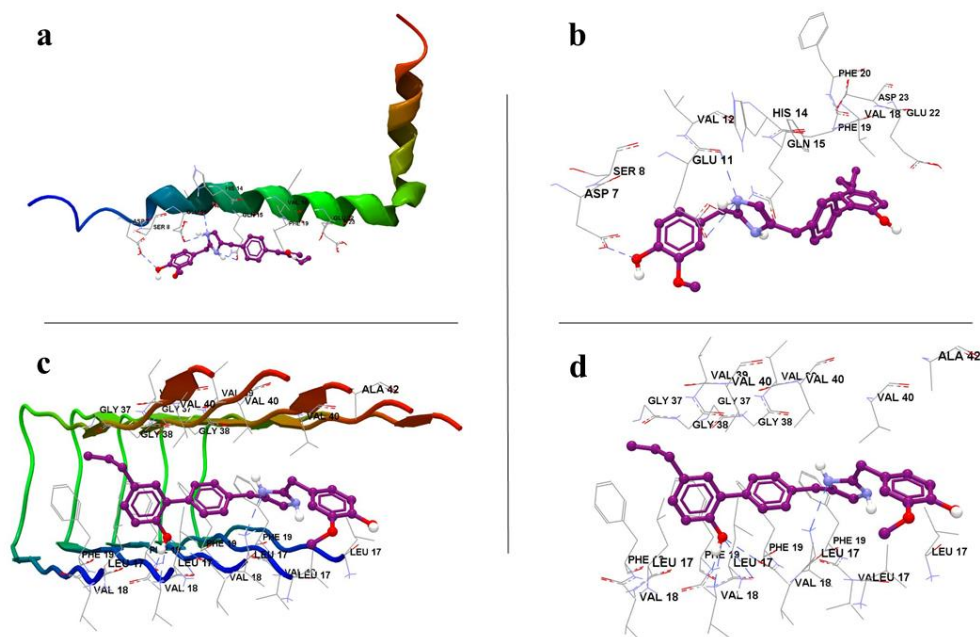


Figure 15. Docking poses of Derivative 7 with A β (a) monomer, (b) Derivative 7 showing proposed binding interaction residues of monomer, (c) oligomer and (d) Derivative 7 showing proposed binding interaction residues of oligomer.

In drug design, Lipinski's rule of five is commonly used as a guide to assess the drug-likeness of a small molecule from its physicochemical properties. These are - i) not more than 5 hydrogen bond donors (nitrogen or oxygen atoms with one or more hydrogen atoms), ii) not more than 10 hydrogen bond acceptors (nitrogen or oxygen atoms), iii) a molecular mass less than 500 daltons, iv) an octanol-water partition coefficient log P not greater than 5. Lipinski's rule also states that no more than one violation of this rule is found in most orally bioavailable drugs (Lipinski, C. A. et al. 1997, 2001). Table 1 describes these physicochemical properties of honokiol and the derivative compounds. All the derivatives have one violation (LogP>5) of this rule of five and honokiol satisfies all of the rules.

Table 1. Molecular properties of honokiol and its derivatives as calculated using the CLC Drug Discovery Workbench (version 2.4.1).

Ligand	Weight (g/mol)	Flexible bonds	Hydrogen donor	Hydrogen acceptor	LogP	Lipinski violations
Honokiol	266.34	5	2	2	4.98	0
Derivative 1	262.35	5	1	1	5.68	1
Derivative 2	338.45	6	1	1	7.17	1
Derivative 3	370.45	6	3	3	6.04	1
Derivative 4	400.47	8	2	4	6.47	1
Derivative 5	490.65	9	1	4	7.00	1
Derivative 6	430.55	8	2	5	5.11	1
Derivative 7	428.53	8	4	5	6.25	1

Table 2. Molecular docking profiles of honokiol and its derivative ligands with A β ₁₋₄₂ monomer (PDB ID: 1IYT).

Ligand	Docking score	H-bonding score	H-bonding residue	Steric interaction score
Honokiol	-45.96	0.00	-	-48.33
Derivative 1	-45.19	0.00	-	-48.26
Derivative 2	-53.97	-2.00	Lys 16	-54.88
Derivative 3	-47.73	0.00	-	-58.31
Derivative 4	-50.61	-2.00	Glu 22	-54.44
Derivative 5	-59.80	0.00	-	-65.05
Derivative 6	-57.15	-2.00	Lys 16	-60.27
Derivative 7	-55.99	-6.19	Gln 15, Glu 11, Asp 7	-56.37

Table 3. Molecular docking profiles of honokiol and its derivative ligands with A β ₁₇₋₄₂ oligomer (PDB ID: 2BEG).

Ligand	Docking score	H-bonding score	H-bonding residue	Steric interaction score
Honokiol	-72.31	-3.87	Leu 17 ^C , Gly 38 ^E	-72.77
Derivative 1	-72.13	-7.65	Leu 17 ^D , Val 18 ^{C,D} , Phe 19 ^D	-68.68
Derivative 2	-79.87	-4.45	Leu 17 ^E , Val 18 ^D , Phe 19 ^D	-90.61
Derivative 3	-73.02	-13.59	Leu 17 ^E , Val 18 ^{D,E} , Phe 19 ^{D,E} , Gly 38 ^E	-66.10
Derivative 4	-73.02	-3.61	Leu 17 ^C , Val 18 ^E	-76.18
Derivative 5	-81.72	-5.07	Leu 17 ^E , Val 18 ^D , Phe 19 ^D	-85.66
Derivative 6	-85.66	-1.98	Gly 37 ^E	-88.31
Derivative 7	-82.10	-8.84	Leu 17 ^{C,D} , Val 18 ^{C,D} , Phe 19 ^D	-78.60

6.3.8 Docking of derivatives with α Synuclein A53T

All the derivatives, except Derivative 1 and 3, were identified as having a favourable docking profile within the binding region of α SA53T (Table 4). The initial structural modification from honokiol to Derivative 1 did not improve its docking profile and the score was marginally reduced, indicating a weaker interaction at the binding pocket (Fig. 16b). In case of Derivative 2, the addition of another benzene ring might have improved its binding through interaction with Thr 33 (Fig. 16c), whereas, in Derivative 3, the two additional -OH groups shifted the ligand orientation towards residue Lys 34, with more predicted H-bonding (Fig. 16d). Absence of these -OH groups and introduction of the -oxy group on the linker chain in Derivative 4's structure improved the docking score, with H-bonding to Lys 23 (Fig. 16e). Derivative 5 had a decreased docking score, possibly due to its larger size compared with other derivatives (Fig.

16f). Derivative 6 displayed superior H-bonding with three residues in this binding pocket (Fig. 16g). Finally, Derivative 7 was found to have the lowest docking score, along with H-bonding to the Lys residues (Fig. 16h, Table 5). The pharmacophore-based ligand design strategy used for Derivative 6 and 7 improved the docking profile, where interestingly, replacing the imidazolidine ring with imidazole ring altered the binding poses and access to Lys 21 and 23 residues (Fig. 16g, h). Lys 21 was previously reported to be a target residue for ligand binding and anti-aggregatory effects towards α S, although Lys 23 and 34 were also involved in this process (Meng, Munishkina et al. 2009). Therefore, Derivative 6 would be the more favourable ligand structure targeting α SA53T than the other Derivatives proposed here.

Table 4. Docking profile of honokiol and all derivatives against α SA53T.

Ligand	Docking score	H-bonding score	H-bonding residue	Steric interaction score
Honokiol	-53.69	-2.00	Lys 23	-55.04
Derivative 1	-50.86	-2.00	Lys 23	-51.97
Derivative 2	-54.22	-3.35	Lys 23, Thr 33	-53.19
Derivative 3	-50.81	-6.00	Lys 34	-51.64
Derivative 4	-56.36	-2.00	Lys 23	-59.09
Derivative 5	-60.43	0.00	-	-65.58
Derivative 6	-56.50	-6.04	Lys 21, 23, Thr 33, Lys 34	-56.25
Derivative 7	-65.25	-3.93	Lys 32, 34	-65.51

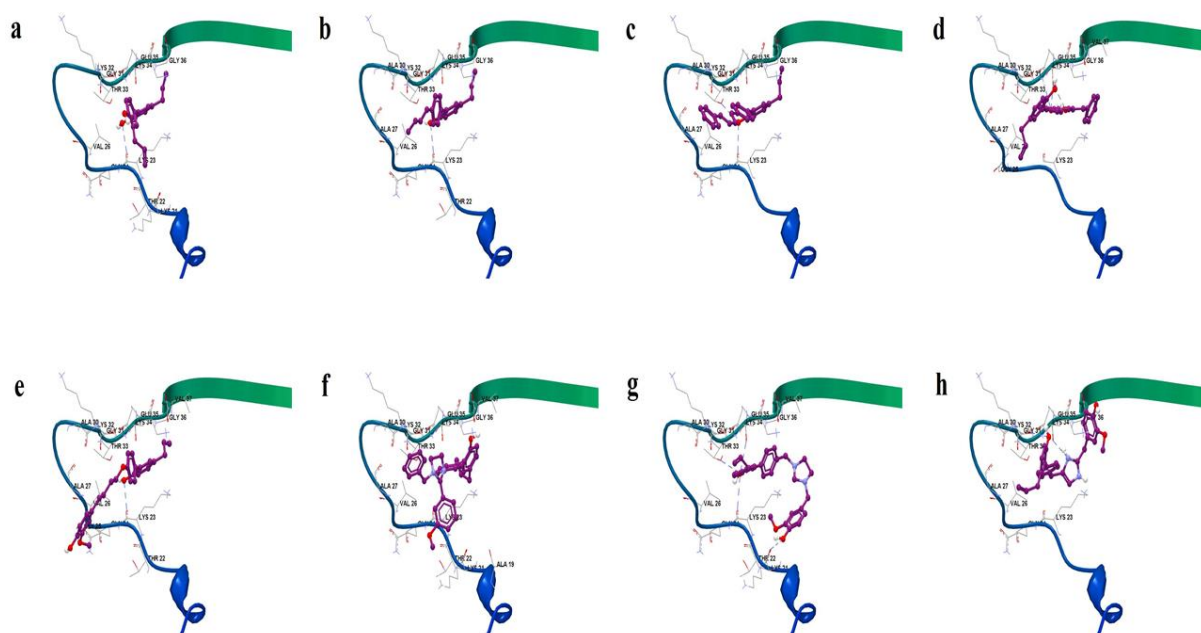


Figure 16. Docking poses of (a) honokiol, (b) Derivative 1, (c) Derivative 2, (d) Derivative 3, (e) Derivative 4, (f) Derivative 5, (g) Derivative 6 and (h) Derivative 7 with α SA53T.

6.3.9 Core fragment and scaffold hopping

This study used molecular docking to derive new ligand structures based on previously known pharmacophores with amyloidogenic affinity and by searching new chemical spaces. By studying the prospective binding interactions of Derivative 6 and 7 in the docking model, a novel scaffold called the ‘core’ structure was designed (Fig. 17). This consisted of a FMH ring connected to a dibenzyl group on both sides (Fig. 17). The FMH ring in the core structure could be either an aromatic ring, such as the imidazole of Derivative 7 or a saturated ring such as the imidazolidine of Derivative 6. This ‘core’ scaffold showed a favourable docking profile against both the A β monomer and oligomer, with an overall score of -43.47 and -73.55 respectively.

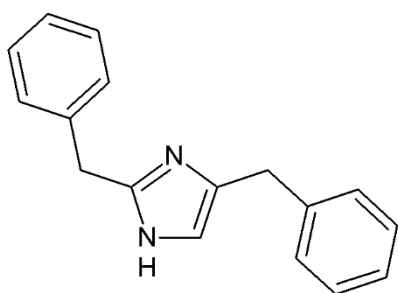


Figure 17. Structure of the ‘core’ scaffold with an imidazole as the FMH ring.

6.3.10 General considerations

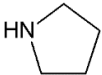
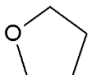
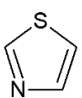

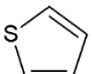
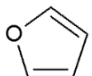
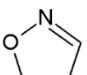
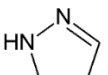
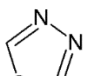

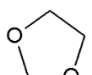
The applications of the novel amyloid binding ligands presented here extend beyond those targeting pathological misfolded proteins in the brain such as A β and α S. A previous study has shown that aminoimidazole analogs having a comparable shape with the ‘core’ structure, act as non-toxic inhibitors of *Pseudoalteromonas sp.* bacterial biofilm formation (Linares, Bottzeck et al. 2011). Amyloidogenic proteins such as curli are associated with biofilm production in uropathogenic bacterial infections (Cegelski, Pinkner et al. 2009). Moreover, the curli functional amyloid system was found in some *Pseudoalteromonas* species (Dueholm, Albertsen et al. 2012). This provides some support to the concept that the pharmacophore-based design of the derivative ligands bearing the ‘core’ fragment might show a generic anti-aggregatory activity against amyloidogenic proteins. Interestingly, a previous study focusing on screening various drugs and natural products structures proposed a ‘BioCore’ scaffold for novel drug design, a similar concept to the ‘core’ scaffold presented here (Kombarov, Altieri et al. 2010).

Imidazole rings have been widely used in medicinal chemistry to discover drugs in the area of cancer chemotherapy, microtubule polymerization inhibitors and kinase inhibitors, in addition

to antifungal drugs (Bukowski, Sheeler et al. 1984, Zhang, Peng et al. 2014). However, the role of imidazole rings for binding to amyloidogenic proteins has not been well documented.

Furthermore, a scaffold hopping approach of the ‘core’ FMH ring would enable additional design of novel derivative ligands targeting A β (Table 5). Scaffold hopping has been a commonly practised approach in medicinal chemistry for changing the central chemical template (Böhm, Flohr et al. 2004). In many drug discovery attempts, scaffold hopping led to the design of successful leads, such as for protein-protein interactions, design of peptide mimetics or selective antagonist of adenosine receptor A_{2A} (Olson, Bolin et al. 1993, Ongini, Monopoli et al. 2001, Böhm, Flohr et al. 2004, Rush, Grant et al. 2005). The 11 FMH ring systems shown in Table 5 were recorded among the most frequently used ring systems in small molecule drugs listed in the FDA Orange Book (Taylor, MacCoss et al. 2014). They were incorporated into docking studies here, where out of these 11 different FMH ring-containing scaffolds, the thiazole moiety at the central core showed the lowest docking scores towards both the monomer and oligomer of A β . This is reflected in the benzothiazole core of thioflavin T structure, a commonly used molecule with high binding affinity towards amyloid fibrils, as used in this thesis. Since thiazoles are present in many drugs and possess various bioactivities desirable for CNS-targeted drug design, the proposed derivative with a thiazole scaffold could be a valuable novel A β ligand in this regard (Mishra, Kumari et al. 2015). Thiazole rings as the benzothiazole group are also present in the FDA approved positron emission tomography (PET) scanning radiopharmaceutical, flutemetamol, that is used clinically to bind A β deposition in AD patients (Curtis, Gamez et al. 2015).

Table 5. Molecular docking profiles of derivatives bearing commonly used FMH rings in small molecule drugs with A β .

FMH rings in Derivative 7	FMH ring structure	Monomer Docking score	Monomer H-bonding score	Oligomer docking score	Oligomer H-bonding score
Pyrrolidine		-49.93	-2.00	-79.10	-6.43
Oxolane		-50.12	0.00	-76.83	-6.43
Thiazole		-59.88	0.00	-88.07	-7.42
Cyclopentane		-55.34	-4.00	-81.26	-7.49
Thiophene		-52.35	-4.95	-84.83	-5.63
Furan		-54.14	-3.80	-83.25	0.00
Oxazole		-50.37	0.00	-83.21	-6.67
Pyrazole		-45.53	-5.43	-82.42	-14.00
Thiadiazole		-55.82	-3.29	-79.03	-9.78
Pyrrole		-44.47	-1.53	-84.27	-8.53
Dioxolane		-47.42	0.00	-83.56	-4.00

There are a set of natural alkaloid compounds found mostly in red marine sponge species *Leucetta chagosensis* and *Lepidium meyenii* that have partial structural similarity with the

dibenzyl imidazole ‘core’ structure presented here (Cui, Zheng et al. 2003, Hassan, Al-Taweel et al. 2009, Koswatta, Kasiri et al. 2017). However, in those natural alkaloids the nitrogen atoms of the imidazole group are connected to the side chains whereas in the ‘core’ structure of this study, the nitrogens are not connected to any group, which accounts for its structural uniqueness. In another study searching for A β inhibitors by a HTS approach, a nitrogen FMH fused ring was identified, namely the indole derivative compound (D737), which has partial similarity with the shape of the ‘core’ structure presented here (McKoy, Chen et al. 2012).

The present study of pharmacophore-based ligand design focused on the presence of nitrogen atoms either as imidazole, imidazolidine or thiazole in the iterative derivation of amyloid binding ligands. These groups possessed an improved docking profile, indicating they might be avid binders to amyloidogenic proteins.

6.4 Conclusion and future direction

This study has introduced a computationally guided drug-design approach from pharmacophores of natural as well as synthetic origin. Beginning from the neolignan biphenyl molecular scaffold of honokiol and later incorporating the dibenzyl imidazolidine scaffold, this study has designed several novel structures along with a novel molecular ‘core’ fragment that was predicted to have a superior binding to amyloidogenic proteins. In order to test this drug-design method as a proof of concept study, a synthetic plan for one or more of these novel derivatives is currently being investigated.

Chapter 7: Final Discussion and Conclusions

7.1 Significance of the study

The first study (Chapter 2) identified honokiol and punicalagin as potent inhibitors of A β ₁₋₄₂ aggregation, detailing their potency of inhibition and extent of neuroprotection from A β ₁₋₄₂ induced neurotoxicity *in vitro*, which was comparable to noted anti-amyloid flavones myricetin and luteolin. The second study (Chapter 3) demonstrated a successful structure-based virtual screening approach validating the predictability of the molecular docking methods, which were subsequently used to understand prospective interactions of small molecules with amyloid-based protein targets used throughout this thesis. The virtual screening not only identified ‘hit’ compounds bearing the desired five-membered heterocycle (FMH) ring fragments, but also identified a novel molecular scaffold. These compounds for the first time were demonstrated to inhibit amyloidogenic protein aggregation of A β and α SA53T and exert neuroprotection. In the third study, we demonstrated inhibition of α SA53T misfolding, amyloidogenic aggregation and exogenous toxicity by two selected synthetic imidazolidine compounds comparable to that observed with honokiol and punicalagin. Such studies highlighted the diverse molecular structural features that can be used as template for further generic amyloid inhibitor drug design. Collectively the results from Chapter 2 and 3 highlighted that the synthetic imidazolidine Compound 2 (1,3-dibenzyl-2-[4-(benzyloxy)-3-methoxyphenyl] imidazolidine) may be a suitable candidate for further development as an amyloidogenic aggregation inhibitor. In Chapter 4, the structure-activity relationships of flavones were further explored and demonstrated that only B-ring vicinal hydroxylation was required to inhibit α SA53T amyloidogenic aggregation and neurotoxicity, exemplified by the antiaggregatory and neuroprotective effects of the semi-synthetic flavone, 2-D08. Chapter 5 revealed the generic

amyloid inhibiting property of the neolignan magnolol, demonstrating an inhibition of aggregation against both A β and particularly α SA53T.

The optimized conformation of these compounds and their proposed binding interactions according to the docking model with model A β ₁₋₄₂ and α SA53T have been foundational to later molecular docking guided design of novel Derivative ligands and fragments targeting A β ₁₋₄₂ and α SA53T as described in Chapter 6. Finally, the novel Derivative ligand design using structural features identified by earlier studies, has provided examples of their application in rational drug design. Overall, the findings of this thesis provide a set of diverse structural features or fragments that might be helpful for early stage design of therapeutics targeting amyloidogenic aggregation, especially targeted to AD and PD. This research of various small molecular proposed interactions with A β and α S is fundamental in this regard, as further drug development is built on the initial favourable molecular structures. Table 1 summarizes the most effective natural and synthetic small molecules identified in the study, which inhibit amyloidogenic protein aggregation as well as protect neuronal cells from amyloid toxicity. Table 1 summarizes the molecular properties of the most effective ligands identified in this study. The physicochemical properties of successful CNS drugs such as polar surface area (PSA) or topological PSA $\leq 90 \text{ \AA}^2$, molecular weight ≤ 400 , LogP ≤ 5 , H-bond donor ≤ 3 and H-bond acceptor ≤ 7 suggests that honokiol, 2-D08 and Compound 1 are suitable for further CNS drug development (Pajouhesh, H. and Lenz, G. R. 2005).

Table 1. Summary of druglike properties of the most effective A β and α SA53T aggregation inhibitors and neuroprotective compounds

Ligand	Weight (g/mol)	Flexible bonds	Hydrogen donor	Hydrogen acceptor	LogP	Polar surface area in \AA^2
Honokiol	266.34	5	2	2	4.98	40.5
Punicalagin	1084.72	0	17	30	1.7	511.0
2-D08	270.24	1	3	5	2.5	87.0
Compound 1	370.45	6	3	3	6.04	15.71
Compound 2	400.47	8	2	4	6.47	24.94
Derivative 7	428.53	8	3	5	6.25	78.37
Derivative 7 with thiazole	443.57	8	2	4	6.13	90.82
Myricetin	318.24	1	6	8	1.85	148.0

7. 2 The neolignan biphenyl scaffold for developing disease modifying therapy in AD and PD

The search for new natural molecules that can be active against a common disease process of both AD and PD which are generally regarded as safe is valuable to facilitate the intensive search for disease-modifying therapeutics. Consequently, the identification of honokiol and magnolol as effective inhibitors of A β ₁₋₄₂ aggregation, the most toxic species of A β , suggests the effectiveness of this neolignan biphenyl scaffold in targeting A β . A previous study found that magnolol was neuroprotective against A β ₁₋₄₀ induced toxicity in PC-12 cells (Hoi, Ho et al. 2010). Additionally, magnolol's neuroprotective potential in PD was further highlighted in a study showing protection from 1-methyl-4-phenyl-1,2,3,6-tetrahydropyridine (MPTP-) induced neurodegeneration both *in vitro* and *in vivo* (Muroyama, Fujita et al. 2012). Likewise,

honokiol acts as a potent scavenger of superoxide and peroxide radicals, owing to its antioxidant activity which may be a further basis for neuroprotection (Dikalov, Losik et al. 2008). In the case of α SA53T, even though honokiol promoted small fibrillar α SA53T structures and magnolol produced small amorphous aggregates, they both demonstrated significant inhibition of aggregation (Chapter 4 and 5). This indicates that the minor structural differences in these two molecules might result in a different binding mode or interaction to the target protein, as suggested by the molecular docking simulations. The binding site for neolignan biphenyl scaffold in α SA53T or α S is not known. However, the docking of magnolol to the NAC-region of α SA53T protein was performed to understand this neolignan biphenyl scaffold interaction in this critical region for aggregation (Cho, Nodet et al. 2009). Thus, the different binding regions for honokiol and magnolol in α SA53T (Chapter 4 and 5) are selected to understand how the neolignan biphenyl scaffold might interact with the modelled flavonoid binding region or NAC region. Previous studies and the experimental studies presented here have not differentiated between honokiol and magnolol in terms of binding affinity towards amyloidogenic proteins such as A β and α SA53T. Nevertheless, the molecular docking studies in this thesis offer some theoretical insights in favour of honokiol having higher binding affinity towards both protein targets.

The generic anti-amyloidogenic activity of both molecules is reflected in their inhibition of human calcitonin aggregation, another amyloidogenic protein (Guo, Ma et al. 2015). The generic anti-aggregative activity along with neuroprotection in the present study and other medical effects such as antidepressant, anxiolytic and neurotrophic properties of honokiol rationalise its use as a template for early drug discovery efforts in dementia (Kuribara, Kishi et al. 2000, Fukuyama, Nakade et al. 2002, Esumi, Makado et al. 2004, Xu, Yi et al. 2008, Qiang, Wang et al. 2009).

Moreover, the neolignan biphenyl scaffold has no catechol-type functional groups, which are often associated with the so called ‘pan assay interference compounds’ or (PAINS) associated with false signalling hits in throughput assays (Baell 2016). Whereas the noted generic amyloid inhibitors such as EGCG, curcumin and other catechol-type flavones have been described as PAINS (Baell 2016, Nelson, Dahlin et al. 2017). The docking studies presented in this thesis suggest that the neolignan biphenyl scaffold might have a more favourable shape and proposed nonpolar interactions with both A β and α SA53T targets when compared with flavones. Shape complementarity plays a critical role in A β amyloidogenic aggregation, as demonstrated by the effect of stereoisomers of key amino acid residues such as Phe19 and Leu34 on A β ₁₋₄₀ aggregation (Chandra, Korn et al. 2017). This study demonstrated that the shape alteration of residues Phe19 and Leu34 does not block fibril formation but does affect the pathway of aggregation (Chandra, Korn et al. 2017). These nonpolar residues have been shown to participate in honokiol and other small molecule binding to A β oligomeric conformations in the docking studies. It is possible that the shape of the neolignan biphenyl scaffold alters the shape of these nonpolar residues, although how the shape of a small molecule inhibitor impacts on the orientation of the key residues is not understood.

In contrast, the molecular mechanisms of flavonoid interactions with A β and α S have been studied and it is known that the *ortho*-quinone formed by the oxidation of vicinal hydroxyl groups common to many flavonoids can covalently modify the lysine residue(s) of both proteins. Non-catechol type flavonoids with no vicinal hydroxyl groups can also interact through π - π interactions with residues His13,14 and Phe19,20 (Sato, Murakami et al. 2013, Hanaki, Murakami et al. 2016). However, the neolignan biphenyl structure is not comparable in this regard, as they are structurally distinct. The computationally predicted favourable shape of the neolignan biphenyl scaffold to bind both A β and α SA53T, coupled with a tractable

structure for derivatization warrants their further research in medicinal chemistry and drug discovery.

In a recent study by Maioli et al., both magnolol and honokiol structures were used to design novel derivatives as an anti-proliferative against hepatocarcinoma cells (Maioli, Basoli et al. 2018). Other studies have also synthesized several analogs of neolignan biphenyls as anti-cancer compounds (Kong, Tzeng et al. 2005). Additionally, some neolignan derivative compounds have demonstrated anti-HIV properties along with anti-tumor activity (Amblard, Govindarajan et al. 2007). These studies validate the suitability of honokiol and magnolol structures as a template for pharmacophore-based drug discovery and serve to highlight a favourable structure for biological activity, which may be exploited towards a number of potential therapeutic applications.

7.3 The novel dibenzyl imidazolidine scaffold and the ‘core’ fragment

In the virtual screening study, the FMH ring fragment-based search identified the dibenzyl imidazolidine scaffold as an inhibitor of amyloidogenic aggregation and toxicity (Chapter 3 and 4). Subsequently, the dibenzyl imidazole ‘core’ fragment was designed based on the molecular docking studies in Chapter 6. Imidazole fragment-bearing compounds have not been thoroughly explored for activity at amyloidogenic protein targets, despite their significant contribution in drug development (Zhang, Peng et al. 2014). Imidazolidine rings without any exocyclic groups or hydantoin structures, are generally lacking in examples of rational drug design. Several FMH rings such as the thiazole or benzothiazole ring are present in the established amyloid binding probe the thioflavin T (ThT) molecule and in flutemetamol, a FDA

approved amyloid PET tracer (Curtis, Gamez et al. 2015). Among the oxygen containing rings, the furan ring in the benzofuran group and oxazole ring in the benzoxazole group have also been used for novel design of A β PET tracers (Ono, Kawashima et al. 2006, Ono, Cheng et al. 2011, Cui, Ono et al. 2012). Additionally, novel compounds bearing benzofuran groups, have been shown to inhibit A β aggregation (Rizzo, Rivière et al. 2008, Ha, Kang et al. 2018). Another FMH ring, the pyrrole group in the indole ring has demonstrated efficacy as an inhibitor of amyloidogenic aggregation (McKoy, Chen et al. 2012). In the abovementioned compounds, the FMH rings have been a part of a bicyclic ring or fused with a benzene ring, whereas the novel scaffold identified here possesses the FMH ring as an individual fragment. Additionally, the dibenzyl groups attached to this central imidazolidine/imidazole ring provide a unique shape to the fragment, which is predicted to be favourable for binding to both A β and α S in the docking simulations. While previous studies have highlighted the usefulness of FMH ring-bearing bicyclic compounds in designing anti-amyloid compounds, the present study provides new structural information about the role of imidazolidine or imidazole FMH ring fragment, as part of this scaffold (Chapter 3, 4 and 6).

7.4 The novel Derivative design as A β and α S ligand

The novel structures presented in this thesis are an example of designing A β and α SA53T binding ligands using the neolignan biphenyl scaffold as a template. Moreover, its hybridisation with the dibenzyl imidazolidine scaffold has provided a novel amyloid ligand design strategy. However, the effectiveness of this design strategy awaits the synthesis and testing of the derivatives. Another application of such a novel ligand might be for the development of an amyloid tracer small molecule for imaging and diagnostic purposes. As mentioned earlier, the presence of the thiazole group in successful amyloid PET tracer

molecules demonstrates the importance of this FMH ring in binding to amyloid β deposits. Molecular docking results predicted high binding affinity of the thiazole ‘core’ structure (Chapter 6) as relevant in this purpose. Notably, the majority of the amyloid tracer molecules, including flutemetamol, are based on the ThT molecular structure, whereas the ‘core’ structure presented in Chapter 6, is distinct. It is not known from the present study whether having the FMH ring without a bicyclic group is a rational approach for designing a selective amyloid binder with a high affinity towards $A\beta$. Notwithstanding this, a major challenge in developing a PET tracer for αS aggregates in Lewy bodies (LB) or Lewy neurites (LN) is an insufficient selectivity for αS over binding to $A\beta$ and another amyloidogenic protein, tau (Kotzbauer, Tu et al. 2017). The versatile binding affinity of the ‘core’ and related derivative structures towards amyloidogenic proteins allude to the challenge of selective PET tracer development. The study is limited to further investigate the structural features that might lead to selective binding to either αS or $A\beta$. Given the similarity between these two amyloidogenic proteins, computer aided ligand-design methods should be combined with detailed biophysical/biochemical understanding of any unique binding sites within each protein.

7.5 Amyloid hypothesis as a target: still work to do

Among the major approaches for overcoming of $A\beta$ and αS associated pathology, reducing the overall production of $A\beta$ and αS and enhancing their clearance have been extensively studied for drug development, as discussed in Chapter 1. By contrast, inhibition of amyloidogenic aggregation by small molecules has not been well-developed but remains a valid target in the context of the amyloid hypothesis. Inhibition of aggregation might be a rational therapeutic choice in scenarios where pathogenic amyloids can act as a seed for further amyloidogenic

aggregation and self-propagation, which occur in a prion protein-like manner (Jucker and Walker 2013).

Notably, targeting amyloidogenic aggregation with a small molecule metal chelator, PBT2 has not been successful in reducing A β burden in clinical trials (Relkin 2008). Subsequently, PBT2 has also been investigated in clinical trials for Huntington's disease, looking at the efficacy of inhibiting huntingtin amyloidogenic protein aggregation (Huntington Study Group Reach2HD Investigators 2015). Another small molecule NPT088, that has been shown to bind amyloidogenic proteins such as α S, A β and tau is still under development and under clinical trial in AD (Levenson, Schroeter et al. 2016)(ClinicalTrials.gov Identifier: NCT03008161).

Active and passive immunization therapies aiming at clearance of amyloid aggregates have largely been unsuccessful in past clinical trials (Morgan 2011). Recently, a monoclonal antibody, aducanumab showed a lowering of amyloid levels and is still under investigation (Haeberlein, Gheuens et al. 2018). However, active and passive immunization therapies have challenges including recurrent infusion and higher cost of production (Lannfelt, Relkin et al. 2014).

Although the jury is still out for efficacy of many other BACE1 inhibitors, the lack of efficacy of verubecestat in a large clinical trial in prodromal AD patients raises doubt more generally about the approach of reducing amyloidogenic protein production (Mullard 2017, Egan, Kost et al. 2018). Previous studies targeting amyloidogenic protein aggregation by all three approaches, have either employed novel synthetic molecules using rigorous medicinal

chemistry efforts or utilized natural products in basic studies and clinical investigations. A hybrid derivative molecule designed from a natural product and synthetic fragment has not been well-documented. Consequently, the novel Derivatives presented in this thesis warrant further investigation to test this concept. Despite arguments about the validity of the amyloid hypothesis in AD, there has not been conclusive evidence to disprove amyloidogenic protein aggregation as a primary viable target for any disease modifying therapy.

7.6 Limitations of this study and future directions

Ligand-based drug design is an inexpensive and fast method in computer-aided drug discovery research. Despite the advantages of this *in silico* approach, there are some disadvantages compared to traditional HTS methods. Synthetic tractability of novel compounds resulting from ligand-based design remains a challenge, especially when the design is guided by *in silico* methods such molecular docking without simultaneous synthesis and testing of fragments. The scope of this study has been limited to novel ligand design, however, these novel ligands have not yet been synthesized to validate the design strategies in experimental models. Therefore, further pharmacological characterisation as well as the toxicity profile of these novel Derivatives await. Preliminary investigations with medicinal chemistry collaborators however have indicated that both the derivative structures and approaches to synthetic pathways are feasible and that synthesis of the core structure has commenced.

The other limitation of this study would be the lack of understanding of a clear mechanism of action for the identified molecular inhibitors of amyloidogenic protein aggregation. Although, studying α SA53T conformational change during early aggregation by IM-MS offers new

insights on various molecular interactions, similar studies on the A β protein could not be undertaken due to methodological limitations for such studies. The present study has been unable to investigate the conformational change of A β proteins in the presence of each of the compounds tested here.

These studies have demonstrated the anti-aggregative properties of various natural and synthetic compounds and tested their neuroprotection *in vitro*, in an attempt to correlate their anti-aggregative property with neuroprotection. The MTT cell viability assay used in this study is somewhat limited to provide an endpoint neuroprotection measure in terms of the viable mitochondria present in cells. This assay is unable to differentiate between different forms of neuroprotective actions of a molecule, such as inhibition of amyloidogenic aggregation, antioxidant or other cell signalling properties. As mentioned earlier, the natural polyphenol inhibitors identified in this study likely possess multiple bioactivities. Thus, the inhibitors might protect neuronal cells by different mechanisms in addition to their antiaggregative properties. Further research on protective mechanisms in addition to their identified antiaggregative properties is needed for understanding the extent of neuroprotection arising from a molecular inhibition of amyloidogenic aggregation. Another important future direction of this study would be to compare the antiaggregative and neuroprotective properties of the identified diverse compounds in appropriate *in vivo* models of AD and PD in the evolution of their preclinical development.

7.7 Conclusions

This study set out with the aim of identifying new naturally occurring small molecule inhibitors of both A β and α SA53T amyloidogenic aggregation that are structurally distinct from known inhibitors such as EGCG or curcumin. A diverse set of such natural inhibitors has been identified and characterised for their effects on amyloidogenic aggregation and neuroprotection. The findings demonstrate honokiol and magnolol as inhibitors of both A β and α SA53T amyloidogenic aggregation. The other aim has been to identify FMH ring-bearing compounds with nitrogen as the heteroatom and without an exocycle C=O/S/N group that can inhibit amyloid aggregation, as well as protect neuronal cells from its toxicity. Two dibenzyl imidazolidine scaffold-bearing compounds, called as Compound 1 and Compound 2 in the thesis, have been identified as not only inhibitors of A β , but also α SA53T amyloidogenic aggregation and toxicity. Subsequently, the final major aim of this study has been to design novel amyloid binding ligands from the various molecular structural features revealed by this study. A set of novel Derivative ligands along with a ‘core’ fragment have been designed *in silico* with predicted high affinity binding to A β and α SA53T.

In conclusion, the studies presented here have highlighted the neolignan biphenyl scaffold as efficacious naturally occurring inhibitors of both A β and α S amyloidogenic protein aggregation and further demonstrated the suitability of using the neolignan biphenyl scaffold for rational drug design. Furthermore, the identification of a novel dibenzyl imidazolidine scaffold with predicted high binding affinity to A β has expanded exploration of new chemical spaces in the search for anti-amyloid compounds. A novel A β and α SA53T binding ligand designed from combining a naturally occurring scaffold with screening ‘hit’ fragment was also revealed. This study testifies as an example of an inexpensive and ligand-based drug design approach. Such approaches may fuel new drug design research and serve the unmet medical need of

discovering new disease-modifying therapeutics for common and currently incurable neurodegenerative diseases.

Chapter 8 : Bibliography

Aarsland, D., K. Laake, J. P. Larsen and C. Janvin (2002). "Donepezil for cognitive impairment in Parkinson's disease: a randomised controlled study." Journal of Neurology, Neurosurgery & Psychiatry **72**(6): 708-712.

Adibhatla, R. M. and J. F. Hatcher (2008). "Phospholipase A2, reactive oxygen species, and lipid peroxidation in CNS pathologies." Journal of Biochemistry and Molecular Biology **41**(8): 560-567.

Ahmad, A., T. Ali, H. Y. Park, H. Badshah, S. U. Rehman and M. O. Kim (2017). "Neuroprotective Effect of Fisetin Against Amyloid-Beta-Induced Cognitive/Synaptic Dysfunction, Neuroinflammation, and Neurodegeneration in Adult Mice." Molecular Neurobiology **54**(3): 2269-2285.

Ahmad, B. and L. J. Lapidus (2012). "Curcumin Prevents Aggregation in α -Synuclein by Increasing Reconfiguration Rate." Journal of Biological Chemistry **287**(12): 9193-9199.

Albani, D., L. Polito, S. Batelli, S. D. Mauro, C. Fracasso, G. Martelli, L. Colombo, C. Manzoni, M. Salmona, S. Caccia, A. Negro and G. Forloni (2009). "The SIRT1 activator resveratrol protects SK-N-BE cells from oxidative stress and against toxicity caused by α -synuclein or amyloid- β (1-42) peptide." Journal of Neurochemistry **110**(5): 1445-1456.

Alvarez-Erviti, L., Y. Couch, J. Richardson, J. M. Cooper and M. J. A. Wood (2011). "Alpha-synuclein release by neurons activates the inflammatory response in a microglial cell line." Neuroscience Research **69**(4): 337-342.

Alzheimer, A. (1911). "Über eigenartige Krankheitsfälle des späteren Alters." Zeitschrift für die gesamte Neurologie und Psychiatrie **4**(1): 356.

Amblard, F., B. Govindarajan, B. Lefkove, K. L. Rapp, M. Detorio, J. L. Arbiser and R. F. Schinazi (2007). "Synthesis, cytotoxicity, and antiviral activities of new neolignans related to honokiol and magnolol." Bioorganic & Medicinal Chemistry Letters **17**(16): 4428-4431.

Ansari, M. A., H. M. Abdul, G. Joshi, W. O. Opii and D. A. Butterfield (2009). "Protective effect of quercetin in primary neurons against A β (1-42): relevance to Alzheimer's disease." The Journal of Nutritional Biochemistry **20**(4): 269-275.

Alzheimer's Association Report 2015. "2015 Alzheimer's disease facts and figures." Alzheimers & Dementia. **11**: 332-384.

Alzheimer's Association Report 2017. "2017 Alzheimer's disease facts and figures." Alzheimer's & Dementia **13**(4): 325-373.

- Australian Bureau of Statistics (2017) *Causes of Death, Australia, 2016* (cat. no. 3303.0)
- Baba, M., S. Nakajo, P. H. Tu, T. Tomita, K. Nakaya, V. M. Lee, J. Q. Trojanowski and T. Iwatsubo (1998). "Aggregation of alpha-synuclein in Lewy bodies of sporadic Parkinson's disease and dementia with Lewy bodies." *The American Journal of Pathology* **152**(4): 879-884.
- Baell, J. B. (2016). "Feeling Nature's PAINS: Natural Products, Natural Product Drugs, and Pan Assay Interference Compounds (PAINS)." *Journal of Natural Products* **79**(3): 616-628.
- Ban, T., D. Hamada, K. Hasegawa, H. Naiki and Y. Goto (2003). "Direct Observation of Amyloid Fibril Growth Monitored by thioflavin T Fluorescence." *Journal of Biological Chemistry* **278**(19): 16462-16465.
- Bastianetto, S., Z. X. Yao, V. Papadopoulos and R. Quirion (2006). "Neuroprotective effects of green and black teas and their catechin gallate esters against β -amyloid-induced toxicity." *European Journal of Neuroscience* **23**(1): 55-64.
- Bhatt, M. A., A. Messer and J. H. Kordower (2013). "Can intrabodies serve as neuroprotective therapies for parkinson's disease? beginning thoughts." *Journal of Parkinson's Disease* **3**(4): 581-591.
- Bieschke, J., M. Herbst, T. Wiglenda, R. P. Friedrich, A. Boeddrich, F. Schiele, D. Kleckers, J. M. Lopez del Amo, B. A. Grüning, Q. Wang, M. R. Schmidt, R. Lurz, R. Anwyl, S. Schnoegl, M. Fändrich, R. F. Frank, B. Reif, S. Günther, D. M. Walsh and E. E. Wanker (2011). "Small-molecule conversion of toxic oligomers to nontoxic β -sheet-rich amyloid fibrils." *Nature Chemical Biology* **8**: 93.
- Bieschke, J., J. Russ, R. P. Friedrich, D. E. Ehrnhoefer, H. Wobst, K. Neugebauer and E. E. Wanker (2010). "EGCG remodels mature α -synuclein and amyloid- β fibrils and reduces cellular toxicity." *Proceedings of the National Academy of Sciences* **107**(17): 7710-7715.
- Bitan, G., B. Tarus, S. S. Vollers, H. A. Lashuel, M. M. Condron, J. E. Straub and D. B. Teplow (2003). "A Molecular Switch in Amyloid Assembly: Met35 and Amyloid β -Protein Oligomerization." *Journal of the American Chemical Society* **125**(50): 15359-15365.
- Böhm, H.-J., A. Flohr and M. Stahl (2004). "Scaffold hopping." *Drug Discovery Today: Technologies* **1**(3): 217-224.
- Bougea, A., C. Koros, M. Stamelou, A. Simitsi, N. Papagiannakis, R. Antonelou, D. Papadimitriou, M. Breza, K. Tasios, S. Fragkiadaki, X. Gericola Trapali, M. Bourboulis, G. Koutsis, S. G. Papageorgiou, E. Kapaki, G. P. Paraskevas and L. Stefanis (2017).

"Frontotemporal dementia as the presenting phenotype of p.A53T mutation carriers in the alpha-synuclein gene." Parkinsonism & Related Disorders **35**: 82-87.

Brys, M., A. Ellenbogen, L. Fanning, N. Penner, M. Yang, M. Welch, E. Koenig, E. David, T. Fox, S. Makh, J. Aldred, I. Goodman, D. Graham, A. Weihofen and J. Cedarbaum (2018). "Randomized, Double-Blind, Placebo-Controlled, Single Ascending Dose Study of Anti-Alpha-Synuclein Antibody BIIB054 in Patients with Parkinson's Disease (S26.001)." Neurology **90**(15 Supplement).

Bucciantini, M., E. Giannoni, F. Chiti, F. Baroni, L. Formigli, J. Zurdo, N. Taddei, G. Ramponi, C. M. Dobson and M. Stefani (2002). "Inherent toxicity of aggregates implies a common mechanism for protein misfolding diseases." Nature **416**: 507.

Bukowski, R. M., L. Sheeler, J. Cunningham and C. Esselstyn (1984). "Successful combination chemotherapy for metastatic parathyroid carcinoma." Archives of Internal Medicine **144**(2): 399-400.

Cao, P. and D. P. Raleigh (2010). "Ester to Amide Switch Peptides Provide a Simple Method for Preparing Monomeric Islet Amyloid Polypeptide under Physiologically Relevant Conditions and Facilitate Investigations of Amyloid Formation." Journal of the American Chemical Society **132**(12): 4052-4053.

Cascella, M., S. Bimonte, M. R. Muzio, V. Schiavone and A. Cuomo (2017). "The efficacy of Epigallocatechin-3-gallate (green tea) in the treatment of Alzheimer's disease: an overview of pre-clinical studies and translational perspectives in clinical practice." Infectious Agents and Cancer **12**(1): 36.

Castellani, R. J., G. Perry, S. L. Siedlak, A. Nunomura, S. Shimohama, J. Zhang, T. Montine, L. M. Sayre and M. A. Smith (2002). "Hydroxynonenal adducts indicate a role for lipid peroxidation in neocortical and brainstem Lewy bodies in humans." Neuroscience Letters **319**(1): 25-28.

Cegelski, L., J. S. Pinkner, N. D. Hammer, C. K. Cusumano, C. S. Hung, E. Chorell, V. Åberg, J. N. Walker, P. C. Seed, F. Almqvist, M. R. Chapman and S. J. Hultgren (2009). "Small-molecule inhibitors target Escherichia coli amyloid biogenesis and biofilm formation." Nature Chemical Biology **5**: 913.

Chandra, B., A. Korn, B. K. Maity, J. Adler, A. Rawat, M. Krueger, D. Huster and S. Maiti (2017). "Stereoisomers Probe Steric Zippers in Amyloid- β ." The Journal of Physical Chemistry B **121**(8): 1835-1842.

Chauhan, K., A. K. Tiwari, N. Chadha, A. Kaul, A. K. Singh and A. Datta (2018). "Chalcone Based Homodimeric PET Agent, 11C-(Chal)2DEA-Me, for Beta Amyloid Imaging: Synthesis and Bioevaluation." Molecular Pharmaceutics **15**(4): 1515-1525.

Cheng, H. Y., M. T. Hsieh, F. S. Tsai, C. R. Wu, C. S. Chiu, M. M. Lee, H. X. Xu, Z. Z. Zhao and W. H. Peng (2010). "Neuroprotective effect of luteolin on amyloid β protein (25–35)-induced toxicity in cultured rat cortical neurons." Phytotherapy Research **24**(S1): S102-S108.

Cheon, M., I. Chang, S. Mohanty, L. M. Luheshi, C. M. Dobson, M. Vendruscolo and G. Favrin (2007). "Structural reorganisation and potential toxicity of oligomeric species formed during the assembly of amyloid fibrils." PLoS Computational Biology **3**(9): 1727-1738.

Chin, Y.-W., M. J. Balunas, H. B. Chai and A. D. Kinghorn (2006). "Drug discovery from natural sources." The AAPS Journal **8**(2): E239-E253.

Cho, M. K., G. Nodet, H. Y. Kim, M. R. Jensen, P. Bernado, C. O. Fernandez, S. Becker, M. Blackledge and M. Zweckstetter (2009). "Structural characterization of α -synuclein in an aggregation prone state." Protein Science **18**(9): 1840-1846.

Choi, B. K., M. G. Choi, J. Y. Kim, Y. Yang, Y. Lai, D. H. Kweon, N. K. Lee and Y. K. Shin (2013). "Large alpha-synuclein oligomers inhibit neuronal SNARE-mediated vesicle docking." Proceedings of the National Academy of Science **110**(10): 4087-4092.

Chromy, B. A., R. J. Nowak, M. P. Lambert, K. L. Viola, L. Chang, P. T. Velasco, B. W. Jones, S. J. Fernandez, P. N. Lacor, P. Horowitz, C. E. Finch, G. A. Krafft and W. L. Klein (2003). "Self-Assembly of A β 1-42 into Globular Neurotoxins." Biochemistry **42**(44): 12749-12760.

Churches, Q. I., J. Caine, K. Cavanagh, V. C. Epa, L. Waddington, C. E. Tranberg, A. G. Meyer, J. N. Varghese, V. Streltsov and P. J. Duggan (2014). "Naturally occurring polyphenolic inhibitors of amyloid beta aggregation." Bioorganic & Medicinal Chemistry Letters **24**(14): 3108-3112.

Coelho-Cerqueira, E., A. S. Pinheiro and C. Follmer (2014). "Pitfalls associated with the use of thioflavin-T to monitor anti-fibrillogenic activity." Bioorganic & Medicinal Chemistry Letters **24**(14): 3194-3198.

Cramer, R. D., D. E. Patterson and J. D. Bunce (1988). "Comparative molecular field analysis (CoMFA). 1. Effect of shape on binding of steroids to carrier proteins." Journal of the American Chemical Society **110**(18): 5959-5967.

Crescenzi, O., S. Tomaselli, R. Guerrini, S. Salvadori, A. M. D'Ursi, P. A. Temussi and D. Picone (2002). "Solution structure of the Alzheimer amyloid beta-peptide (1-42) in an apolar microenvironment. Similarity with a virus fusion domain." European Journal of Biochemistry **269**(22): 5642-5648.

Cui, B., B. L. Zheng, K. He and Q. Y. Zheng (2003). "Imidazole Alkaloids from *Lepidium meyenii*." Journal of Natural Products **66**(8): 1101-1103.

Cui, M., M. Ono, H. Kimura, M. Ueda, Y. Nakamoto, K. Togashi, Y. Okamoto, M. Ihara, R. Takahashi, B. Liu and H. Saji (2012). "Novel 18F-Labeled Benzoxazole Derivatives as Potential Positron Emission Tomography Probes for Imaging of Cerebral β -Amyloid Plaques in Alzheimer's Disease." Journal of Medicinal Chemistry **55**(21): 9136-9145.

Culvenor, J. G., C. A. McLean, S. Cutt, B. C. V. Campbell, F. Maher, P. Jäkälä, T. Hartmann, K. Beyreuther, C. L. Masters and Q.-X. Li (1999). "Non-A β Component of Alzheimer's Disease Amyloid (NAC) Revisited: NAC and α -Synuclein Are Not Associated with A β Amyloid." The American Journal of Pathology **155**(4): 1173-1181.

Curtis, C., J. E. Gamez, U. Singh and et al. (2015). "Phase 3 trial of flutemetamol labeled with radioactive fluorine 18 imaging and neuritic plaque density." Journal of American Medical Association Neurology **72**(3): 287-294.

Dalfo, E., M. Barrachina, J. L. Rosa, S. Ambrosio and I. Ferrer (2004). "Abnormal alpha-synuclein interactions with rab3a and rabphilin in diffuse Lewy body disease." Neurobiology of Disease **16**(1): 92-97.

Das, S. and S. D. Smid (2017). "Identification of dibenzyl imidazolidine and triazole acetamide derivatives through virtual screening targeting amyloid beta aggregation and neurotoxicity in PC12 cells." European Journal of Medicinal Chemistry **130**: 354-364.

Das, S., L. Stark, I. F. Musgrave, T. Pukala and S. D. Smid (2016). "Bioactive polyphenol interactions with [small beta] amyloid: a comparison of binding modelling, effects on fibril and aggregate formation and neuroprotective capacity." Food & Function **7**(2): 1138-1146.

de Queiroz, R. B., F. L. de Carvalho, D. V. Fonseca, J. M. Barbosa-Filho, P. R. Salgado, L. L. Paulo, A. B. de Queiroz, L. C. Pordeus, S. A. de Souza, H. D. Souza, B. F. Lira and P. F. de Athayde-Filho (2015). "Antinociceptive effect of hydantoin 3-phenyl-5-(4-ethylphenyl)-imidazolidine-2,4-dione in mice." Molecules **20**(1): 974-986.

DeMaagd, G. and A. Philip (2015). "Part 2: Introduction to the Pharmacotherapy of Parkinson's Disease, With a Focus on the Use of Dopaminergic Agents." Pharmacy and Therapeutics **40**(9): 590-600.

Dikalov, S., T. Losik and J. L. Arbiser (2008). "Honokiol is a potent scavenger of superoxide and peroxy radicals." Biochemical Pharmacology **76**(5): 589-596.

Doig, A. J. and P. Derreumaux (2015). "Inhibition of protein aggregation and amyloid formation by small molecules." Current Opinion in Structural Biology **30**: 50-56.

Dueholm, M. S., M. Albertsen, D. Otzen and P. H. Nielsen (2012). "Curli Functional Amyloid Systems Are Phylogenetically Widespread and Display Large Diversity in Operon and Protein Structure." PLOS ONE **7**(12): e51274.

Efimova, S. S., V. V. Zakharov and O. S. Ostroumova (2015). "Effects of dipole modifiers on channel-forming activity of amyloid and amyloid-like peptides in lipid bilayers." Cell and Tissue Biology **9**(3): 250-259.

Egan, M. F., J. Kost, P. N. Tariot, P. S. Aisen, J. L. Cummings, B. Vellas, C. Sur, Y. Mukai, T. Voss, C. Furtek, E. Mahoney, L. Harper Mozley, R. Vandenberghe, Y. Mo and D. Michelson (2018). "Randomized Trial of Verubecestat for Mild-to-Moderate Alzheimer's Disease." New England Journal of Medicine **378**(18): 1691-1703.

Ehrnhoefer, D. E., J. Bieschke, A. Boeddrich, M. Herbst, L. Masino, R. Lurz, S. Engemann, A. Pastore and E. E. Wanker (2008). "EGCG redirects amyloidogenic polypeptides into unstructured, off-pathway oligomers." Nature Structural & Molecular Biology **15**: 558.

Eisele, Y. S., C. Monteiro, C. Fearn, S. E. Encalada, R. L. Wiseman, E. T. Powers and J. W. Kelly (2015). "Targeting protein aggregation for the treatment of degenerative diseases." Nature Reviews Drug Discovery **14**: 759.

El-Azhary, A. A. and H. U. Suter (1996). "Comparison between Optimized Geometries and Vibrational Frequencies Calculated by the DFT Methods." The Journal of Physical Chemistry **100**(37): 15056-15063.

Eliezer, D., E. Kutluay, R. Bussell and G. Browne (2001). "Conformational properties of α -synuclein in its free and lipid-associated states" Edited by P. E. Wright." Journal of Molecular Biology **307**(4): 1061-1073.

Erlanson, D. A. (2012). Introduction to fragment-based drug discovery. Topics in Current Chemistry. **317**: 1-32.

Espargaró, A., T. Ginex, M. d. M. Vadell, M. A. Busquets, J. Estelrich, D. Muñoz-Torrero, F. J. Luque and R. Sabate (2017). "Combined in Vitro Cell-Based/in Silico Screening of Naturally Occurring Flavonoids and Phenolic Compounds as Potential Anti-Alzheimer Drugs." Journal of Natural Products **80**(2): 278-289.

- Esumi, T., G. Makado, H. Zhai, Y. Shimizu, Y. Mitsumoto and Y. Fukuyama (2004). "Efficient synthesis and structure–activity relationship of honokiol, a neurotrophic biphenyl-type neolignan." Bioorganic & Medicinal Chemistry Letters **14**(10): 2621-2625.
- Fernandez-Ruiz, J., C. Garcia, O. Sagredo, M. Gomez-Ruiz and E. de Lago (2010). "The endocannabinoid system as a target for the treatment of neuronal damage." Expert Opinion in Therapeutic Targets **14**(4): 387-404.
- Ferrazzoli, D., A. Carter, F. S. Ustun, G. Palamara, P. Ortelli, R. Maestri, M. Yücel and G. Frazzitta (2016). "Dopamine Replacement Therapy, Learning and Reward Prediction in Parkinson's Disease: Implications for Rehabilitation." Frontiers in Behavioral Neuroscience **10**(121).
- Ferri, C. P., M. Prince, C. Brayne, H. Brodaty, L. Fratiglioni, M. Ganguli, K. Hall, K. Hasegawa, H. Hendrie, Y. Huang, A. Jorm, C. Mathers, P. R. Menezes, E. Rimmer and M. Scazufca (2006). "Global prevalence of dementia: a Delphi consensus study." The Lancet **366**(9503): 2112-2117.
- Fischer, C., S. L. Zultanski, H. Zhou, J. L. Methot, W. C. Brown, D. M. Mampreian, A. J. Schell, S. Shah, H. Nuthall, B. L. Hughes, N. Smotrov, C. M. Kenific, J. C. Cruz, D. Walker, M. Bouthillette, G. N. Nikov, D. F. Savage, V. V. Jeliaskova-Mecheva, D. Diaz, A. A. Szewczak, N. Bays, R. E. Middleton, B. Munoz and M. S. Shearman (2011). "Triazoles as γ -secretase modulators." Bioorganic & Medicinal Chemistry Letters **21**(13): 4083-4087.
- Floor, E. and M. G. Wetzel (1998). "Increased protein oxidation in human substantia nigra pars compacta in comparison with basal ganglia and prefrontal cortex measured with an improved dinitrophenylhydrazine assay." Journal of Neurochemistry **70**(1): 268-275.
- Fosso, M. Y., K. McCarty, E. Head, S. Garneau-Tsodikova and H. LeVine (2016). "Differential Effects of Structural Modifications on the Competition of Chalcones for the PIB Amyloid Imaging Ligand-Binding Site in Alzheimer's Disease Brain and Synthetic A β Fibrils." ACS Chemical Neuroscience **7**(2): 171-176.
- Frimpong, A. K., R. R. Abzalimov, V. N. Uversky and I. A. Kaltashov (2010). "Characterization of intrinsically disordered proteins with electrospray ionization mass spectrometry: Conformational heterogeneity of α -synuclein." Proteins: Structure, Function, and Bioinformatics **78**(3): 714-722.
- Frisch, M., G. Trucks, H. Schlegel, G. Scuseria, M. Robb, J. Cheeseman, J. Montgomery Jr, T. Vreven, K. Kudin and J. Burant (2016). "GAUSSIAN 03, Gaussian Inc., Pittsburgh, PA, 2003."

- Fukuyama, Y., K. Nakade, Y. Minoshima, R. Yokoyama, H. Zhai and Y. Mitsumoto (2002). "Neurotrophic activity of honokiol on the cultures of fetal rat cortical neurons." Bioorganic & Medicinal Chemistry Letters **12**(8): 1163-1166.
- Gai, W. P., J. H. T. Power, P. C. Blumbergs and W. W. Blessing "Multiple-system atrophy: a new α -synuclein disease?" The Lancet **352**(9127): 547-548.
- Ganesan, A. (2008). "The impact of natural products upon modern drug discovery." Current Opinion in Chemical Biology **12**(3): 306-317.
- Gerhard, A., N. Pavese, G. Hotton, F. Turkheimer, M. Es, A. Hammers, K. Eggert, W. Oertel, R. B. Banati and D. J. Brooks (2006). "In vivo imaging of microglial activation with [¹¹C](R)-PK11195 PET in idiopathic Parkinson's disease." Neurobiology of Disease **21**(2): 404-412.
- Goate, A., M.-C. Chartier-Harlin, M. Mullan, J. Brown, F. Crawford, L. Fidani, L. Giuffra, A. Haynes, N. Irving, L. James, R. Mant, P. Newton, K. Rooke, P. Roques, C. Talbot, M. Pericak-Vance, A. Roses, R. Williamson, M. Rossor, M. Owen and J. Hardy (1991). "Segregation of a missense mutation in the amyloid precursor protein gene with familial Alzheimer's disease." Nature **349**: 704.
- Gonçalves, D., G. Alves, A. Fortuna, P. Soares-da-Silva and A. Falcão (2017). "Pharmacokinetics of opicapone, a third-generation COMT inhibitor, after single and multiple oral administration: A comparative study in the rat." Toxicology and Applied Pharmacology **323**: 9-15.
- Gorenberg, E. L. and S. S. Chandra (2017). "The Role of Co-chaperones in Synaptic Proteostasis and Neurodegenerative Disease." Frontiers in Neuroscience **11**(248).
- Gou, M. L., M. Dai, X. Y. Li, X. H. Wang, C. Y. Gong, Y. Xie, K. Wang, X. Zhao, Z. Y. Qian and Y. Q. Wei (2008). "Preparation and characterization of honokiol nanoparticles." Journal of Materials Science: Materials in Medicine **19**(7): 2605-2608.
- Gremer, L., D. Scholzel, C. Schenk, E. Reinartz, J. Labahn, R. B. G. Ravelli, M. Tusche, C. Lopez-Iglesias, W. Hoyer, H. Heise, D. Willbold and G. F. Schroder (2017). "Fibril structure of amyloid-beta(1-42) by cryo-electron microscopy." Science **358**(6359): 116-119.
- Grinter, S. and X. Zou (2014). "Challenges, Applications, and Recent Advances of Protein-Ligand Docking in Structure-Based Drug Design." Molecules **19**(7): 10150.
- Guo, C., L. Ma, Y. Zhao, A. Peng, B. Cheng, Q. Zhou, L. Zheng and K. Huang (2015). "Inhibitory effects of magnolol and honokiol on human calcitonin aggregation." Scientific Reports **5**: 13556.

- Guo, C., L. Ma, Y. Zhao, A. Peng, B. Cheng, Q. Zhou, L. Zheng and K. Huang (2015). "Inhibitory effects of magnolol and honokiol on human calcitonin aggregation." Scientific Reports **5**: 13556.
- Gustot, A., José I. Gallea, R. Sarroukh, María S. Celej, J.-M. Ruyschaert and V. Raussens (2015). "Amyloid fibrils are the molecular trigger of inflammation in Parkinson's disease." Biochemical Journal **471**(3): 323-333.
- Ha, H.-J., D. W. Kang, H.-M. Kim, J.-M. Kang, J. Ann, H. J. Hyun, J. H. Lee, S. H. Kim, H. Kim, K. Choi, H.-S. Hong, Y. Kim, D.-G. Jo, J. Lee and J. Lee (2018). "Discovery of an Orally Bioavailable Benzofuran Analogue That Serves as a β -Amyloid Aggregation Inhibitor for the Potential Treatment of Alzheimer's Disease." Journal of Medicinal Chemistry **61**(1): 396-402.
- Haerberlein, S. B., S. Gheuens, T. Chen, J. O'Gorman, P. von Rosenstiel, P. Chiao, G. Wang, C. von Hehn, L. Skordos, C. Hock, R. Nitsch and A. Sandrock (2018). "Aducanumab 36-month data from PRIME: a randomized, double-blind, placebo-controlled Phase 1b study in patients with prodromal or mild Alzheimer's disease (S2.004)." Neurology **90**(15 Supplement).
- Hamilton, R. L. (2000). "Lewy Bodies in Alzheimer's Disease: A Neuropathological Review of 145 Cases Using α -Synuclein Immunohistochemistry." Brain Pathology **10**(3): 378-384.
- Hanaki, M., K. Murakami, K.-i. Akagi and K. Irie (2016). "Structural insights into mechanisms for inhibiting amyloid β 42 aggregation by non-catechol-type flavonoids." Bioorganic & Medicinal Chemistry **24**(2): 304-313.
- Hanasaki, Y., S. Ogawa and S. Fukui (1994). "The correlation between active oxygens scavenging and antioxidative effects of flavonoids." Free Radical Biology & Medicine **16**(6): 845-850.
- Hardy, J. and D. J. Selkoe (2002). "The Amyloid Hypothesis of Alzheimer's Disease: Progress and Problems on the Road to Therapeutics." Science **297**(5580): 353-356.
- Hardy, J. A. and G. A. Higgins (1992). "Alzheimer's disease: the amyloid cascade hypothesis." Science **256**(5054): 184-185.
- Harper, J. D., C. M. Lieber and P. T. Lansbury (1997). "Atomic force microscopic imaging of seeded fibril formation and fibril branching by the Alzheimer's disease amyloid- β protein." Chemistry & Biology **4**(12): 951-959.

Harper, J. D., S. S. Wong, C. M. Lieber and P. T. Lansbury (1999). "Assembly of A β Amyloid Protofibrils: An in Vitro Model for a Possible Early Event in Alzheimer's Disease." Biochemistry **38**(28): 8972-8980.

Harte, N. P., I. Klyubin, E. K. McCarthy, S. Min, S. A. Garrahy, Y. Xie, G. P. Davey, J. J. Boland, M. J. Rowan and K. H. Mok (2015). "Amyloid Oligomers and Mature Fibrils Prepared from an Innocuous Protein Cause Diverging Cellular Death Mechanisms." Journal of Biological Chemistry **290**(47): 28343-28352.

Hartley, D. M., D. M. Walsh, C. P. Ye, T. Diehl, S. Vasquez, P. M. Vassilev, D. B. Teplow and D. J. Selkoe (1999). "Protofibrillar intermediates of amyloid beta-protein induce acute electrophysiological changes and progressive neurotoxicity in cortical neurons." Journal of Neuroscience **19**(20): 8876-8884.

Harvey, A. L. (2008). "Natural products in drug discovery." Drug Discovery Today **13**(19–20): 894-901.

Hassan, W. H. B., A. M. Al-Taweel and P. Proksch (2009). "Two new imidazole alkaloids from *Leucetta chagosensis* sponge." Saudi Pharmaceutical Journal **17**(4): 295-298.

Hatters, D.M., Lindner, R.A., Carver, J.A. and G.J. Howlett (2001). "The Molecular Chaperone, α -Crystallin, Inhibits Amyloid Formation by Apolipoprotein C-II". Journal of Biological Chemistry **276**: 33755-33761.

Hertel, C., E. Terzi, N. Hauser, R. Jakob-Røtne, J. Seelig and J. A. Kemp (1997). "Inhibition of the electrostatic interaction between β -amyloid peptide and membranes prevents β -amyloid-induced toxicity." Proceedings of the National Academy of Sciences **94**(17): 9412-9416.

Hoi, C. P., Y. P. Ho, L. Baum and A. H. L. Chow (2010). "Neuroprotective effect of honokiol and magnolol, compounds from *Magnolia officinalis*, on beta-amyloid-induced toxicity in PC12 cells." Phytotherapy Research **24**(10): 1538-1542.

Hong, D.-P., A. L. Fink and V. N. Uversky (2008). "Structural Characteristics of α -Synuclein Oligomers Stabilized by the Flavonoid Baicalein." Journal of Molecular Biology **383**(1): 214-223.

Honma, T. (2003). "Recent advances in de novo design strategy for practical lead identification." Medicinal Research Reviews **23**(5): 606-632.

Honma, T., K. Hayashi, T. Aoyama, N. Hashimoto, T. Machida, K. Fukasawa, T. Iwama, C. Ikeura, M. Ikuta, I. Suzuki-Takahashi, Y. Iwasawa, T. Hayama, S. Nishimura and H. Morishima (2001). "Structure-Based Generation of a New Class of Potent Cdk4 Inhibitors:

New de Novo Design Strategy and Library Design." Journal of Medicinal Chemistry **44**(26): 4615-4627.

Hsieh, H.-L. and C.-M. Yang (2013). "Role of Redox Signaling in Neuroinflammation and Neurodegenerative Diseases." BioMed Research International **2013**: 18.

Hudson, S. A., H. Ecroyd, T. W. Kee and J. A. Carver (2009). "The thioflavin T fluorescence assay for amyloid fibril detection can be biased by the presence of exogenous compounds." The FEBS Journal **276**(20): 5960-5972.

Huntington Study Group Reach2HD Investigators (2015). "Safety, tolerability, and efficacy of PBT2 in Huntington's disease: a phase 2, randomised, double-blind, placebo-controlled trial." The Lancet Neurology **14**(1): 39-47.

Ingelsson, M. (2016). "Alpha-Synuclein Oligomers-Neurotoxic Molecules in Parkinson's Disease and Other Lewy Body Disorders." Frontiers in Neuroscience **10**: 408.

Inoue, E., Y. Shimizu, R. Masui, T. Hayakawa, T. Tsubonoya, S. Hori and K. Sudoh (2017). "Effects of saffron and its constituents, crocin-1, crocin-2, and crocetin on α -synuclein fibrils." Journal of Natural Medicines **72**(1): 274-279.

Iwatsubo, T., T. C. Saido, D. M. Mann, V. M. Lee and J. Q. Trojanowski (1996). "Full-length amyloid-beta (1-42(43)) and amino-terminally modified and truncated amyloid-beta 42(43) deposit in diffuse plaques." The American Journal of Pathology **149**(6): 1823-1830.

Jain, V. S., D. K. Vora and C. S. Ramaa (2013). "Thiazolidine-2,4-diones: Progress towards multifarious applications." Bioorganic & Medicinal Chemistry **21**(7): 1599-1620.

Janefjord, E., J. L. Maag, B. S. Harvey and S. D. Smid (2014). "Cannabinoid effects on beta amyloid fibril and aggregate formation, neuronal and microglial-activated neurotoxicity in vitro." Cellular and Molecular Neurobiology **34**(1): 31-42.

Janezic, S., S. Threlfell, P. D. Dodson, M. J. Dowie, T. N. Taylor, D. Potgieter, L. Parkkinen, S. L. Senior, S. Anwar, B. Ryan, T. Deltheil, P. Kosillo, M. Cioroch, K. Wagner, O. Ansorge, D. M. Bannerman, J. P. Bolam, P. J. Magill, S. J. Cragg and R. Wade-Martins (2013). "Deficits in dopaminergic transmission precede neuron loss and dysfunction in a new Parkinson model." Proceedings of the National Academy of Sciences **110**(42): E4016-E4025.

Jeon, S.-Y., K. Bae, Y.-H. Seong and K.-S. Song (2003). "Green tea catechins as a BACE1 (β -Secretase) inhibitor." Bioorganic & Medicinal Chemistry Letters **13**(22): 3905-3908.

Ji, H., W. Zhang, M. Zhang, M. Kudo, Y. Aoyama, Y. Yoshida, C. Sheng, Y. Song, S. Yang, Y. Zhou, J. Lü and J. Zhu (2003). "Structure-Based de Novo Design, Synthesis, and

Biological Evaluation of Non-Azole Inhibitors Specific for Lanosterol 14 α -Demethylase of Fungi." Journal of Medicinal Chemistry **46**(4): 474-485.

Jillian, M., W. Xiaoyan, B. D. R. and M. D. A. (2009). "Evaluation of β -Alanine- and GABA-Substituted Peptides as Inhibitors of Disease-Linked Protein Aggregation." ChemBioChem **10**(12): 1982-1987.

Jing, X., X. Wei, M. Ren, L. Wang, X. Zhang and H. Lou (2016). "Neuroprotective Effects of Tanshinone I Against 6-OHDA-Induced Oxidative Stress in Cellular and Mouse Model of Parkinson's Disease Through Upregulating Nrf2." Neurochemical Research **41**(4): 779-786.

Jucker, M. and L. C. Walker (2013). "Self-propagation of pathogenic protein aggregates in neurodegenerative diseases." Nature **501**: 45.

Jung, H. A., S. E. Jin, R. J. Choi, D. H. Kim, Y. S. Kim, J. H. Ryu, D.-W. Kim, Y. K. Son, J. J. Park and J. S. Choi (2010). "Anti-amnesic activity of neferine with antioxidant and anti-inflammatory capacities, as well as inhibition of ChEs and BACE1." Life Sciences **87**(13): 420-430.

Jurneczko, E. and P. E. Barran (2011). "How useful is ion mobility mass spectrometry for structural biology? The relationship between protein crystal structures and their collision cross sections in the gas phase." Analyst **136**(1): 20-28.

Jurneczko, E., F. Cruickshank, M. Porrini, P. Nikolova, Iain D. G. Campuzano, M. Morris and Perdita E. Barran (2012). "Intrinsic disorder in proteins: a challenge for (un)structural biology met by ion mobility–mass spectrometry." Biochemical Society Transactions **40**(5): 1021-1026.

Kadowaki, H., H. Nishitoh, F. Urano, C. Sadamitsu, A. Matsuzawa, K. Takeda, H. Masutani, J. Yodoi, Y. Urano, T. Nagano and H. Ichijo (2004). "Amyloid β induces neuronal cell death through ROS-mediated ASK1 activation." Cell Death And Differentiation **12**: 19.

Kantham, S., S. Chan, G. McColl, J. A. Miles, S. K. Veliyath, G. S. Deora, S. N. Dighe, S. Khabbazi, M.-O. Parat and B. P. Ross (2017). "Effect of the Biphenyl Neolignan Honokiol on A β 42-Induced Toxicity in *Caenorhabditis elegans*, A β 42 Fibrillation, Cholinesterase Activity, DPPH Radicals, and Iron(II) Chelation." ACS Chemical Neuroscience **8**(9): 1901-1912.

Katarkar, A., P. K. Haldar and K. Chaudhuri (2015). "De novo design based pharmacophore query generation and virtual screening for the discovery of Hsp-47 inhibitors." Biochemical and Biophysical Research Communications **456**(3): 707-713.

Kennedy, M. E., A. W. Stamford, X. Chen, K. Cox, J. N. Cumming, M. F. Dockendorf, M. Egan, L. Ereshefsky, R. A. Hodgson, L. A. Hyde, S. Jhee, H. J. Kleijn, R. Kuvelkar, W. Li, B. A. Mattson, H. Mei, J. Palcza, J. D. Scott, M. Tanen, M. D. Troyer, J. L. Tseng, J. A. Stone, E. M. Parker and M. S. Forman (2016). "The BACE1 inhibitor verubecestat (MK-8931) reduces CNS β -amyloid in animal models and in Alzheimer's disease patients." Science Translational Medicine **8**(363): 363ra150-363ra150.

Khurana, R., C. Coleman, C. Ionescu-Zanetti, S. A. Carter, V. Krishna, R. K. Grover, R. Roy and S. Singh (2005). "Mechanism of thioflavin T binding to amyloid fibrils." Journal of Structural Biology **151**(3): 229-238.

Klebe, G., U. Abraham and T. Mietzner (1994). "Molecular Similarity Indices in a Comparative Analysis (CoMSIA) of Drug Molecules to Correlate and Predict Their Biological Activity." Journal of Medicinal Chemistry **37**(24): 4130-4146.

Knehans, T., A. Schüller, D. N. Doan, K. Nacro, J. Hill, P. Güntert, M. S. Madhusudhan, T. Weil and S. G. Vasudevan (2011). "Structure-guided fragment-based in silico drug design of dengue protease inhibitors." Journal of Computer-Aided Molecular Design **25**(3): 263-274.

Kodali, R. and R. Wetzel (2007). "Polymorphism in the intermediates and products of amyloid assembly." Current Opinion in Structural Biology **17**(1): 48-57.

Kohn, W., A. D. Becke and R. G. Parr (1996). "Density Functional Theory of Electronic Structure." Journal of Physical Chemistry **100**(31): 12974-12980.

Kombarov, R., A. Altieri, D. Genis, M. Kirpichenok, V. Kochubey, N. Rakitina and Z. Titarenko (2010). "BioCores: identification of a drug/natural product-based privileged structural motif for small-molecule lead discovery." Molecular Diversity **14**(1): 193-200.

Kong, Z.-L., S.-C. Tzeng and Y.-C. Liu (2005). "Cytotoxic neolignans: an SAR study." Bioorganic & Medicinal Chemistry Letters **15**(1): 163-166.

Koppel, J. and P. Davies (2008). "Targeting the endocannabinoid system in Alzheimer's disease." Journal of Alzheimer's Disease **15**(3): 495-504.

Korb, O., T. Stütze and T. E. Exner (2009). "Empirical Scoring Functions for Advanced Protein-Ligand Docking with PLANTS." Journal of Chemical Information and Modeling **49**(1): 84-96.

Korshavn, K. J., C. Satriano, Y. Lin, R. Zhang, M. Dulchavsky, A. Bhunia, M. I. Ivanova, Y.-H. Lee, C. La Rosa, M. H. Lim and A. Ramamoorthy (2017). "Reduced Lipid Bilayer Thickness Regulates the Aggregation and Cytotoxicity of Amyloid- β ." Journal of Biological Chemistry **292**(11): 4638-4650.

- Koswatta, P. B., S. Kasiri, J. K. Das, A. Bhan, H. M. Lima, B. Garcia-Barboza, N. N. Khatibi, M. Yousufuddin, S. S. Mandal and C. J. Lovely (2017). "Total synthesis and cytotoxicity of Leucetta alkaloids." Bioorganic & Medicinal Chemistry **25**(5): 1608-1621.
- Kotzbauer, P. T., Z. Tu and R. H. Mach (2017). "Current status of the development of PET radiotracers for imaging alpha synuclein aggregates in Lewy bodies and Lewy neurites." Clinical and Translational Imaging **5**(1): 3-14.
- Koutsoukas, A., B. Simms, J. Kirchmair, P. J. Bond, A. V. Whitmore, S. Zimmer, M. P. Young, J. L. Jenkins, M. Glick, R. C. Glen and A. Bender (2011). "From in silico target prediction to multi-target drug design: Current databases, methods and applications." Journal of Proteomics **74**(12): 2554-2574.
- Kowalewski, T. and D. M. Holtzman (1999). "In situ atomic force microscopy study of Alzheimer's beta-amyloid peptide on different substrates: new insights into mechanism of beta-sheet formation." Proceedings of the National Academy of Sciences **96**(7): 3688-3693.
- Kraziński, B. E., J. Radecki and H. Radecka (2011). "Surface Plasmon Resonance Based Biosensors for Exploring the Influence of Alkaloids on Aggregation of Amyloid- β Peptide." Sensors **11**(4): 4030-4042.
- Krebs, M. R., E. H. Bromley and A. M. Donald (2005). "The binding of thioflavin-T to amyloid fibrils: localisation and implications." Journal of Structural Biology **149**(1): 30-37.
- Krishnan, R., H. Tsubery, M. Y. Proschitsky, E. Asp, M. Lulu, S. Gilead, M. Gartner, J. P. Waltho, P. J. Davis, A. M. Hounslow, D. A. Kirschner, H. Inouye, D. G. Myszka, J. Wright, B. Solomon and R. A. Fisher (2014). "A Bacteriophage Capsid Protein Provides a General Amyloid Interaction Motif (GAIM) That Binds and Remodels Misfolded Protein Assemblies." Journal of Molecular Biology **426**(13): 2500-2519.
- Kuo, Y.-M., M. R. Emmerling, C. Vigo-Pelfrey, T. C. Kasunic, J. B. Kirkpatrick, G. H. Murdoch, M. J. Ball and A. E. Roher (1996). "Water-soluble A(N-40, N-42) Oligomers in Normal and Alzheimer Disease Brains." Journal of Biological Chemistry **271**(8): 4077-4081.
- Kuribara, H., E. Kishi, N. Hattori, M. Okada and Y. Maruyama (2000). "The Anxiolytic Effect of Two Oriental Herbal Drugs in Japan Attributed to Honokiol from Magnolia Bark." Journal of Pharmacy and Pharmacology **52**(11): 1425-1429.
- Kwak, H.-M., S.-Y. Jeon, B.-H. Sohng, J.-G. Kim, J.-M. Lee, K.-B. Lee, H.-H. Jeong, J.-M. Hur, Y.-H. Kang and K.-S. Song (2005). " β -Secretase(BACE1) inhibitors from pomegranate (*Punica granatum*) husk." Archives of Pharmaceutical Research **28**(12): 1328-1332.

Lambert, M. P., A. K. Barlow, B. A. Chromy, C. Edwards, R. Freed, M. Liosatos, T. E. Morgan, I. Rozovsky, B. Trommer, K. L. Viola, P. Wals, C. Zhang, C. E. Finch, G. A. Krafft and W. L. Klein (1998). "Diffusible, nonfibrillar ligands derived from A β 1–42 are potent central nervous system neurotoxins." Proceedings of the National Academy of Sciences **95**(11): 6448-6453.

Lannfelt, L., N. R. Relkin and E. R. Siemers (2014). "Amyloid- β -directed immunotherapy for Alzheimer's disease." Journal of Internal Medicine **275**(3): 284-295.

Lashuel, H. A., D. Hartley, B. M. Petre, T. Walz and P. T. Lansbury Jr (2002). "Amyloid pores from pathogenic mutations." Nature **418**: 291.

Leavell, M. D., S. P. Gaucher, J. A. Leary, J. A. Taraszka and D. E. Clemmer (2002). "Conformational studies of Zn-ligand-hexose diastereomers using ion mobility measurements and density functional theory calculations." Journal of the American Society for Mass Spectrometry **13**(3): 284-293.

Lecanu, L., W. Yao, G. L. Teper, Z.-X. Yao, J. Greeson and V. Papadopoulos (2004). "Identification of naturally occurring spirostenols preventing beta-amyloid-induced neurotoxicity." Steroids **69**(1): 1-16.

Lee, H.-J., E.-J. Bae and S.-J. Lee (2014). "Extracellular α -synuclein—a novel and crucial factor in Lewy body diseases." Nature Reviews Neurology **10**: 92.

Lee, H.-J., J.-E. Suk, C. Patrick, E.-J. Bae, J.-H. Cho, S. Rho, D. Hwang, E. Masliah and S.-J. Lee (2010). "Direct Transfer of α -Synuclein from Neuron to Astroglia Causes Inflammatory Responses in Synucleinopathies." Journal of Biological Chemistry **285**(12): 9262-9272.

Lee, H. J., R. A. Kerr, K. J. Korshavn, J. Lee, J. Kang, A. Ramamoorthy, B. T. Ruotolo and M. H. Lim (2016). "Effects of hydroxyl group variations on a flavonoid backbone toward modulation of metal-free and metal-induced amyloid-[small beta] aggregation." Inorganic Chemistry Frontiers **3**(3): 381-392.

Lee, T. P., M. L. Matteliano and E. Middleton, Jr. (1982). "Effect of quercetin on human polymorphonuclear leukocyte lysosomal enzyme release and phospholipid metabolism." Life Science **31**(24): 2765-2774.

Lemere, C. A., F. Lopera, K. S. Kosik, C. L. Lendon, J. Ossa, T. C. Saido, H. Yamaguchi, A. Ruiz, A. Martinez, L. Madrigal, L. Hincapie, J. C. Arango L, D. C. Anthony, E. H. Koo, A. M. Goate, D. J. Selkoe and J. C. Arango V (1996). "The E280A presenilin 1 Alzheimer mutation produces increased A β 42 deposition and severe cerebellar pathology." Nature Medicine **2**: 1146.

- Leopoldini, M., N. Russo and M. Toscano (2011). "The molecular basis of working mechanism of natural polyphenolic antioxidants." Food Chemistry **125**(2): 288-306.
- Levenson, J. M., S. Schroeter, J. C. Carroll, V. Cullen, E. Asp, M. Proschitsky, C. H. Y. Chung, S. Gilead, M. Nadeem, H. B. Dodiya, S. Shoaga, E. J. Mufson, H. Tsubery, R. Krishnan, J. Wright, B. Solomon, R. Fisher and K. S. Gannon (2016). "NPT088 reduces both amyloid- β and tau pathologies in transgenic mice." Alzheimer's & Dementia : Translational Research & Clinical Interventions **2**(3): 141-155.
- Levin, J., S. Maaß, M. Schuberth, G. Respondek, F. Paul, U. Mansmann, W. H. Oertel, S. Lorenzl, F. Krismer, K. Seppi, W. Poewe, G. Wenning, A. Giese, K. Bötzel and G. Höglinger (2016). "The PROMESA-protocol: progression rate of multiple system atrophy under EGCG supplementation as anti-aggregation-approach." Journal of Neural Transmission **123**(4): 439-445.
- Li, J., V. N. Uversky and A. L. Fink (2001). "Effect of familial Parkinson's disease point mutations A30P and A53T on the structural properties, aggregation, and fibrillation of human alpha-synuclein." Biochemistry **40**(38): 11604-11613.
- Li, R.-S., X.-B. Wang, X.-J. Hu and L.-Y. Kong (2013). "Design, synthesis and evaluation of flavonoid derivatives as potential multifunctional acetylcholinesterase inhibitors against Alzheimer's disease." Bioorganic & Medicinal Chemistry Letters **23**(9): 2636-2641.
- Lill, C. M. (2016). "Genetics of Parkinson's disease." Molecular and Cellular Probes **30**(6): 386-396.
- Lin, J.-W., J.-T. Chen, C.-Y. Hong, Y.-L. Lin, K.-T. Wang, C.-J. Yao, G.-M. Lai and R.-M. Chen (2012). "Honokiol traverses the blood-brain barrier and induces apoptosis of neuroblastoma cells via an intrinsic bax-mitochondrion-cytochrome c-caspase protease pathway." Neuro-Oncology **14**(3): 302-314.
- Linares, D., O. Bottzeck, O. Pereira, A. Praud-Tabariès and Y. Blache (2011). "Designing 2-aminoimidazole alkaloids analogs with anti-biofilm activities: Structure–activities relationships of polysubstituted triazoles." Bioorganic & Medicinal Chemistry Letters **21**(22): 6751-6755.
- Lipinski, C. A., Lombardo, F., Dominy, B. W. and P. J. Feeney (1997). "Experimental and computational approaches to estimate solubility and permeability in drug discovery and development settings." Advanced Drug Delivery Reviews **23**(1-3): 3-25.
- Lipinski, C. A., Lombardo, F., Dominy, B. W. and P. J. Feeney (2001). "Experimental and computational approaches to estimate solubility and permeability in drug discovery and development settings." Advanced Drug Delivery Reviews **46**(1-3): 3-26.

Lippa, C. F., H. Fujiwara, D. M. A. Mann, B. Giasson, M. Baba, M. L. Schmidt, L. E. Nee, B. O'Connell, D. A. Pollen, P. St. George-Hyslop, B. Ghetti, D. Nochlin, T. D. Bird, N. J. Cairns, V. M. Y. Lee, T. Iwatsubo and J. Q. Trojanowski (1998). "Lewy Bodies Contain Altered α -Synuclein in Brains of Many Familial Alzheimer's Disease Patients with Mutations in Presenilin and Amyloid Precursor Protein Genes." The American Journal of Pathology **153**(5): 1365-1370.

Liu, Y., J. A. Carver, A. N. Calabrese and T. L. Pukala (2014). "Gallic acid interacts with α -synuclein to prevent the structural collapse necessary for its aggregation." Biochimica et Biophysica Acta (BBA) - Proteins and Proteomics **1844**(9): 1481-1485.

Liu, Y., M. Graetz, L. Ho and T. L. Pukala (2015). "Ion Mobility—Mass Spectrometry-Based Screening for Inhibition of α -Synuclein Aggregation." European Journal of Mass Spectrometry **21**(3): 255-264.

Lorenzen, N., S. B. Nielsen, Y. Yoshimura, B. S. Vad, C. B. Andersen, C. Betzer, J. D. Kaspersen, G. Christiansen, J. S. Pedersen, P. H. Jensen, F. A. A. Mulder and D. E. Otzen (2014). "How Epigallocatechin Gallate Can Inhibit α -Synuclein Oligomer Toxicity in Vitro." Journal of Biological Chemistry **289**(31): 21299-21310.

Lovell, M. A., W. D. Ehmann, M. P. Mattson and W. R. Markesbery (1997). "Elevated 4-Hydroxynonenal in Ventricular Fluid in Alzheimer's Disease." Neurobiology of Aging **18**(5): 457-461.

Lovering, F., J. Bikker and C. Humblet (2009). "Escape from Flatland: Increasing Saturation as an Approach to Improving Clinical Success." Journal of Medicinal Chemistry **52**(21): 6752-6756.

Lu, J.-X., W. Qiang, W.-M. Yau, Charles D. Schwieters, Stephen C. Meredith and R. Tycko (2013). "Molecular Structure of β -Amyloid Fibrils in Alzheimer's Disease Brain Tissue." Cell **154**(6): 1257-1268.

Lu, J. H., M. T. Ardah, S. S. K. Durairajan, L. F. Liu, L. X. Xie, W. F. D. Fong, M. Y. Hasan, J. D. Huang, O. M. A. El-Agnaf and M. Li (2011). "Baicalein Inhibits Formation of α -Synuclein Oligomers within Living Cells and Prevents A β Peptide Fibrillation and Oligomerisation." ChemBioChem **12**(4): 615-624.

Luhurs, T., C. Ritter, M. Adrian, D. Riek-Loher, B. Bohrmann, H. Dobeli, D. Schubert and R. Riek (2005). "3D structure of Alzheimer's amyloid-beta(1-42) fibrils." Proceedings of the National Academy of Sciences **102**(48): 17342-17347.

Lührs, T., C. Ritter, M. Adrian, D. Riek-Loher, B. Bohrmann, H. Döbeli, D. Schubert and R. Riek (2005). "3D structure of Alzheimer's amyloid- β (1–42) fibrils." Proceedings of the National Academy of Sciences **102**(48): 17342-17347.

Luk, K. C., V. Kehm, J. Carroll, B. Zhang, P. O'Brien, J. Q. Trojanowski and V. M.-Y. Lee (2012). "Pathological α -Synuclein Transmission Initiates Parkinson-like Neurodegeneration in Nontransgenic Mice." Science **338**(6109): 949-953.

Luo, Y., J. V. Smith, V. Paramasivam, A. Burdick, K. J. Curry, J. P. Buford, I. Khan, W. J. Netzer, H. Xu and P. Butko (2002). "Inhibition of amyloid- β aggregation and caspase-3 activation by the Ginkgo biloba extract EGb761." Proceedings of the National Academy of Sciences **99**(19): 12197-12202.

M. J. Frisch, G. W. T., H. B. Schlegel, G. E. Scuseria, M. A. Robb, J. R. Cheeseman, G. Scalmani, V. Barone, G. A. Petersson, H. Nakatsuji, X. Li, M. Caricato, A. Marenich, J. Bloino, B. G. Janesko, R. Gomperts, B. Mennucci, H. P. Hratchian, J. V. Ortiz, A. F. Izmaylov, J. L. Sonnenberg, D. Williams-Young, F. Ding, F. Lipparini, F. Egidi, J. Goings, B. Peng, A. Petrone, T. Henderson, D. Ranasinghe, V. G. Zakrzewski, J. Gao, N. Rega, G. Zheng, W. Liang, M. Hada, M. Ehara, K. Toyota, R. Fukuda, J. Hasegawa, M. Ishida, T. Nakajima, Y. Honda, O. Kitao, H. Nakai, T. Vreven, K. Throssell, J. A. Montgomery, Jr., J. E. Peralta, F. Ogliaro, M. Bearpark, J. J. Heyd, E. Brothers, K. N. Kudin, V. N. Staroverov, T. Keith, R. Kobayashi, J. Normand, K. Raghavachari, A. Rendell, J. C. Burant, S. S. Iyengar, J. Tomasi, M. Cossi, J. M. Millam, M. Klene, C. Adamo, R. Cammi, J. W. Ochterski, R. L. Martin, K. Morokuma, O. Farkas, J. B. Foresman, and D. J. Fox, Gaussian, Inc., Wallingford CT. (2016). "Gaussian 09."

Maioli, M., V. Basoli, P. Carta, D. Fabbri, M. A. Dettori, S. Cruciani, P. A. Serra and G. Delogu (2018). "Synthesis of magnolol and honokiol derivatives and their effect against hepatocarcinoma cells." PLOS ONE **13**(2): e0192178.

Maione, F., M. Piccolo, S. De Vita, M. G. Chini, C. Cristiano, C. De Caro, P. Lippiello, M. C. Miniaci, R. Santamaria, C. Irace, V. De Feo, A. Calignano, N. Mascolo and G. Bifulco (2018). "Down regulation of pro-inflammatory pathways by tanshinone IIA and cryptotanshinone in a non-genetic mouse model of Alzheimer's disease." Pharmacological Research **129**: 482-490.

Manach, C., A. Scalbert, C. Morand, C. Rémésy and L. Jiménez (2004). "Polyphenols: food sources and bioavailability." The American Journal of Clinical Nutrition **79**(5): 727-747.

Marambaud, P., H. Zhao and P. Davies (2005). "Resveratrol Promotes Clearance of Alzheimer's Disease Amyloid- β Peptides." Journal of Biological Chemistry **280**(45): 37377-37382.

- Marsh, D. T., S. Das, J. Ridell and S. D. Smid (2017). "Structure-activity relationships for flavone interactions with amyloid β reveal a novel anti-aggregatory and neuroprotective effect of 2',3',4'-trihydroxyflavone (2-D08)." Bioorganic & Medicinal Chemistry **25**(14): 3827-3834.
- Masters, C. L., G. Multhaup, G. Simms, J. Pottgiesser, R. N. Martins and K. Beyreuther (1985). "Neuronal origin of a cerebral amyloid: neurofibrillary tangles of Alzheimer's disease contain the same protein as the amyloid of plaque cores and blood vessels." Embo journal **4**(11): 2757-2763.
- Masters, C. L., G. Simms, N. A. Weinman, G. Multhaup, B. L. McDonald and K. Beyreuther (1985). "Amyloid plaque core protein in Alzheimer disease and Down syndrome." Proceedings of the National Academy of Sciences **82**(12): 4245-4249.
- McGeer, P. L., S. Itagaki, B. E. Boyes and E. G. McGeer (1988). "Reactive microglia are positive for HLA-DR in the: Substantia nigra of Parkinson's and Alzheimer's disease brains." Neurology **38**(8): 1285-1291.
- McKoy, A. F., J. Chen, T. Schupbach and M. H. Hecht (2012). "A Novel Inhibitor of Amyloid β (A β) Peptide Aggregation: From high throughput screening to efficacy in an animal model of Alzheimer disease" Journal of Biological Chemistry **287**(46): 38992-39000.
- Mecocci, P. and M. C. Polidori (2012). "Antioxidant clinical trials in mild cognitive impairment and Alzheimer's disease." Biochimica et Biophysica Acta (BBA) - Molecular Basis of Disease **1822**(5): 631-638.
- Mendgen, T., C. Steuer and C. D. Klein (2012). "Privileged Scaffolds or Promiscuous Binders: A Comparative Study on Rhodanines and Related Heterocycles in Medicinal Chemistry." Journal of Medicinal Chemistry **55**(2): 743-753.
- Meng, X.-Y., H.-X. Zhang, M. Mezei and M. Cui (2011). "Molecular Docking: A powerful approach for structure-based drug discovery." Current computer-aided drug design **7**(2): 146-157.
- Meng, X., L. A. Munishkina, A. L. Fink and V. N. Uversky (2009). "Molecular Mechanisms Underlying the Flavonoid-Induced Inhibition of α -Synuclein Fibrillation." Biochemistry **48**(34): 8206-8224.
- Meng, X., L. A. Munishkina, A. L. Fink and V. N. Uversky (2010). "Effects of Various Flavonoids on the -Synuclein Fibrillation Process." Parkinson's Disease **2010**: 16.
- Mereles, D. and W. Hunstein (2011). "Epigallocatechin-3-gallate (EGCG) for Clinical Trials: More Pitfalls than Promises?" International Journal of Molecular Sciences **12**(9): 5592.

- Meusel, M. and M. Gütschow (2004). "Recent developments in hydantoin chemistry. A review." Organic Preparations and Procedures International **36**(5): 391-443.
- Mishra, C. B., S. Kumari and M. Tiwari (2015). "Thiazole: A promising heterocycle for the development of potent CNS active agents." European Journal of Medicinal Chemistry **92**: 1-34.
- Mittal, S., K. Bjørnevik, D. S. Im, A. Flierl, X. Dong, J. J. Locascio, K. M. Abo, E. Long, M. Jin, B. Xu, Y. K. Xiang, J.-C. Rochet, A. Engeland, P. Rizzu, P. Heutink, T. Bartels, D. J. Selkoe, B. J. Caldarone, M. A. Glicksman, V. Khurana, B. Schüle, D. S. Park, T. Riise and C. R. Scherzer (2017). " β 2-Adrenoreceptor is a regulator of the α -synuclein gene driving risk of Parkinson's disease." Science **357**(6354): 891-898.
- Mizuno, Y., S. Ohta, M. Tanaka, S. Takamiya, K. Suzuki, T. Sato, H. Oya, T. Ozawa and Y. Kagawa (1989). "Deficiencies in Complex I subunits of the respiratory chain in Parkinson's disease." Biochemical and Biophysical Research Communications **163**(3): 1450-1455.
- Moors, T. E., J. J. M. Hoozemans, A. Ingrassia, T. Beccari, L. Parnetti, M.-C. Chartier-Harlin and W. D. J. van de Berg (2017). "Therapeutic potential of autophagy-enhancing agents in Parkinson's disease." Molecular Neurodegeneration **12**(1): 11.
- Morgan, D. (2011). "Immunotherapy for Alzheimer's Disease." Journal of internal medicine **269**(1): 54-63.
- Mori, H., K. Takio, M. Ogawara and D. J. Selkoe (1992). "Mass spectrometry of purified amyloid beta protein in Alzheimer's disease." Journal of Biological Chemistry **267**(24): 17082-17086.
- Moroney, M. A., Alcaraz M. J., Forder R. A., Carey F. and Hault J. R. S. (1988). "Selectivity of Neutrophil 5-Lipoxygenase and Cyclo-oxygenase Inhibition by an Anti-inflammatory Flavonoid Glycoside and Related Aglycone Flavonoids." Journal of Pharmacy and Pharmacology **40**(11): 787-792.
- Mrak, R. E. and W. S. T. Griffin (2005). "Potential Inflammatory biomarkers in Alzheimer's disease." Journal of Alzheimer's Disease **8**(4): 369-375.
- Muccioli, G. G., N. Fazio, G. K. E. Scriba, W. Poppitz, F. Cannata, J. H. Poupaert, J. Wouters and D. M. Lambert (2006). "Substituted 2-Thioxoimidazolidin-4-ones and Imidazolidine-2,4-diones as Fatty Acid Amide Hydrolase Inhibitors Templates." Journal of Medicinal Chemistry **49**(1): 417-425.
- Mullard, A. (2017). "BACE inhibitor bust in Alzheimer trial." Nature Reviews Drug Discovery **16**: 155.

- Muroyama, A., A. Fujita, C. Lv, S. Kobayashi, Y. Fukuyama and Y. Mitsumoto (2012). "Magnolol Protects against MPTP/MPP+-Induced Toxicity via Inhibition of Oxidative Stress in In Vivo and In Vitro Models of Parkinson's Disease." Parkinson's Disease **2012**: 9.
- Murray, C. W., M. L. Verdonk and D. C. Rees (2012). "Experiences in fragment-based drug discovery." Trends in Pharmacological Sciences **33**(5): 224-232.
- Murray, I. V. J., L. Liu, H. Komatsu, K. Uryu, G. Xiao, J. A. Lawson and P. H. Axelsen (2007). "Membrane-mediated Amyloidogenesis and the Promotion of Oxidative Lipid Damage by Amyloid β Proteins." Journal of Biological Chemistry **282**(13): 9335-9345.
- Mutisya, E. M., A. C. Bowling and M. F. Beal (1994). "Cortical Cytochrome Oxidase Activity Is Reduced in Alzheimer's Disease." Journal of Neurochemistry **63**(6): 2179-2184.
- Naiki, H., K. Higuchi, M. Hosokawa and T. Takeda (1989). "Fluorometric determination of amyloid fibrils in vitro using the fluorescent dye, thioflavine T." Analytical Biochemistry **177**(2): 244-249.
- Nakagami, Y., S. Nishimura, T. Murasugi, I. Kaneko, M. Meguro, S. Marumoto, H. Kogen, K. Koyama and T. Oda (2002). "A novel β -sheet breaker, RS-0406, reverses amyloid β -induced cytotoxicity and impairment of long-term potentiation in vitro." British Journal of Pharmacology **137**(5): 676-682.
- Narhi, L., S. J. Wood, S. Steavenson, Y. Jiang, G. M. Wu, D. Anafi, S. A. Kaufman, F. Martin, K. Sitney, P. Denis, J.-C. Louis, J. Wypych, A. L. Biere and M. Citron (1999). "Both Familial Parkinson's Disease Mutations Accelerate α -Synuclein Aggregation." Journal of Biological Chemistry **274**(14): 9843-9846.
- Nelson, K. M., J. L. Dahlin, J. Bisson, J. Graham, G. F. Pauli and M. A. Walters (2017). "The Essential Medicinal Chemistry of Curcumin." Journal of Medicinal Chemistry **60**(5): 1620-1637.
- Newman, D. J. and G. M. Cragg (2007). "Natural Products as Sources of New Drugs over the Last 25 Years." Journal of Natural Products **70**(3): 461-477.
- Nordberg, A. and A.-L. Svensson (1998). "Cholinesterase Inhibitors in the Treatment of Alzheimer's Disease." Drug Safety **19**(6): 465-480.
- Olson, G. L., D. R. Bolin, M. P. Bonner, M. Bos, C. M. Cook, D. C. Fry, B. J. Graves, M. Hatada and D. E. Hill (1993). "Concepts and progress in the development of peptide mimetics." Journal of Medicinal Chemistry **36**(21): 3039-3049.
- Ongini, E., A. Monopoli, B. Cacciari and P. Giovanni Baraldi (2001). "Selective adenosine A2A receptor antagonists." Il Farmaco **56**(1): 87-90.

- Ono, M., Y. Cheng, H. Kimura, M. Cui, S. Kagawa, R. Nishii and H. Saji (2011). "Novel ^{18}F -Labeled Benzofuran Derivatives with Improved Properties for Positron Emission Tomography (PET) Imaging of β -Amyloid Plaques in Alzheimer's Brains." Journal of Medicinal Chemistry **54**(8): 2971-2979.
- Ono, M., M. Hori, M. Haratake, T. Tomiyama, H. Mori and M. Nakayama (2007). "Structure-activity relationship of chalcones and related derivatives as ligands for detecting of β -amyloid plaques in the brain." Bioorganic & Medicinal Chemistry **15**(19): 6388-6396.
- Ono, M., R. Ikeoka, H. Watanabe, H. Kimura, T. Fuchigami, M. Haratake, H. Saji and M. Nakayama (2010). "Synthesis and Evaluation of Novel Chalcone Derivatives with $^{99\text{m}}\text{Tc}/\text{Re}$ Complexes as Potential Probes for Detection of β -Amyloid Plaques." ACS Chemical Neuroscience **1**(9): 598-607.
- Ono, M., H. Kawashima, A. Nonaka, T. Kawai, M. Haratake, H. Mori, M.P. Kung, H. F. Kung, H. Saji and M. Nakayama (2006). "Novel Benzofuran Derivatives for PET Imaging of β -Amyloid Plaques in Alzheimer's Disease Brains." Journal of Medicinal Chemistry **49**(9): 2725-2730.
- Pajouhesh, H. and G.R. Lenz (2005). " Medicinal Chemical Properties of Successful Central Nervous System Drugs." NeuroRx **2**(4): 541-553.
- Pandey, K. B. and S. I. Rizvi (2009). "Plant polyphenols as dietary antioxidants in human health and disease." Oxidative Medicine and Cellular Longevity **2**(5): 270-278.
- Papandreou, M. A., C. D. Kanakis, M. G. Polissiou, S. Efthimiopoulos, P. Cordopatis, M. Margarity and F. N. Lamari (2006). "Inhibitory Activity on Amyloid- β Aggregation and Antioxidant Properties of Crocus sativus Stigmas Extract and Its Crocin Constituents." Journal of Agricultural and Food Chemistry **54**(23): 8762-8768.
- Parker, W. D., Jr., C. M. Filley and J. K. Parks (1990). "Cytochrome oxidase deficiency in Alzheimer's disease." Neurology **40**(8): 1302-1303.
- Patridge, E., P. Gareiss, M. S. Kinch and D. Hoyer (2016). "An analysis of FDA-approved drugs: natural products and their derivatives." Drug Discovery Today **21**(2): 204-207.
- Perl, D. P. (2010). "Neuropathology of Alzheimer's Disease." The Mount Sinai Journal of Medicine, New York **77**(1): 32-42.
- Perron, N. R. and J. L. Brumaghim (2009). "A Review of the Antioxidant Mechanisms of Polyphenol Compounds Related to Iron Binding." Cell Biochemistry and Biophysics **53**(2): 75-100.

Petkova, A. T., R. D. Leapman, Z. Guo, W.-M. Yau, M. P. Mattson and R. Tycko (2005). "Self-Propagating, Molecular-Level Polymorphism in Alzheimer's β -Amyloid Fibrils." Science **307**(5707): 262-265.

Poewe, W., K. Seppi, C. M. Tanner, G. M. Halliday, P. Brundin, J. Volkmann, A.-E. Schrag and A. E. Lang (2017). "Parkinson disease." Nature Reviews Disease Primers **3**: 17013.

Porat, Y., A. Abramowitz and E. Gazit (2006). "Inhibition of Amyloid Fibril Formation by Polyphenols: Structural Similarity and Aromatic Interactions as a Common Inhibition Mechanism." Chemical Biology & Drug Design **67**(1): 27-37.

Prince, M., R. Bryce, E. Albanese, A. Wimo, W. Ribeiro and C. P. Ferri (2013). "The global prevalence of dementia: A systematic review and metaanalysis." Alzheimer's & Dementia **9**(1): 63-75.e62.

Pringsheim, T., N. Jette, A. Frolkis and T. D. Steeves (2014). "The prevalence of Parkinson's disease: a systematic review and meta-analysis." Movement Disorder **29**(13): 1583-1590.

Qiang, L.-Q., C.-P. Wang, F.-M. Wang, Y. Pan, L.-T. Yi, X. Zhang and L.-D. Kong (2009). "Combined administration of the mixture of honokiol and magnolol and ginger oil evokes antidepressant-like synergism in rats." Archives of Pharmacal Research **32**(9): 1281-1292.

Qu, W., M.-P. Kung, C. Hou, S. Oya and H. F. Kung (2007). "Quick Assembly of 1,4-Diphenyltriazoles as Probes Targeting β -Amyloid Aggregates in Alzheimer's Disease." Journal of Medicinal Chemistry **50**(14): 3380-3387.

Rabey, J. M., I. Sagi, M. Huberman, E. Melamed, A. Korczyn, N. Giladi, R. Inzelberg, R. Djaldetti, C. Klein, G. Berecz and R. S. Group (2000). "Rasagiline Mesylate, a New Mao-B Inhibitor for the Treatment of Parkinson's Disease: A Double-Blind Study as Adjunctive Therapy to Levodopa." Clinical Neuropharmacology **23**(6): 324-330.

Reinke, A. A. and J. E. Gestwicki (2007). "Structure–activity Relationships of Amyloid Beta-aggregation Inhibitors Based on Curcumin: Influence of Linker Length and Flexibility." Chemical Biology & Drug Design **70**(3): 206-215.

Rekas, A., Adda C. G., Andrew, A. J., Barnham, K.J., Sunde, M., Galatis, D., Williamson N.A., Masters, C.L., Anders, R.F., Robinson, C.V., Cappai, R. and J.A. Carver (2004). "Interaction of the molecular chaperone α B-crystallin with α -synuclein: effects on amyloid fibril formation and chaperone activity." Journal of Molecular Biology **340**(5): 1167-83.

Relkin, N. R. (2008). "Testing the mettle of PBT2 for Alzheimer's disease." The Lancet Neurology **7**(9): 762-763.

Rezai-Zadeh, K., G. W. Arendash, H. Hou, F. Fernandez, M. Jensen, M. Runfeldt, R. D. Shytle and J. Tan (2008). "Green tea epigallocatechin-3-gallate (EGCG) reduces β -amyloid mediated cognitive impairment and modulates tau pathology in Alzheimer transgenic mice." Brain Research **1214**: 177-187.

Riederer, P. and Laux, G. (2011). "MAO-inhibitors in Parkinson's Disease." Experimntal Neurobiology **20**(1): 1-17.

Rizzo, S., C. Rivière, L. Piazzzi, A. Bisi, S. Gobbi, M. Bartolini, V. Andrisano, F. Morroni, A. Tarozzi, J.-P. Monti and A. Rampa (2008). "Benzofuran-Based Hybrid Compounds for the Inhibition of Cholinesterase Activity, β Amyloid Aggregation, and A β Neurotoxicity." Journal of Medicinal Chemistry **51**(10): 2883-2886.

Rodrigues, T., D. Reker, P. Schneider and G. Schneider (2016). "Counting on natural products for drug design." Nature Chemistry **8**: 531.

Rodriguez, J. A., M. I. Ivanova, M. R. Sawaya, D. Cascio, F. E. Reyes, D. Shi, S. Sangwan, E. L. Guenther, L. M. Johnson, M. Zhang, L. Jiang, M. A. Arbing, B. L. Nannenga, J. Hattne, J. Whitelegge, A. S. Brewster, M. Messerschmidt, S. Boutet, N. K. Sauter, T. Gonen and D. S. Eisenberg (2015). "Structure of the toxic core of alpha-synuclein from invisible crystals." Nature **525**(7570): 486-490.

Ruottinen, H.M., and Rinne, U.K. (1998). "COMT inhibition in the treatment of Parkinson's disease." Journal of Neurology **245**(11 Supplement 3): 25-34.

Rush, T. S., J. A. Grant, L. Mosyak and A. Nicholls (2005). "A Shape-Based 3-D Scaffold Hopping Method and Its Application to a Bacterial Protein-Protein Interaction." Journal of Medicinal Chemistry **48**(5): 1489-1495.

Salminen, A., J. Ojala, A. Kauppinen, K. Kaarniranta and T. Suuronen (2009). "Inflammation in Alzheimer's disease: Amyloid- β oligomers trigger innate immunity defence via pattern recognition receptors." Progress in Neurobiology **87**(3): 181-194.

Sandrine, A., O. Pierre-Jean, C. Nicola, O. Mehemed, M.-F. Helene and V. Bruno (2008). "GuidAge Study: A 5-Year Double Blind, Randomised Trial of EGb 761 for the Prevention of Alzheimers Disease in Elderly Subjects with Memory Complaints. I. Rationale, Design and Baseline Data." Current Alzheimer Research **5**(4): 406-415.

Sardi, S. P., S. H. Cheng and L. S. Shihabuddin (2015). "Gaucher-related synucleinopathies: The examination of sporadic neurodegeneration from a rare (disease) angle." Progress in Neurobiology **125**: 47-62.

- Sarni-Manchado, P. and V. Cheynier (2002). "Study of non-covalent complexation between catechin derivatives and peptides by electrospray ionization mass spectrometry." Journal of Mass Spectrometry **37**(6): 609-616.
- Sato, M., K. Murakami, M. Uno, Y. Nakagawa, S. Katayama, K.-i. Akagi, Y. Masuda, K. Takegoshi and K. Irie (2013). "Site-specific Inhibitory Mechanism for Amyloid β 42 Aggregation by Catechol-type Flavonoids Targeting the Lys Residues." Journal of Biological Chemistry **288**(32): 23212-23224.
- Schapiro, A. H. V., J. M. Cooper, D. Dexter, J. B. Clark, P. Jenner and C. D. Marsden (1990). "Mitochondrial Complex I Deficiency in Parkinson's Disease." Journal of Neurochemistry **54**(3): 823-827.
- Schenk, D. B., M. Koller, D. K. Ness, S. G. Griffith, M. Grundman, W. Zago, J. Soto, G. Atiee, S. Ostrowitzki and G. G. Kinney (2017). "First-in-human assessment of PRX002, an anti- α -synuclein monoclonal antibody, in healthy volunteers." Movement Disorders **32**(2): 211-218.
- Scheuner, D., C. Eckman, M. Jensen, X. Song, M. Citron, N. Suzuki, T. D. Bird, J. Hardy, M. Hutton, W. Kukull, E. Larson, L. Levy-Lahad, M. Viitanen, E. Peskind, P. Poorkaj, G. Schellenberg, R. Tanzi, W. Wasco, L. Lannfelt, D. Selkoe and S. Younkin (1996). "Secreted amyloid [beta]-protein similar to that in the senile plaques of Alzheimer's disease is increased in vivo by the presenilin 1 and 2 and APP mutations linked to familial Alzheimer's disease." Nature Medicine **2**(8): 864-870.
- Schneider, G., O. Clément-Chomienne, L. Hilfiger, P. Schneider, S. Kirsch, H. J. Böhm and W. Neidhart (2000). "Virtual Screening for Bioactive Molecules by Evolutionary De Novo Design." Angewandte Chemie International Edition **39**(22): 4130-4133.
- Schneider, G., W. Neidhart, T. Giller and G. Schmid (1999). "'Scaffold-Hopping' by Topological Pharmacophore Search: A Contribution to Virtual Screening." Angewandte Chemie International Edition **38**(19): 2894-2896.
- Schrag, A., L. Horsfall, K. Walters, A. Noyce and I. Petersen (2015). "Prediagnostic presentations of Parkinson's disease in primary care: a case-control study." The Lancet Neurology **14**(1): 57-64.
- Schreiber, S. L. (2000). "Target-Oriented and Diversity-Oriented Organic Synthesis in Drug Discovery." Science **287**(5460): 1964-1969.
- Sevigny, J., P. Chiao, T. Bussière, P. H. Weinreb, L. Williams, M. Maier, R. Dunstan, S. Salloway, T. Chen, Y. Ling, J. O'Gorman, F. Qian, M. Arastu, M. Li, S. Chollate, M. S. Brennan, O. Quintero-Monzon, R. H. Scannevin, H. M. Arnold, T. Engber, K. Rhodes, J.

- Ferrero, Y. Hang, A. Mikulskis, J. Grimm, C. Hock, R. M. Nitsch and A. Sandrock (2016). "The antibody aducanumab reduces A β plaques in Alzheimer's disease." Nature **537**: 50-56.
- Shang, E., Y. Yuan, X. Chen, Y. Liu, J. Pei and L. Lai (2014). "De Novo Design of Multitarget Ligands with an Iterative Fragment-Growing Strategy." Journal of Chemical Information and Modeling **54**(4): 1235-1241.
- Shi, C., L. Zhao, B. Zhu, Q. Li, D. T. Yew, Z. Yao and J. Xu (2009). "Protective effects of Ginkgo biloba extract (EGb761) and its constituents quercetin and ginkgolide B against β -amyloid peptide-induced toxicity in SH-SY5Y cells." Chemico-Biological Interactions **181**(1): 115-123.
- Shimmyo, Y., T. Kihara, A. Akaike, T. Niidome and H. Sugimoto (2008). "Multifunction of myricetin on A β : Neuroprotection via a conformational change of A β and reduction of A β via the interference of secretases." Journal of Neuroscience Research **86**(2): 368-377.
- Shuker, S. B., P. J. Hajduk, R. P. Meadows and S. W. Fesik (1996). "Discovering high-affinity ligands for proteins: SAR by NMR." Science **274**(5292): 1531-1534.
- Singh, S. K., R. Gaur, A. Kumar, R. Fatima, L. Mishra and S. Srikrishna (2014). "The Flavonoid Derivative 2-(4' Benzyloxyphenyl)-3-hydroxy-chromen-4-one Protects Against A β 42-Induced Neurodegeneration in Transgenic Drosophila: Insights from In Silico and In Vivo Studies." Neurotoxicity Research **26**(4): 331-350.
- Smid, S. D., J. L. Maag and I. F. Musgrave (2012). "Dietary polyphenol-derived protection against neurotoxic beta-amyloid protein: from molecular to clinical." Food & Function **3**(12): 1242-1250.
- Spillantini, M. G. and M. Goedert (2000). "The alpha-synucleinopathies: Parkinson's disease, dementia with Lewy bodies, and multiple system atrophy." Annals of the New York Academy of Sciences **920**: 16-27.
- Stamford, A. and C. Strickland (2013). "Inhibitors of BACE for treating Alzheimer's disease: a fragment-based drug discovery story." Current Opinion in Chemical Biology **17**(3): 320-328.
- Stsiapura, V. I., A. A. Maskevich, V. A. Kuzmitsky, K. K. Turoverov and I. M. Kuznetsova (2007). "Computational Study of thioflavin T Torsional Relaxation in the Excited State." The Journal of Physical Chemistry A **111**(22): 4829-4835.
- Tang, S. Q., Y. Y. I. Lee, D. S. Packiaraj, H. K. Ho and C. L. L. Chai (2015). "Systematic Evaluation of the Metabolism and Toxicity of Thiazolidinone and Imidazolidinone Heterocycles." Chemical Research in Toxicology **28**(10): 2019-2033.

Tariot, P. N., M. R. Farlow, G. T. Grossberg and et al. (2004). "Memantine treatment in patients with moderate to severe alzheimer disease already receiving donepezil: A randomized controlled trial." Journal of American Medical Association **291**(3): 317-324.

Taylor, R. D., M. MacCoss and A. D. G. Lawson (2014). "Rings in Drugs." Journal of Medicinal Chemistry **57**(14): 5845-5859.

The National Centre for Social and Economic Modelling NATSEM (2016) *Economic Cost of Dementia in Australia 2016-2056*

Thomsen, R. and M. H. Christensen (2006). "MolDock: a new technique for high-accuracy molecular docking." Journal of Medicinal Chemistry **49**(11): 3315-3321.

Tomasic, T. and L. P. Masic (2009). "Rhodanine as a Privileged Scaffold in Drug Discovery." Current Medicinal Chemistry **16**(13): 1596-1629.

Tosatto, L., M. H. Horrocks, A. J. Dear, T. P. Knowles, M. Dalla Serra, N. Cremades, C. M. Dobson and D. Klenerman (2015). "Single-molecule FRET studies on alpha-synuclein oligomerization of Parkinson's disease genetically related mutants." Scientific Report **5**: 16696.

Touboul, D., L. Maillard, A. Grässlin, R. Moumne, M. Seitz, J. Robinson and R. Zenobi (2009). "How to Deal with Weak Interactions in Noncovalent Complexes Analyzed by Electrospray Mass Spectrometry: Cyclopeptidic Inhibitors of the Nuclear Receptor Coactivator 1-STAT6." Journal of the American Society for Mass Spectrometry **20**(2): 303-311.

Trinh, N., J. Hoblyn, S. Mohanty and K. Yaffe (2003). "Efficacy of cholinesterase inhibitors in the treatment of neuropsychiatric symptoms and functional impairment in alzheimer disease: A meta-analysis." Journal of American Medical Association **289**(2): 210-216.

Turner, P. R., K. O'Connor, W. P. Tate and W. C. Abraham (2003). "Roles of amyloid precursor protein and its fragments in regulating neural activity, plasticity and memory." Progress in Neurobiology **70**(1): 1-32.

Tuttle, M. D., G. Comellas, A. J. Nieuwkoop, D. J. Covell, D. A. Berthold, K. D. Kloepper, J. M. Courtney, J. K. Kim, A. M. Barclay, A. Kendall, W. Wan, G. Stubbs, C. D. Schwieters, V. M. Lee, J. M. George and C. M. Rienstra (2016). "Solid-state NMR structure of a pathogenic fibril of full-length human alpha-synuclein." Nature Structural Molecular Biology **23**(5): 409-415.

Tycko, R. (2015). "Amyloid Polymorphism: Structural Basis and Neurobiological Relevance." Neuron **86**(3): 632-645.

- Tysnes, O. B. and A. Storstein (2017). "Epidemiology of Parkinson's disease." Journal of Neural Transmission (Vienna) **124**(8): 901-905.
- Ufer, M., M.-L. Rouzade-Dominguez, G. Huledal, N. Pezous, A. Avrameas, O. David, S. Kretz, K. Kucher, U. Neumann, J.-H. Cha, A. Graf and C. Lopez-Lopez (2016). " Results from a first-in-human study with the BACE inhibitor CNP520." Alzheimer's & Dementia: The Journal of the Alzheimer's Association **12**(7): P200.
- Uversky, V. N. (2011). "Intrinsically disordered proteins from A to Z." The International Journal of Biochemistry & Cell Biology **43**(8): 1090-1103.
- van der Stelt, M., J. Cals, S. Broeders-Josten, J. Cottney, A. A. van der Doelen, M. Hermkens, V. de Kimpe, A. King, J. Klomp, J. Oosterom, I. Pols-de Rooij, J. de Roos, M. van Tilborg, S. Boyce and J. Baker (2011). "Discovery and Optimization of 1-(4-(Pyridin-2-yl)benzyl)imidazolidine-2,4-dione Derivatives As a Novel Class of Selective Cannabinoid CB2 Receptor Agonists." Journal of Medicinal Chemistry **54**(20): 7350-7362.
- Volles, M. J. and P. T. Lansbury Jr (2007). "Relationships between the Sequence of α -Synuclein and its Membrane Affinity, Fibrillization Propensity, and Yeast Toxicity." Journal of Molecular Biology **366**(5): 1510-1522.
- Volpicelli-Daley, L. A., K. C. Luk, T. P. Patel, S. A. Tanik, D. M. Riddle, A. Stieber, D. F. Meaney, J. Q. Trojanowski and V. M. Lee (2011). "Exogenous alpha-synuclein fibrils induce Lewy body pathology leading to synaptic dysfunction and neuron death." Neuron **72**(1): 57-71.
- Walsh, D. M., D. M. Hartley, Y. Kusumoto, Y. Fezoui, M. M. Condron, A. Lomakin, G. B. Benedek, D. J. Selkoe and D. B. Teplow (1999). "Amyloid β -Protein Fibrillogenesis: Structure and biological activity of protofibrillar intermediates." Journal of Biological Chemistry **274**(36): 25945-25952.
- Walsh, D. M., A. Lomakin, G. B. Benedek, M. M. Condron and D. B. Teplow (1997). "Amyloid β -Protein Fibrillogenesis: Detection of a protofibrillar intermediate." Journal of Biological Chemistry **272**(35): 22364-22372.
- Wang, S., H. Jing, H. Yang, Z. Liu, H. Guo, L. Chai and L. Hu (2015). "Tanshinone I selectively suppresses pro-inflammatory genes expression in activated microglia and prevents nigrostriatal dopaminergic neurodegeneration in a mouse model of Parkinson's disease." Journal of Ethnopharmacology **164**: 247-255.
- Wang, X., X. Duan, G. Yang, X. Zhang, L. Deng, H. Zheng, C. Deng, J. Wen, N. Wang, C. Peng, X. Zhao, Y. Wei and L. Chen (2011). "Honokiol Crosses BBB and BCSFB, and

Inhibits Brain Tumor Growth in Rat 9L Intracerebral Gliosarcoma Model and Human U251 Xenograft Glioma Model." PLOS ONE **6**(4): e18490.

Wermuth, C. G., C. R. Ganellin, P. Lindberg and L. A. Mitscher (1998). Glossary of terms used in medicinal chemistry (IUPAC Recommendations 1998). Pure and Applied Chemistry. **70**: 1129-1143.

Werner, C. J., R. Heyny-von Haussen, G. Mall and S. Wolf (2008). "Proteome analysis of human substantia nigra in Parkinson's disease." Proteome Sci **6**: 8.

Wong, V., A. Wu, J. Wang, L. Liu and B. Law (2015). "Neferine Attenuates the Protein Level and Toxicity of Mutant Huntingtin in PC-12 Cells via Induction of Autophagy." Molecules **20**(3): 3496.

Wu, Y., Z. Wu, P. Butko, Y. Christen, M. P. Lambert, W. L. Klein, C. D. Link and Y. Luo (2006). "Amyloid- β -Induced Pathological Behaviors Are Suppressed by Ginkgo biloba Extract EGb 761 and Ginkgolides in Transgenic *Caenorhabditis elegans*." The Journal of Neuroscience **26**(50): 13102-13113.

Xiao, Y., B. Ma, D. McElheny, S. Parthasarathy, F. Long, M. Hoshi, R. Nussinov and Y. Ishii (2015). "A β (1-42) fibril structure illuminates self-recognition and replication of amyloid in Alzheimer's disease." Nature Structural Molecular Biology **22**(6): 499-505.

Xu, Q., L.-T. Yi, Y. Pan, X. Wang, Y.-C. Li, J.-M. Li, C.-P. Wang and L.-D. Kong (2008). "Antidepressant-like effects of the mixture of honokiol and magnolol from the barks of *Magnolia officinalis* in stressed rodents." Progress in Neuro-Psychopharmacology and Biological Psychiatry **32**(3): 715-725.

Yamaguchi, H., S. Hirai, M. Morimatsu, M. Shoji and Y. Nakazato (1989). "Diffuse type of senile plaques in the cerebellum of Alzheimer-type dementia demonstrated by beta protein immunostain." Acta Neuropathologica **77**(3): 314-319.

Yan, R. (2016). "Stepping closer to treating Alzheimer's disease patients with BACE1 inhibitor drugs." Translational Neurodegeneration **5**(1): 13.

Yan, R. and R. Vassar (2014). "Targeting the β secretase BACE1 for Alzheimer's disease therapy." The Lancet Neurology **13**(3): 319-329.

Yanagisawa, D., N. Shirai, T. Amatsubo, H. Taguchi, K. Hirao, M. Urushitani, S. Morikawa, T. Inubushi, M. Kato, F. Kato, K. Morino, H. Kimura, I. Nakano, C. Yoshida, T. Okada, M. Sano, Y. Wada, K.-n. Wada, A. Yamamoto and I. Tooyama (2010). "Relationship between the tautomeric structures of curcumin derivatives and their A β -binding activities in the context of therapies for Alzheimer's disease." Biomaterials **31**(14): 4179-4185.

- Yanagisawa, D., H. Taguchi, S. Morikawa, T. Kato, K. Hirao, N. Shirai and I. Tooyama (2015). "Novel curcumin derivatives as potent inhibitors of amyloid β aggregation." Biochemistry and Biophysics Reports **4**: 357-368.
- Yang, F., G. P. Lim, A. N. Begum, O. J. Ubeda, M. R. Simmons, S. S. Ambegaokar, P. P. Chen, R. Kaye, C. G. Glabe, S. A. Frautschy and G. M. Cole (2005). "Curcumin Inhibits Formation of Amyloid β Oligomers and Fibrils, Binds Plaques, and Reduces Amyloid in Vivo." Journal of Biological Chemistry **280**(7): 5892-5901.
- Yang, X., M. Wang and M. C. Fitzgerald (2004). "Analysis of protein folding and function using backbone modified proteins." Bioorganic Chemistry **32**(5): 438-449.
- Yankner, B. A. and M.-M. Mesulam (1991). " β -Amyloid and the Pathogenesis of Alzheimer's Disease." New England Journal of Medicine **325**(26): 1849-1857.
- Yoo, K.-Y. and S.-Y. Park (2012). "Terpenoids as Potential Anti-Alzheimer's Disease Therapeutics." Molecules **17**(3): 3524.
- Yoritaka, A., N. Hattori, K. Uchida, M. Tanaka, E. R. Stadtman and Y. Mizuno (1996). "Immunohistochemical detection of 4-hydroxynonenal protein adducts in Parkinson disease." Proceedings of the National Academy of Sciences **93**(7): 2696-2701.
- Yu, W., S. Chen, L. Cao, J. Tang, W. Xiao and B. Xiao (2017). "Ginkgolide K promotes the clearance of A53T mutation alpha-synuclein in SH-SY5Y cells." Cell Biology and Toxicology.
- Zeng, H., P. Huang, X. Wang, J. Wu, M. Wu and J. Huang (2015). "Galangin-induced down-regulation of BACE1 by epigenetic mechanisms in SH-SY5Y cells." Neuroscience **294**: 172-181.
- Zhang, C., A. Browne, D. Child and R. E. Tanzi (2010). "Curcumin Decreases Amyloid- β Peptide Levels by Attenuating the Maturation of Amyloid- β Precursor Protein." Journal of Biological Chemistry **285**(37): 28472-28480.
- Zhang, L., X. M. Peng, G. L. V. Damu, R. X. Geng and C. H. Zhou (2014). "Comprehensive Review in Current Developments of Imidazole-Based Medicinal Chemistry." Medicinal Research Reviews **34**(2): 340-437.
- Zharikov, A. D., J. R. Cannon, V. Tapias, Q. Bai, M. P. Horowitz, V. Shah, A. El Ayadi, T. G. Hastings, J. T. Greenamyre and E. A. Burton (2015). "shRNA targeting α -synuclein prevents neurodegeneration in a Parkinson's disease model." The Journal of Clinical Investigation **125**(7): 2721-2735.

Zheng, J., H. Kong, J. M. Wilson, J. Guo, Y. Chang, M. Yang, G. Xiao and P. Sun (2014). "Insight into the Interactions between Novel Isoquinolin-1,3-Dione Derivatives and Cyclin-Dependent Kinase 4 Combining QSAR and Molecular Docking." PLOS ONE **9**(4): e93704.

Zhu, J. T. T., R. C. Y. Choi, G. K. Y. Chu, A. W. H. Cheung, Q. T. Gao, J. Li, Z. Y. Jiang, T. T. X. Dong and K. W. K. Tsim (2007). "Flavonoids Possess Neuroprotective Effects on Cultured Pheochromocytoma PC12 Cells: A Comparison of Different Flavonoids in Activating Estrogenic Effect and in Preventing β -Amyloid-Induced Cell Death." Journal of Agricultural and Food Chemistry **55**(6): 2438-2445.

Zoete, V., A. Grosdidier and O. Michielin (2009). "Docking, virtual high throughput screening and in silico fragment-based drug design." Journal of Cellular and Molecular Medicine **13**(2): 238-248.